Report to BEIS

**Long-Term Atmospheric
Measurement and Interpretation
of Radiatively Active Trace Gases**

**Annual Report
Sept 2018 – Sept 2019**

Date: 4th Oct 2019

Met Office: Alison Redington, Alistair Manning
University of Bristol: Simon O'Doherty, Dan Say, Matt Rigby, Daniel Hoare, Adam Wisher
NPL: Chris Rennick, Tim Arnold
Terra Modus Consultants: Dickon Young
INSCON: Peter Simmonds

Contents

1 Executive Summary

- The overriding aim of the project is to estimate UK emissions of the principle greenhouse gases using the UK Deriving Emissions related to Climate Change (DECC) network of observations and compare these to the compiled inventory. The Inversion Technique for Emission Modelling (InTEM) has been developed to deliver these estimates. These comparisons enable BEIS to be more informed in their inventory improvement programme.

- The northern hemisphere atmospheric concentrations of ALL the 'Kyoto basket' of gases, except HFC-152a, are increasing.

- InTEM estimates for UK methane show good agreement from 2012 onwards.

- The trend in UK emissions of nitrous oxide is in good agreement with the inventory but the InTEM estimates are consistently higher.

- The UK emissions of all the HFCs are estimated to be lower using InTEM compared to the inventory, the only exceptions being HFC-23 which is higher and HFC-245fa which is the same magnitude.

- InTEM estimates of UK PFC-14 & SF_6 have good agreement with the inventory, PFC-116 & PFC-218 under-estimate and PFC-318 over-estimates.

- The northern hemisphere rate of decline of atmospheric CFC-11 has slowed considerably since 2012 but the InTEM modelled emissions from the UK continue to decline at a constant rate.

1.1 Project Summary

Monitoring the atmospheric concentrations of gases is important in assessing the impact of international policies related to the atmospheric environment. The effects of control measures on greenhouse gases in the so called 'Kyoto basket' of gases: carbon dioxide (CO_2), methane (CH_4), nitrous oxide (N_2O), hydrofluorocarbons (HFC), perfluorocarbons (PFC), nitrogen trifluoride (NF_3) and sulphur hexafluoride (SF_6), should now be observable. Likewise, measures introduced under the Montreal Protocol to protect the stratospheric ozone layer are being observed in the atmosphere. Understanding the effectiveness and impacts of policies on the atmospheric abundance of these key gases is vitally important to policy makers.

This project has two principle aims:

- **Estimate the background atmospheric concentrations of the principle greenhouse and ozone-depleting gases from the DECC network of observations.**

- **Estimate the UK emissions of the principle greenhouse gases using the DECC network of observations and compare these to the compiled inventory.**

Since 1987, high frequency, real time measurements of the principal halocarbons and radiatively active trace gases have been made as part of the Global Atmospheric Gases Experiment (GAGE) and Advanced Global Atmospheric Gases Experiment (AGAGE) at Mace Head, County Galway, Ireland. For much of the time, the Mace Head measurement station (MHD), which is situated on the Atlantic coast, monitors clean westerly air that has travelled across the North Atlantic Ocean. However, when the winds are easterly, MHD receives substantial regional scale pollution in air that has travelled from the populated and industrial regions of Europe. The site is therefore uniquely situated to record trace gas concentrations associated with both the northern hemisphere background levels and with the more polluted air arising from European emissions.

To this aim, the UK has developed a network of observation stations called the UK Deriving Emissions related to Climate Change (DECC) network. Along with MHD, it consists of four tall tower stations: Ridge Hill (RGL) near Hereford; Tacolneston (TAC) near Norwich; Bilsdale (BSD) in North Yorkshire (originally Angus (TTA) near Dundee); and Heathfield (HFD), Sussex. RGL became operational in February 2012 and TAC in July 2012. TTA began operating for the network in April 2012 but was decommissioned and replaced with BSD in September 2015 (BSD began operation in Jan 2014 under the NERC GAUGE programme). HFD began operation in Nov 2013 under the NERC GAUGE programme but became fully part of the network in Sept. 2018. The expanded network makes it possible to resolve emissions on a higher resolution, both spatially and temporally, across the UK.

The UK DECC network measures, to very high precision, all of the principle greenhouse gases in the inventory 'Kyoto basket' of gases as well as many ozone-depleting gases.

The Inversion Technique for Emission Modelling (InTEM) has been developed to use these observations to estimate both Northern Hemisphere concentration trends and UK emissions of each gas. The InTEM emission estimates, as well as those reported through the inventory process, have uncertainties. The comparisons between the inventory and InTEM estimates enable BEIS to be more informed in their inventory improvement programme.

The atmospheric measurements and emission estimates of greenhouse gases provide an important independent cross-check for the national GreenHouse Gas Inventory (GHGI) of emissions submitted annually to the United Nations Framework Convention on Climate Change (UNFCCC). The GHGI are estimated through in-country submissions of Activity Data and Emission Factors that are, in some cases, very uncertain. Independent emissions verification is considered good practice by the Intergovernmental Panel on Climate Change (IPCC).

The UK is one of only three countries worldwide (Switzerland and Australia are the others) that currently routinely verify their reported inventory emissions as part of their annual UNFCCC submission of emissions. The UK is the only country to do so for all of the principle Kyoto gases and has done so for longest.

1.2   Summary of the main findings on inventory verification

- The northern hemisphere atmospheric concentrations of all 'Kyoto basket' gases except HFC-152a are increasing.

- Methane (CH_4): The UK InTEM estimates are lower than the UK inventory (GHGI) estimates (as reported to the UNFCCC in 2017) in the 1990s and 2000s. By 2012 the uncertainties of the two methods overlap and from 2012 onwards there is good agreement. The inclusion of the extended DECC network observations and data from Cabauw in the Netherlands and Weybourne (run by the University of East Anglia) has allowed the InTEM time frame to be reduced from 3-years to under a year. The 8-site, 2-month inversions closely match the inventory estimates with no discernible seasonal pattern.

- Nitrous oxide (N_2O): The UK GHGI and InTEM trend in UK estimates are similar but the InTEM estimates are ~20 Gg yr^{-1} higher. The 5-site, 2-month inversions agree reasonably well with the 3-year MHD-only inversion estimates from 2012 onwards. The InTEM 2-month results show a strong seasonal cycle in UK N_2O emissions with peaks in spring.

- HFC-134a: The UK InTEM is approximately 50% lower than that estimated by the GHGI and the uncertainties of the two methods do not overlap. Both estimates have remained flat since 2009.

- HFC-32: The UK GHGI estimates (used in refrigerant blends) are increasing. UK InTEM estimates are approximately 40% lower than the GHGI but with a similar trend.

- HFC-125: The UK GHGI estimates have started to decrease since 2015. UK InTEM estimates are approximately 40% lower than the GHGI. From 2013 the InTEM emission estimates have been relatively flat.

- HFC-143a and HFC-43-10-mee: UK InTEM estimates are approximately 30% lower than the GHGI in recent years, with good agreement to the decreasing trend.

- HFC-245fa: UK InTEM estimates agree very well with the inventory.

- HFC-365mfc: UK InTEM agrees reasonably well with the GHGI until 2016 onwards where the model estimate decreases as the GHGI continues to increase.

- HFC-227ea: UK InTEM estimates are significantly lower (~60%) than reported in the inventory.

- Sulphur hexafluoride (SF_6): The UK InTEM estimates are in good agreement with the GHGI.

- PFCs: The InTEM estimate for PFC-14 shows good agreement with the inventory; PFC-116 and PFC-218 under-estimate the inventory; PFC-318 over-estimates compared to the inventory.

- CFC-11: InTEM estimates of UK emissions fell rapidly in the early 1990s and has since slowly declined.

1.3   Summary of Progress

Significant progress has been made during the first 12 months of the current contract period. The report includes a chapter on the use of satellite data for estimating UK methane emissions and a chapter specifically on UK HFC-125 emissions. Global emissions and trends of the key greenhouse gases have also been updated.

- **Mace Head** continues to be a baseline station at the forefront of global atmospheric research. This is evident through the high volume of peer-reviewed publications related to work using the MHD observational record. The recent publications related to this contract are detailed in the publication section of this report. In addition, the inclusion of MHD in many EU funded atmospheric research programmes, such as ICOS, InGOS, ACTRIS, and continued support from other global programmes such as AGAGE and NOAA-ESRL indicates its international significance.

- **Radon detectors have been built and are awaiting shipment from ANSTO, Australia.** As part of the NERC Advanced UK Observing Network for Air Quality, Public Health and Greenhouse Gas award (NE/R011532/1) award, three radon detectors are being built by ANSTO, Australia, and will be installed at Tacolneston, Ridge Hill and Heathfield to measure atmospheric radon and help better constrain inversion models.

- **Meteorological equipment will be installed on the tall towers at Tacolneston, Ridge Hill and Heathfield.** As part of the NE/R011532/1 award, wind speed and direction, temperature, humidity, and barometric pressure will be measured at each of these three UK DECC sites. Instrumentation has been selected and is awaiting installation on the tall towers.

- **Optical N_2O and CO analysers installed.** A Picarro G5310 was purchased as part of the NE/R011532/1 award and installed at Bilsdale in March 2019. A Picarro G5310 was installed at Heathfield in October 2018.

- **Mid-latitude Northern Hemisphere baseline trends have been updated.** The trends have been extended up to and including August 2019 observations.

- **UK emission estimates**. Inversion emission estimates for the UK are reported up to and including 2019 and have been compared to the UK GHGI inventory submitted in 2019 (the 2019 GHGI submission covers UK emissions up to and including 2017).

- **UNFCCC verification appendix chapter** for the UK National Inventory Report (NIR) submission was delivered (February 2019).

1.4   Future Plans

- High resolution NAME modelling (~5 km compared to the current ~25 km) of the areas directly surrounding each station may improve the overall modelling of the observations. This will be investigated using the Tacolneston station.

- There is a new ECMWF meteorological re-analysis data (ERA-5) available that covers the period 1987-2002. This is at a higher resolution (~30 km compared to ~80 km) compared to the ERA-Interim that is available. The plan is run NAME for this period using the improved meteorology and compare to the existing results.

- The UK DECC network will be utilised within DARE-UK (Detection and Attribution of Regional greenhouse gas Emissions in the United Kingdom), a 4-year NERC funded research project that will seek to develop systems for estimating greenhouse gas emissions in order to improve the accuracy of the UK inventory. In addition to the existing instrumentation, DARE-UK will incorporate in-situ radon (^{222}Rn) measurements from Ridge Hill, Tacolneston and Heathfield (to be used as a tool for the evaluation of NAME-InTEM model uncertainty) and radiocarbon (^{14}C) flask measurements from Tacolneston and Heathfield (for the estimation of fossil fuel CO_2 emissions). DARE-UK focuses on the three major greenhouse gases responsible for global warming: carbon dioxide (CO_2), methane (CH_4) and nitrous oxide (N_2O).

- The HUGS (A HUb for Greenhouse gas data Science) feasibility study aims to create a cloud-based data analysis 'hub' for greenhouse gas measurements, modelling and data analysis. Following on from the success of the feasibility study, funding is currently being sought for a full project. HUGS aims to streamline the process for data sharing, analysis and visualisation and add value through automated processes such as atmospheric chemistry transport model runs associated with uploaded data. Interaction with the data and associated products will be facilitated via a simple web interface with more functionality available via Jupyter notebooks. This platform builds on the expertise used to create the "Acquire" and "Cluster-in-the-Cloud" architecture developed within the Advanced Computing Research Centre at the University of Bristol.

- In the first quarter of 2020, the Ridge Hill station will officially become an ICOS (Integrated Carbon Observation Network) observatory, feeding CO_2 and CH_4 observations from the on-site Picarro G2301 into the ICOS Carbon Portal. Data from this portal supports climate science that informs scientists and society on natural and human emissions and uptake of these greenhouse gases from ocean, land ecosystems and atmosphere. In order to become a recognised observatory, the Ridge Hill Picarro will be sent to LSCE (Laboratoire des Sciences du Climat et de l'Environnement) in France for quality control measures. It will return with a new set of calibration cylinders provided by ICOS. University of Bristol operatives will also visit LSCE to be trained-up on ICOS quality control/assurance procedures.

- The installation of the Picarro G5310 at Bilsdale means that as of March 2019, there are two instruments on-site measuring CO simultaneously. In contrast, Ridge Hill does not currently have any capability for this gas. A swap is therefore planned, to switch the Bilsdale G2401 (CO_2, CH_4 and CO) with the Ridge Hill G2301 (CO_2 and CH_4), allowing for analysis of CO at Ridge Hill without loss of capability at Bilsdale. Confirmation of this swap will be required before January 2020, when the Picarro to be situated at Ridge Hill is sent to LSCE as part of the ICOS procedure.

- NPL are deploying a new instrument to measure isotope ratios in methane at high frequency from ambient air, with the aim to help distinguish emissions sources at regional scales. This deployment is initially scheduled for an ambient sampling laboratory at NPL, followed by a move to Heathfield in 2020 under the DARE-UK project.

- Two instruments at Heathfield and Bilsdale are capable of measuring N_2O: the GC-ECD and the Picarro G5310. The Picarro was installed in October 2018 as an upgrade, providing higher precision measurements. Analysis of the overlapping data will also provide quantitative insight into the value of high-frequency measurements in capturing short duration pollution events.

- NPL will prepare a set of gravimetric calibration standards containing CO and N_2O to verify instrument linearity across the sites.

1.5   2018 and 2019 Publications

Adcock, K. E., … O'Doherty, S., et al.: **Continued increase of CFC-113a (CCl3CF3) mixing ratios in the global atmosphere: emissions, occurrence and potential sources**, Atmos. Chem. Phys., 18(7), 4737–4751, doi:10.5194/acp-18-4737-2018, 2018.

Arnold, T., Manning, A., … O'Doherty, S., **Inverse modelling of CF4 and NF3 emissions in East Asia,** Atmos. Chem. Phys., 18, 13305-13320, doi:10.5194/acp-18-13305-2018, 2018

Bergamaschi, P., … Manning, A. J., et al.: **Inverse modelling of European CH4 emissions during using different inverse models and reassessed atmospheric observations**, Atmos. Chem. Phys, 18, 901–920, doi:10.5194/acp-18-901-2018, 2018.

Brophy K., H. Graven, A. J. Manning, E. White, T. Arnold, … M. Rigby: **Characterizing Uncertainties in Atmospheric Inversions of Fossil Fuel CO2 Emissions in California**; Atmos. Chem. Phys., 19, 2991-3006, doi:10.5194/acp-19-2991-2019, 2019

Derwent, R. G., Manning, A. J., Simmonds, P. G., Spain, T. G. and O'Doherty, S.: **Long-term trends in ozone in baseline and European regionally-polluted air at Mace Head, Ireland over a 30-year period**; Atmos. Environ., 179, 279–287, doi:10.1016/j.atmosenv.2018.02.024, 2018

Derwent, R., P. Simmonds, S. O'Doherty, A.J. Manning, T. G. Spain: **A 24-year record of high-frequency, in situ, observations of hydrogen at the Atmospheric Research Station at Mace Head, Ireland**; Atmos. Environ., 203, 28-34, doi:10.1016/j.atmosenv.2019.01.050, 2019

Fang, X., S. Park, T. Saito, R. Tunnicliffe, A. L. Ganesan, M. Rigby, … S. O'Doherty, … P. G. Simmonds, … D. Young, M. F. Lunt, A. J. Manning, et al : **A potential new threat to ozone layer recovery from a rapid increase in chloroform emissions from China**; Nature Geoscience, 12(2), 89-93, doi:10.1038/s41561-018-0278-2, 2018

Helfter, C., Mullinger, N., Vieno, M., O'Doherty, S., Ramonet, M., Palmer, P. I., and Nemitz, E.: **Country-scale greenhouse gas budgets using shipborne measurements: a case study for the UK and Ireland**, Atmos. Chem. Phys., 19, 3043–3063, doi:10.5194/acp-19-3043-2019, 2019.

Hernández-Paniagua, I. Y., … O'Doherty, S., et al.: **Diurnal, seasonal, and annual trends in tropospheric CO in Southwest London during 2000–2015: Wind sector analysis and**

comparisons with urban and remote sites, Atmos. Environ., 177, 262–274, doi:10.1016/j.atmosenv.2018.01.027, 2018.

Hossaini, R., Atlas, … O'Doherty, S., Young, D., Maione, M., Arduini, J. and Lunder, C. R.: **Recent Trends in Stratospheric Chlorine From Very Short-Lived Substances**, J. Geophys. Res. Atmos., 124(4), 2318–2335, doi:10.1029/2018JD029400, 2019.

Kuyper, B., Lesch, T., Labuschagne, C., Martin, D., Young, D., Khan, M. A. H., Williams, A. G., O'Doherty, et. al.: **Volatile halocarbon measurements in the marine boundary layer at Cape Point, South Africa**, Atmos. Environ., doi:10.1016/j.atmosenv.2019.116833, 2019.

Kuyper, B., D. Say, … D. Young, M. Anwar Khan, M. Rigby, A. Ganesan, M. Lunt, C. O'Dowd, A. J. **Manning**, S. O'Doherty, et. al. **HCFCs and HFCs in the atmosphere at Cape Point, South Africa**; Environ. Sci. & Tech., 53, 15, 8967-8975, doi:10.1021/acs.est.9b01612, 2019

Li, S., … O'Doherty, S., et al.: **Chemical evidence of inter-hemispheric air mass intrusion into the Northern Hemisphere mid-latitudes**, Sci. Rep., 8(1), doi:10.1038/s41598-018-22266-0, 2018.

Lunt, M., S. Park, S. Li, S. Henne, A. J. Manning, A. Ganesan, … S. O'Doherty, … M. Rigby: **Continued Emissions of the Ozone Depleting Substance Carbon Tetrachloride from Eastern Asia**, Geophysical Res. Lett., 45, 20, doi:10.1029/2018GL079500, 2018

Montzka, S. A., …Rigby, M., Manning, et al.: **An unexpected and persistent increase in global emissions of ozone-depleting CFC-11**, Nature, 557, 413-417, doi:10.1038/s41586-018-0106-2, 2018.

Mühle, J., C. M. Trudinger, M. Rigby, L. M. Western, M. K. Vollmer, S. Park, A. J. Manning, D. Say, A. L. Ganesan, …T. Arnold, S. Li, A. Stohl, … S. O'Doherty, … D. Young, K. M. Stanley, … P. G. Simmonds, et al, **Perfluorocyclobutane (PFC-318, c-C4F8) in the global atmosphere,** Atmos. Chem. Phys., 19, 10335-10359, doi:10.5194/acp-19-10335-2019, 2019

Palmer, P., S. O'Doherty, … A. J. Manning, … M. Rigby, and D. Young; **A measurement-based verification framework for UK greenhouse gas emissions: an overview of the Greenhouse gAs Uk and Global Emissions (GAUGE) project.** Atmos. Chem. Phys., 18, 11753-11777, 2018, doi:10.5194/acp-18-11753-2018

Park, S., Li, S., Mühle, J., O'Doherty, S., Weiss, R. F., et al.: **Toward resolving the budget discrepancy of ozone-depleting carbon tetrachloride (CCl4): an analysis of top-down emissions from China**, Atmos. Chem. Phys., 18(16), 11729–11738, doi:10.5194/acp-18-11729-2018, 2018.

Parrish, D. D., Derwent, R. G., O'Doherty, S., and Simmonds, P. G.: **Flexible approach for quantifying average long-term changes and seasonal cycles of tropospheric trace species**, Atmos. Meas. Tech., 12, 3383–3394, doi:10.5194/amt-12-3383-2019, 2019.

Pison, I., … Ganesan, A., O 'Doherty, S., Spain, T. G., et al.: **How a European network may help with estimating methane emissions on the French national scale**, Atmos. Chem. Phys, 185194, 3779–3798, doi:10.5194/acp-18-3779-2018, 2018.

Pitt, J. , G. Allen, … A. J. Manning, P. Palmer: **Assessing London CO_2, CH_4 and CO emissions using aircraft measurements and dispersion modelling,** Atmos. Chem. Phys., 19, 8931-8945, doi:10.5194/acp-2018-1033, 2019

Prignon, M., Chabrillat, S., Minganti, D., O'Doherty, et. al.: **Improved FTIR retrieval strategy for HCFC-22 (CHClF2), comparisons with in situ and satellite datasets with the support of models, and determination of its long-term trend above Jungfraujoch**, Atmos. Chem. Phys., 19, 12309–12324, doi:10.5194/acp-19-12309-2019, 2019.

Prinn, R. G., … Arnold, T., Ganesan, A. L., Manning, A. J., O'Doherty, S., Rigby, M., Simmonds, P. G., Young, D. et al.: **History of chemically and radiatively important atmospheric gases from**

the Advanced Global Atmospheric Gases Experiment (AGAGE), Earth Syst. Sci. Data, 10, 985–1018, doi:10.3334/CDIAC, 2018.

Riddick, S. N., D. L. Mauzerall, … and A. J. Manning: **Methane emissions from oil and gas platforms in the North Sea**, Atmos. Chem. Phys., 19, 9787-9796, doi:10.5194/acp-19-9787-2019, 2019

Rigby, M.,S. Park, T. Saito, L. M. Western, A. L. Redington, … A. J. Manning, … A. L. Ganesan, … S. O'Doherty, … P. Simmonds, R. L. Tunnicliffe, … D. Young: **Increase in CFC-11 emissions from eastern China based on atmospheric observations**, Nature, 569, 546-550, doi:10.1038/s41586-019-1193-4, 2019

Say D., A. L. Ganesan, M. F. Lunt, M. Rigby, S. O'Doherty, C. M. Harth, A. J. Manning, P. B. Krummel, S. Bauguitte; **Emissions of halocarbons from India inferred through atmospheric measurements**, Atmos. Chem. Phys., 19, 9865-9885, doi:10.5194/acp-19-9865-2019, 2019

Schoenenberger, F., … O'Doherty, S., et al., **Abundance and sources of atmospheric halocarbons in the Eastern Mediterranean**, Atmos. Chem. Phys., 18(6), 4069–4092, doi:10.5194/acp-18-4069-2018, 2018.

Simmonds, P. G., Rigby, … O'Doherty, S., Manning, A. J., Young, D., et al.: **Recent increases in the atmospheric growth rate and emissions of HFC-23 (CHF3) and the link to HCFC-22 (CHClF2) production**, Atmos. Chem. Phys., 18(6), 4153–4169, doi:10.5194/acp-18-4153-2018, 2018.

Stanley, K. M., …, O'Doherty, S., Young, D., Manning, A.J., Spain, T. G., Simmonds, P. G., et al.: **Greenhouse gas measurements from a UK network of tall towers: technical description and first results**, Atmos. Meas. Tech., 11(3), 1437–1458, doi:10.5194/amt-11-1437-2018, 2018.

Stavert A. R., S. O'Doherty, K. Stanley, D. Young, A. J. Manning, M. F. Lunt, C. Rennick, T. Arnold**: UK greenhouse gas measurements at two new tall towers for aiding emissions verification**, Atmos. Meas. Tech., 12, 1103-1121, doi:10.5194/amt-12-1103-2019, 2019

Vollmer, M. K., Young, D., … Rigby, M., O'Doherty, S., Simmonds, P. G., et al.: **Atmospheric histories and emissions of chlorofluorocarbons CFC-13 (CClF3), ΣCFC-114 (C2Cl2F4) and CFC-115 (C2ClF5)**, Atmos. Chem. Phys., 18, 979–1002, doi:10.5194/acp-18-979-2018, 2018.

Wells, K. C., … O'Doherty, S., Young, D., et al.: **Top-down constraints on global N$_2$O emissions at optimal resolution: application of a new dimension reduction technique**, Atmos. Chem. Phys., 18(2), 735–756, doi:10.5194/acp-18-735-2018, 2018.

White, E. D., M. Rigby, M. F. Lunt, … A. J. Manning, A. L. Ganesan, S. O'Doherty, A. R. Stavert, K. M. Stanley, et al; **Quantifying the UK's Carbon Dioxide Flux: An atmospheric inverse modelling approach using a regional measurement network**, Atmos. Chem. Phys., 19, 4345-4365, doi:10.5194/acp-19-4345-2019, 2019

Yu, D., Yao, B., Lin, W., Vollmer, M. K., Ge, B., Zhang, G., Li, Y., Xu, H., O'Doherty, S., Chen, L. and Reimann, S.: **Atmospheric CH3CCl3 observations in China: Historical trends and implications**, Atmos. Res., doi:10.1016/j.atmosres.2019.104658, 2020.

1.6   Meetings

- AGAGE meeting (USA, October 2018)
- NISC meeting (London, November 2018)
- COP 24 (Poland, December 2018)
- CFC-11 SPARC meeting (Vienna, March 2019)
- AGAGE meeting (Switzerland, May 2019)
- NCGG8 conference (Amsterdam, June 2019)
- DECC network meeting (Exeter, July 2019)

1.7 Related information

www.gov.uk/government/publications/uk-greenhouse-gas-emissions-monitoring-and-verification

Methodology Report (Dec 2018)

Technical Document (May 2016)

1.8 Acknowledgements

We would like to thank the following groups for providing observational data for this report:

- ALICE High Performance Computing Facility at the University of Leicester for production of the GOSAT XCH_4 data

- Empa, Switzerland, for Jungfraujoch (JFJ) data

- TNO, The Netherlands, for Cabauw (CBW) data

- University of East Anglia (UEA), UK, for Weybourne Atmospheric Observatory (WAO) data

- University of Urbino, Italy, for Monte Cimone (CMN) data

2 Instrumentation

2.1 Sites

A brief summary of site operations is presented below.

2.1.1 Mace Head (MHD)

- General: A new water-chiller air-conditioning system has been approved by National University of Ireland Galway (NUIG), but as yet no date has been confirmed for installation. This will replace the existing air-conditioning unit, whose leakage of R-410A (50% by weight HFC-125, 50% by weight HFC-32) has compromised large periods of Medusa GCMS data for these compounds. Both storm Gareth (13th March 2019) and storm Hannah (24th April 2019) passed without issue. On the 30th of March, a 40 ft sperm whale washed up on the shore close to the observatory, resulting in a significant increase in traffic near the site.

- Medusa GCMS: The Medusa performed well throughout the last 12 months. On the 5th of November 2018, a new quaternary standard (H-342) was installed. 7 days of data were lost from the 9th to the 15th of December, due to a failing EI (Electron Ionisation) filament. After this failure, CI (Chemical Ionisation) filaments were installed. A new PoraBOND Q column was installed on the 8th of January 2019. The Cryotiger was conditioned on the 23rd of January 2019, in order to address an increasing baseplate temperature (which was first noted on the 21st). On the 1st of February 2019, H-343 replaced the existing quaternary standard. On the 2nd of May 2019, the existing quaternary and tertiary standards were replaced with H-359 and J-223 respectively. On the 5th of July 2019, a new quaternary (H-364) was installed. On the 16th of August 2019 a valve fault was detected. A replacement valve and rotor were ordered on the 21st of August 2019. The replacement rotor was installed on the 27th August but failed to fully fix the problem. Further testing revealed that the GasPro column had developed a leak and a replacement was installed on 20th September and sampling restarted.

- GC-MD: The Mace Head GC-MD performed well over the last 12 months. Christoph Zwellweger (EMPA) performed a GAW audit of the instrument, analysing a series of tanks between 15th and 26th of November 2018. The EKOM compressor showed signs of failure on the 15th of February and was immediately replaced by a new GAST compressor. The failing unit was returned to the University of Bristol for servicing/repair. A gradual loss of precision in channel2 data (particularly CFC-11) after of a loss of power for two days starting on 26th of January 2019. To resolve this problem a number of operations were performed, starting on 2nd of April 2019 – balanced backflush flows, checked for leaks, baked out clean-up traps, baked out column, valve 6 rotor was cleaned. It was also noted that there was slight movement in valve 6 when actuated. The valve was realigned and tightened (no movement now) on the 10th of April 2019. The precision of CFC-11 and CFC-113 improved immediately. On the 26th of April 2019, a new working standard (J-223) replaced the previous standard, J-218. On the 24th of June 2019, a suite of NOAA calibration cylinders was analysed. These cylinders were analysed again on the 16th of July 2019. The EKOM compressor was also re-installed on the 24th June. On the 29th of July, the EKOM compressor was briefly removed following a power cut. It was reinstalled shortly after when it was discovered that the internal breaker had tripped.

2.1.2 Tacolneston (TAC)

- General: A power cut on the 4th of December 2018 led to the failure of the laboratory air-conditioning, TOC generator and compressor and subsequent shutdown of all

instruments on site. The problem was exacerbated by the presence of riggers on site, which prevented access to the laboratory on safety grounds. The issue was resolved on the 11th of December 2018 when access was granted. On the 29th of January, the 40-micron filters on the 54 m and 185 m lines were replaced. The 54 m line pump failed on the 20th of August. The Picarro G2301 and LGR instruments sampled from the other two heights exclusively, until a replacement pump was installed two days later.

- Medusa GCMS: The Tacolneston Medusa GCMS underwent a comprehensive upgrade during the reporting period, with the installation of a new Agilent 7890 Gas Chromatograph (GC) and 5977B Mass Spectrometric Detector (MSD) in October 2018. These upgrades have led to a significant improvement in the precision of many Kyoto basket species. Significant data loss was observed over the course of this upgrade, and afterwards during related instrumental problems. On the 24th October 2018, 8 days of data were lost due to a slowly deteriorating MS filament. Starting on the 31st of October 2018, 23 days of data were lost due to a dirty HED (High Energy Dynode). On the 15th of January, the existing quaternary standard (H-346) was replaced with H-347. A new tertiary cylinder, J-217, was installed on site on the 5th of February 2019. On the 9th of February 2019, 11 days of data were lost due to a failing filament, with a further 9 days of data loss starting on 6th of May 2019 due to the same issue. Following this data loss, the previously preferred CI filaments were replaced with EI filaments, in order to maximise filament lifespan. On the 21st of May 2019, H-347 was replaced with a new quaternary standard, H-361. This cylinder was itself replaced on the 25th of June 2019 by H-367. H-367 was spiked with a range of low abundance compounds during filling at Mace Head, including several hydrofluorolefins (HFOs), to allow for more accurate calibration of these species.

- Picarro G2301: The G2301 operated well over the course of the last 12 months. A new target cylinder, UoB-14, was installed on the 31st of October 2013. On the 10th of November 2018, the G2301 was configured to sample the calibration cylinders (UoB-07, UoB-08, UoB-11 and H-288) already sampled by the LGR, replacing the existing calibration suite. 8 days of data were lost as a result of the power cut on the 4th of December 2018. Loss of communication between the instrument and GCWerks led to a further 15 days of data loss, beginning on the 13th of December 2018. A further 4 days of data were lost, starting on the 26th of January 2019, due to a redundant line in the instrument runfile.

- LGR: The LGR performed well throughout the last 12 months, with the only significant loss of data corresponding with the laboratory power cut on the 4th of December 2018. The LGR began analysis of a new target cylinder, UoB-14 (which is shared between this instrument and the G2301) on the 8th of November 2018. On the 29th of January 2019, the 7-micron filter on the LGR's 185 m sample line was changed, and on the 16th of April 2019 the LGR cooling fans were cleaned. GCWerks lost communication with the LGR on the 30th of May 2019. The issue was resolved by restarting the GCWerks software.

2.1.3 Ridge Hill (RGL)

- General: On the 6th of February 2019, the Ridge Hill laboratory was serviced. All compressor/TOC filters, line filters, line pumps and water traps were replaced. A new pressure sensor was installed on the 9th of April 2019, allowing for remote monitoring of carrier gas pressure. In addition, the carrier gas configuration was modified to have two cylinders inline at any one time, reducing the frequency of carrier gas changeovers. Post-installation, there have been issues with the pressure sensor failing to return a reading despite sufficient carrier gas. Investigations into the cause of this are ongoing. The 45 m line pump failed on the 21st of June 2019 and was replaced on

the 5th of July 2019. In the interim, the Picarro G2301 sampled exclusively from the 90 m line.

- GC-ECD: The Ridge Hill GC-ECD performed well over the last 12 months. On the 2nd of October 2018, H-231 was replaced by a new cylinder (H-299) that became the new working standard. At the same time, the on-site TOC (Total Organic Carbon) gas generator was replaced with an identical unit from the University of Bristol, to allow the older unit to be serviced. 5 days of data were lost, starting on the 9th April 2019, as a result of highly variable sample module temperature. On the 7th of July, the sample module temperature again became highly variable, suggesting that the heater unit was failing. The heater was therefore switched off, allowing the sample module temperature at Ridge Hill to vary in line with laboratory temperature. Since the Ridge Hill laboratory is only very weakly temperature controlled, there is a high degree of variability that occasionally results in spurious N_2O data. These data are routinely flagged, and investigations into methods for better temperature control/replacement options for the existing sample module heater are ongoing.

- Picarro G2301: The G2301 performed well over the last 12 months, with very few reported issues. 4 days of data loss, starting on the 28th October 2018, due to an issue with the GCWerks software. On the 11th of February 2019, a notable increase in instrument cycle time (the time taken for each laser pulse to decay within the instrument cavity) was observed. A hard reboot of the instrument resolved the issue. On the 1st of May 2019, H-311 was replaced by UoB-29, which became the new working standard. A target cylinder (UoB-61) was installed on the same date.

2.1.4 Bilsdale (BSD)

- General: The layout of the laboratory was reconfigured in March 2019 to accommodate the new Picarro G5310 instrument. As part of these works, a new cylinder rack was installed to house the standard, target, and calibration suite cylinders. Four new calibration suite cylinders (UoB-32, UoB-34, UoB-35 and UoB-36) and one new target cylinder (UoB-33) were installed as part of the G5310 installation.

- GC-ECD: The Bilsdale GC-ECD performed well throughout the last 12 months. 10 days of data were lost, starting on the 16th of October 2018, due to instability of the sample module temperature. On the 8th of November this instability was observed again, with the sample module heater unable to maintain a consistent temperature. The heater was therefore switched off, and the temperature of the sample module allowed to vary in line with the temperature of the laboratory. The quality of the data was not seen to be affected in the months following this change. On the 4th of March 2019, the compressor (used to provide air for the Nafion counter-purge) was found to have failed. The compressor was removed and returned to Bristol for maintenance. During this period, the instrument operated without a Nafion counter-purge, and hence samples were not dried. Again, this did not affect the quality of the data. On the 3rd of May, the compressor was reinstalled. On the 3rd of May, a routine carrier gas changeover resulted in an appreciable reduction of instrument precision, most notably for SF_6. Careful investigation did not result in a cause, however the change to a new standard (H-366) on the 16th of July rectified the issue, suggesting a possible issue with the old standard regulator.

- Picarro G2401: The G2401 performed well throughout the last 12 months. 4 days of data was lost starting on the 4th of March 2019, due to a reconfiguration of the lab required to accommodate the new Picarro G5310.

- Picarro G5310: This new instrument (measuring N_2O and CO) was installed in March 2019, following extensive testing at the University of Bristol. The first atmospheric measurements were acquired on the 6th of March 2019. The G5310 has, in general,

performed well during the period since its installation, with a clear improvement in N_2O measurement precision compared to the GC-ECD. There is an ongoing issue whereby very high CO concentrations result in a slow-down in data acquisition (which affects both gases). This issue was raised with Picarro, who said that it was both expected and unavoidable. Further investigation is planned to quantify the total amount of data lost due to this phenomenon.

2.1.5 Heathfield (HFD)

- General: The 50 m line-pump failed at the beginning of May, requiring a replacement. The Picarro G2401 sequence was changed to sample from only the 100 m inlet until the pump was replaced on the 23rd May. The 40 µm filter for the 50 m inlet was also replaced in December 2018 and July 2019. There have been two mains failures at the site, on 22nd June 2019 and 30th July 2019. The instruments were protected by the UPS during these events and no data were lost, although the compressor supplying drying air to the GC-MD did not automatically restart. The instruments were shut down remotely for 5 days from the 24th July as a precaution against overheating. The laboratory temperature reached 40 °C and the instruments were restarted when this had decreased to 35 °C.

- GC-ECD: There was one period of data loss between March 2019 and May 2019 due to low carrier gas pressure. There was a second shutdown in July to protect the instruments from overheating, as described above. The compressor supplying the TOC generator, used to dry the sample, was found off during a site visit. It is likely that the power failure on 30th July tripped the circuit breaker. The samples were therefore not dried but the data are unaffected. The compressor has been left disconnected until it is serviced.

- Picarro G2401: The Picarro has run well with a period of data loss due to the planned shutdown for high lab temperatures, described above. 5 days of data were also lost in June 2019 as the instrument restarted without any apparent cause. The instrument communication is now monitored, which will generate an email alert for future communication issues. A new gas standard was installed in October 2018: serial number H-358, filled in Mace Head and calibrated at EMPA. This standard was used to calibrate the outgoing gas, UEA-001.

- Picarro G5310: This instrument was installed in October 2018 to measure N_2O with better precision than the GC-ECD. Air is sampled from the 50 m and 100 m inlets for 20 minutes and 40 minutes out of each hour respectively. The calibration standard is H-358, also used for the G2401 instrument. The G5310 has run well over the year, with three periods of data loss due to an unexplained instrument reset, which is under investigation.

2.2 Linearity

A suite of five calibration synthetic air mixtures have been prepared gravimetrically by NPL containing CH_4, CO_2, CO and N_2O over a range of concentrations that spans the atmospheric baseline and pollution events. These have been used to independently verify the calibration strategy currently employed for the Picarro G2401 at Heathfield, which uses standards based on natural air that are referenced to the WMO scales for these species.

The proportionality of the instrument response to the sample concentration should be linear over the range expected in the atmosphere. This proportionality may change with time and is determined using a suite of three standards (so-called span tanks) and comparing the instrument response with the known amount fraction. This relationship is used to generate a correction (here termed a nonlinearity correction) that is applied to the

measurement of air samples, with the aim of improving the instrument reliability over time and compatibility between measurement sites.

The span calibration standards are a set of three tanks filled at Mace Head, with a known CO_2 value measured by the EMPA Central Calibration Laboratory (CCL) on the WMO-CO_2-X2007 scale. The CO_2 concentration of the reference standards is also reported on the same scale. The mixtures in these tanks have been measured over two periods of time, when two different reference standards were in use: H-285 from September 2017, replaced by H-358 in September 2018. During these times the two sets of tanks were measured monthly. Figure 1 plots the measured value for these gases, and the atmospheric concentration, for carbon dioxide.
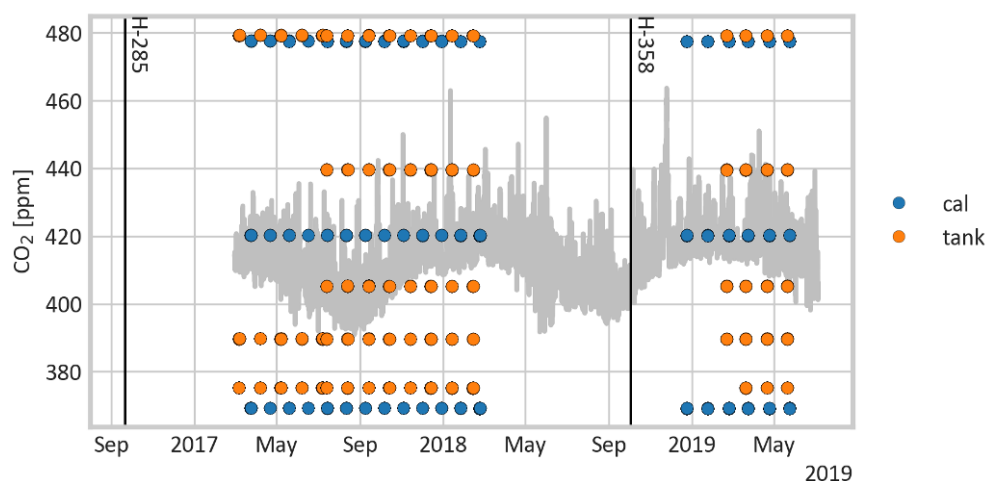
Figure 1 Time series of WMO-scale calibration standards (cal) and validation tanks prepared gravimetrically by NPL (tank). The vertical lines denote change in reference standard. The atmospheric concentration of carbon dioxide is shown in light grey for reference.

Instrumental drift is corrected by comparing each air measurement (or tank measurement) to the reference standard. The set of three span calibration (labelled cal in Figure 1) standards are then used to fit the true concentration relative to the drift-corrected instrument response. This results in a correction function that is applied to the air data to retrieve an estimate of the true amount fraction of CO_2 in the atmospheric sample. The magnitude of this nonlinearity correction is represented in Figure 2 as the difference between the raw measurement and corrected value for the two reference standards. The shaded areas represent the 95% confidence interval of the correction, determined from the fit to the calibration data. This plot shows that the correction varies with CO_2 concentration, with near-background levels around 410 ppm corrected by -0.02 ppm and pollution events at 450 ppm corrected by -0.07 ppm. These corrections are small and within the instrumental uncertainty.

15
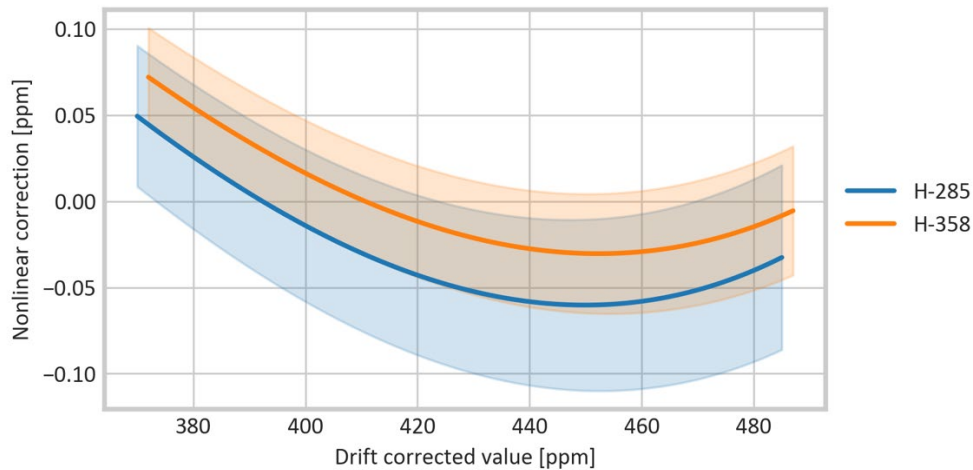
Figure 2 Magnitude of the correction applied to a measurement, expressed as the difference between the corrected and uncorrected values.

2.3 Verifying the Instrument Correction

The set of gravimetric standards provide an independent validation of this calibration procedure. The calibrated value for measured amount fraction of CO_2 in each gravimetric mixture is plotted in Figure 3 as the difference between the calibrated and gravimetric amount fractions, the error bar indicates the 95% confidence interval from the nonlinearity calibration fit and does not include the systematic error from the assignment of the span and calibration standard gases, which will be correlated between all measurements and result in a bias. Each isolated black bar in Figure 3 is the lower bound for the uncertainty in the amount fraction of CO_2 from the gravimetric preparation (95% confidence).
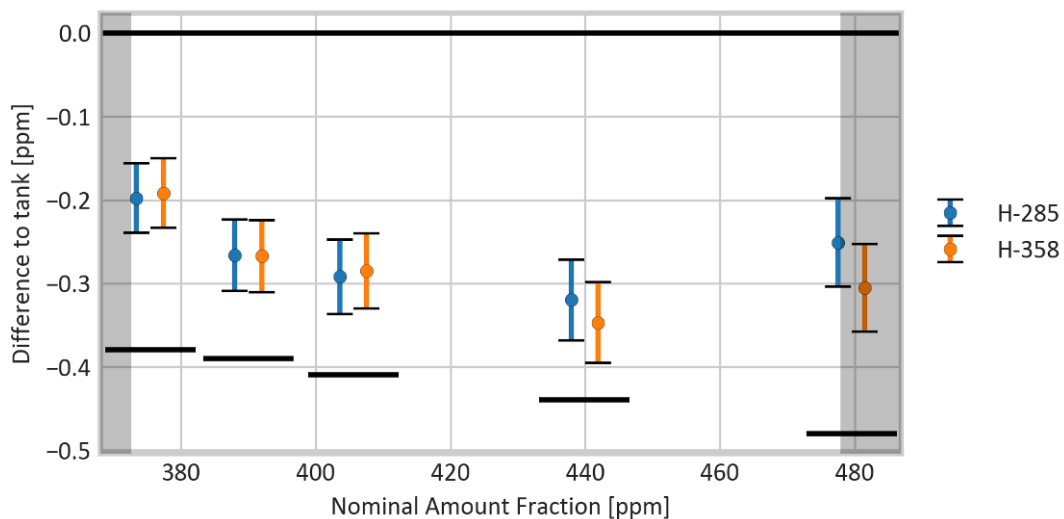
Figure 3 Calibrated, nonlinearity corrected, values for the set of gravimetric mixtures under two different standards, expressed as the difference between the measurement and assigned value. The grey shaded regions indicate the limits of the nonlinearity correction using the span standards. The points for H-358 have been offset horizontally for clarity.

The calibrated measurement of the amount fraction of CO_2 in the gas mixtures prepared by NPL is within the uncertainty of the gravimetric value and is stable over time and for different reference standards. There remains an apparent bias in the measured amount fraction of CO_2 relative to the assigned gravimetric value. This difference may be a result of the instrument calibration being performed using standards measured on the WMO-CO_2-X2007 scale, whereas the gravimetric tanks are traceable to the international mass

standard. A bias of this magnitude has been seen previously in comparison of gravimetric standards with the NOAA scale[1].

2.4 Stability of Correction

Monthly measurements of the gravimetric tanks are shown in Figure 4 as the difference between the corrected measurement and the assigned value. This shows that the measured value drifts by less than 0.05 ppm over the 10 months of measurement under reference standard H-285.
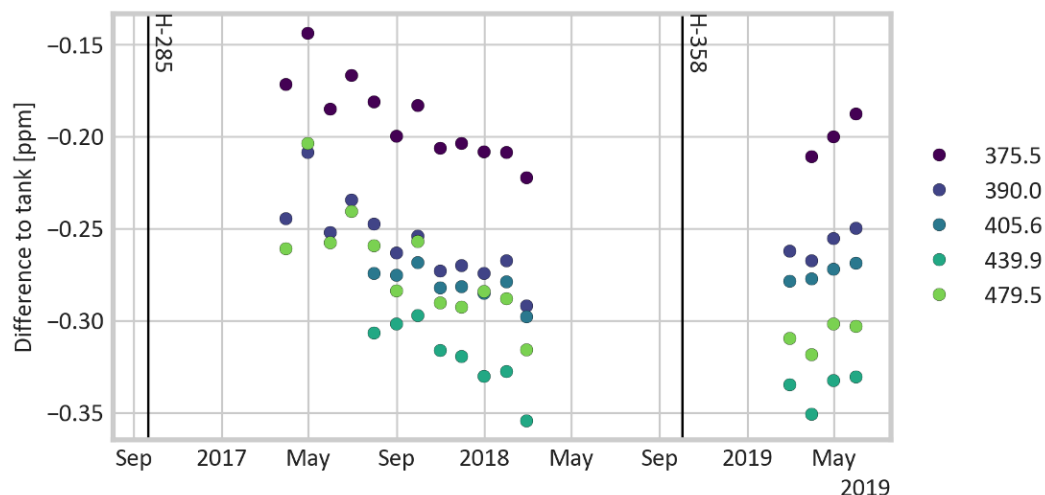
Figure 4 Amount fraction of CO_2 in each gravimetric standard plotted as the difference between the corrected measurement and the assigned value. The vertical lines denote changes to the reference standard, a different nonlinearity correction is calculated for each standard.

2.5 Summary

The drift and nonlinearity correction applied to the raw data from the Picarro G2401 has been validated by measurement of independently-prepared gas mixtures for CO_2 (shown above) and CH_4 and CO (not shown). The instrument response to CO_2 and CH_4 is stable with time and after changes of reference standards, providing calibrated measurements over a range of amount fraction seen in the atmospheric baseline and pollution events. Analysis of the CO data shows that calibration requires a larger correction and carries a much larger uncertainty. This is a known problem as the amount fraction of CO in an air mixture stored in a tank drifts with time due to chemical reactions with the tank material. Further work will aim to determine if this drift can be accounted for in the CO calibration procedure and reduce the uncertainty in atmospheric measurements. This analysis indicates that the whole-air calibration standards could be substituted by gravimetric standards for these species.

NPL participated in a key comparison exercise with other NMI (CCQM-K120.a, carbon dioxide in air at background level) which notes that the gravimetric standards submitted for the comparison were prepared using CO_2 from a range of sources with δ-13C values that varied between -67‰ and 0‰, and δ-18O values that varied between -35‰ and 0‰. This range of isotopic composition could result in a measurement bias of up to 0.3 ppm when these standards are used in optical instruments without accounting for the isotopic composition. Adsorption of CO_2 onto the walls of the high-pressure cylinder has also been found to cause deviation from the gravimetric amount fraction by up to 0.1 ppm.

3 Annual Northern Hemispheric trends

3.1 Baseline Mole Fractions

For each gas observed at Mace Head a baseline analysis has been performed. ECMWF meteorology is used from 1989 – 2002 inclusive and Met Office meteorology from 2003 – 2019 inclusive. For each gas, monthly and annual northern hemisphere (NH) baselines, annual growth rates and the average seasonal cycle seen within the observations are calculated. Table 1 – Table 4 summarises the annual baseline mole fractions for each of the gases observed.

Gas	CH4	N2O	CO2	HFC-125	HFC-134a	HFC-143a	HFC-152a	HFC-23	HFC-32
Unit	ppb	ppb	ppm	ppt	ppt	ppt	ppt	ppt	ppt
1990	1788	309							
1991	1807	310							
1992	1799	310							
1993	1809	311	357						
1994	1813	312	359						
1995	1814	312	360		2		1.2		
1996	1820	313	363		4		1.3		
1997	1818	314	364		6		1.4		
1998	1831	315	367	1.2	10		1.9		
1999	1835	315	369	1.4	13		2.2		
2000	1838	317	369	1.8	17		2.5		
2001	1838	317	371	2.3	21		2.9		
2002	1839	318	373	2.6	25		3.4		
2003	1849	319	375	3.3	30		4.1		
2004	1846	319	378	3.9	35	5.5	4.8		1.1
2005	1844	320	379	4.6	39	6.4	5.6		1.6
2006	1843	321	382	5.4	44	7.4	6.7		2.1
2007	1853	322	384	6.3	48	8.4	7.9		2.7
2008	1862	323	386	7.5	53	9.6	8.9	22.5	3.4
2009	1865	323	387	8.6	58	10.7	8.9	23	4.1
2010	1867	324	390	10	63	11.9	9.4	23.7	5.2
2011	1872	325	392	11.7	68	13.2	9.9	24.7	6.5
2012	1880	326	394	13.5	73	14.5	10	25.6	7.7
2013	1885	327	397	15.5	79	16	10.1	26.6	9.2
2014	1895	328	398	17.8	84	17.4	10	27.8	10.9
2015	1906	329	401	20.1	89	18.8	9.8	28.8	12.7
2016	1917	330	404	22.7	96	20.5	10	29.6	15
2017	1923	331	407	25.8	103	22.2	10	30.7	18.2
2018	1929	332	409	28.9	108	23.8	10.1	31.9	21.4
2019	1937	333							
AvGrow	5.19	0.8	2.07	1.44	4.66	1.32	0.4	0.96	1.51
AvGr12	6.62	1.05	2.46	3.19	5.9	1.56	0.24	1.27	3.39

Table 1: Annual Northern Hemisphere (NH) baseline mass mixing ratios for Kyoto gases measured at Mace Head (ppt unless stated) and growth rates (ppt yr-1 unless stated). AvGrow = Average growth since records began and AvGr12 = Average growth over most recent year (2017).

Gas	HFC-227ea	HFC-245fa	HFC-4310mee	HFC-365mfc	PFC-14	PFC-116	PFC-218	PFC-318	SF6	NF3
Unit	ppt	ppt	ppt	ppt	ppt	ppt	ppt	ppt	ppt	ppt
2004				0.2	74.9	3.6	0.4		5.6	
2005				0.3	75.5	3.7	0.5		5.8	
2006				0.4	76.2	3.8	0.5		6.1	
2007	0.5	1.1		0.5	76.9	3.9	0.5		6.3	
2008	0.5	1.3		0.6	77.6	4	0.5		6.6	
2009	0.6	1.4		0.6	78.1	4.1	0.5		6.9	
2010	0.7	1.5		0.7	78.7	4.1	0.6		7.2	
2011	0.8	1.8	0.2	0.8	79.5	4.2	0.6	1.3	7.5	
2012	0.9	2	0.2	0.9	80.3	4.3	0.6	1.4	7.8	
2013	1	2.2	0.2	0.9	81.1	4.4	0.6	1.4	8.1	
2014	1.1	2.4	0.3	1	81.8	4.5	0.6	1.5	8.4	1.3
2015	1.2	2.6	0.3	1.1	82.6	4.6	0.6	1.5	8.8	1.4
2016	1.3	2.8	0.3	1.2	83.5	4.6	0.6	1.6	9.1	1.6
2017	1.5	3.1	0.3	1.2	84.3	4.7	0.7	1.7	9.4	1.8
2018	1.6	3.2	0.3	1.3	85.3	4.8	0.7	1.7	9.8	2
AvGrow	0.1	0.2	0.01	0.08	0.75	0.08	0.02	0.06	0.3	0.18
AvGr12	0.13	0.21	0	0.05	0.91	0.09	0.02	0.07	0.34	0.23

Table 2: Annual NH baseline mass mixing ratios for Kyoto gases measured at Mace Head (ppt) and growth rates (ppt yr-1). AvGrow = Average growth since records began and AvGr12 = Average growth over most recent year (2017).

Gas	CFC-11	CFC-12	CFC-113	HCFC-124	HCFC-141b	HCFC-142b	HCFC-22	HFC-236fa	SO2F2	CH3Cl	CH2Cl2
Unit	ppt	ppt	ppt	ppt	ppt	ppt	ppt	ppt	ppt	ppt	ppt
1990	264	496	75.5								
1991	267	506	80.8								
1992	268	516	84.2								
1993	269	522	85								
1994	268	528	84.3								
1995	267	533	84.4		5.3	8.1					36.6
1996	266	538	84.3		7.4	9.3					37.3
1997	265	541	83.7		9.8	10.7					37.6
1998	263	542	83.1	1.1	11.4	11.5				549	33.3
1999	261	544	82.6	1.3	13.3	12.5	145			542	32.2
2000	260	546	82.2	1.4	15.1	13.7	151			525	30.5
2001	259	546	81.4	1.6	16.3	14.6	158			523	30.1
2002	257	546	80.6	1.6	17.6	15.1	164			519	29.5
2003	255	546	80	1.6	18.6	15.6	169			531	31.4
2004	253	545	79.3	1.6	19.2	16.3	174			524	30.5
2005	251	544	78.7	1.6	19.1	17	180		1.5	529	30.2
2006	248	543	77.9	1.6	19.5	18.1	187		1.5	520	31.9
2007	246	541	77.1	1.7	20.2	19.3	195	0.1	1.6	531	34.1
2008	244	538	76.7	1.6	20.9	20.6	204	0.1	1.6	535	35.9
2009	242	535	76	1.6	21.3	21.4	211	0.1	1.7	532	36.1
2010	240	533	75.2	1.5	22	21.9	219	0.1	1.7	530	39.6
2011	238	530	74.5	1.4	23.1	22.7	226	0.1	1.8	519	
2012	236	527	74	1.4	24.1	23	230	0.1	1.9	525	
2013	235	524	73.4	1.3	24.9	23.3	236	0.1	2	537	
2014	234	522	72.8	1.3	25.3	23.4	241	0.1	2.1	533	
2015	232	519	72	1.2	25.7	23.3	245	0.1	2.2	539	
2016	231	515	71.5	1.2	26	23.4	249	0.2	2.3	541	
2017	230	512	71	1.1	25.9	23.4	252	0.2	2.5	529	57.3
2018	229	509	70.3	1	25.6	23.3	254	0.2	2.5	529	54.5
AvGrow	-1.17	0.6	-0.11	-0.01	0.86	0.65	5.76	0.01	0.08	-1.27	0.26
AvGr12	-1.34	-3.0	-0.61	-0.08	-0.28	-0.13	2.3	0.02	0.07	-0.75	-1.19

Table 3: Annual NH baseline mass mixing ratios for gases measured at Mace Head (ppt) and growth rates (ppt yr-1). AvGrow = Average growth since records began and AvGr12 = Average growth over most recent year (2017).

Gas	CHCl3	CCl4	CH3CCl3	C2Cl4	CH3Br	Halon-1211	Halon-1301	Halon-2402	CO	H2	O3
Unit	ppt	ppt	ppt	ppt	ppt	ppt	ppt	ppt	ppb		
1990		108	150								34
1991		105	151								34.
1992		105	149								34
1993		104	139								34
1994	12.2	104	125							50	35.
1995	12.9	102	111							50	34.
1996	12.7	101	95							51	37
1997	12.3	100	79						119	50	36.
1998	12.7	99	66			4	2.7		148	52	39.
1999	11.9	98	55		11	4.2	2.8		124	52	40.
2000	11.5	97	46		10.5	4.3	2.9		119	51	39.
2001	11.8	96	39	5.4	9.9	4.4	3		116	50	38.
2002	11.4	95	32	4.8	9.1	4.4	3		121	51	39.
2003	11.6	94	27	4.8	8.9	4.4	3.1		136	51	40.
2004	11.5	93	23	4.4	9.4	4.5	3.1	0.5	123	50	39.
2005	11.5	93	19	3.8	10.2	4.5	3.2	0.5	124	51	39
2006	11.5	91	16	3.8	9.4	4.5	3.2	0.5	122	51	40.
2007	11.5	90	13	3.6	9.1	4.4	3.2	0.5	121	51	39
2008	11.6	89	11	3.5	9.1	4.4	3.3	0.5	120	51	41
2009	11	88	9	3	8.6	4.3	3.3	0.5	115	51	40.
2010	11.7	87	8	3.1	8.3	4.2	3.3	0.5	122	51	39.
2011	11.6	86	7	2.7	8.3	4.2	3.3	0.5	116	51	40
2012	11.6	85	5	2.5	8.2	4.1	3.3	0.4	123	51	40.
2013	12.8	84	4	2.5	8.3	4	3.4	0.4	119	52	41.
2014	13.8	83	4	2.4	7.7	3.9	3.4	0.4	119	51	40
2015	14.6	82	3	2.4	7.5	3.8	3.4	0.4	120	51	40.
2016	15.2	80	3	2.3	7.4	3.6	3.4	0.4	116	51	39.
2017	15.9	80	2	2.4	7.3	3.5	3.4	0.4	113	51	40.
2018	15.5	79	2	2.2	7.2	3.4	3.4	0.4	113	52	
AvGrow	0.11	-1.05	-5.11	-0.17	-0.2	-0.04	0.03	-0.01	-0.38	0.6	0.2
AvGr12	-0.93	-0.68	-0.36	-0.09	-0.18	-0.1	0	-0.01	-0.25	2.8	0.4

Table 4: Annual NH baseline mass mixing ratios for gases measured at Mace Head (ppt) and growth rates (ppt yr-1). AvGrow = Average growth since records began and AvGr12 = Average growth over most recent year (2017).

4 Regional emission estimation

4.1 Introduction

This chapter presents the InTEM inversion results, showing the atmospheric trends and regional emissions of the gases that are measured in the UK DECC network and that are reported to the UNFCCC (United Nations Framework Convention on Climate Change). For each gas, the mid-latitude Northern Hemisphere baselines are presented along with the background mole fractions measured at some additional AGAGE (Advanced Global Atmospheric Gases Experiment) stations that span both hemispheres. UK estimated emissions follow where a comparison is made between the InTEM results and the reported UNFCCC inventory values (April 2019 submission). Finally, for each gas the InTEM estimates for North West Europe (NWEU = IRL + UK + FRA + BEL + NLD + LUX + DEU) are compared to UNFCCC estimates (April 2019 submission). For methane and nitrous oxide, where observations from southern and central Europe have not been used, the comparison is made to NWEU$_{north}$ which excludes the south of France and the east of Germany as these areas are not well represented by the observations used.

InTEM is briefly presented but for more information the reader is referred to the Methodology report. The uses, atmospheric lifetimes, and global warming potentials for the different gases reported under the UNFCCC are presented in Table 5.

4.2 Summary of InTEM inverse modelling

Each observation is comprised of two parts; a time-varying Northern Hemisphere baseline concentration and a perturbation above baseline. The perturbations above baseline, observed across the UK DECC network, are driven by emissions on regional scales that have yet to be fully mixed on the hemisphere scale and are the principle information used to estimate surface emissions across north-west Europe. A method for estimating emissions from observations, referred to as 'Inversion Technique for Emission Modelling' (InTEM), has been developed over many years and is used here to estimate UK emissions using the observations from the UK DECC network, and other networks where available.

InTEM links the observation time-series with the 2-hour NAME air history estimates of how surface emissions dilute as they travel to the observation stations. An estimated emission distribution, when combined with the NAME output, can be transformed into a modelled time-series at each of the measurement stations. The modelled and the observed time-series can be compared using a single or a range of statistics (referred to as cost functions) to produce a skill score for that particular emission distribution. InTEM uses a Bayesian statistical technique with a non-negative least squares solver to find the emission distributions that produces the modelled times-series at each observation station that has the best statistical match to the observations. The Bayesian method requires the use of a prior emission distribution with associated uncertainties as the starting point for the inversion. The prior information can influence and inform the inversion (posterior) solution. In this work the prior emission information has been chosen to be either land-based but population weighted (HFCs, SF_6) or spread uniformly across the land (CH_4, N_2O, PFCs, NF_3). However, to preserve the independence of the inversion results presented here from the prior estimates, the priors were given very large uncertainties thus ensuring the inversion was negligibly constrained by the prior.

For InTEM to provide robust solutions for every area within the modelled domain, each region needs to significantly contribute to the air concentrations at the UK DECC network sites on a reasonable number of time periods. If the signal from an area is only rarely or poorly seen by the network, then its impact on the cost function is minimal and the inversion method will have little skill at determining its true emission. The contributions that different grid boxes make to the observed air concentration varies from grid to grid.

Grid boxes that are distant from the observation site contribute little to the observation, whereas those that are close have a large impact. To balance the contributions from different grid boxes, those that are more distant are grouped together into increasingly larger regions. The grouping cannot extend beyond country, region or Devolved Administration (DA) boundaries. The country boundaries can extend into the surrounding seas to reflect both emissions from shipping, off-shore installations and river runoff but also because the inversion has geographical uncertainty.

For each greenhouse gas three types of inversion are performed. The first, using only Mace Head data, were performed with an inversion timeframe of 3 years. For CH_4 and N_2O, the inversions were started in 1989 to coincide with the availability of ECMWF ERA-Interim meteorology, for the other gases the inversions were started from when the observations were first available. For each gas 3-year inversions were performed covering entire calendar years. Each 3-year inversion was repeated 24 times, each time with the observations from 8, randomly chosen, blocks of 5-days per year removed from the dataset (approximately 10% of each year). Annual emission estimates were made by averaging the inversion results covering the appropriate year. The second inversion covered 2-year periods and included data from Jungfraujoch (JFJ, Switzerland) and Monte Cimone (CMN, Italy). The third type of inversion follows the same process but includes additionally the observations from the UK DECC network and were performed over smaller inversion time-windows. For CH_4, N_2O and SF_6, where observations are available from 5 to 8 sites, the inversion time-window was set to 2-months, for the remaining compounds, where only TAC, MHD, JFJ and CMN data are available, the inversion time-window was 1-year. The repeating of each inversion multiple times and the random removal of ~10% of the observations from each inversion improves the estimates of uncertainty.

There are a range of uncertainties in the emissions that are estimated. Uncertainty arises from many factors: errors in the baseline estimate; emissions that vary over time-scales shorter than the inversion time-window e.g. diurnal, seasonal or intermittent; heterogeneous emissions i.e. emissions that vary within the regions solved for; errors in the transport model (NAME) or the underpinning 3-dimensional meteorology; errors in the observations themselves. The potential magnitudes of these uncertainties have been estimated and are incorporated within InTEM to inform the uncertainty of the modelled results.

At RGL, HFD, TAC and BSD CH_4 is observed at two or more heights. If, during a 2-hour period the observed CH_4 at different or the same height varies significantly, it is an indication that the meteorology is particularly complex and therefore the modelled meteorology will have significant uncertainty. At the other stations, in low boundary layer, low wind speed or stable conditions, it is also assumed that the meteorological model will have higher uncertainty. Such 2-hour periods are identified at each observation station and are excluded from the inverse modelling.

Estimating the model and observation uncertainty is an important part of InTEM. The observation uncertainty is estimated each day by repeatedly measuring the same tank of air. The standard deviation of these measurements is defined as the observation uncertainty for that day's observations of that gas. For the high frequency (1-minute) Picarro observations the variability over each 2-hour period is defined as the observation uncertainty. The model uncertainty is defined as having two components; a baseline uncertainty and a meteorological uncertainty. The baseline uncertainty is estimated during the fitting of the Northern Hemisphere baseline trend to the baseline observations. The meteorological uncertainty is proportional to the magnitude of the pollution event with an imposed minimum of twice the median pollution event for that gas for that year.

4.3   Summary of the greenhouse gases reported to the UNFCCC

Table 5 describes the principle uses of each of the gases, their radiative efficiency, atmospheric lifetime and global warming potential in a 100-year framework (GWP_{100}).

Gas	Chemical Formula	Main Use	Radiative Efficiency (W m^{-2}ppb^{-1})	Atmos. lifetime (years)	GWP$_{100}$
Methane	CH4	Landfill, farming, energy, wetlands	0.00036	12.4	28
Nitrous Oxide	N_2O	Nylon manufacture, farming	0.003	121	265
Carbon Dioxide	CO_2	Combustion	0.0000138	indefinite	1
HFC-125	CHF_2CF_3	Refrigeration blend, fire suppression	0.23	28.2	3,170
HFC-134a	CH_2FCF_3	Mobile air conditioner	0.16	13.4	1,300
HFC-143a	CH_3CF_3	Refrigeration blend	0.16	47.1	4,800
HFC-152a	CH_3CHF_2	Aerosol propellant, foam-blowing agent	0.10	1.5	138
HFC-23	CHF_3	Bi-product of manufacture of HCFC-22	0.18	222	12,400
HFC-32	CH_2F_2	Refrigeration blend	0.11	5.2	677
HFC-227ea	CF_3CHFCF_3	Fire suppression, inhalers, foam blowing	0.26	38.9	3,350
HFC-245fa	$C_3H_3F_5$	Blowing and insulation agent	0.24	7.7	858
HFC-43-10mee	$C_5H_2F_{10}$	Electronics industry	0.42	16.1	1,650
HFC-365mfc	$C_4H_5F_5$	Foam blowing	0.22	8.7	804
PFC-14	CF_4	Bi-product alum. production, electronics	0.09	50,000	6,630
PFC-116	C_2F_6	Electronics, bi-product alum. production	0.25	>10,000	11,100
PFC-218	C_3F_8	Electronics, bi-product alum. production	0.28	2,600	8,900
PFC-318	C_4F_8	Semiconductor and electronics industries	0.32	3,200	9,540
Sulphur Hexafluoride	SF_6	Circuit breaker in high voltage switchgear	0.57	3,200	23,500
Nitrogen Trifluoride	NF_3	Electronics	0.2	500	16,100

Table 5: The principle use, radiative efficiency, atmospheric lifetime and 100-year global warming potential of the gases measured by the UK DECC network and that are reported to the UNFCCC. Data taken from the 5th IPCC Assessment Report Chapter 8 Appendix 8.A
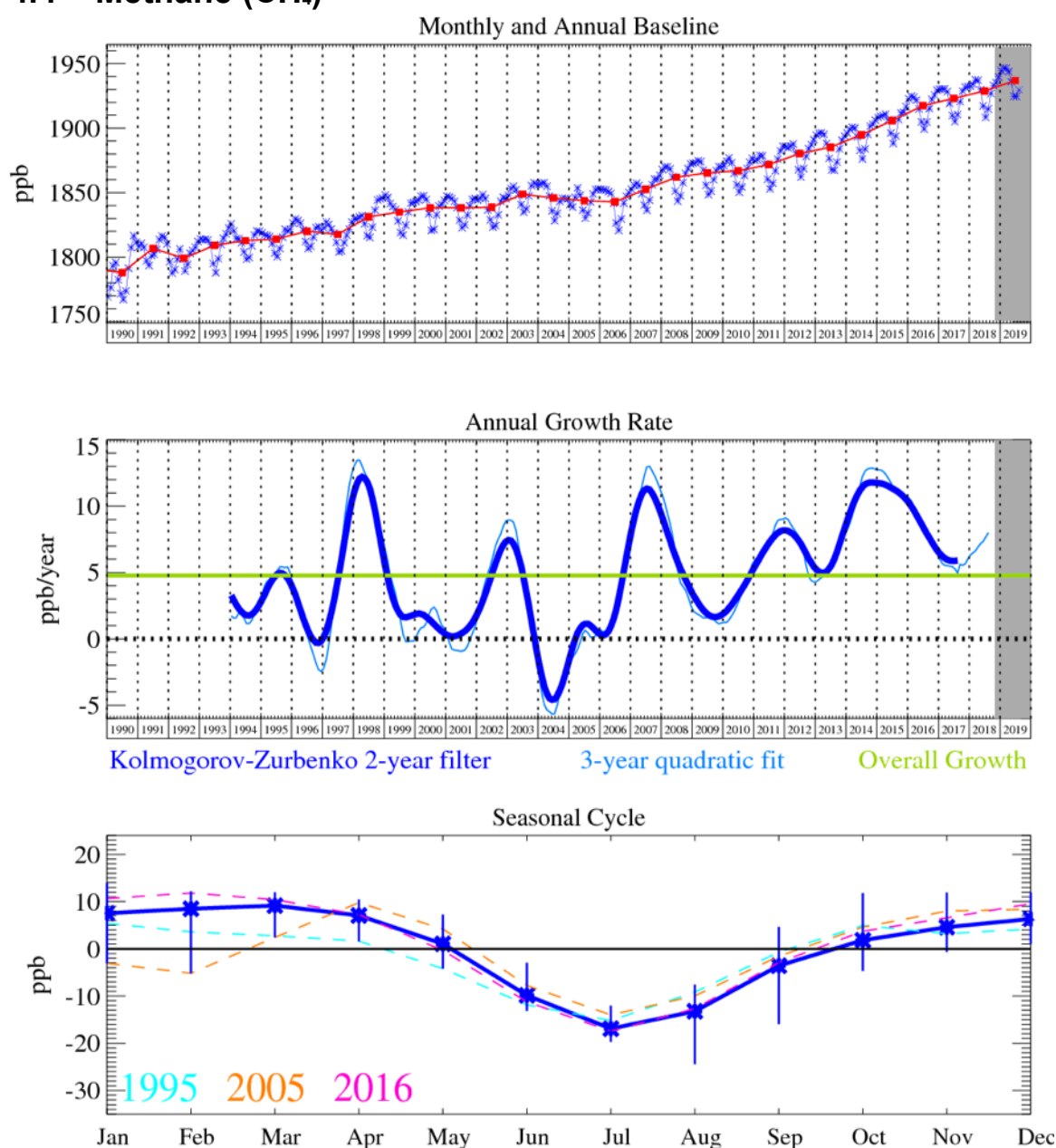
4.4 Methane (CH₄)

Figure 5: Methane: Monthly (blue) and annual (red) Northern Hemisphere baseline mole fractions (top plot). Annual (blue) and overall (green) average growth rate (middle plot). Seasonal cycle (de-trended) with year-to-year variability (lower plot). Grey area covers un-ratified provisional data.

The amount of CH_4 in the atmosphere continues to grow at a strong rate although slowed to 6 ppb yr^{-1} in 2017. It has a strong seasonal cycle, with the dip in the summer caused by its chemical removal by the OH radical.

The InTEM UK methane estimates are presented alongside the UNFCCC inventory for methane from 1990. The blue line shows the inversion estimate with 2 sites (MHD and CBW) from 1990 using global meteorology and the orange line shows the estimate made using 8 observation sites and UKV meteorology. The InTEM estimated emissions for the UK for CH_4 are much lower than that reported in the inventory in the 1990s and also show a slower decline over the 28 years, from ~2800 Gg yr^{-1} to ~1600 Gg yr^{-1}. The inventory has declined from 5300 Gg yr^{-1} to 2100 Gg yr^{-1} over the same period. Both methods have significant uncertainty, especially InTEM in the early 1990s when the observations were less precise and the meteorology more coarse. The uncertainties between the two

methods overlap from 2013 onwards. The use of the extended UK DECC network (TAC, RGL and TTA) from mid-2012, including the towers at Bilsdale (formerly GAUGE now in the UK DECC network), Heathfield (formerly GAUGE now operated by NPL) and Weybourne (operated by NERC), has yielded results that are similar to the MHD-CBW inversions but which allows much greater time and spatial resolution.

The InTEM results for NWEU$_{north}$ are in much better agreement with the inventory in terms of magnitude than for the UK, however the trend does not follow the inventory and the estimates remain approximately flat throughout, hence under-predicting the inventory until 2005, and thereafter over-predicting the inventory. From 2015 there is a rise in emissions from the MHD-CBW inversion estimate but this is not seen in the 8-site inversion estimate.

The 2-month InTEM inversions using 8-sites do not show much evidence of a seasonality in the emissions at either the UK or the NWEU$_{north}$ scale.
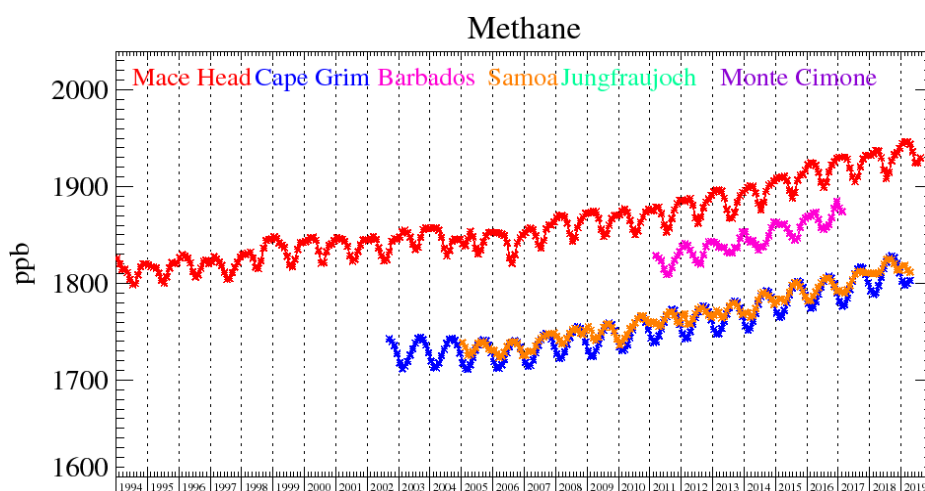

Figure 6: Background methane mole fractions at several global AGAGE stations both in the Northern and Southern Hemispheres.
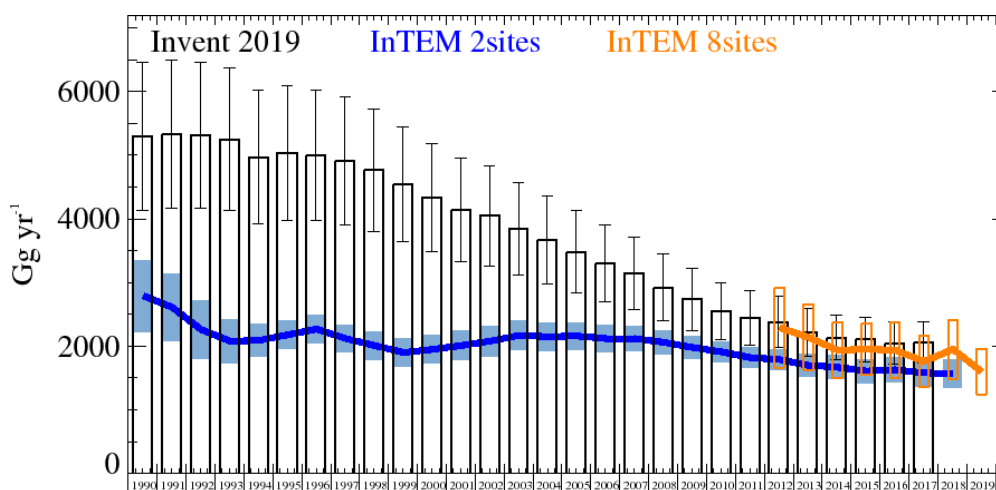

Figure 7: CH$_4$ UK emission estimates (Gg yr^{-1}) from the UNFCCC Inventory (black) and InTEM (annually averaged): (a) MHD+CBW with global meteorology (blue) and (b) DECC + CBW + WAO with UKV 1.5 km meteorology (orange). The uncertainty bars represent 1 std.
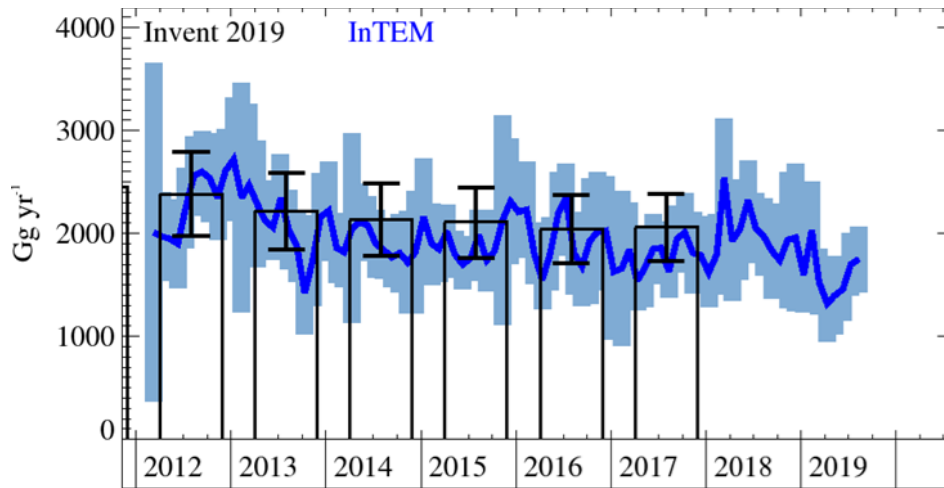
Figure 8: CH$_4$ UK emission estimates (Gg yr^{-1}) from the UNFCCC Inventory (black) and InTEM 2-month DECC + CBW + WAO with UKV 1.5 km meteorology (blue). The uncertainty bars represent 1 std.
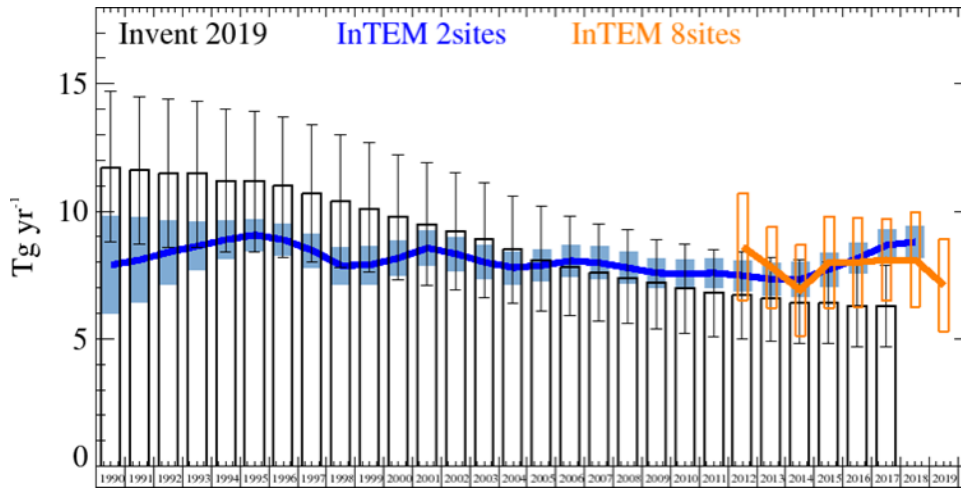
Figure 9: CH$_4$ NWEU$_{north}$ emission estimates (Gg yr^{-1}) from the UNFCCC Inventory (black) and InTEM (annually averaged): (a) MHD+CBW with global meteorology (blue) and (b) DECC + CBW + WAO with UKV 1.5 km meteorology (orange). The uncertainty bars represent 1 std.

Figure 10: CH$_4$ NWEU$_{north}$ emission estimates (Gg yr^{-1}) from the UNFCCC Inventory (black) and InTEM 2-month DECC + CBW + WAO with UKV 1.5 km meteorology (blue). The uncertainty bars represent 1 std.
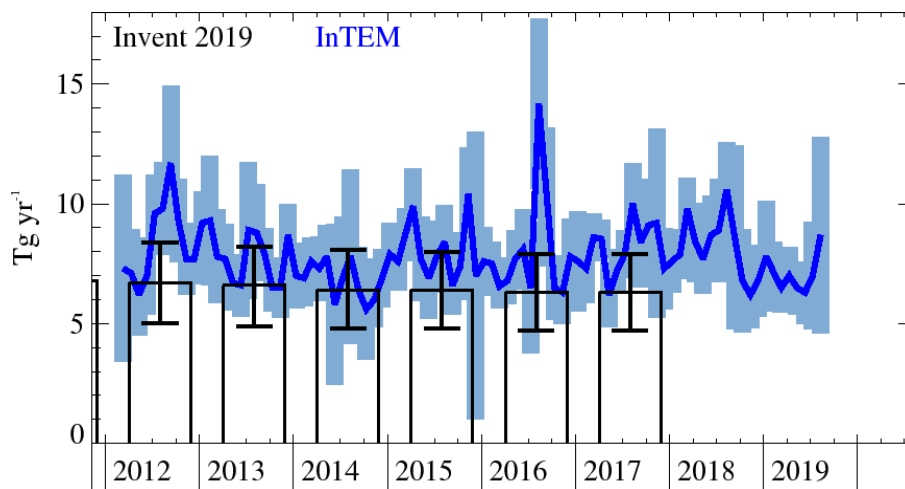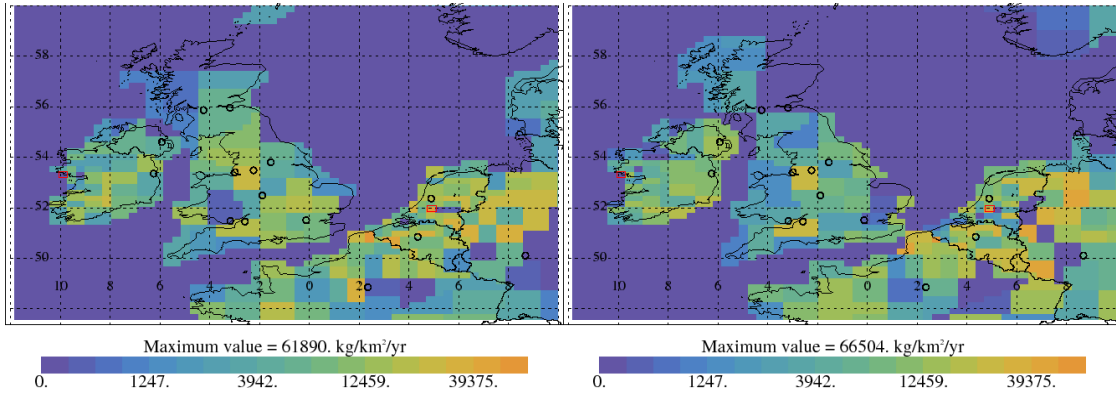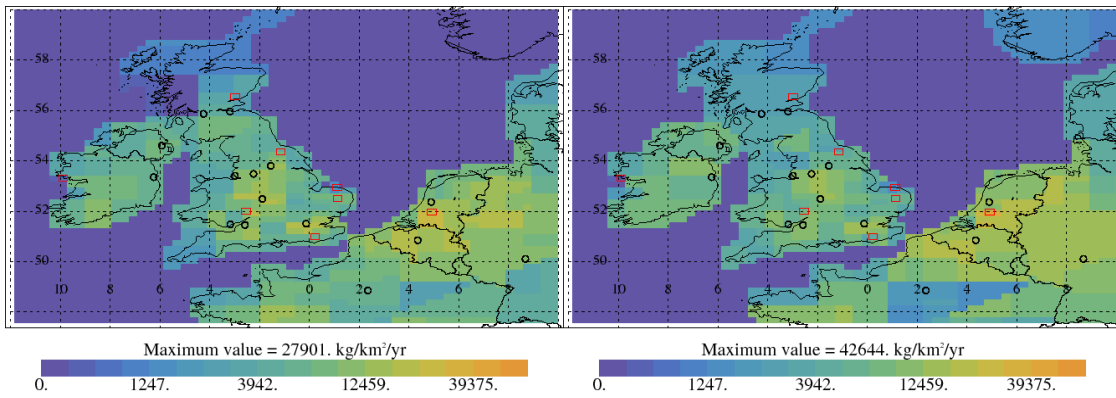
Maximum value = 61890. kg/km²/yr

0.   1247.   3942.   12459.   39375.

Maximum value = 66504. kg/km²/yr

0.   1247.   3942.   12459.   39375.

Figure 11: CH₄: emission estimate using MHD+CBW data and global meteorology for 2004-2008 (left) and 2014-2018 (right). Major cities shown as black circles and observation sites shown as red rectangle.

Maximum value = 27901. kg/km²/yr

0.   1247.   3942.   12459.   39375.

Maximum value = 42644. kg/km²/yr

0.   1247.   3942.   12459.   39375.

Figure 12: CH₄ emission estimate using data from 8 sites and UKV meteorology for 2013-2015 (left) and 2016-2018 (right). Major cities shown as black circles and observation sites shown as red rectangle.
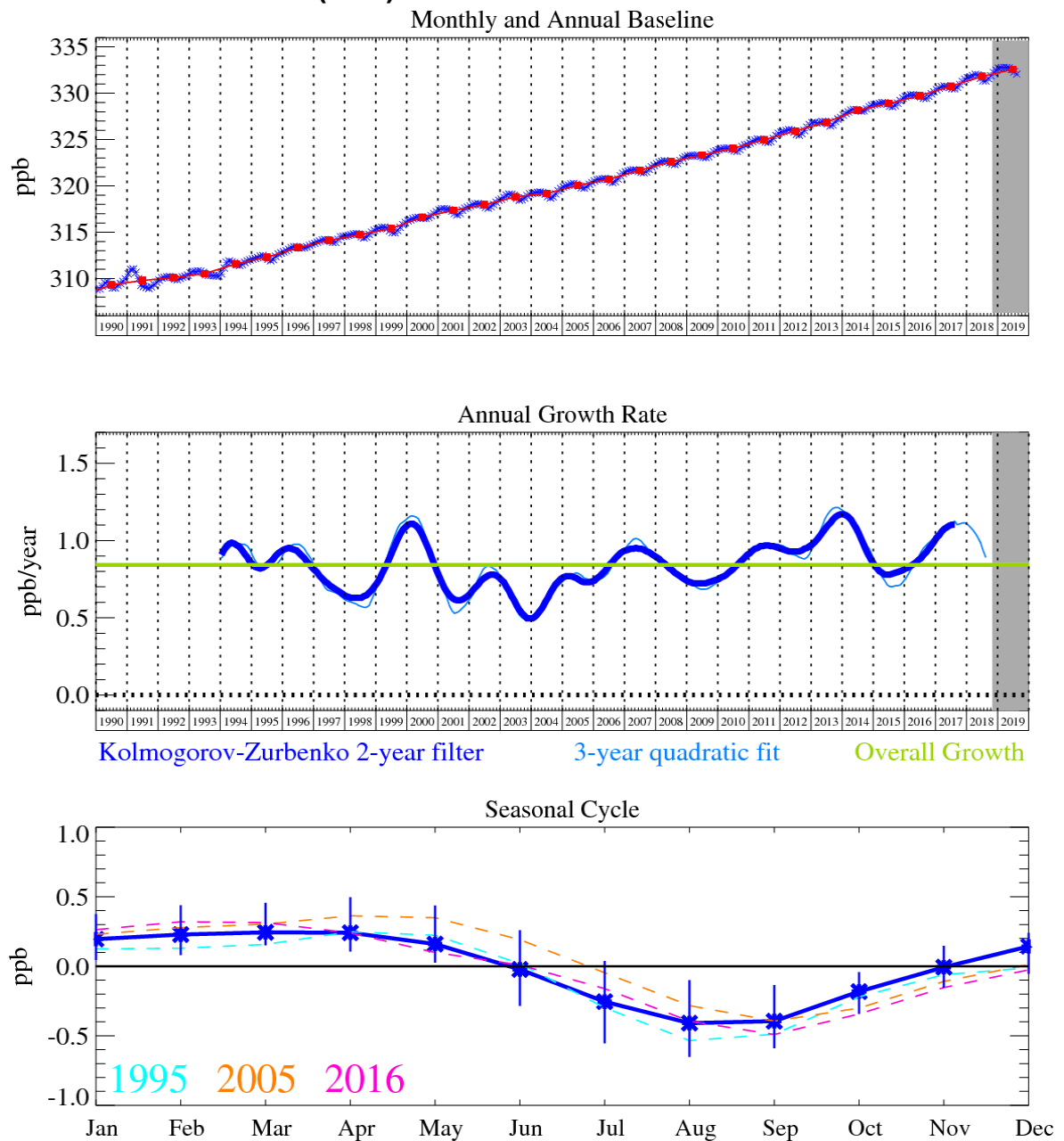
Years	Inventory	MHD+CBW	8 sites
1990	5300. (4130.-6460.)	2790. (2220.-3350.)	
1991	5330. (4170.-6490.)	2610. (2080.-3140.)	
1992	5320. (4170.-6460.)	2260. (1810.-2710.)	
1993	5250. (4130.-6370.)	2080. (1740.-2420.)	
1994	4970. (3920.-6030.)	2090. (1830.-2340.)	
1995	5040. (3980.-6090.)	2180. (1960.-2400.)	
1996	5000. (3970.-6030.)	2270. (2050.-2490.)	
1997	4910. (3900.-5910.)	2120. (1900.-2340.)	
1998	4770. (3800.-5730.)	2010. (1790.-2240.)	
1999	4540. (3640.-5450.)	1900. (1680.-2130.)	
2000	4340. (3480.-5190.)	1950. (1730.-2170.)	
2001	4140. (3330.-4950.)	2010. (1780.-2240.)	
2002	4050. (3260.-4830.)	2080. (1840.-2310.)	
2003	3840. (3110.-4570.)	2170. (1940.-2410.)	
2004	3670. (2970.-4360.)	2150. (1930.-2370.)	
2005	3480. (2830.-4130.)	2160. (1950.-2380.)	
2006	3300. (2690.-3910.)	2120. (1910.-2330.)	
2007	3150. (2570.-3720.)	2120. (1920.-2320.)	
2008	2920. (2400.-3450.)	2060. (1870.-2250.)	
2009	2740. (2250.-3230.)	1980. (1810.-2160.)	
2010	2550. (2110.-3000.)	1910. (1740.-2070.)	
2011	2450. (2020.-2870.)	1820. (1660.-1980.)	
2012	2380. (1980.-2790.)	1790. (1630.-1960.)	2290. (1660.-2920.)
2013	2220. (1840.-2590.)	1700. (1520.-1880.)	2140. (1620.-2660.)
2014	2130. (1780.-2490.)	1670. (1490.-1860.)	1940. (1500.-2370.)
2015	2110. (1760.-2450.)	1610. (1430.-1800.)	1950. (1550.-2360.)
2016	2040. (1710.-2380.)	1630. (1440.-1820.)	1940. (1500.-2380.)
2017	2060. (1730.-2390.)	1580. (1370.-1790.)	1760. (1360.-2160.)
2018		1570. (1340.-1790.)	1950. (1480.-2410.)
2019			1600. (1240.-1960.)

Table 6: CH$_4$ emission (Gg yr^{-1}) estimates for the UK with uncertainty (1std).

Years	Inventory	MHD+CBW	8 sites
1990	11.7 (8.8-14.7)	7.9 (6.0-9.8)	
1991	11.6 (8.7-14.5)	8.1 (6.4-9.7)	
1992	11.5 (8.6-14.4)	8.4 (7.1-9.6)	
1993	11.5 (8.6-14.3)	8.64 (7.70-9.58)	
1994	11.2 (8.4-14.0)	8.89 (8.15-9.63)	
1995	11.2 (8.4-13.9)	9.07 (8.44-9.69)	
1996	11.0 (8.2-13.7)	8.88 (8.27-9.49)	
1997	10.7 (8.0-13.4)	8.46 (7.79-9.13)	
1998	10.4 (7.8-13.0)	7.87 (7.13-8.60)	
1999	10.1 (7.6-12.7)	7.90 (7.15-8.66)	
2000	9.8 (7.3-12.2)	8.17 (7.47-8.87)	
2001	9.5 (7.1-11.9)	8.56 (7.89-9.23)	
2002	9.2 (6.9-11.5)	8.33 (7.67-8.99)	
2003	8.9 (6.6-11.1)	8.00 (7.34-8.66)	
2004	8.5 (6.4-10.6)	7.79 (7.15-8.43)	
2005	8.1 (6.1-10.2)	7.88 (7.26-8.50)	
2006	7.8 (5.9-9.8)	8.06 (7.43-8.69)	
2007	7.6 (5.7-9.5)	7.98 (7.35-8.62)	
2008	7.4 (5.6-9.3)	7.78 (7.16-8.39)	
2009	7.2 (5.4-8.9)	7.58 (6.99-8.16)	
2010	7.0 (5.2-8.7)	7.55 (6.99-8.11)	
2011	6.8 (5.1-8.5)	7.58 (7.01-8.14)	
2012	6.7 (5.0-8.4)	7.48 (6.88-8.08)	8.6 (6.5-10.7)
2013	6.6 (4.9-8.2)	7.34 (6.69-7.99)	7.8 (6.2-9.4)
2014	6.4 (4.8-8.1)	7.34 (6.67-8.02)	6.9 (5.1-8.7)
2015	6.4 (4.8-8.0)	7.72 (7.06-8.38)	8.0 (6.2-9.8)
2016	6.3 (4.7-7.9)	8.16 (7.55-8.78)	8.0 (6.2-9.7)
2017	6.3 (4.7-7.9)	8.67 (8.05-9.29)	8.1 (6.5-9.7)
2018		8.80 (8.16-9.43)	8.1 (6.3-10.0)
2019			7.1 (5.3-8.9)

Table 7: CH$_4$ emission (Tg yr^{-1}) estimates for NWEU$_{north}$ with uncertainty (1std).

4.5   Nitrous oxide (N₂O)

Monthly and Annual Baseline

Annual Growth Rate

Kolmogorov-Zurbenko 2-year filter   3-year quadratic fit   Overall Growth

Seasonal Cycle

1995   2005   2016

Figure 13: N₂O: Monthly (blue) and annual (red) Northern Hemisphere baseline mole fractions (top plot). Annual (blue) and overall (green) average growth rate (middle plot). Seasonal cycle (de-trended) with year-to-year variability (lower plot). Grey area covers un-ratified provisional data.

The atmospheric concentration of N₂O continues to grow strongly. The seasonal cycle in the baseline is driven by the seasonal cycle in the interaction of the stratosphere (relatively low concentration) with the troposphere (relatively high concentration). The stratosphere is the main atmospheric sink of N₂O.
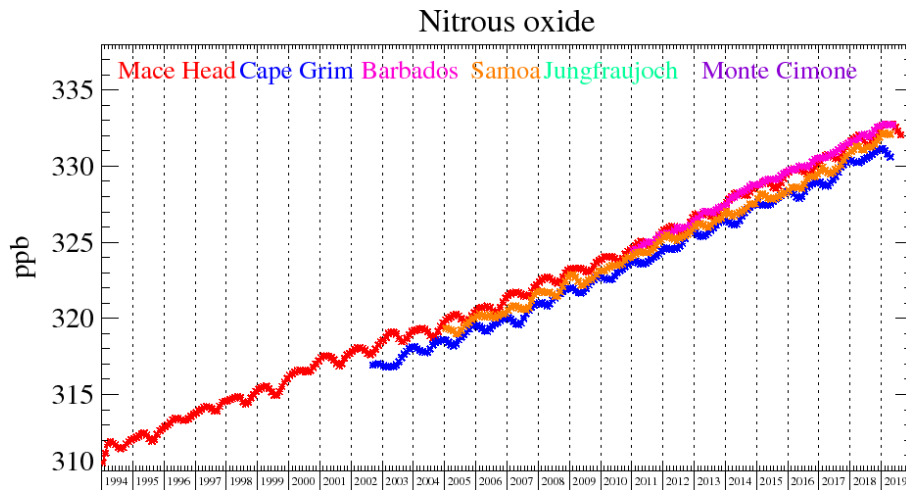
Figure 14: Background nitrous oxide mole fractions at several global AGAGE stations both in the Northern and Southern Hemispheres.
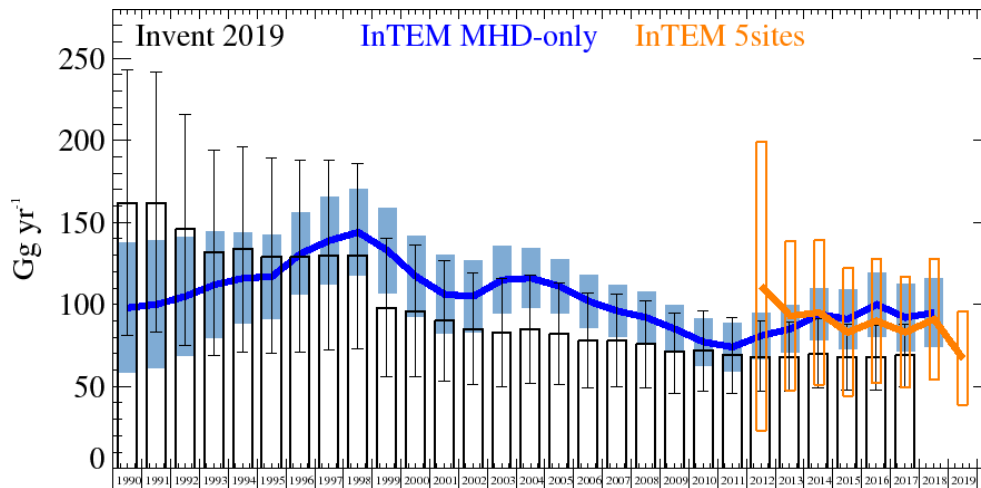

Figure 15: N$_2$O: UK emission estimates (Gg yr^{-1}) from the UNFCCC Inventory (black) and InTEM (annually averaged): (a) MHD with global meteorology (blue) and (b) DECC with UKV 1.5 km meteorology (orange). The uncertainty bars represent 1 std.

Figure 16: N$_2$O: UK emission estimates (Gg yr^{-1}) from the UNFCCC Inventory (black) and InTEM 2-month DECC with UKV 1.5 km meteorology (blue). The uncertainty bars represent 1 std.

Figure 17: N₂O: NWEU$_{north}$ emission estimates (Gg yr^{-1}) from the UNFCCC Inventory (black) and InTEM (annually averaged): (a) MHD with global meteorology (blue) and (b) DECC with UKV 1.5 km meteorology (orange). The uncertainty bars represent 1 std (UNFCCC std assumed 80%).
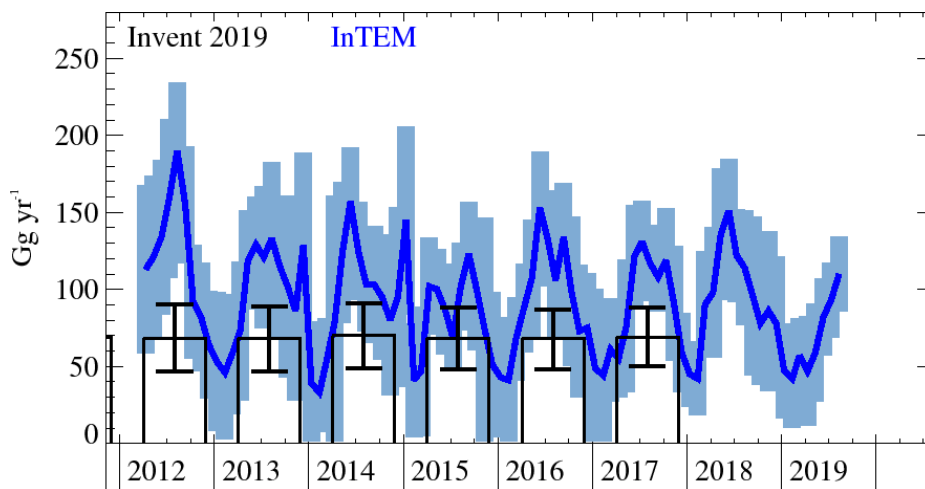

Figure 18: N₂O: NWEU$_{north}$ emission estimates (Gg yr^{-1}) from the UNFCCC Inventory (black) and InTEM 2-month DECC with UKV 1.5 km meteorology (blue). The uncertainty bars represent 1 std (UNFCCC std assumed 80%).
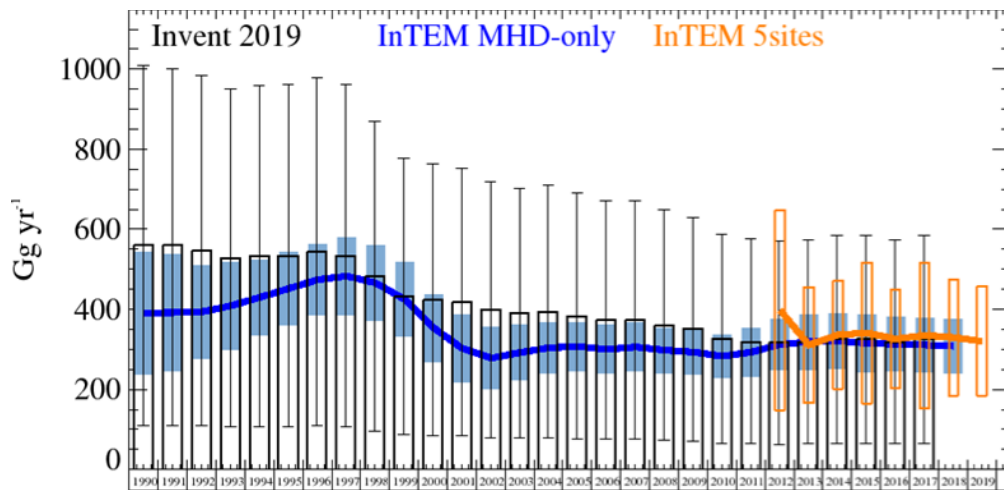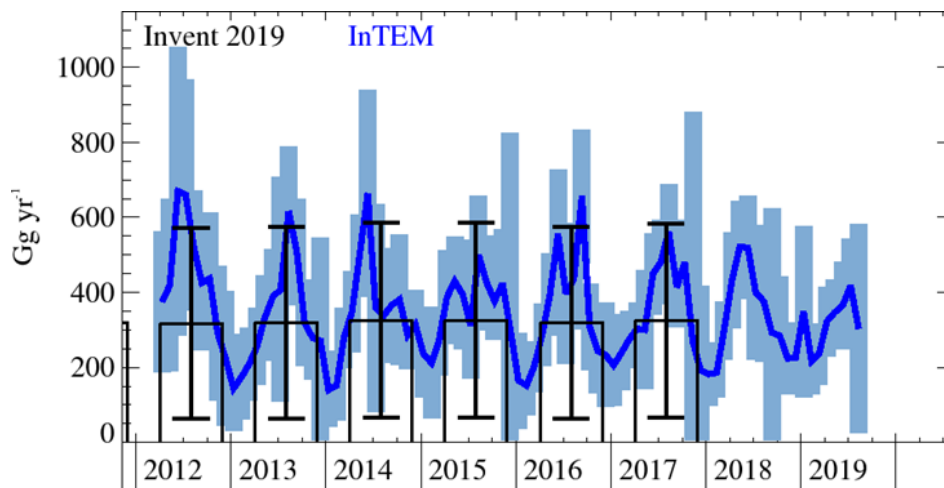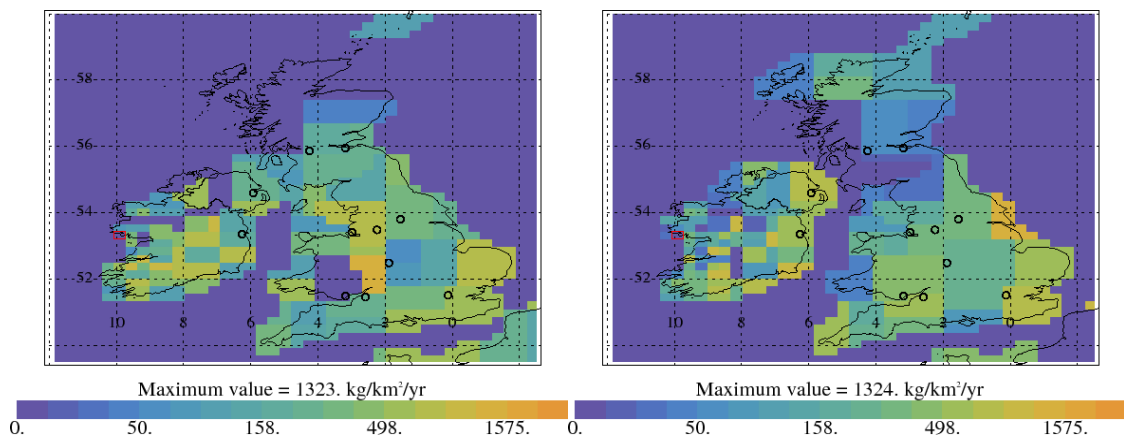

Figure 19: N₂O: emission estimate using MHD data for 2004-2008 (left) and 2014-2018 (right). Major cities shown as black circles and observation sites shown as red rectangle.
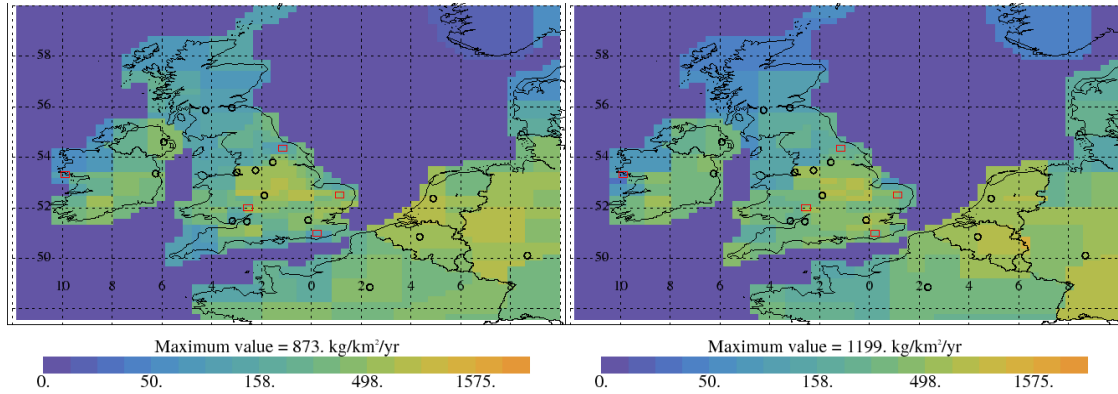
Maximum value = 873. kg/km²/yr

| 0. | 50. | 158. | 498. | 1575. |

Maximum value = 1199. kg/km²/yr

| 0. | 50. | 158. | 498. | 1575. |

Figure 20: N₂O emission estimate using data from 5 sites for 2013-2015 (left) and 2016-2018 (right). Major cities shown as black circles and observation sites shown as red rectangle.

The UK InTEM estimate is initially a little lower than the inventory, reaching good agreement in 1996, after which the InTEM estimate is consistently higher than the inventory, with the MHD-only InTEM estimate being greater than the multi-site estimate. By 2017 the MHD-only estimate is 33% higher than the inventory and the multi-site estimate 20% higher, though the uncertainties of all three overlap. When 2-month inversions are run, a strong seasonal cycle can be seen in the InTEM estimates with a strong peak in spring/summer and a minimum in winter, in line with the application of fertilizer.

Years	Inventory	MHD	5 sites
1990	162. (81.-243.)	98. (58.-137.)	
1991	162. (83.-242.)	100. (61.-139.)	
1992	146. (75.-216.)	105. (69.-141.)	
1993	132. (69.-194.)	112. (79.-144.)	
1994	134. (71.-196.)	116. (89.-144.)	
1995	129. (70.-189.)	117. (92.-143.)	
1996	129. (71.-188.)	131. (106.-156.)	
1997	130. (72.-188.)	139. (113.-166.)	
1998	130. (73.-186.)	144. (118.-171.)	
1999	98. (56.-140.)	133. (107.-159.)	
2000	96. (56.-136.)	117. (92.-141.)	
2001	90. (53.-127.)	106. (82.-130.)	
2002	85. (51.-119.)	105. (83.-127.)	
2003	83. (50.-116.)	115. (94.-135.)	
2004	85. (52.-118.)	116. (98.-134.)	
2005	82. (51.-113.)	111. (95.-128.)	
2006	78. (49.-107.)	102. (86.-118.)	
2007	78. (50.-106.)	96. (80.-112.)	
2008	76. (49.-102.)	92. (76.-107.)	
2009	71. (46.-95.)	85. (71.-100.)	
2010	72. (47.-96.)	77. (63.-92.)	
2011	69. (46.-92.)	74. (60.-89.)	
2012	68. (47.-90.)	81. (67.-95.)	111. (23.-199.)
2013	68. (47.-89.)	85. (71.-100.)	93. (47.-138.)
2014	70. (49.-91.)	94. (78.-110.)	95. (51.-139.)
2015	68. (48.-88.)	91. (73.-109.)	83. (44.-122.)
2016	68. (48.-87.)	100. (81.-120.)	90. (52.-128.)
2017	69. (50.-88.)	92. (71.-112.)	83. (49.-116.)
2018		95. (74.-116.)	91. (54.-128.)
2019			67. (39.-96.)

Table 8: N₂O emission (Gg yr⁻¹) estimates for the UK with uncertainty (1std).

The NWEU$_{north}$ InTEM estimate is generally slightly lower than the inventory but follows the trend very well. From 2012 there is excellent agreement for both InTEM inversions.

The inventory estimates have been changed significantly over different UNFCCC submissions, for example the UK 2011 inventory estimates were 110 Gg yr^{-1} in the 2013 submission, 117 Gg yr^{-1} in 2014, 93 Gg yr^{-1} in 2015, 72 Gg yr^{-1} in 2016, 77 Gg yr^{-1} in 2017, 73 Gg yr^{-1} in 2018 and 69 Gg yr^{-1} in the 2019 submission.

Discussions are ongoing with the inventory team to try and understand the differences between the inventory and the InTEM estimates. The spatial distribution indicate that the emissions are wide-spread across the UK. The clear benefit of having the network of observations, compared to just MHD, allows smaller inversion time-windows and thus a clearer understanding of seasonality and spatial patterns.

Years	Inventory	MHD	5 sites
1990	560. (110.-1010.)	391. (237.-544.)	
1991	560. (110.-1000.)	392. (246.-537.)	
1992	546. (109.-983.)	394. (277.-511.)	
1993	528. (106.-950.)	409. (300.-518.)	
1994	533. (107.-960.)	430. (336.-523.)	
1995	534. (107.-961.)	452. (361.-543.)	
1996	543. (109.-978.)	474. (386.-562.)	
1997	534. (107.-961.)	483. (387.-579.)	
1998	483. (97.-870.)	466. (373.-559.)	
1999	432. (86.-778.)	425. (332.-517.)	
2000	424. (85.-763.)	354. (270.-439.)	
2001	418. (84.-752.)	302. (218.-387.)	
2002	400. (80.-720.)	278. (201.-355.)	
2003	391. (78.-703.)	292. (223.-362.)	
2004	394. (79.-710.)	304. (241.-368.)	
2005	383. (77.-690.)	307. (246.-368.)	
2006	373. (75.-671.)	300. (239.-361.)	
2007	373. (75.-671.)	306. (245.-366.)	
2008	360. (72.-648.)	298. (241.-354.)	
2009	350. (70.-630.)	293. (238.-348.)	
2010	326. (65.-587.)	283. (229.-336.)	
2011	319. (64.-575.)	293. (233.-353.)	
2012	317. (63.-571.)	312. (250.-375.)	398. (149.-648.)
2013	319. (64.-574.)	319. (250.-388.)	311. (166.-456.)
2014	325. (65.-585.)	321. (252.-390.)	336. (200.-471.)
2015	325. (65.-585.)	315. (243.-387.)	341. (165.-517.)
2016	319. (64.-574.)	313. (246.-381.)	326. (202.-450.)
2017	325. (65.-584.)	311. (243.-380.)	335. (153.-517.)
2018		308. (241.-375.)	330. (185.-476.)
2019			320. (183.-457.)

Table 9: N$_2$O emission (Gg yr^{-1}) estimates for NWEU$_{north}$ with uncertainty (1std).

4.6   Carbon dioxide (CO₂)
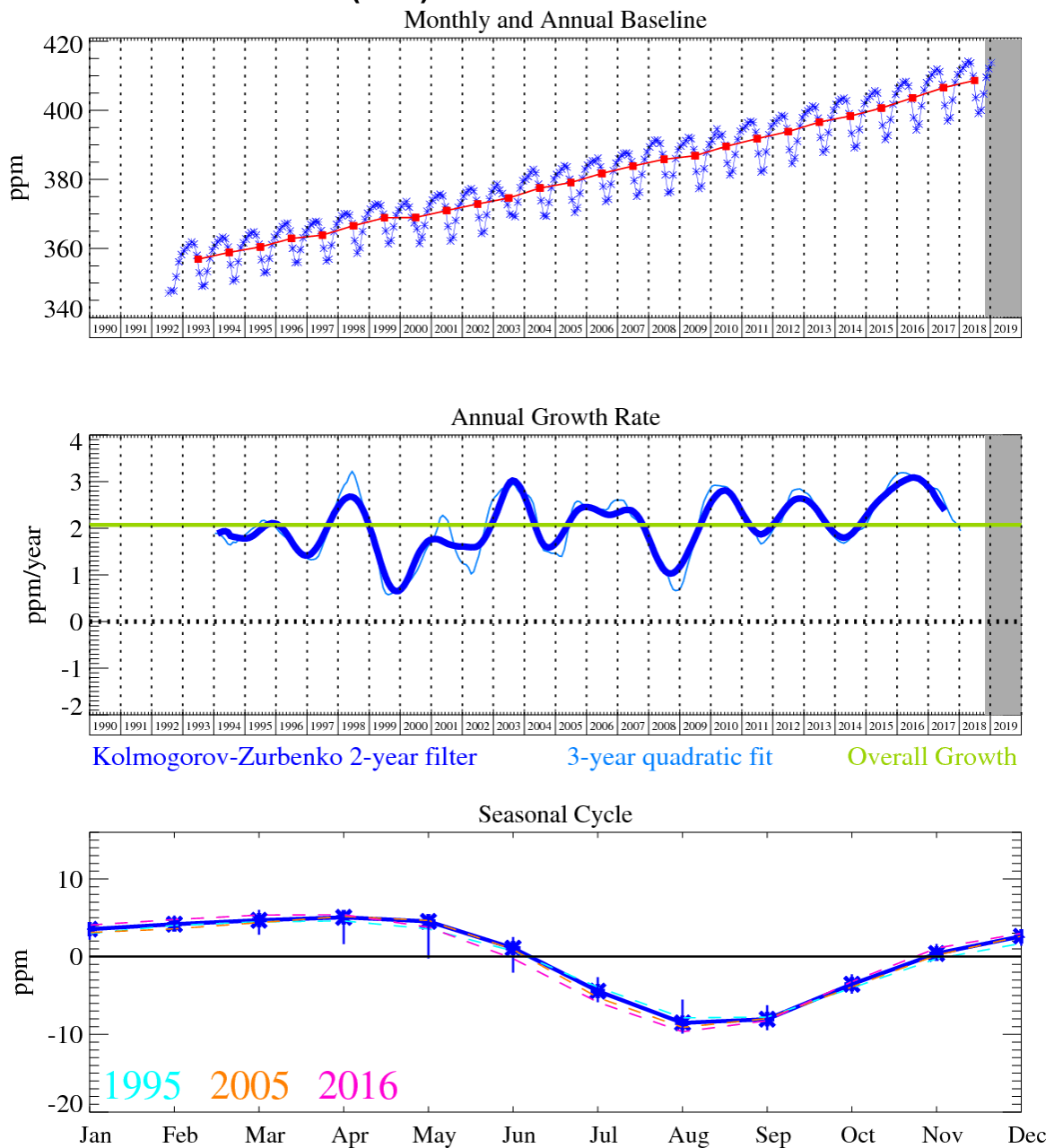
Figure 21: CO₂: Monthly (blue) and annual (red) Northern Hemisphere baseline mole fractions (top plot). Annual (blue) and overall (green) average growth rate (middle plot). Seasonal cycle (de-trended) with year-to-year variability (lower plot). Grey area covers un-ratified provisional data.

CO_2 is the most important greenhouse gas. It has steadily grown at an annual average rate of 2 ppm yr^{-1}. Since 2012 the growth rate has averaged more than 2 ppm yr^{-1}. It has now reached an average annual mole fraction of 409 ppm (2018), the highest yet recorded at Mace Head, Ireland. There have been positive growth rate anomalies in several years (1998-99, 2002-03, 2009-10, 2012-13 and 2015-17) with some of these being directly linked to significant global biomass burning events. The average annual baseline mole fraction in the mid-latitude northern hemisphere surpassed 400 ppm in 2015.

4.7 HFC-125
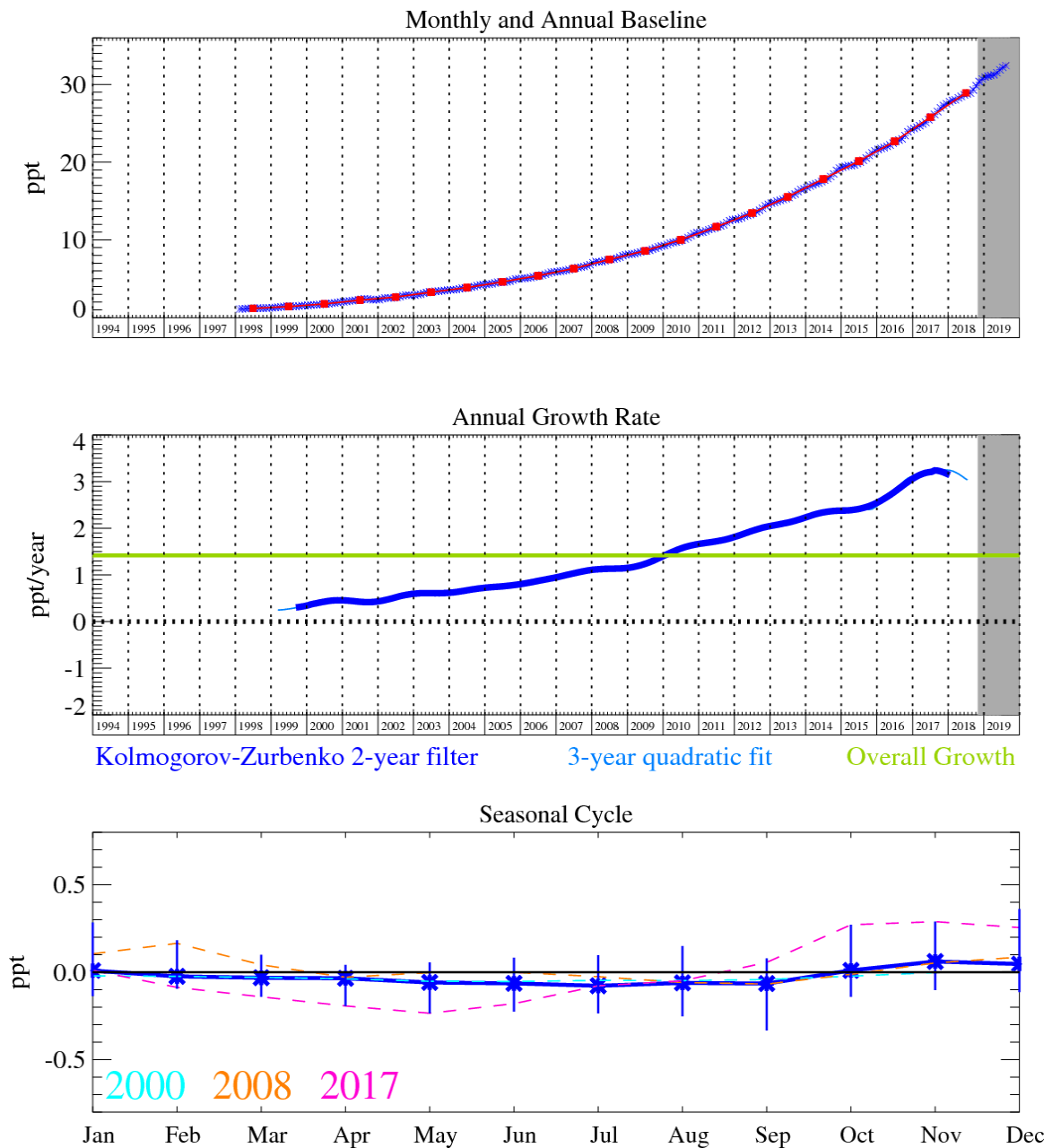
Figure 22: HFC-125: Monthly (blue) and annual (red) Northern Hemisphere baseline mole fractions (top plot). Annual (blue) and overall (green) average growth rate (middle plot). Seasonal cycle (de-trended) with year-to-year variability (lower plot). Grey area covers un-ratified provisional data.

Unfortunately, the observations of HFC-125 (and HFC-32) at Mace Head were compromised by contamination from the air conditioning system (May 2014 – June 2015) and these data had to be removed. The current working solution is to flush the air sample module with clean ambient air to minimise contamination from laboratory air. A long-term solution will require modification of the air conditioner to use a chilled water heat exchanger with the refrigerant gases contained in a unit external to the laboratory. The northern hemisphere baseline during this period has been estimated using another AGAGE northern hemisphere station, Zeppelin (Ny-Ålesund). The Northern Hemisphere mole fraction is currently about 5 ppt above that of the Southern Hemisphere which is indicating an 18-month lag between the two hemispheres.

Relative to the magnitude of the baseline the pollution events are very significant. Therefore, InTEM has plenty of clear information on which to base the emission estimates. The agreement in trend between the inventory and InTEM for the UK is good. However, the rate of increase in the inventory is greater than that estimated by InTEM. The InTEM estimates using the AGAGE network (MHD and MHD+JFJ+CMN) have shown no overall trend since 2012, the 4-site inversion does however indicate a possible decline in UK emissions over the 7 years 2013-2019. The UK InTEM estimates are currently about 50% of those reported through the inventory. The NWEU InTEM emissions follow a very similar pattern to those for the UK, under-predicting the inventory, the main difference being the divergence of the 3-site model away from the other results from 2014-2017.
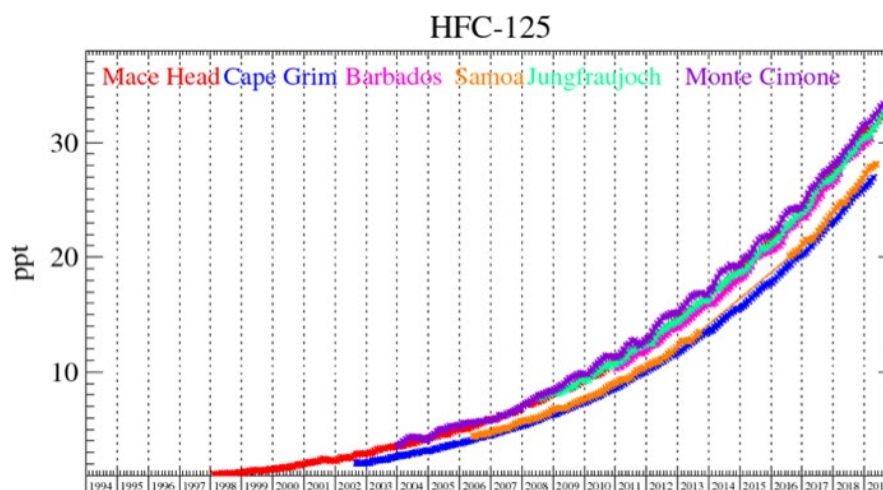
Figure 23: Background HFC-125 mole fractions at several global AGAGE stations both in the Northern and Southern Hemispheres.

Figure 24: HFC-125: UK emission estimates (Gg yr^{-1}) from the UNFCCC Inventory (black) and InTEM (annually averaged): (a) MHD (3yr) with global meteorology (blue), (b) 3 sites (2yr) (MHD+JFJ+CMN) with global meteorology (orange), and (c) 4 sites (1yr) (MHD+JFJ+CMN+TAC) with UKV 1.5 km nested in global meteorology (green). The uncertainty bars represent 1 std.

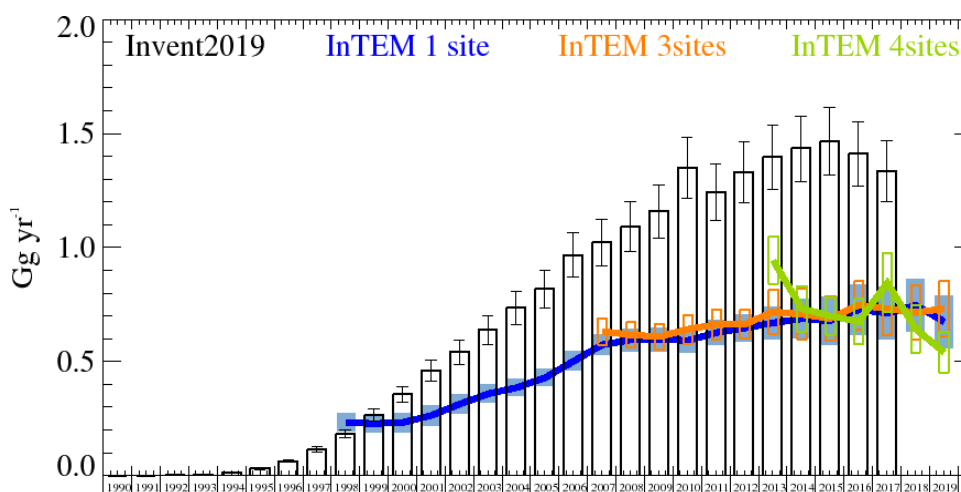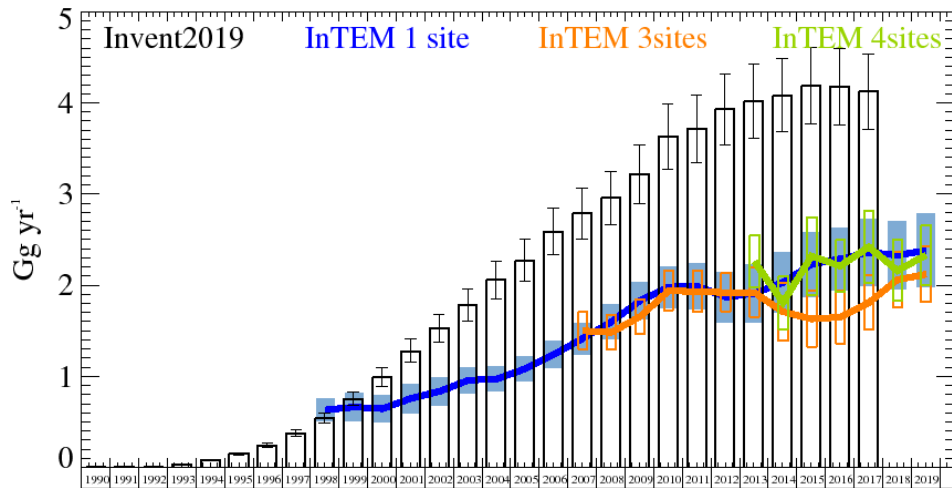**Figure 25: HFC-125: NWEU emission estimates (Gg yr^{-1}) from the UNFCCC Inventory (black) and InTEM (annually averaged): (a) MHD (3yr) with global meteorology (blue), (b) 3 sites (2yr) (MHD+JFJ+CMN) with global meteorology (orange), and (c) 4 sites (1yr) (MHD+JFJ+CMN+TAC) with UKV 1.5 km nested in global meteorology (green). The uncertainty bars represent 1 std.**

Figure 26: HFC-125 emission estimate using MHD data for 2004-2008 (left) and 2014-2018 (right). Major cities shown as black circles and observation sites shown as red rectangle.

Figure 27: HFC-125 emission estimate using data from 4 sites for 2013-2015 (left) and 2016-2018 (right). Major cities shown as black circles and observation sites shown as red rectangle.

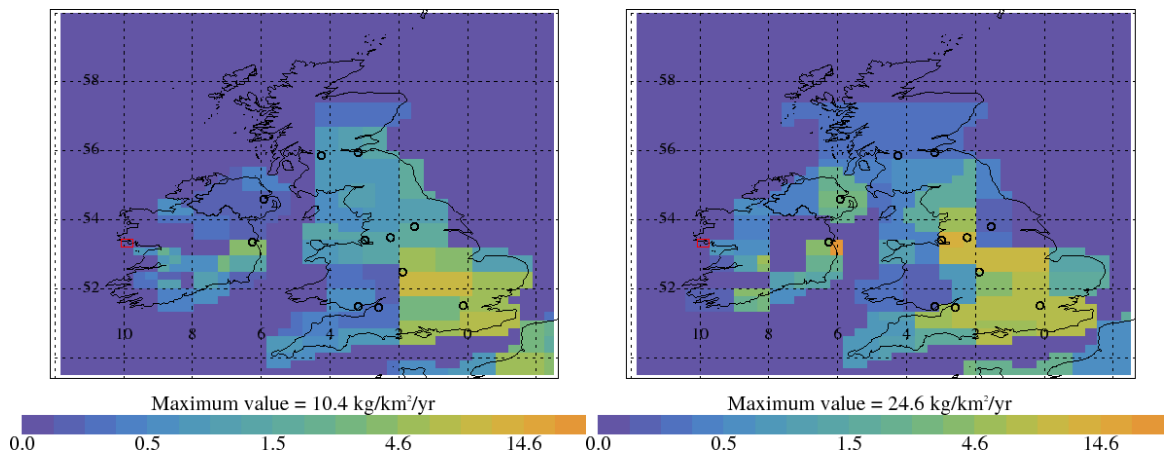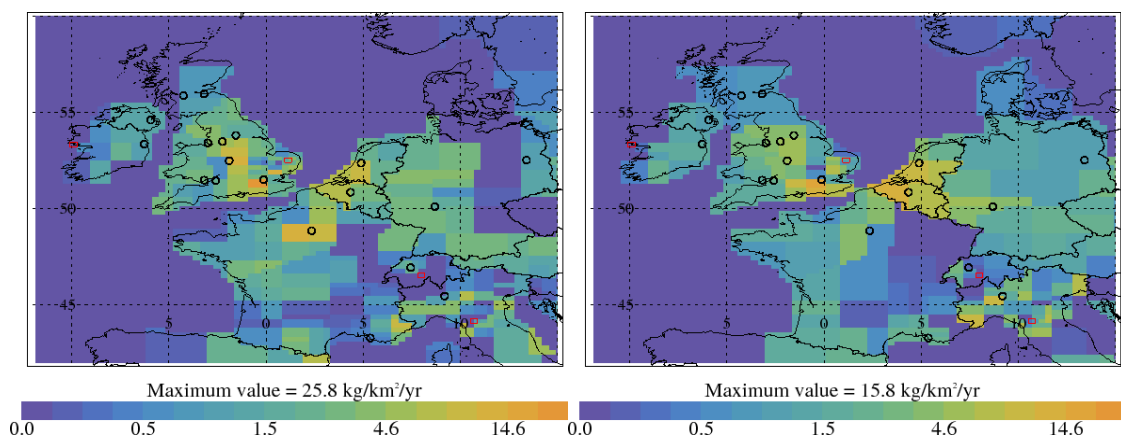| Years	Inventory	MHD	3 sites	4 sites
1994	0.0120 (0.0110-0.0130)			
1995	0.0301 (0.0271-0.0331)			
1996	0.0634 (0.0571-0.0698)			
1997	0.1143 (0.1029-0.1257)			
1998	0.1831 (0.1648-0.2014)	0.233 (0.192-0.273)		
1999	0.265 (0.239-0.292)	0.228 (0.187-0.269)		
2000	0.356 (0.321-0.392)	0.233 (0.191-0.274)		
2001	0.462 (0.416-0.508)	0.264 (0.221-0.308)		
2002	0.541 (0.487-0.595)	0.314 (0.271-0.356)		
2003	0.638 (0.574-0.702)	0.359 (0.319-0.399)		
2004	0.735 (0.661-0.808)	0.386 (0.349-0.424)		
2005	0.819 (0.737-0.901)	0.430 (0.391-0.468)		
2006	0.968 (0.871-1.065)	0.503 (0.461-0.545)		
2007	1.023 (0.921-1.126)	0.574 (0.529-0.620)	0.632 (0.574-0.690)	
2008	1.091 (0.982-1.200)	0.595 (0.547-0.644)	0.617 (0.560-0.674)	
2009	1.158 (1.042-1.274)	0.598 (0.547-0.650)	0.609 (0.552-0.666)	
2010	1.349 (1.214-1.484)	0.592 (0.540-0.645)	0.642 (0.579-0.706)	
2011	1.243 (1.118-1.367)	0.627 (0.572-0.682)	0.663 (0.598-0.728)	
2012	1.332 (1.199-1.465)	0.647 (0.589-0.706)	0.664 (0.600-0.728)	
2013	1.397 (1.257-1.536)	0.670 (0.597-0.743)	0.718 (0.623-0.813)	0.943 (0.839-1.047)
2014	1.435 (1.291-1.578)	0.688 (0.601-0.775)	0.707 (0.596-0.818)	0.732 (0.632-0.832)
2015	1.466 (1.320-1.613)	0.679 (0.576-0.783)	0.689 (0.590-0.788)	0.700 (0.617-0.783)
2016	1.412 (1.270-1.553)	0.728 (0.616-0.839)	0.748 (0.641-0.854)	0.675 (0.576-0.775)
2017	1.337 (1.203-1.471)	0.712 (0.596-0.827)	0.732 (0.614-0.850)	0.845 (0.716-0.974)
2018		0.747 (0.630-0.863)	0.715 (0.594-0.836)	0.643 (0.539-0.747)
2019		0.675 (0.561-0.790)	0.732 (0.611-0.854)	0.541 (0.452-0.629)

Table 10: HFC-125 emission (Gg yr^{-1}) estimates for the UK with uncertainty (1std).

Years	Inventory 1yr	1s 3y	3s 2y	4s 1y
1994	0.0825 (0.0742-0.0907)			
1995	0.1483 (0.1335-0.1632)			
1996	0.243 (0.219-0.267)			
1997	0.377 (0.339-0.415)			
1998	0.541 (0.487-0.595)	0.827 (0.665-0.990)		
1999	0.753 (0.678-0.829)	0.870 (0.670-1.007)		
2000	0.994 (0.894-1.093)	0.846 (0.651-1.041)		
2001	1.278 (1.151-1.406)	1.000 (0.780-1.210)		
2002	1.529 (1.376-1.682)	1.095 (0.898-1.292)		
2003	1.779 (1.601-1.957)	1.255 (1.066-1.444)		
2004	2.06 (1.85-2.26)	1.273 (1.098-1.448)		
2005	2.27 (2.04-2.50)	1.422 (1.248-1.596)		
2006	2.59 (2.33-2.85)	1.63 (1.43-1.83)		
2007	2.79 (2.51-3.07)	1.86 (1.63-2.08)	1.94 (1.72-2.16)	
2008	2.96 (2.66-3.25)	2.09 (1.85-2.34)	1.84 (1.63-2.05)	
2009	3.21 (2.89-3.54)	2.40 (2.13-2.67)	1.88 (1.68-2.09)	
2010	3.63 (3.27-3.99)	2.60 (2.30-2.90)	2.20 (1.97-2.44)	
2011	3.71 (3.34-4.08)	2.61 (2.27-2.94)	2.38 (2.14-2.63)	
2012	3.93 (3.54-4.32)	2.45 (2.09-2.81)	2.47 (2.22-2.71)	
2013	4.02 (3.61-4.42)	2.50 (2.09-2.91)	2.39 (2.09-2.68)	2.84 (2.52-3.16)
2014	4.08 (3.68-4.49)	2.65 (2.21-3.09)	2.09 (1.75-2.43)	2.38 (2.04-2.73)
2015	4.19 (3.77-4.61)	2.92 (2.45-3.38)	2.12 (1.80-2.44)	3.05 (2.60-3.50)
2016	4.18 (3.76-4.59)	3.00 (2.55-3.45)	2.25 (1.95-2.56)	2.88 (2.57-3.19)
2017	4.13 (3.71-4.54)	3.09 (2.61-3.56)	2.29 (1.99-2.60)	2.84 (2.43-3.26)
2018		3.06 (2.57-3.54)	2.42 (2.11-2.73)	2.57 (2.22-2.92)
2019		3.11 (2.59-3.64)	2.48 (2.17-2.78)	2.88 (2.52-3.23)

Table 11: HFC-125 emission (Gg yr^{-1}) estimates for the NWEU with uncertainty (1std).
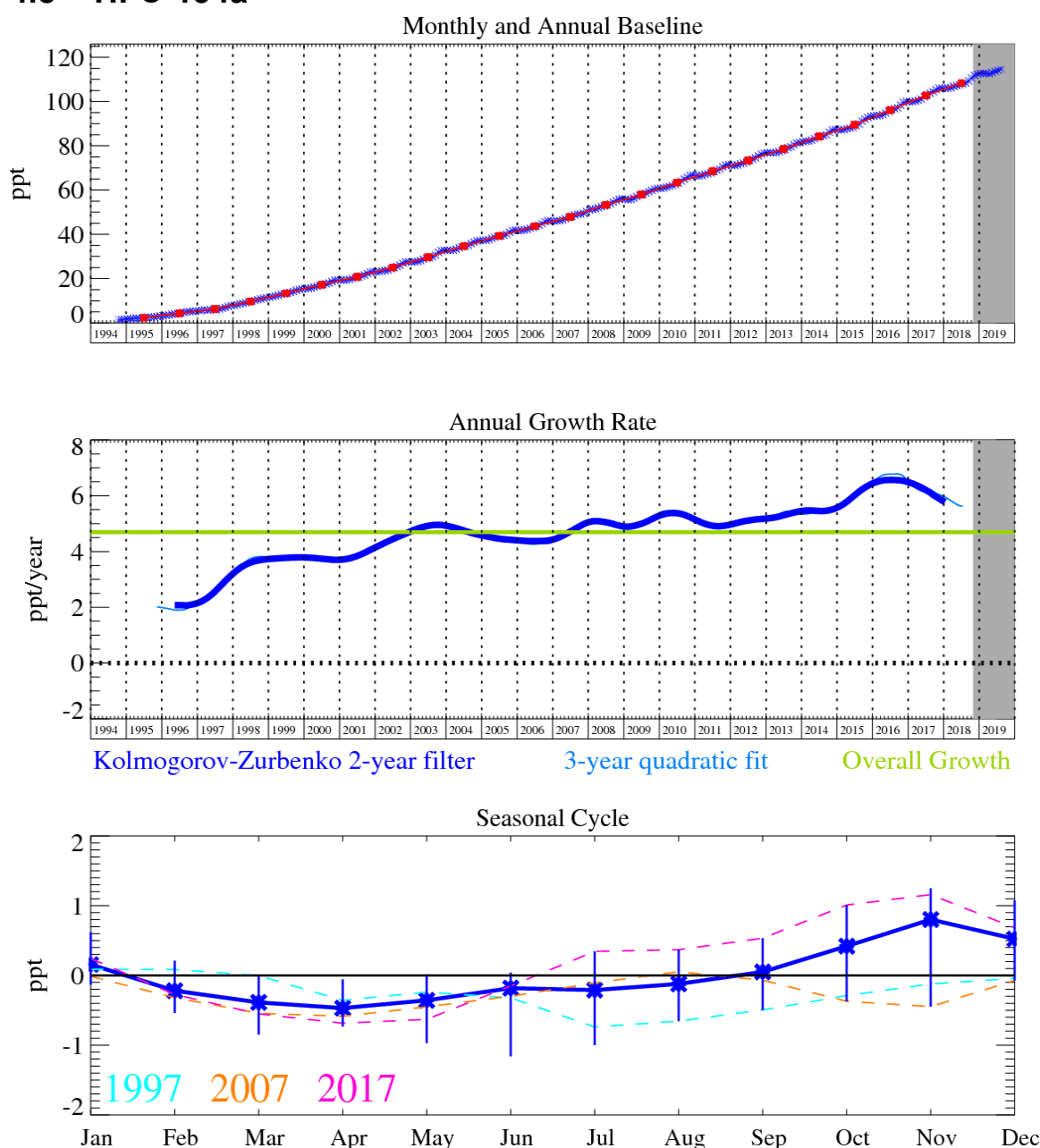
4.8 HFC-134a

Figure 28: HFC-134a: Monthly (blue) and annual (red) Northern Hemisphere baseline mole fractions (top plot). Annual (blue) and overall (green) average growth rate (middle plot). Seasonal cycle (de-trended) with year-to-year variability (lower plot). Grey area covers un-ratified provisional data.

Globally HFC-134a (CH_2FCF_3) is the most abundant HFC present in the atmosphere and is used predominantly in refrigeration and mobile air conditioning (MAC). Due to its long lifetime, 13.5 years, and relatively high GWP_{100} of 1370, the use of HFC-134a (and any other HFCs with a GWP_{100} >150) was phased out in Europe between 2011 and 2017. It is proposed that a very gradual phase-out of the use of HFC-134a in cars will also take place outside Europe because of the global nature of the car industry. However, in developing countries the potential for growth of HFC-134a is still large [*Velders et al.*, 2009].

The UK inventory and InTEM estimates (initially flat) increase until around 2009 when the estimates level off. However, the InTEM estimates for the UK are consistently around half of the inventory estimates. A very similar picture can be seen in the NWEU estimates, with the main difference being that the NWEU InTEM 3-site inversion under-estimates

compared with the MHD-only run, causing it to flatten off sooner. A significant proportion of the HFC-134a emitted is estimated to come from in-use vehicles (it is used in mobile air conditioning units). The UK inventory was modified downwards (5%) for the 2017 submission for data from 2009 onwards after further work on the activity data and emission factors used was undertaken. However, a key factor, the annual re-fill frequency, was kept at the conservative, albeit unrealistic, rate of 100% because of a limitation present in the inventory model.
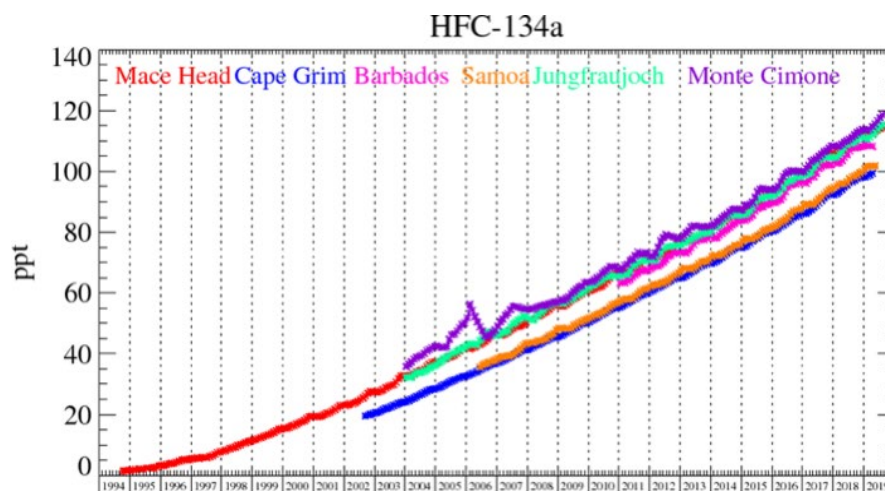
Figure 29: Background HFC-134a mole fractions at several global AGAGE stations both in the Northern and Southern Hemispheres.
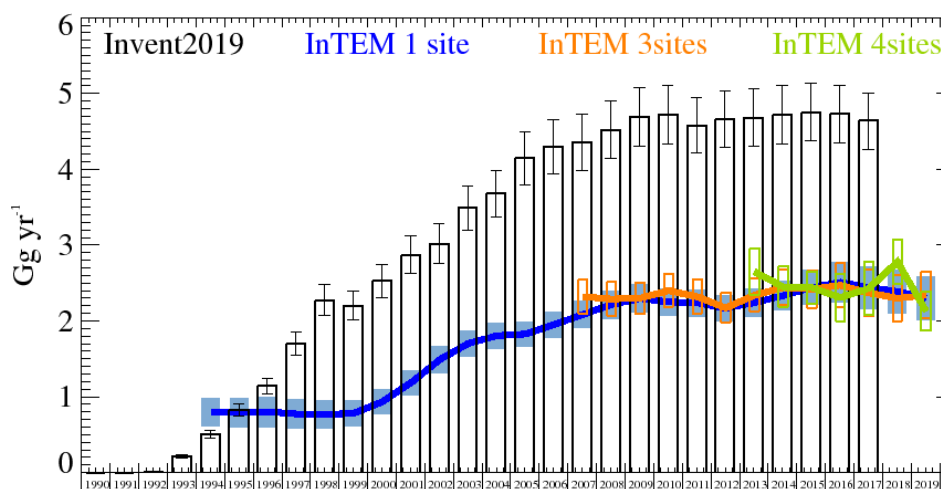
Figure 30: HFC-134a: UK emission estimates (Gg yr⁻¹) from the UNFCCC Inventory (black) and InTEM (annually averaged): (a) MHD (3yr) with global meteorology (blue), (b) 3 sites (2yr) (MHD+JFJ+CMN) with global meteorology (orange), and (c) 4 sites (1yr) (MHD+JFJ+CMN+TAC) with UKV 1.5 km nested in global meteorology (green). The uncertainty bars represent 1 std.
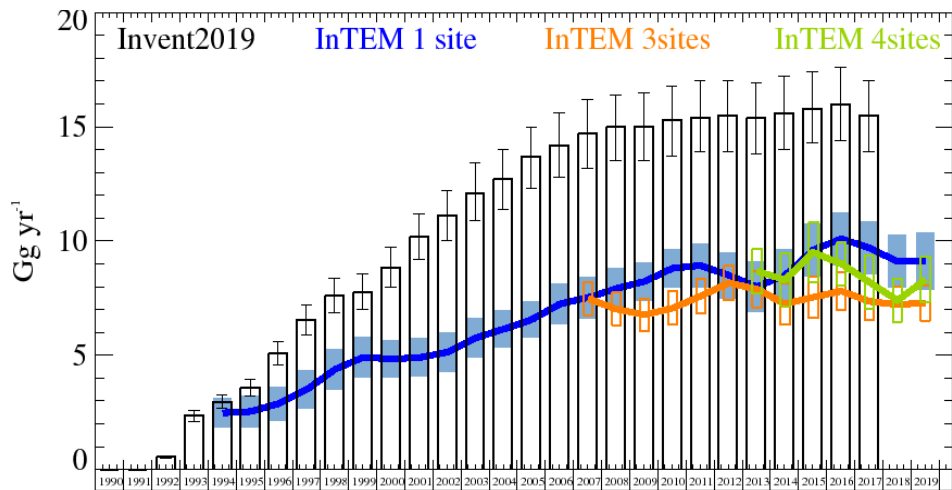
Figure 31: HFC-134a: NWEU emission estimates (Gg yr^{-1}) from the UNFCCC Inventory (black) and InTEM (annually averaged): (a) MHD (3yr) with global meteorology (blue), (b) 3 sites (2yr) (MHD+JFJ+CMN) with global meteorology (orange), and (c) 4 sites (1yr) (MHD+JFJ+CMN+TAC) with UKV 1.5 km nested in global meteorology (green). The uncertainty bars represent 1 std.


Figure 32: HFC-134a emission estimate using MHD data for 2004-2008 (left) and 2014-2018 (right). Major cities shown as black circles and observation sites shown as red rectangle.

Figure 33: HFC-134a emission estimate using data from 4 sites for 2013-2015 (left) and 2016-2018 (right). Major cities shown as black circles and observation sites shown as red rectangle.

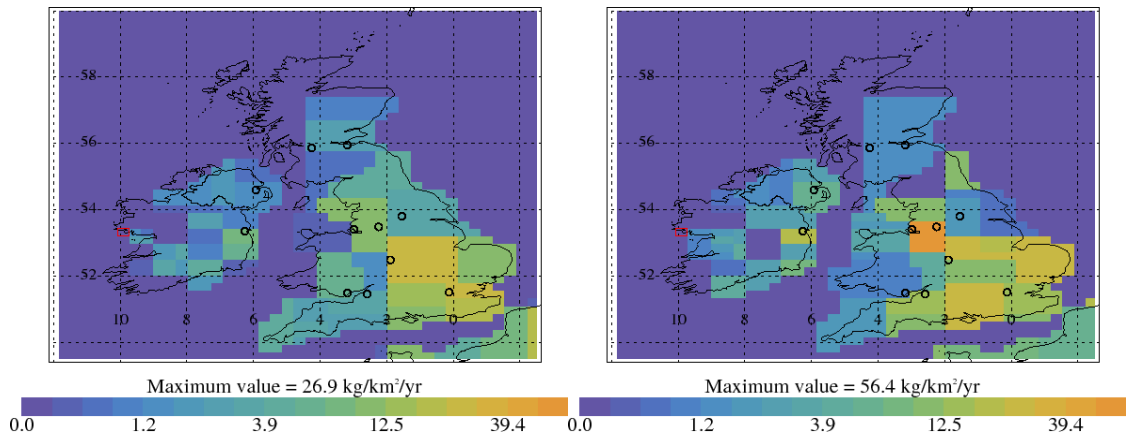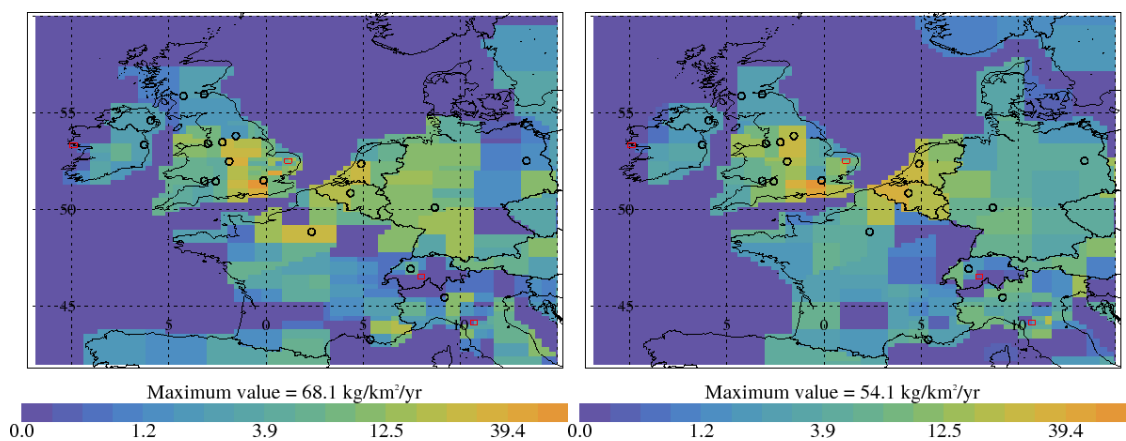| Years	Inventory 1yr	MHD	3 sites	4 sites
1994	0.508 (0.454-0.562)	0.796 (0.605-0.986)		
1995	0.828 (0.753-0.902)	0.794 (0.605-0.983)		
1996	1.146 (1.043-1.248)	0.802 (0.605-0.999)		
1997	1.700 (1.549-1.851)	0.773 (0.579-0.967)		
1998	2.27 (2.07-2.48)	0.766 (0.580-0.952)		
1999	2.202 (2.009-2.395)	0.783 (0.617-0.950)		
2000	2.53 (2.31-2.75)	0.936 (0.774-1.099)		
2001	2.87 (2.62-3.12)	1.187 (1.020-1.354)		
2002	3.02 (2.76-3.28)	1.490 (1.315-1.665)		
2003	3.49 (3.19-3.78)	1.704 (1.530-1.878)		
2004	3.68 (3.37-3.99)	1.806 (1.638-1.974)		
2005	4.15 (3.80-4.49)	1.828 (1.665-1.991)		
2006	4.30 (3.94-4.66)	1.952 (1.781-2.124)		
2007	4.36 (3.99-4.72)	2.085 (1.905-2.264)	2.32 (2.09-2.54)	
2008	4.52 (4.15-4.90)	2.216 (2.033-2.399)	2.29 (2.07-2.52)	
2009	4.69 (4.30-5.07)	2.296 (2.112-2.479)	2.30 (2.09-2.51)	
2010	4.72 (4.34-5.10)	2.251 (2.072-2.429)	2.40 (2.19-2.62)	
2011	4.58 (4.21-4.95)	2.239 (2.060-2.418)	2.32 (2.10-2.54)	
2012	4.66 (4.29-5.04)	2.167 (1.997-2.337)	2.17 (1.98-2.37)	
2013	4.68 (4.31-5.06)	2.242 (2.062-2.421)	2.34 (2.12-2.55)	2.65 (2.35-2.95)
2014	4.72 (4.34-5.10)	2.334 (2.138-2.529)	2.44 (2.21-2.68)	2.45 (2.18-2.72)
2015	4.75 (4.37-5.13)	2.44 (2.21-2.67)	2.42 (2.18-2.67)	2.44 (2.23-2.66)
2016	4.73 (4.35-5.11)	2.51 (2.24-2.77)	2.47 (2.18-2.76)	2.31 (2.00-2.63)
2017	4.64 (4.26-5.01)	2.44 (2.16-2.72)	2.37 (2.06-2.68)	2.43 (2.08-2.77)
2018		2.39 (2.11-2.68)	2.30 (1.99-2.60)	2.78 (2.49-3.08)
2019		2.30 (2.01-2.58)	2.34 (2.03-2.65)	2.13 (1.87-2.39)

Table 12: HFC-134a emission (Gg yr^{-1}) estimates for the UK with uncertainty (1std).

Years	Inventory 1yr	1s 3y	3s 2y	4s 1y
1994	2.96 (2.66-3.25)	2.48 (1.85-3.11)		
1995	3.59 (3.23-3.95)	2.54 (1.86-3.21)		
1996	5.09 (4.58-5.60)	2.89 (2.15-3.62)		
1997	6.56 (5.90-7.21)	3.51 (2.69-4.33)		
1998	7.62 (6.86-8.38)	4.39 (3.51-5.27)		
1999	7.77 (6.99-8.55)	4.91 (4.03-5.78)		
2000	8.85 (7.97-9.74)	4.84 (4.01-5.66)		
2001	10.2 (9.2-11.2)	4.90 (4.07-5.74)		
2002	11.1 (10.0-12.2)	5.14 (4.29-5.98)		
2003	12.1 (10.9-13.4)	5.76 (4.90-6.62)		
2004	12.7 (11.4-14.0)	6.15 (5.32-6.97)		
2005	13.7 (12.3-15.0)	6.57 (5.79-7.35)		
2006	14.2 (12.8-15.6)	7.25 (6.38-8.11)		
2007	14.7 (13.2-16.2)	7.53 (6.62-8.44)	7.48 (6.75-8.21)	
2008	15.0 (13.5-16.4)	7.92 (7.01-8.82)	7.02 (6.30-7.74)	
2009	15.0 (13.5-16.5)	8.23 (7.39-9.08)	6.77 (6.07-7.47)	
2010	15.3 (13.7-16.8)	8.81 (7.99-9.63)	7.06 (6.34-7.79)	
2011	15.4 (13.9-17.0)	8.93 (7.99-9.88)	7.59 (6.82-8.36)	
2012	15.5 (13.9-17.0)	8.5 (7.5-9.5)	8.17 (7.41-8.93)	
2013	15.4 (13.8-16.9)	8.0 (6.9-9.1)	7.89 (7.08-8.70)	8.68 (7.70-9.66)
2014	15.6 (14.0-17.2)	8.5 (7.3-9.6)	7.25 (6.33-8.17)	8.30 (7.20-9.50)
2015	15.8 (14.3-17.4)	9.6 (8.4-10.7)	7.54 (6.63-8.46)	9.50 (8.20-10.8)
2016	16.0 (14.4-17.6)	10.1 (8.9-11.2)	7.81 (6.96-8.66)	9.01 (8.07-9.95)
2017	15.5 (13.9-17.0)	9.7 (8.6-10.9)	7.36 (6.55-8.17)	8.20 (7.00-9.30)
2018		9.1 (8.0-10.3)	7.22 (6.44-8.00)	7.40 (6.46-8.34)
2019		9.1 (7.8-10.3)	7.29 (6.52-8.07)	8.31 (7.31-9.30)

Table 13: HFC-134a emission (Gg yr^{-1}) estimates for the NWEU with uncertainty (1std).
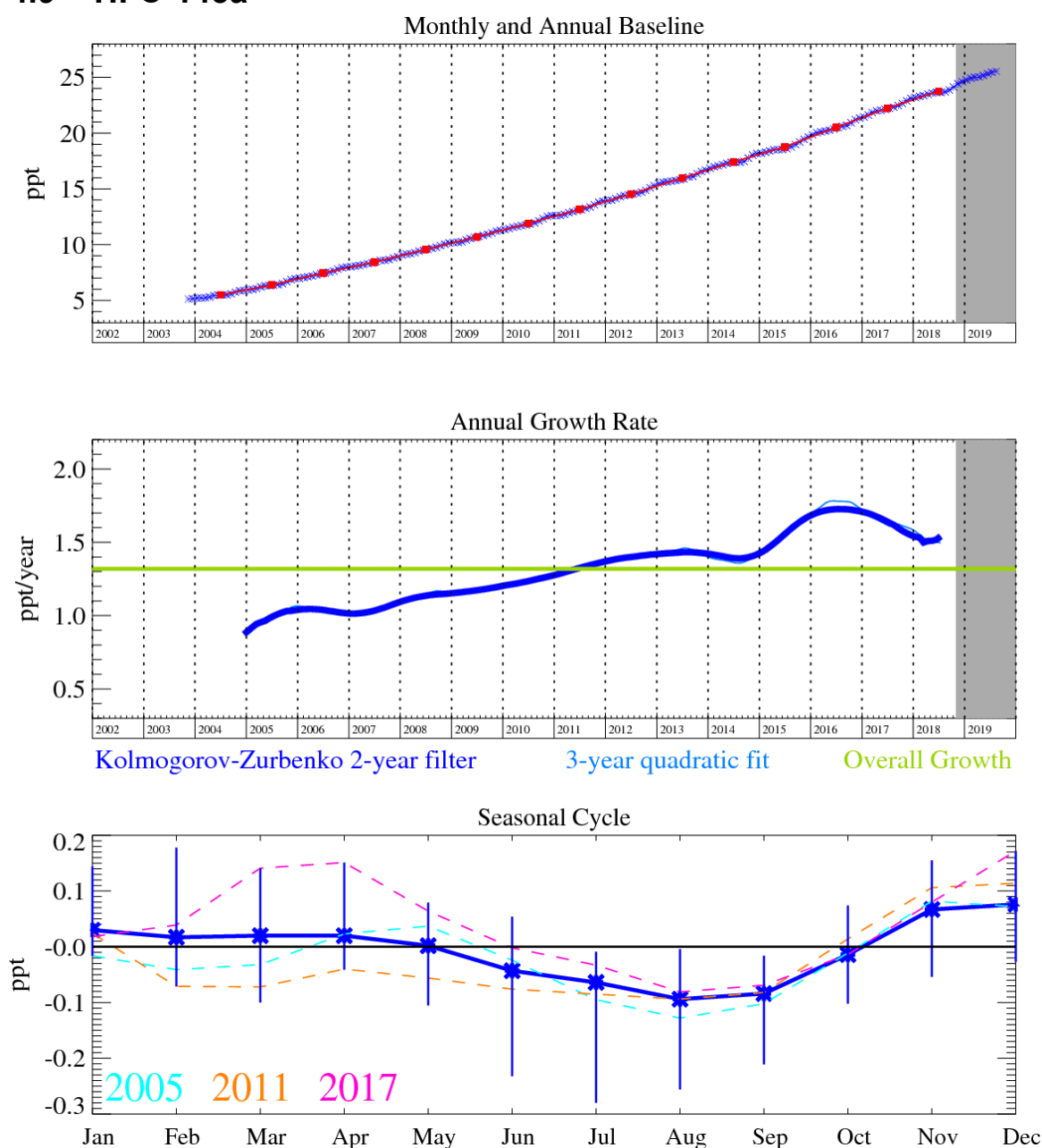
4.9 HFC-143a

Figure 34: HFC-143a: Monthly (blue) and annual (red) Northern Hemisphere baseline mole fractions (top plot). Annual (blue) and overall (green) average growth rate (middle plot). Seasonal cycle (de-trended) with year-to-year variability (lower plot). Grey area covers un-ratified provisional data.

HFC-143a (CH_3CF_3) is used mainly as a working fluid in refrigerant blends (R-404A and R-507A) for low and medium temperature commercial refrigeration systems. In 2016 the NH baseline mole exceeded 20 ppt for the first time. These levels have increased dramatically from the low levels observed in 2003 with an increasing growth rate. It has a relatively long atmospheric lifetime of 51.4 years and a significant radiative forcing value (third largest of all the HFCs) with a GWP_{100} of 4400.

There is a reasonable correlation between the inventory and the UK InTEM estimates, with the InTEM estimate being approximately 2/3rds of the inventory estimate, though this does vary over time and with the different combinations of measurement sites used for the inversions. The significant step down in the inventory in 2010-2011 is somewhat muted in the InTEM MHD-only inversions as they span 3-years. There are significant step-downs

in the inventory estimates going from 2015 to 2016 and 2016 to 2017 which are also seen in the inversion estimates. There is good agreement in 2016 but despite the downward trend in the inversion model estimates they are not as low in 2017 as the inventory estimate. The InTEM results for 2018 and 2019 indicate that UK emissions of HFC-143a are continuing to fall. Looking at NWEU emission estimates the InTEM estimates are considerably lower than the inventory estimate for 2017 and show a slight downward trend.
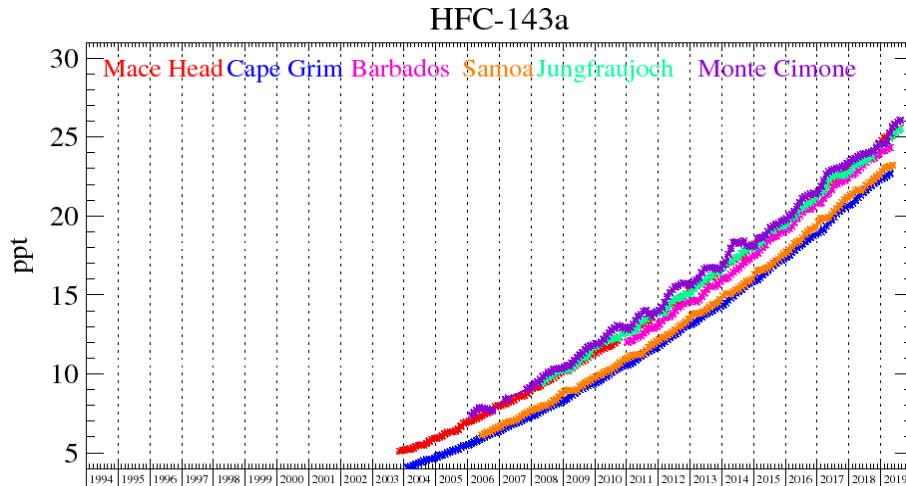
Figure 35: Background HFC-143a mole fractions at several global AGAGE stations both in the Northern and Southern Hemispheres.
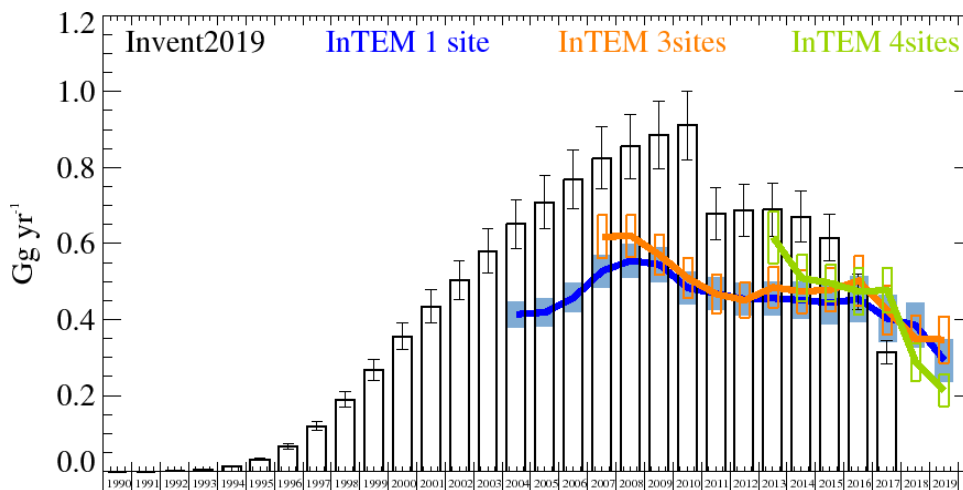
Figure 36: HFC-143a: UK emission estimates (Gg yr⁻¹) from the UNFCCC Inventory (black) and InTEM (annually averaged): (a) MHD (3yr) with global meteorology (blue), (b) 3 sites (2yr) (MHD+JFJ+CMN) with global meteorology (orange), and (c) 4 sites (1yr) (MHD+JFJ+CMN+TAC) with UKV 1.5 km nested in global meteorology (green). The uncertainty bars represent 1 std.
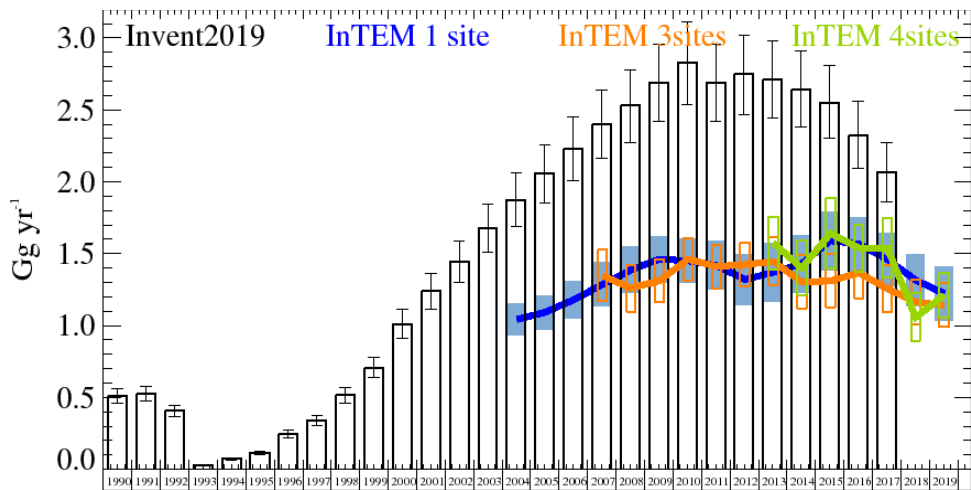
Figure 37: HFC-143a: NWEU emission estimates (Gg yr^{-1}) from the UNFCCC Inventory (black) and InTEM (annually averaged): (a) MHD (3yr) with global meteorology (blue), (b) 3 sites (2yr) (MHD+JFJ+CMN) with global meteorology (orange), and (c) 4 sites (1yr) (MHD+JFJ+CMN+TAC) with UKV 1.5 km nested in global meteorology (green). The uncertainty bars represent 1 std.

Figure 38: HFC-143a emission estimate using MHD data for 2004-2008 (left) and 2014-2018 (right). Major cities shown as black circles and observation sites shown as red rectangle.

Figure 39: HFC-143a emission estimate using data from 4 sites for 2013-2015 (left) and 2016-2018 (right). Major cities shown as black circles and observation sites shown as red rectangle.

46

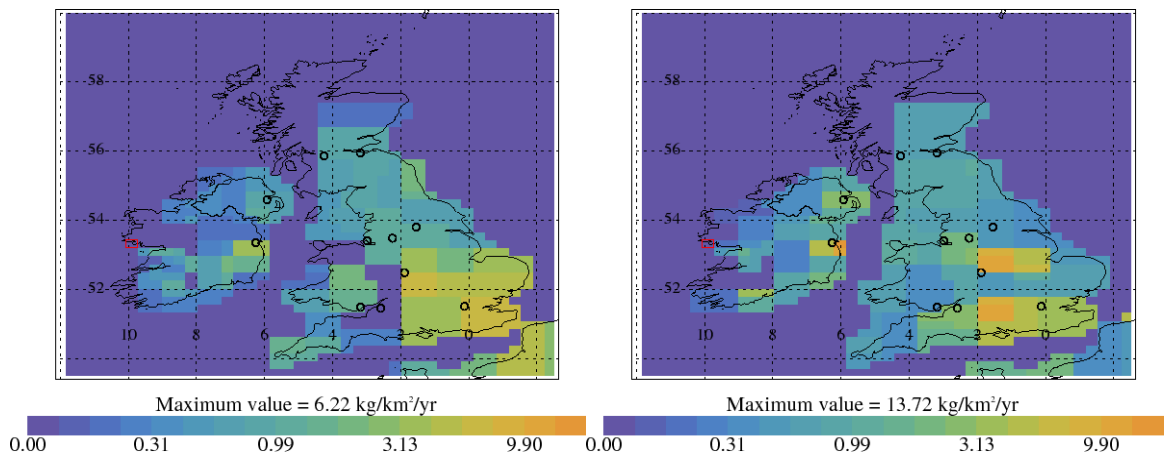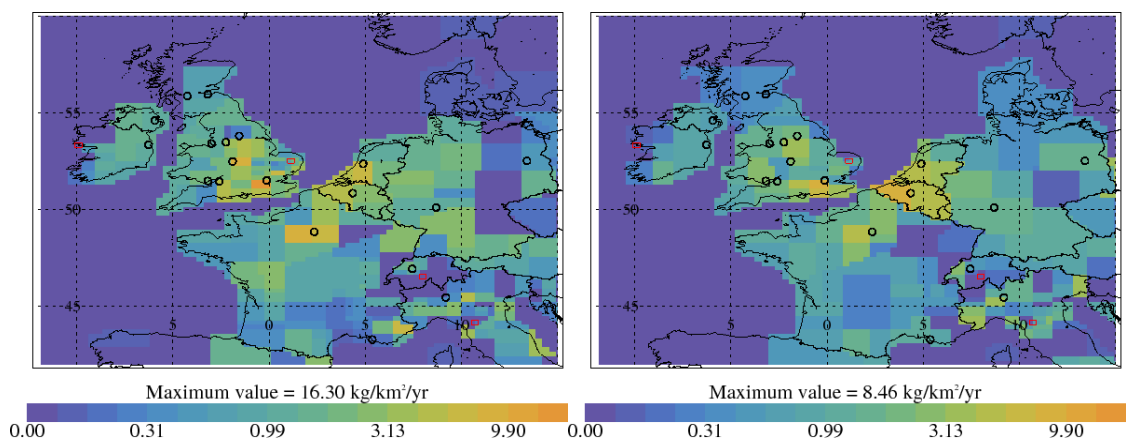| Years	Inventory 1yr	MHD	3 sites	4 sites
1994	0.0130 (0.0120-0.0140)			
1995	0.0321 (0.0289-0.0353)			
1996	0.0670 (0.0603-0.0737)			
1997	0.1194 (0.1075-0.1314)			
1998	0.1900 (0.1710-0.2091)			
1999	0.268 (0.241-0.295)			
2000	0.356 (0.320-0.391)			
2001	0.435 (0.391-0.478)			
2002	0.505 (0.454-0.555)			
2003	0.580 (0.522-0.638)			
2004	0.651 (0.586-0.716)	0.414 (0.379-0.448)		
2005	0.709 (0.638-0.780)	0.419 (0.383-0.455)		
2006	0.769 (0.692-0.846)	0.458 (0.419-0.496)		
2007	0.825 (0.743-0.908)	0.528 (0.485-0.571)	0.618 (0.561-0.675)	
2008	0.855 (0.769-0.940)	0.555 (0.510-0.600)	0.620 (0.564-0.676)	
2009	0.886 (0.797-0.974)	0.545 (0.498-0.591)	0.570 (0.518-0.623)	
2010	0.911 (0.820-1.002)	0.483 (0.439-0.527)	0.509 (0.456-0.563)	
2011	0.679 (0.611-0.746)	0.468 (0.424-0.511)	0.467 (0.416-0.518)	
2012	0.688 (0.619-0.757)	0.454 (0.413-0.496)	0.451 (0.405-0.498)	
2013	0.689 (0.620-0.758)	0.456 (0.412-0.501)	0.485 (0.431-0.539)	0.616 (0.548-0.684)
2014	0.671 (0.604-0.738)	0.451 (0.403-0.500)	0.474 (0.418-0.531)	0.509 (0.449-0.570)
2015	0.615 (0.554-0.677)	0.444 (0.388-0.499)	0.478 (0.421-0.535)	0.496 (0.449-0.543)
2016	0.474 (0.426-0.521)	0.454 (0.394-0.514)	0.502 (0.437-0.566)	0.474 (0.412-0.535)
2017	0.315 (0.283-0.346)	0.403 (0.342-0.464)	0.424 (0.360-0.488)	0.477 (0.418-0.535)
2018		0.385 (0.325-0.444)	0.350 (0.289-0.411)	0.289 (0.240-0.339)
2019		0.293 (0.237-0.350)	0.347 (0.286-0.408)	0.213 (0.171-0.255)

Table 14: HFC-143a emission (Gg yr^{-1}) estimates for the UK with uncertainty (1std).

Years	Inventory 1yr	MHD	3 sites	4sites
1994	0.074 (0.067-0.082)			
1995	0.117 (0.105-0.128)			
1996	0.245 (0.221-0.270)			
1997	0.343 (0.308-0.377)			
1998	0.515 (0.464-0.567)			
1999	0.706 (0.636-0.777)			
2000	1.012 (0.911-1.113)			
2001	1.241 (1.117-1.365)			
2002	1.446 (1.302-1.591)			
2003	1.677 (1.509-1.845)			
2004	1.875 (1.687-2.062)	1.367 (1.221-1.512)		
2005	2.06 (1.85-2.26)	1.432 (1.277-1.586)		
2006	2.23 (2.01-2.45)	1.547 (1.375-1.720)		
2007	2.40 (2.16-2.64)	1.68 (1.48-1.88)	1.713 (1.520-1.906)	
2008	2.53 (2.27-2.78)	1.82 (1.61-2.03)	1.561 (1.385-1.737)	
2009	2.69 (2.42-2.96)	1.91 (1.70-2.13)	1.503 (1.344-1.661)	
2010	2.83 (2.54-3.11)	1.90 (1.70-2.10)	1.671 (1.509-1.832)	
2011	2.69 (2.42-2.96)	1.86 (1.64-2.08)	1.745 (1.580-1.910)	
2012	2.75 (2.47-3.02)	1.73 (1.50-1.96)	1.816 (1.650-1.983)	
2013	2.71 (2.44-2.98)	1.79 (1.53-2.06)	1.801 (1.622-1.981)	2.09 (1.89-2.30)
2014	2.64 (2.38-2.91)	1.88 (1.61-2.14)	1.631 (1.437-1.824)	1.88 (1.66-2.10)
2015	2.55 (2.30-2.81)	2.08 (1.81-2.34)	1.659 (1.468-1.850)	2.15 (1.90-2.41)
2016	2.32 (2.09-2.56)	2.05 (1.81-2.30)	1.724 (1.544-1.904)	2.04 (1.86-2.22)
2017	2.07 (1.86-2.27)	1.91 (1.67-2.16)	1.541 (1.374-1.709)	1.77 (1.55-1.99)
2018		1.72 (1.49-1.96)	1.381 (1.225-1.537)	1.32 (1.15-1.49)
2019		1.60 (1.35-1.85)	1.356 (1.205-1.507)	1.45 (1.28-1.63)

Table 15: HFC-143a emission (Gg yr^{-1}) estimates for the NWEU with uncertainty (1std).

4.10 HFC-152a
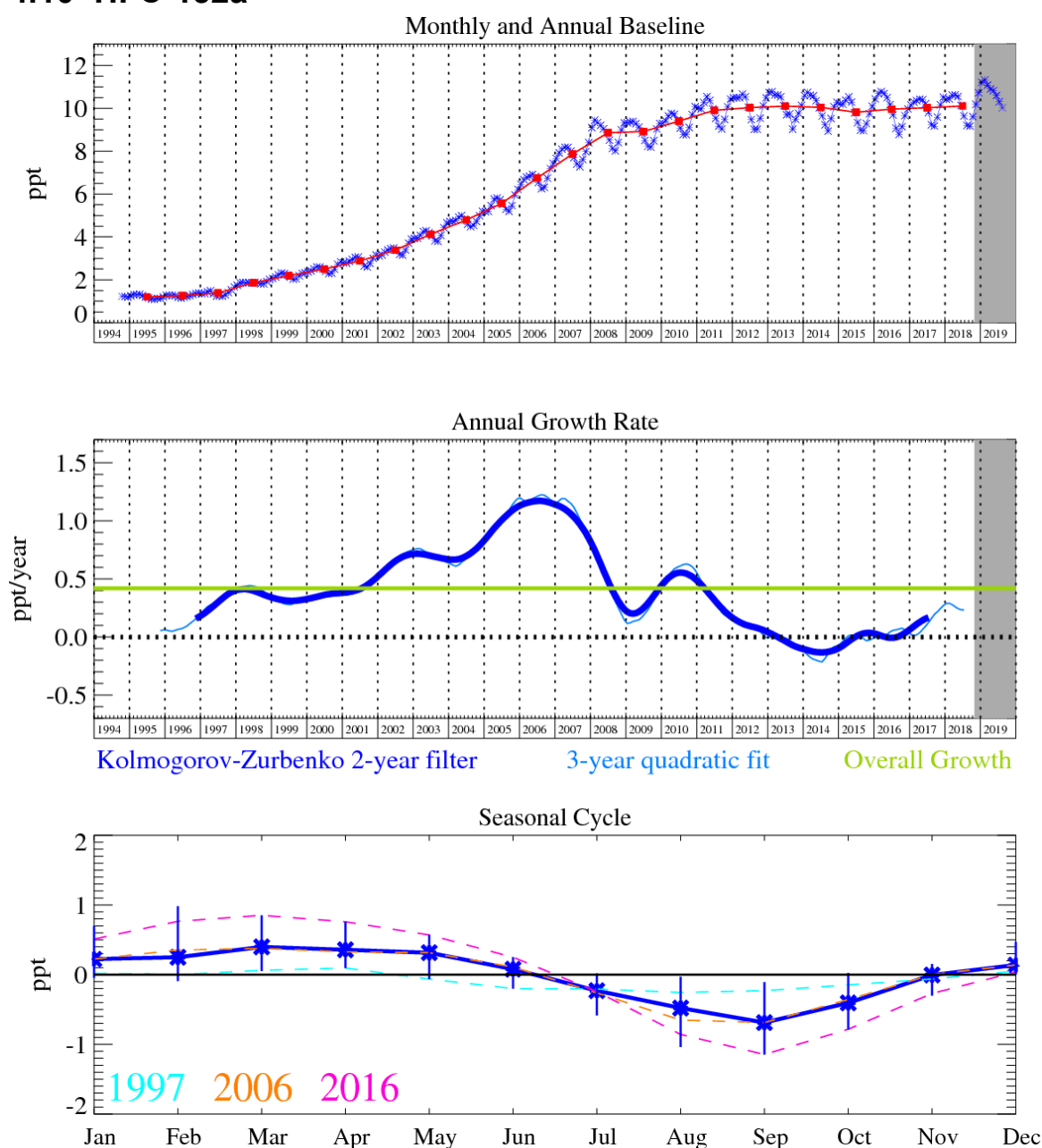
Figure 40: HFC-152a: Monthly (blue) and annual (red) Northern Hemisphere baseline mole fractions (top plot). Annual (blue) and overall (green) average growth rate (middle plot). Seasonal cycle (de-trended) with year-to-year variability (lower plot). Grey area covers un-ratified provisional data.

HFC-152a (CH_3CHF_2) has a relatively short lifetime of 1.6 years due to its efficient removal by OH oxidation in the troposphere, consequently it has the smallest GWP_{100} at 133 of all the major HFCs. It is used as a foam-blowing agent and aerosol propellant and given its short lifetime has exhibited substantial growth in the atmosphere since measurements began in 1994, implying a substantial increase in emissions in these years. However, in the last few years the rate of growth slowed considerably and is now zero to negative. The maximum NH monthly mole fraction reached was 10.7 ppt (Apr 2012).
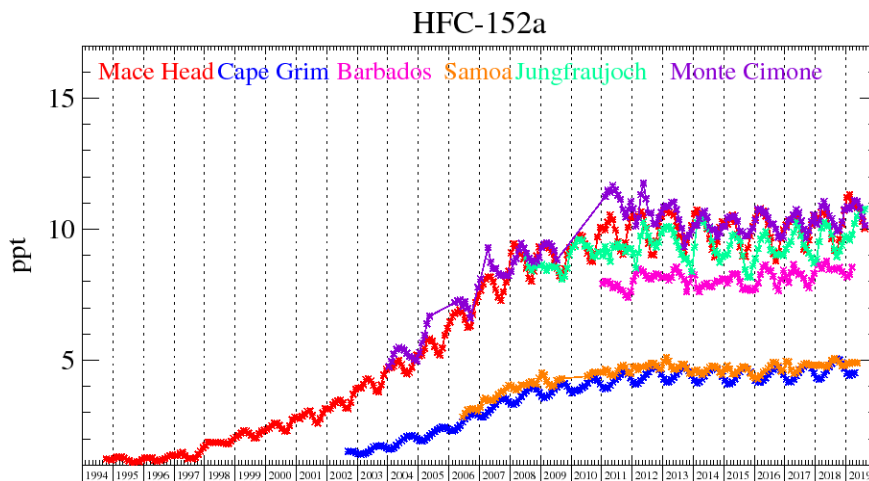
Figure 41: Background HFC-152a mole fractions at several global AGAGE stations both in the Northern and Southern Hemispheres.
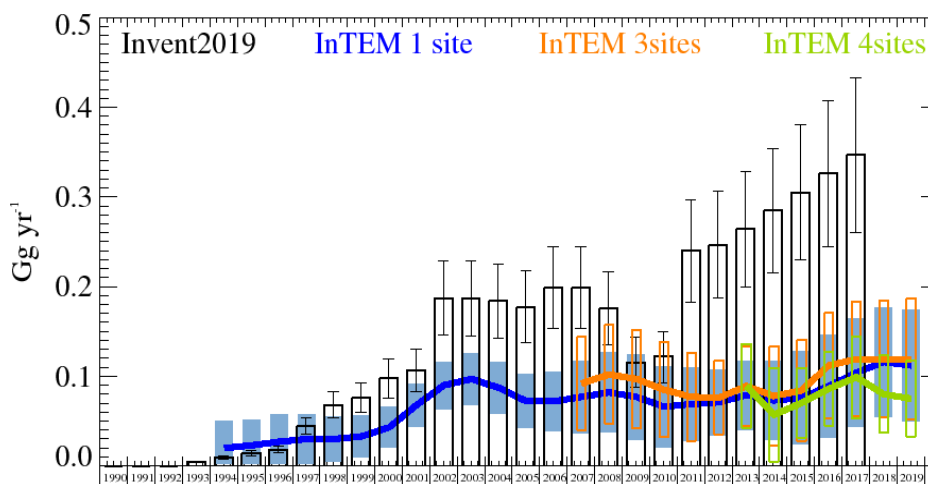
Figure 42: HFC-152a: UK emission estimates (Gg yr^{-1}) from the UNFCCC Inventory (black) and InTEM (annually averaged): (a) MHD (3yr) with global meteorology (blue), (b) 3 sites (2yr) (MHD+JFJ+CMN) with global meteorology (orange), and (c) 4 sites (1yr) (MHD+JFJ+CMN+TAC) with UKV 1.5 km nested in global meteorology (green). The uncertainty bars represent 1 std.

Figure 43: HFC-152a: NWEU emission estimates (Gg yr^{-1}) from the UNFCCC Inventory (black) and InTEM (annually averaged): (a) MHD (3yr) with global meteorology (blue), (b) 3 sites (2yr) (MHD+JFJ+CMN) with global meteorology (orange), and (c) 4 sites (1yr) (MHD+JFJ+CMN+TAC) with UKV 1.5 km nested in global meteorology (green). The uncertainty bars represent 1 std.

Maximum value = 3.35 kg/km²/yr   Maximum value = 4.07 kg/km²/yr

| 0.00 | 0.09 | 0.30 | 0.94 | 2.98 | 0.00 | 0.09 | 0.30 | 0.94 | 2.98 |

Figure 44: HFC-152a emission estimate using MHD data for 2004-2008 (left) and 2014-2018 (right). Major cities shown as black circles and observation sites shown as red rectangle.

Maximum value = 5.31 kg/km²/yr   Maximum value = 3.42 kg/km²/yr

| 0.00 | 0.09 | 0.30 | 0.95 | 2.99 | 0.00 | 0.09 | 0.30 | 0.94 | 2.98 |

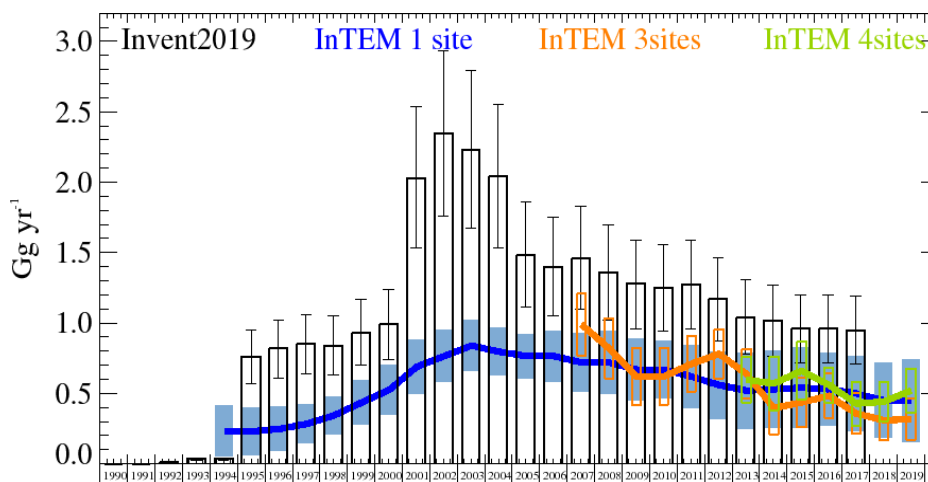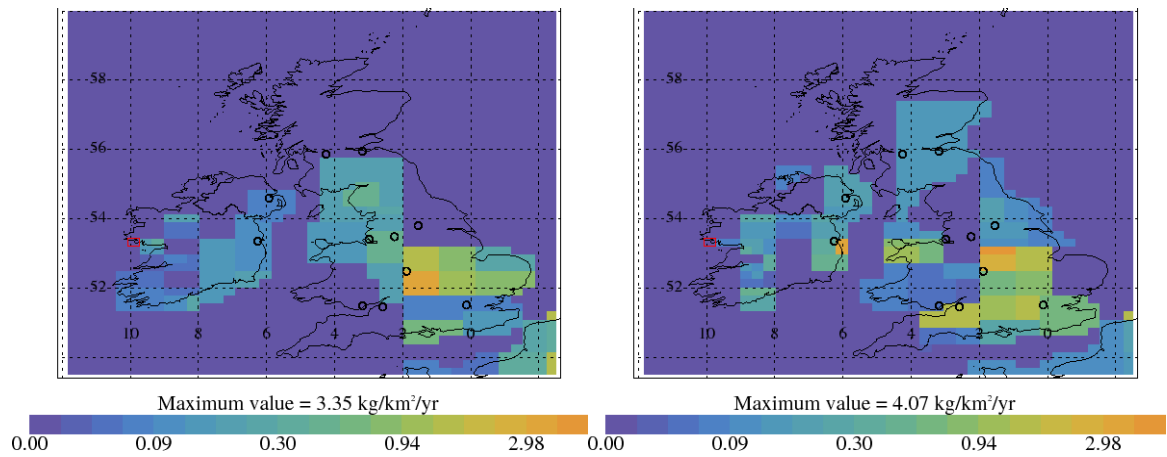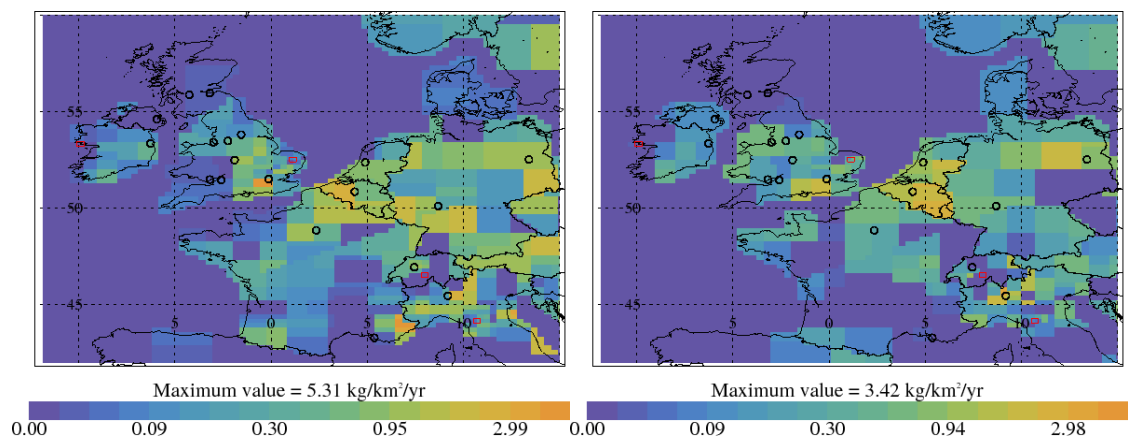**Figure 45: HFC-152a emission estimate using data from 4 sites for 2013-2015 (left) and 2016-2018 (right). Major cities shown as black circles and observation sites shown as red rectangle.**

The comparison for the UK shows that the InTEM estimates are substantially lower than the inventory although the uncertainties do overlap in the early years and in 2009 and 2010. The steadily rising UK emissions reported in the inventory are not reflected in the InTEM results. The improved InTEM resolution achieved with the additional observations estimates the UK emissions primarily come from the south although the uncertainties are large. Belgium is also estimated to be a significant source of HFC-152a. InTEM is showing a slight rise in UK emissions from 2016. The InTEM results for NWEU show a similar profile to that for the UK, however the estimates are flat or possibly declining from 2016 and whilst still underestimating the inventory they show a better agreement than for the UK and have overlapping uncertainties in recent years.

Years	Inventory 1yr	MHD	3 sites	4 sites
1994	0.0094 (0.0074-0.0113)	0.020 (0.000-0.061)		
1995	0.0141 (0.0111-0.0170)	0.023 (0.000-0.057)		
1996	0.0183 (0.0145-0.0222)	0.027 (0.000-0.060)		
1997	0.0443 (0.0349-0.0537)	0.030 (0.002-0.057)		
1998	0.0681 (0.0535-0.0827)	0.030 (0.005-0.056)		
1999	0.0757 (0.0593-0.0921)	0.033 (0.010-0.056)		
2000	0.098 (0.076-0.119)	0.043 (0.021-0.066)		
2001	0.107 (0.083-0.130)	0.068 (0.044-0.092)		
2002	0.187 (0.146-0.229)	0.090 (0.063-0.116)		
2003	0.187 (0.145-0.229)	0.097 (0.068-0.125)		
2004	0.184 (0.142-0.225)	0.087 (0.058-0.116)		
2005	0.177 (0.137-0.218)	0.072 (0.042-0.102)		
2006	0.199 (0.153-0.245)	0.072 (0.039-0.106)		
2007	0.199 (0.153-0.245)	0.077 (0.037-0.117)	0.092 (0.040-0.144)	
2008	0.176 (0.135-0.217)	0.082 (0.037-0.126)	0.102 (0.047-0.157)	
2009	0.115 (0.088-0.143)	0.077 (0.029-0.124)	0.097 (0.042-0.151)	
2010	0.122 (0.093-0.150)	0.066 (0.021-0.111)	0.085 (0.032-0.138)	
2011	0.240 (0.183-0.297)	0.069 (0.028-0.110)	0.077 (0.027-0.126)	
2012	0.246 (0.187-0.306)	0.071 (0.034-0.107)	0.076 (0.035-0.117)	
2013	0.264 (0.200-0.328)	0.079 (0.041-0.118)	0.089 (0.045-0.133)	0.089 (0.042-0.136)
2014	0.285 (0.215-0.354)	0.073 (0.029-0.117)	0.078 (0.023-0.133)	0.057 (0.004-0.109)
2015	0.305 (0.230-0.381)	0.076 (0.024-0.128)	0.084 (0.028-0.140)	0.070 (0.031-0.108)
2016	0.326 (0.245-0.407)	0.089 (0.032-0.146)	0.112 (0.053-0.170)	0.086 (0.044-0.127)
2017	0.347 (0.260-0.433)	0.104 (0.044-0.164)	0.119 (0.056-0.183)	0.099 (0.053-0.144)
2018		0.116 (0.055-0.177)	0.119 (0.054-0.184)	0.080 (0.037-0.123)
2019		0.112 (0.050-0.174)	0.119 (0.052-0.187)	0.075 (0.033-0.118)

Table 16: HFC-152a emission (Gg yr^{-1}) estimates for the UK with uncertainty (1std).

Years	Inventory 1yr	MHD	3 sites	4 sites
1994	0.0340 (0.0255-0.0425)	0.234 (0.054-0.414)		
1995	0.763 (0.572-0.954)	0.231 (0.065-0.397)		
1996	0.82 (0.61-1.02)	0.247 (0.090-0.404)		
1997	0.85 (0.64-1.06)	0.284 (0.144-0.424)		
1998	0.84 (0.63-1.05)	0.344 (0.208-0.480)		
1999	0.93 (0.70-1.17)	0.435 (0.277-0.593)		
2000	0.99 (0.74-1.24)	0.525 (0.347-0.702)		
2001	2.03 (1.53-2.54)	0.689 (0.496-0.881)		
2002	2.35 (1.76-2.93)	0.765 (0.579-0.951)		
2003	2.23 (1.67-2.79)	0.840 (0.662-1.018)		
2004	2.04 (1.53-2.55)	0.796 (0.627-0.964)		
2005	1.48 (1.11-1.86)	0.765 (0.606-0.924)		
2006	1.40 (1.05-1.75)	0.765 (0.585-0.946)		
2007	1.46 (1.10-1.83)	0.72 (0.51-0.92)	0.99 (0.77-1.21)	
2008	1.36 (1.02-1.70)	0.72 (0.50-0.94)	0.82 (0.61-1.04)	
2009	1.28 (0.96-1.59)	0.67 (0.45-0.89)	0.62 (0.42-0.82)	
2010	1.25 (0.94-1.56)	0.67 (0.46-0.87)	0.62 (0.42-0.82)	
2011	1.27 (0.96-1.59)	0.62 (0.39-0.84)	0.710 (0.511-0.909)	
2012	1.17 (0.87-1.46)	0.56 (0.32-0.80)	0.781 (0.607-0.955)	
2013	1.04 (0.78-1.31)	0.52 (0.25-0.79)	0.638 (0.464-0.812)	0.597 (0.433-0.761)
2014	1.02 (0.76-1.27)	0.53 (0.25-0.80)	0.396 (0.211-0.582)	0.570 (0.380-0.760)
2015	0.96 (0.72-1.20)	0.54 (0.26-0.83)	0.435 (0.258-0.611)	0.66 (0.46-0.87)
2016	0.96 (0.72-1.20)	0.53 (0.27-0.79)	0.483 (0.324-0.641)	0.561 (0.436-0.685)
2017	0.95 (0.71-1.19)	0.50 (0.23-0.76)	0.357 (0.215-0.500)	0.428 (0.272-0.584)
2018		0.45 (0.19-0.72)	0.310 (0.167-0.454)	0.441 (0.301-0.580)
2019		0.45 (0.15-0.74)	0.316 (0.169-0.463)	0.521 (0.366-0.677)

Table 17: HFC-152a emission (Gg yr^{-1}) estimates for the NWEU with uncertainty (1std).
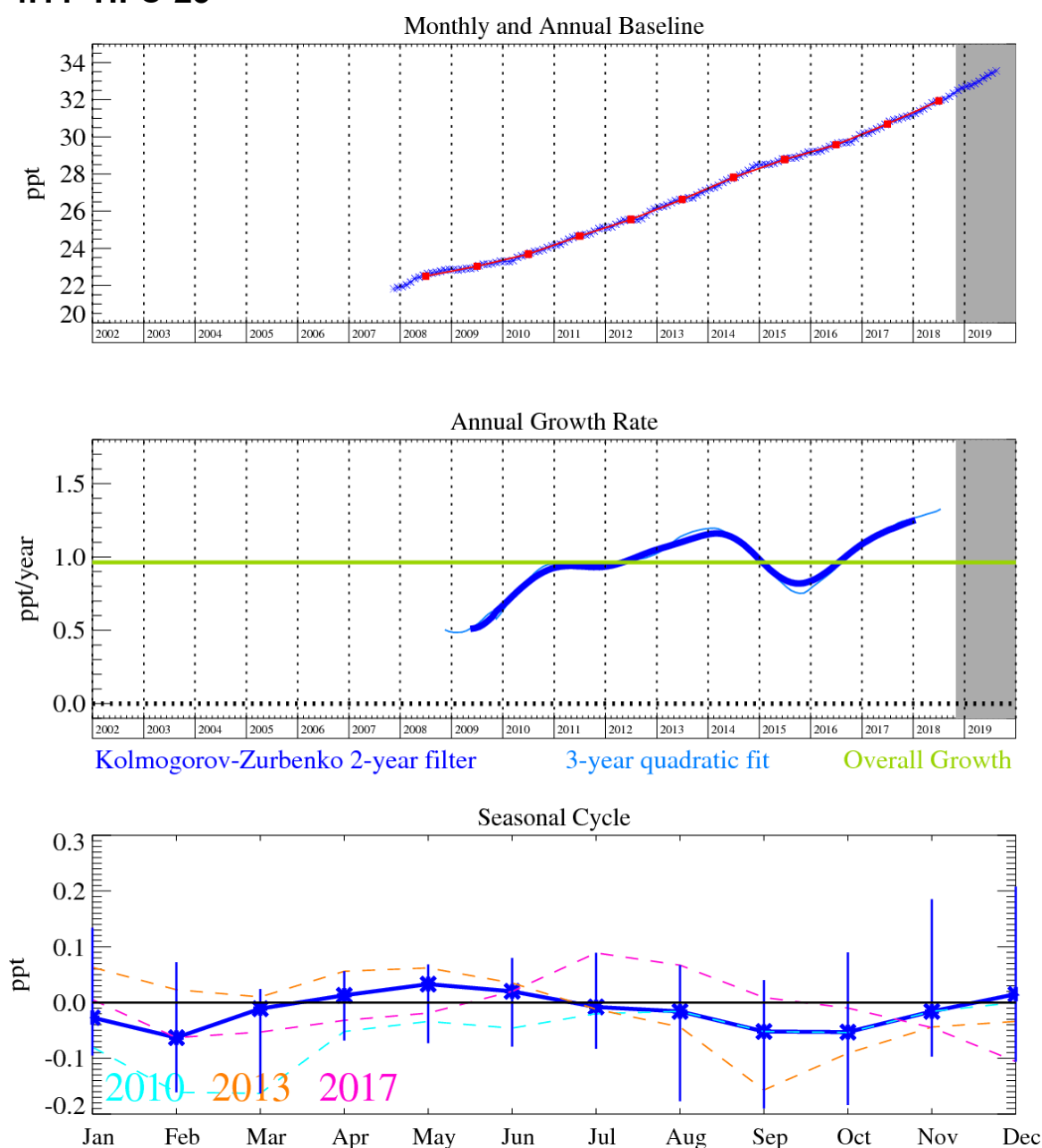
4.11 HFC-23

Figure 46: HFC-23: Monthly (blue) and annual (red) Northern Hemisphere baseline mole fractions (top plot). Annual (blue) and overall (green) average growth rate (middle plot). Seasonal cycle (de-trended) with year-to-year variability (lower plot). Grey area covers un-ratified provisional data.

HFC-23 (CHF$_3$) is primarily a by-product formed by the over fluorination of chloroform during the production of HCFC-22. Other minor emissions arise from the electronic industry and fire extinguishers. It is the second most abundant HFC in the atmosphere after HFC-134a; this, combined with a long atmospheric lifetime of 228 years, makes this compound a potent GHG. Emissions of HFC-23 in developed countries have declined due to the Montreal Protocol phase-out schedule for HCFC-22; however, emissions from developing countries continues to drive global atmospheric concentrations up.

The InTEM estimates for the UK over-estimate the inventory and the uncertainty ranges do not overlap, however, the emissions are very small. There are no clear geographical areas where the emissions are particularly strong. The annual results for NWEU are very similar, with possible increased emissions showing in Belgium and Northern Italy.
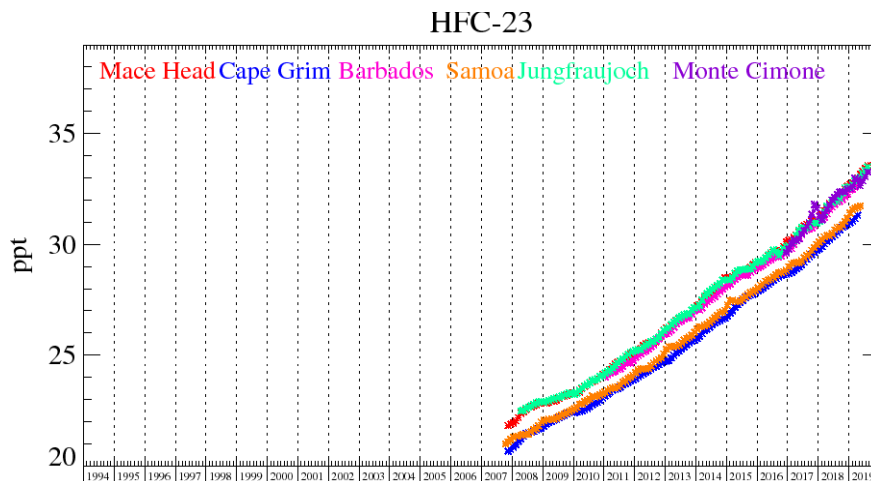
Figure 47: Background HFC-23 mole fractions at several global AGAGE stations both in the Northern and Southern Hemispheres.

Figure 48: HFC-23: UK emission estimates (Gg yr⁻¹) from the UNFCCC Inventory (black) and InTEM (annually averaged): (a) MHD (3yr) with global meteorology (blue), (b) 3 sites (2yr) (MHD+JFJ+CMN) with global meteorology (orange), and (c) 4 sites (1yr) (MHD+JFJ+CMN+TAC) with UKV 1.5 km nested in global meteorology (green). The uncertainty bars represent 1 std.
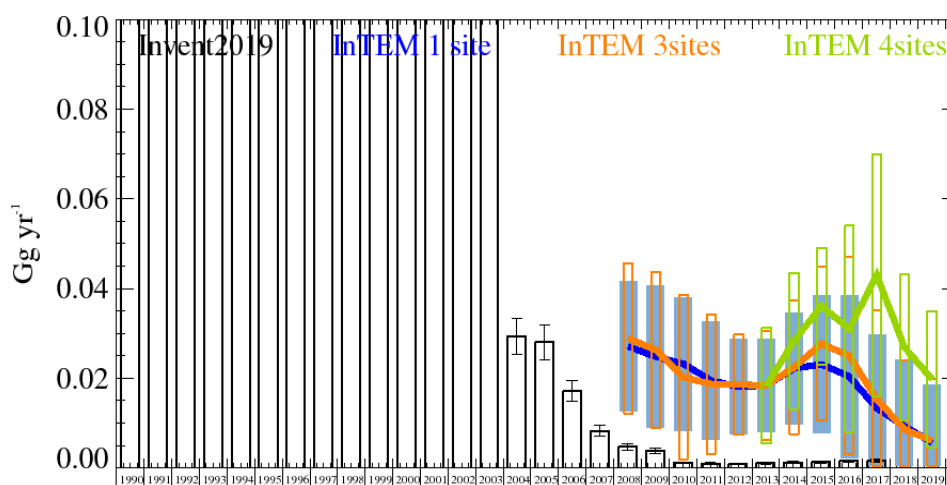
Figure 49: HFC-23: (Expanded Y-axis) UK emission estimates (Gg yr⁻¹) from the UNFCCC Inventory (black) and InTEM (annually averaged): (a) MHD (3yr) with global meteorology (blue), (b) 3 sites (2yr) (MHD+JFJ+CMN) with global meteorology (orange), and (c) 4 sites (1yr) (MHD+JFJ+CMN+TAC) with UKV 1.5 km nested in global meteorology (green). The uncertainty bars represent 1 std.
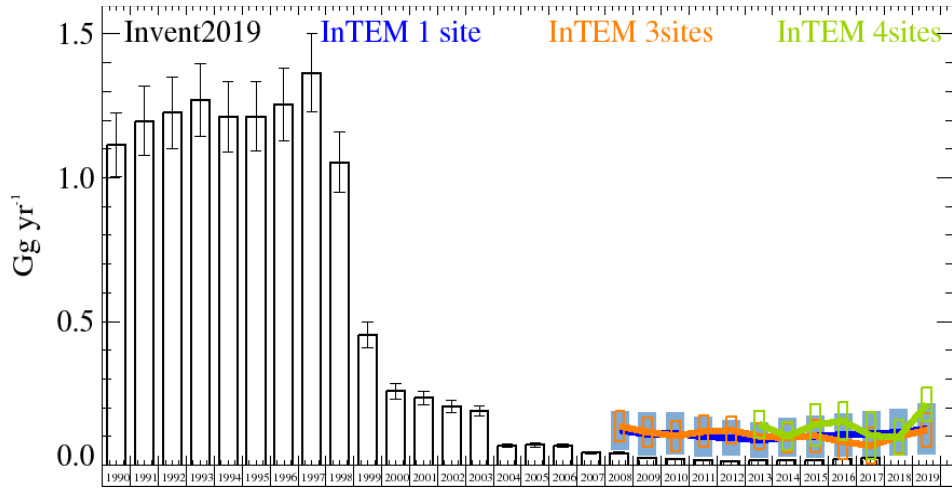
Figure 50: HFC-23: NWEU emission estimates (Gg yr⁻¹) from the UNFCCC Inventory (black) and InTEM (annually averaged): (a) MHD (3yr) with global meteorology (blue), (b) 3 sites (2yr) (MHD+JFJ+CMN) with global meteorology (orange), and (c) 4 sites (1yr) (MHD+JFJ+CMN+TAC) with UKV 1.5 km nested in global meteorology (green). The uncertainty bars represent 1 std.

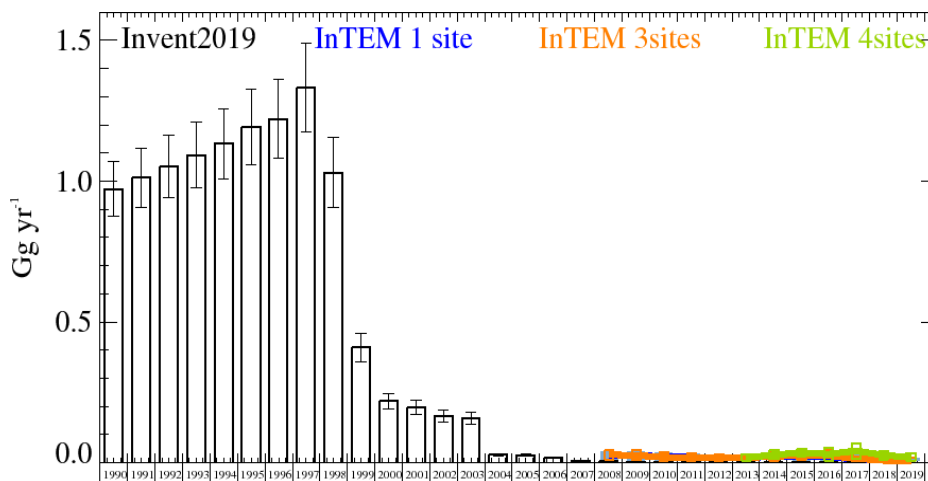**Figure 51: HFC-23: (Expanded Y-axis) NWEU emission estimates (Gg yr⁻¹) from the UNFCCC Inventory (black) and InTEM (annually averaged): (a) MHD (3yr) with global meteorology (blue), (b) 3 sites (2yr) (MHD+JFJ+CMN) with global meteorology (orange), and (c) 4 sites (1yr) (MHD+JFJ+CMN+TAC) with UKV 1.5 km nested in global meteorology (green). The uncertainty bars represent 1 std.**
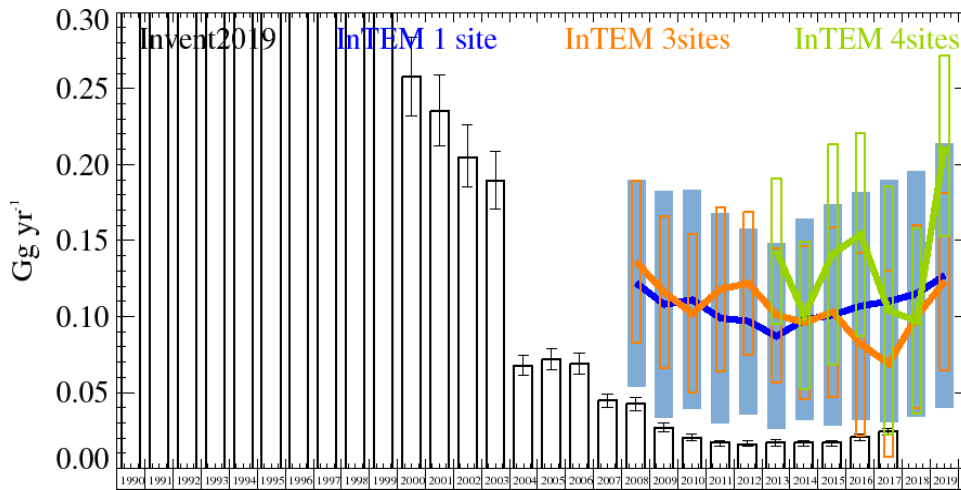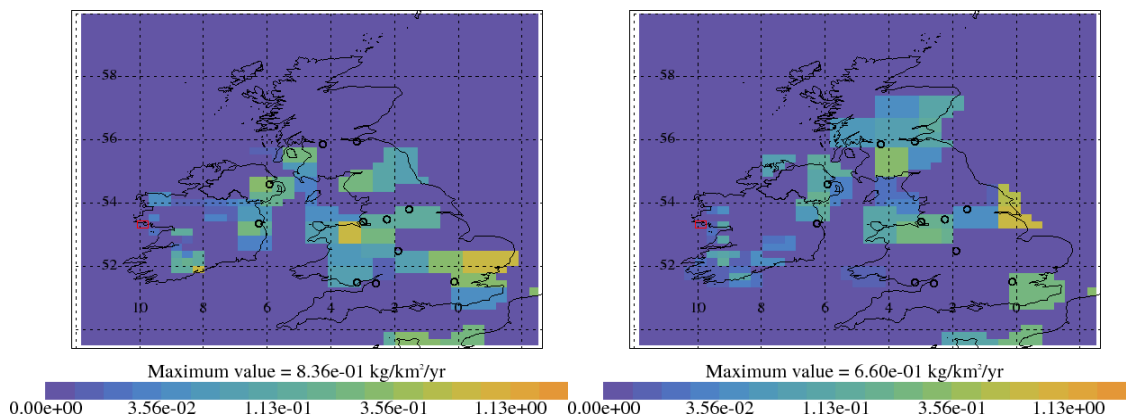

Figure 52: HFC-23 emission estimate using MHD data for 2008-2012 (left) and 2014-2018 (right). Major cities shown as black circles and observation sites shown as red rectangle.

54
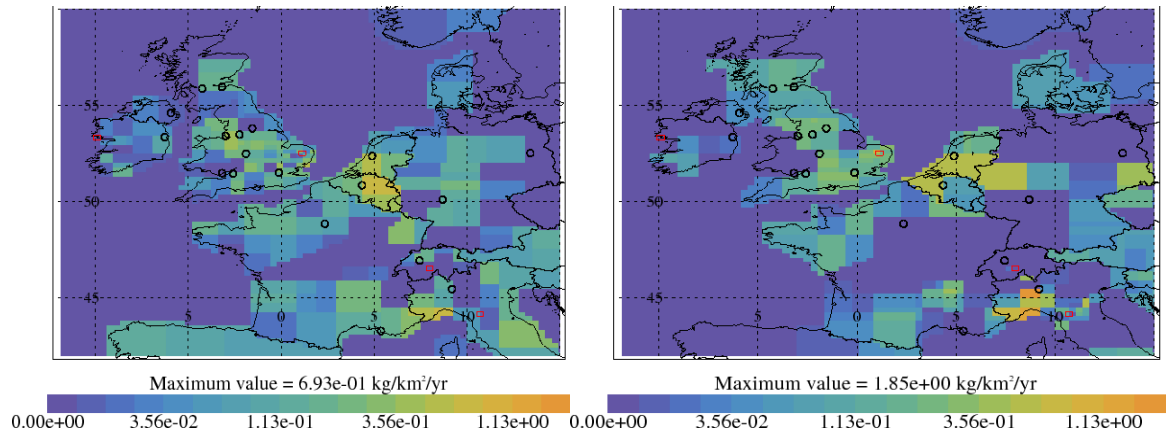
Figure 53: HFC-23 emission estimate using data from 4 sites for 2013-2015 (left) and 2016-2018 (right). Major cities shown as black circles and observation sites shown as red rectangle.

Years	Inventory 1yr	MHD	3 sites	4 sites
1990	0.972 (0.875-1.070)			
1991	1.012 (0.908-1.116)			
1992	1.052 (0.942-1.163)			
1993	1.092 (0.975-1.210)			
1994	1.133 (1.008-1.258)			
1995	1.193 (1.058-1.327)			
1996	1.221 (1.080-1.362)			
1997	1.331 (1.174-1.488)			
1998	1.030 (0.906-1.155)			
1999	0.410 (0.359-0.460)			
2000	0.219 (0.191-0.247)			
2001	0.197 (0.172-0.222)			
2002	0.165 (0.144-0.187)			
2003	0.159 (0.138-0.180)			
2004	0.0294 (0.0254-0.0334)			
2005	0.0280 (0.0241-0.0319)			
2006	0.0172 (0.0148-0.0196)			
2007	0.0083 (0.0071-0.0095)			
2008	0.0047 (0.0040-0.0054)	0.0271 (0.0126-0.0416)	0.0289 (0.0121-0.0457)	
2009	0.0038 (0.0032-0.0044)	0.0248 (0.0089-0.0407)	0.0263 (0.0090-0.0436)	
2010	0.0011 (0.0010-0.0013)	0.0232 (0.0083-0.0381)	0.0202 (0.0019-0.0385)	
2011	0.0010 (0.0009-0.0012)	0.0195 (0.0063-0.0327)	0.0187 (0.0031-0.0343)	
2012	0.0009 (0.0008-0.0010)	0.0181 (0.0075-0.0287)	0.0186 (0.0074-0.0298)	
2013	0.0010 (0.0009-0.0012)	0.0184 (0.0081-0.0287)	0.0184 (0.0063-0.0305)	0.0183 (0.0054-0.0312)
2014	0.0012 (0.0010-0.0014)	0.0222 (0.0097-0.0347)	0.0224 (0.0075-0.0373)	0.0283 (0.0131-0.0435)
2015	0.0014 (0.0011-0.0016)	0.0231 (0.0078-0.0384)	0.0277 (0.0105-0.0449)	0.0361 (0.0231-0.0491)
2016	0.0015 (0.0012-0.0017)	0.0204 (0.0022-0.0386)	0.0250 (0.0030-0.0470)	0.0310 (0.0080-0.0540)
2017	0.0016 (0.0013-0.0019)	0.0133 (0.0000-0.0329)	0.0153 (0.0000-0.0395)	0.0430 (0.0160-0.0700)
2018		0.0093 (0.0000-0.0297)	0.0086 (0.0000-0.0310)	0.0269 (0.0105-0.0433)
2019		0.0057 (0.0000-0.0259)	0.0061 (0.0000-0.0275)	0.0198 (0.0046-0.0350)

Table 18: HFC-23 emission (Gg yr^{-1}) estimates for the UK with uncertainty (1std).

Years	Inventory 1yr	MHD	3 sites	4 sites
1990	1.114 (1.003-1.226)			
1991	1.197 (1.077-1.317)			
1992	1.226 (1.103-1.349)			
1993	1.270 (1.143-1.397)			
1994	1.213 (1.091-1.334)			
1995	1.213 (1.092-1.335)			
1996	1.256 (1.130-1.381)			
1997	1.365 (1.229-1.502)			
1998	1.054 (0.949-1.160)			
1999	0.453 (0.408-0.499)			
2000	0.258 (0.232-0.284)			
2001	0.235 (0.212-0.259)			
2002	0.205 (0.185-0.226)			
2003	0.189 (0.171-0.208)			
2004	0.068 (0.061-0.075)			
2005	0.072 (0.065-0.079)			
2006	0.069 (0.062-0.076)			
2007	0.045 (0.040-0.049)			
2008	0.043 (0.038-0.047)	0.122 (0.054-0.190)	0.136 (0.083-0.189)	
2009	0.027 (0.024-0.030)	0.108 (0.034-0.183)	0.116 (0.066-0.166)	
2010	0.020 (0.018-0.022)	0.111 (0.039-0.183)	0.102 (0.050-0.154)	
2011	0.017 (0.015-0.018)	0.099 (0.030-0.168)	0.118 (0.064-0.172)	
2012	0.016 (0.015-0.018)	0.097 (0.036-0.158)	0.122 (0.075-0.169)	
2013	0.017 (0.015-0.019)	0.087 (0.026-0.148)	0.101 (0.057-0.145)	0.143 (0.095-0.191)
2014	0.017 (0.015-0.018)	0.098 (0.032-0.164)	0.096 (0.046-0.146)	0.101 (0.053-0.150)
2015	0.017 (0.015-0.018)	0.101 (0.028-0.173)	0.103 (0.047-0.159)	0.141 (0.069-0.214)
2016	0.021 (0.019-0.023)	0.107 (0.032-0.182)	0.082 (0.022-0.142)	0.154 (0.087-0.221)
2017	0.024 (0.022-0.027)	0.110 (0.030-0.189)	0.069 (0.008-0.131)	0.104 (0.022-0.185)
2018		0.115 (0.035-0.196)	0.100 (0.040-0.160)	0.097 (0.036-0.158)
2019		0.127 (0.040-0.214)	0.123 (0.065-0.181)	0.212 (0.153-0.272)

Table 19: HFC-23 emission (Gg yr^{-1}) estimates for the NWEU with uncertainty (1std).

4.12 HFC-32
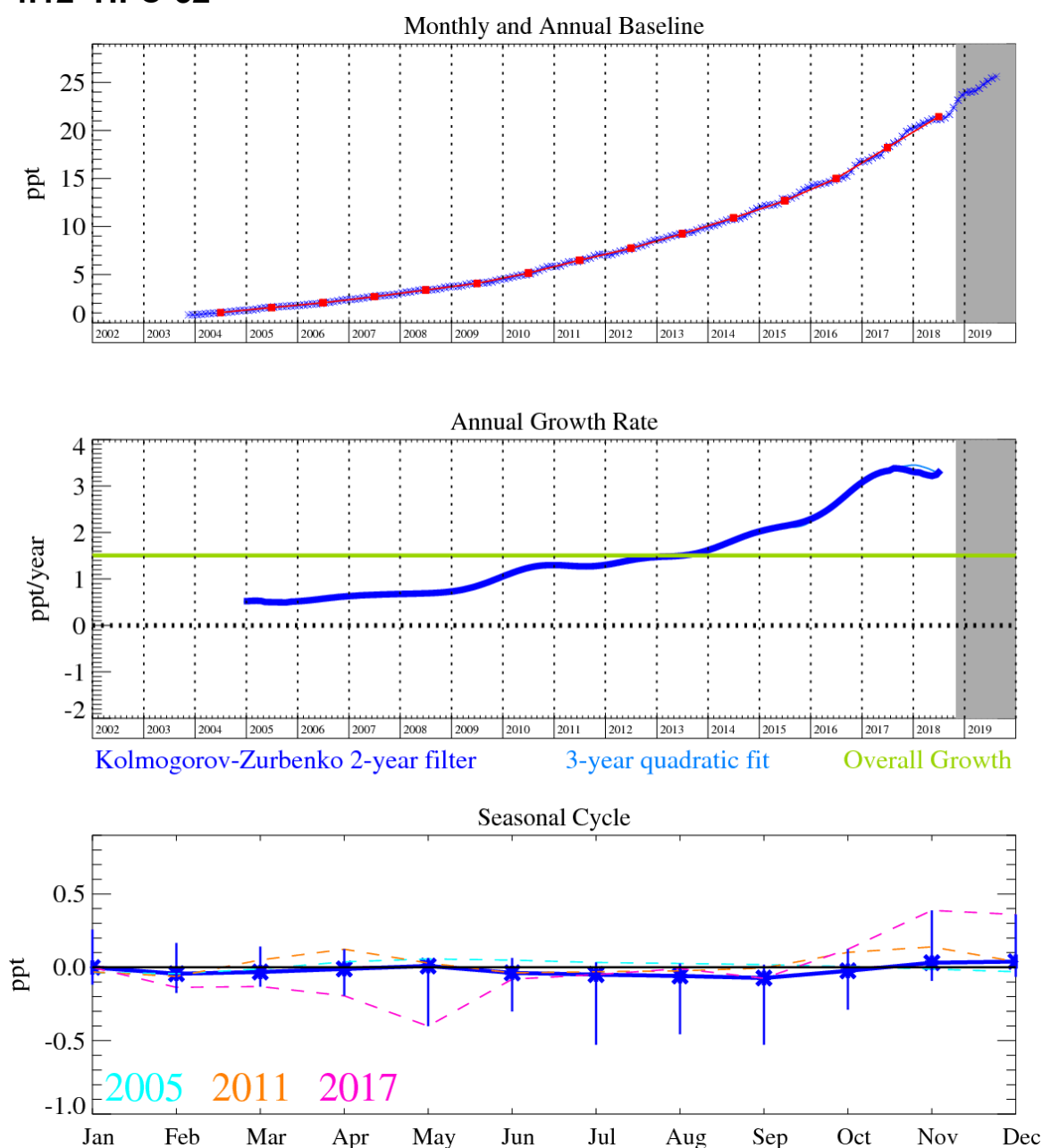
Figure 54: HFC-32: Monthly (blue) and annual (red) Northern Hemisphere baseline mole fractions (top plot). Annual (blue) and overall (green) average growth rate (middle plot). Seasonal cycle (de-trended) with year-to-year variability (lower plot). Grey area covers un-ratified provisional data.

HFC-32 (CH_2F_2) has an atmospheric lifetime of 5.4 years and a GWP_{100} of 716. It is used in air conditioning and refrigeration applications; R-410A (50% HFC-32, 50% HFC-125 by weight) and R-407C (23% HFC-32, 52% HFC-134a, 25% HFC-125 by weight) are used as replacements to HCFC-22. As the phase-out of HCFC-22 gains momentum it might be expected that demand for these refrigerant blends will increase. The pollution events measured at Mace Head are highly correlated with those of HFC-125.

Unfortunately, the observations of HFC-32 at Mace Head, like those of HFC-125, were compromised by contamination from the air conditioning system (May 2014 – June 2015) and these data had to be removed. Like HFC-125, during this period the NH baseline has been estimated using another AGAGE NH station, Zeppelin (Ny-Ålesund).
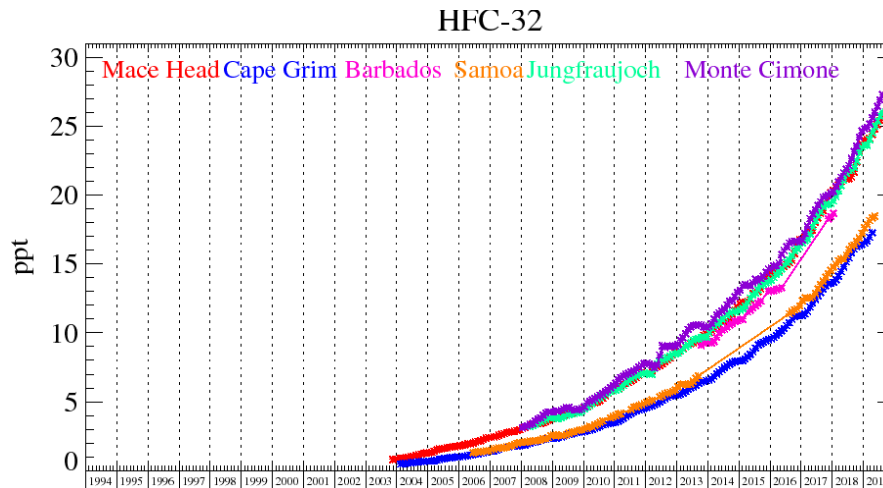
Figure 55: Background HFC-32 mole fractions at several global AGAGE stations both in the Northern and Southern Hemispheres.
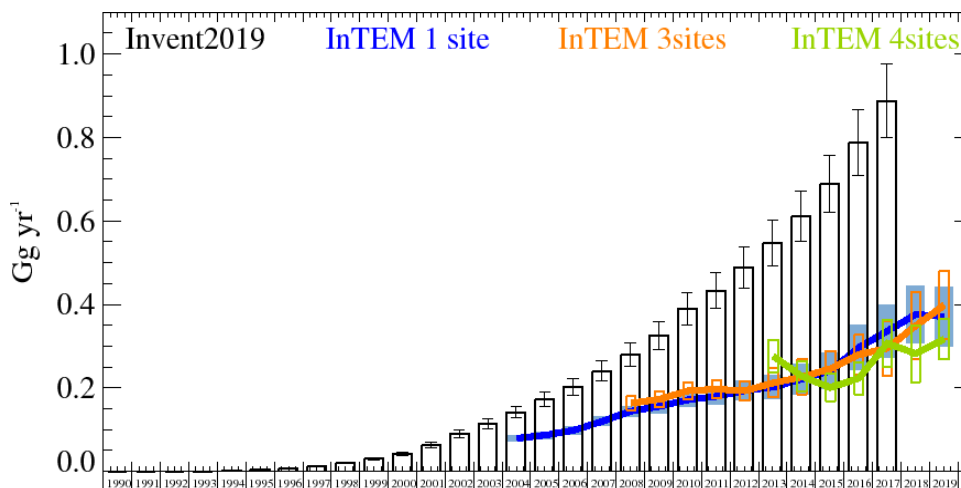
Figure 56: HFC-32: UK emission estimates (Gg yr^{-1}) from the UNFCCC Inventory (black) and InTEM (annually averaged): (a) MHD (3yr) with global meteorology (blue), (b) 3 sites (2yr) (MHD+JFJ+CMN) with global meteorology (orange), and (c) 4 sites (1yr) (MHD+JFJ+CMN+TAC) with UKV 1.5 km nested in global meteorology (green). The uncertainty bars represent 1 std.

The UK inventory estimates grow throughout the time-series. The InTEM estimates using only MHD data are increasing throughout. The InTEM estimates for the UK using the additional observations at 3 sites show very similar results. The estimates made including 4 sites is much less smooth and doesn't show such a pronounced increase. These inversions are 1 year only which is likely to account for the less smooth result and are also using UKV meteorology rather than global. The reason for the difference between the inventory and InTEM results warrant some further investigation. The InTEM results using either data set are lower than the inventory estimates and the uncertainties do not overlap. The emissions are broadly population based.
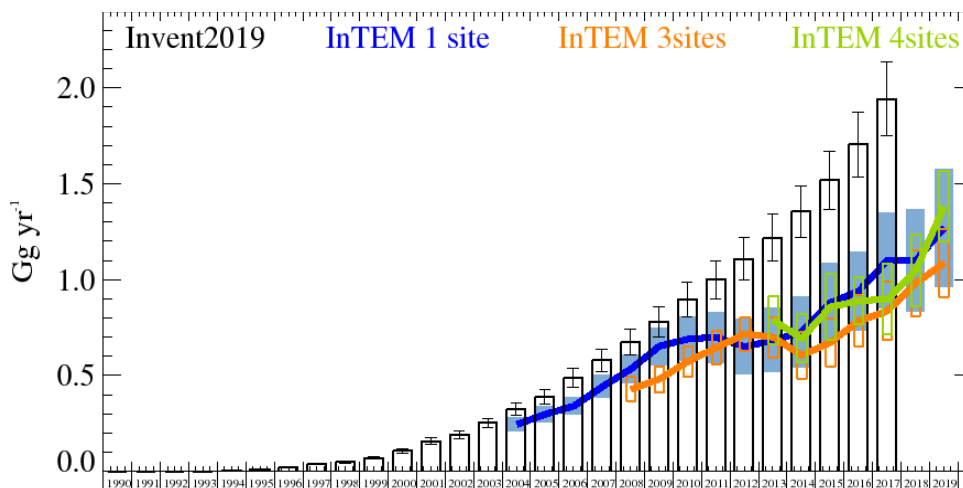
Figure 57: HFC-32: NWEU emission estimates (Gg yr^{-1}) from the UNFCCC Inventory (black) and InTEM (annually averaged): (a) MHD (3yr) with global meteorology (blue), (b) 3 sites (2yr) (MHD+JFJ+CMN) with global meteorology (orange), and (c) 4 sites (1yr) (MHD+JFJ+CMN+TAC) with UKV 1.5 km nested in global meteorology (green). The uncertainty bars represent 1 std.

Figure 58: HFC-32 emission estimate using MHD data for 2004-2008 (left) and 2014-2018 (right). Major cities shown as black circles and observation sites shown as red rectangle.

Figure 59: HFC-32 emission estimate using data from 4 sites for 2013-2015 (left) and 2016-2018 (right). Major cities shown as black circles and observation sites shown as red rectangle.

59

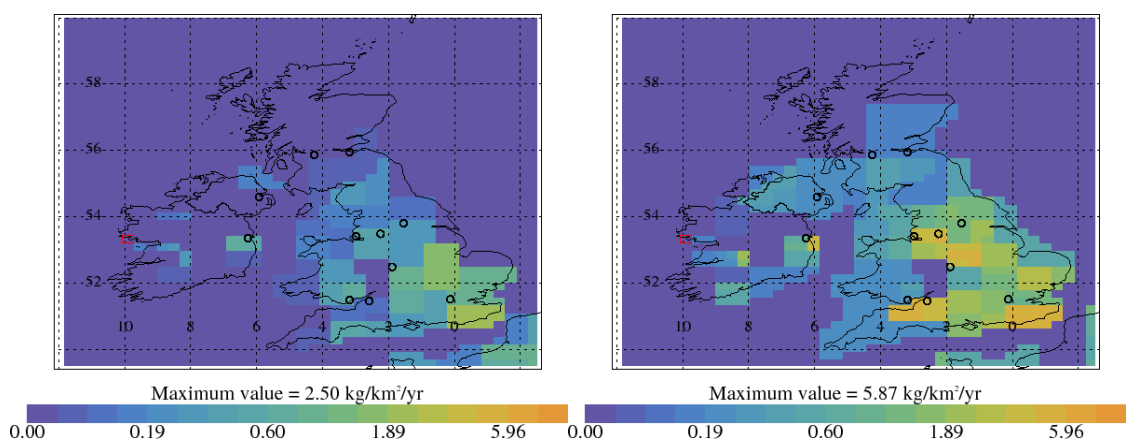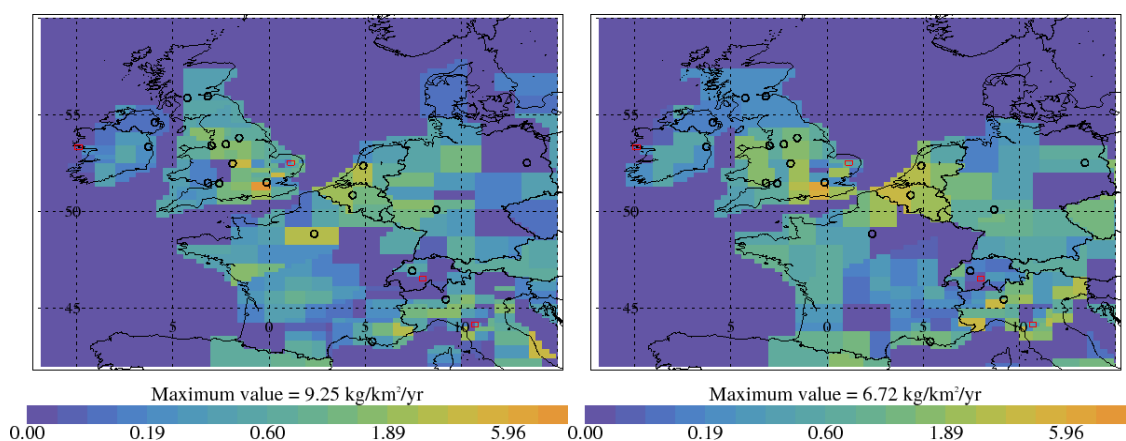| Years	Inventory 1yr	MHD	3 sites	4 sites
1994	0.0013 (0.0012-0.0014)			
1995	0.0033 (0.0030-0.0037)			
1996	0.0071 (0.0064-0.0079)			
1997	0.013 (0.011-0.014)			
1998	0.020 (0.018-0.021)			
1999	0.0308 (0.0277-0.0338)			
2000	0.0429 (0.0386-0.0471)			
2001	0.0626 (0.0563-0.0688)			
2002	0.0898 (0.0808-0.0988)			
2003	0.1141 (0.1027-0.1255)			
2004	0.1421 (0.1279-0.1563)	0.080 (0.071-0.088)		
2005	0.1723 (0.1551-0.1895)	0.087 (0.078-0.096)		
2006	0.203 (0.183-0.223)	0.099 (0.089-0.108)		
2007	0.240 (0.216-0.264)	0.120 (0.109-0.131)		
2008	0.280 (0.252-0.308)	0.144 (0.131-0.157)	0.164 (0.147-0.180)	
2009	0.326 (0.293-0.358)	0.156 (0.140-0.172)	0.173 (0.155-0.191)	
2010	0.390 (0.351-0.429)	0.172 (0.154-0.189)	0.193 (0.172-0.214)	
2011	0.433 (0.390-0.477)	0.180 (0.160-0.200)	0.197 (0.174-0.219)	
2012	0.489 (0.440-0.538)	0.194 (0.171-0.217)	0.193 (0.169-0.217)	
2013	0.547 (0.492-0.602)	0.202 (0.173-0.231)	0.212 (0.178-0.247)	0.276 (0.236-0.315)
2014	0.611 (0.550-0.672)	0.221 (0.185-0.258)	0.226 (0.183-0.268)	0.228 (0.192-0.264)
2015	0.688 (0.620-0.757)	0.241 (0.197-0.286)	0.246 (0.204-0.289)	0.201 (0.169-0.234)
2016	0.787 (0.709-0.866)	0.297 (0.243-0.351)	0.280 (0.232-0.328)	0.223 (0.184-0.263)
2017	0.888 (0.800-0.977)	0.336 (0.273-0.400)	0.295 (0.229-0.361)	0.307 (0.250-0.364)
2018		0.376 (0.307-0.445)	0.349 (0.269-0.429)	0.282 (0.214-0.350)
2019		0.371 (0.299-0.443)	0.398 (0.316-0.479)	0.317 (0.269-0.366)

Table 20: HFC-32 emission (Gg yr^{-1}) estimates for the UK with uncertainty (1std).

Years	Inventory 1yr	MHD	3 sites	4 sites
1994	0.0032 (0.0029-0.0036)			
1995	0.0110 (0.0100-0.0120)			
1996	0.0215 (0.0194-0.0237)			
1997	0.0370 (0.0333-0.0407)			
1998	0.0490 (0.0441-0.0539)			
1999	0.0698 (0.0628-0.0768)			
2000	0.1063 (0.0956-0.1169)			
2001	0.1582 (0.1424-0.1741)			
2002	0.1914 (0.1723-0.2106)			
2003	0.252 (0.227-0.277)			
2004	0.322 (0.290-0.354)	0.245 (0.208-0.283)		
2005	0.388 (0.349-0.427)	0.298 (0.257-0.340)		
2006	0.488 (0.439-0.537)	0.341 (0.295-0.387)		
2007	0.580 (0.522-0.638)	0.442 (0.382-0.501)		
2008	0.674 (0.607-0.742)	0.534 (0.459-0.608)	0.428 (0.365-0.492)	
2009	0.778 (0.700-0.856)	0.653 (0.556-0.751)	0.481 (0.413-0.548)	
2010	0.897 (0.808-0.987)	0.690 (0.575-0.806)	0.573 (0.492-0.653)	
2011	0.999 (0.899-1.099)	0.700 (0.566-0.833)	0.645 (0.558-0.731)	
2012	1.108 (0.997-1.219)	0.650 (0.506-0.793)	0.717 (0.630-0.804)	
2013	1.218 (1.097-1.340)	0.684 (0.516-0.852)	0.700 (0.595-0.806)	0.789 (0.666-0.912)
2014	1.355 (1.220-1.491)	0.727 (0.544-0.911)	0.605 (0.484-0.727)	0.693 (0.568-0.818)
2015	1.520 (1.368-1.672)	0.88 (0.67-1.08)	0.672 (0.545-0.798)	0.857 (0.686-1.028)
2016	1.705 (1.535-1.876)	0.94 (0.73-1.14)	0.785 (0.652-0.918)	0.889 (0.766-1.011)
2017	1.943 (1.749-2.138)	1.10 (0.85-1.35)	0.836 (0.683-0.988)	0.899 (0.713-1.085)
2018		1.10 (0.84-1.37)	0.982 (0.809-1.155)	1.048 (0.862-1.234)
2019		1.27 (0.97-1.58)	1.086 (0.910-1.262)	1.382 (1.197-1.567)

Table 21: HFC-32 emission (Gg yr^{-1}) estimates for the NWEU with uncertainty (1std).

4.13 HFC-227ea
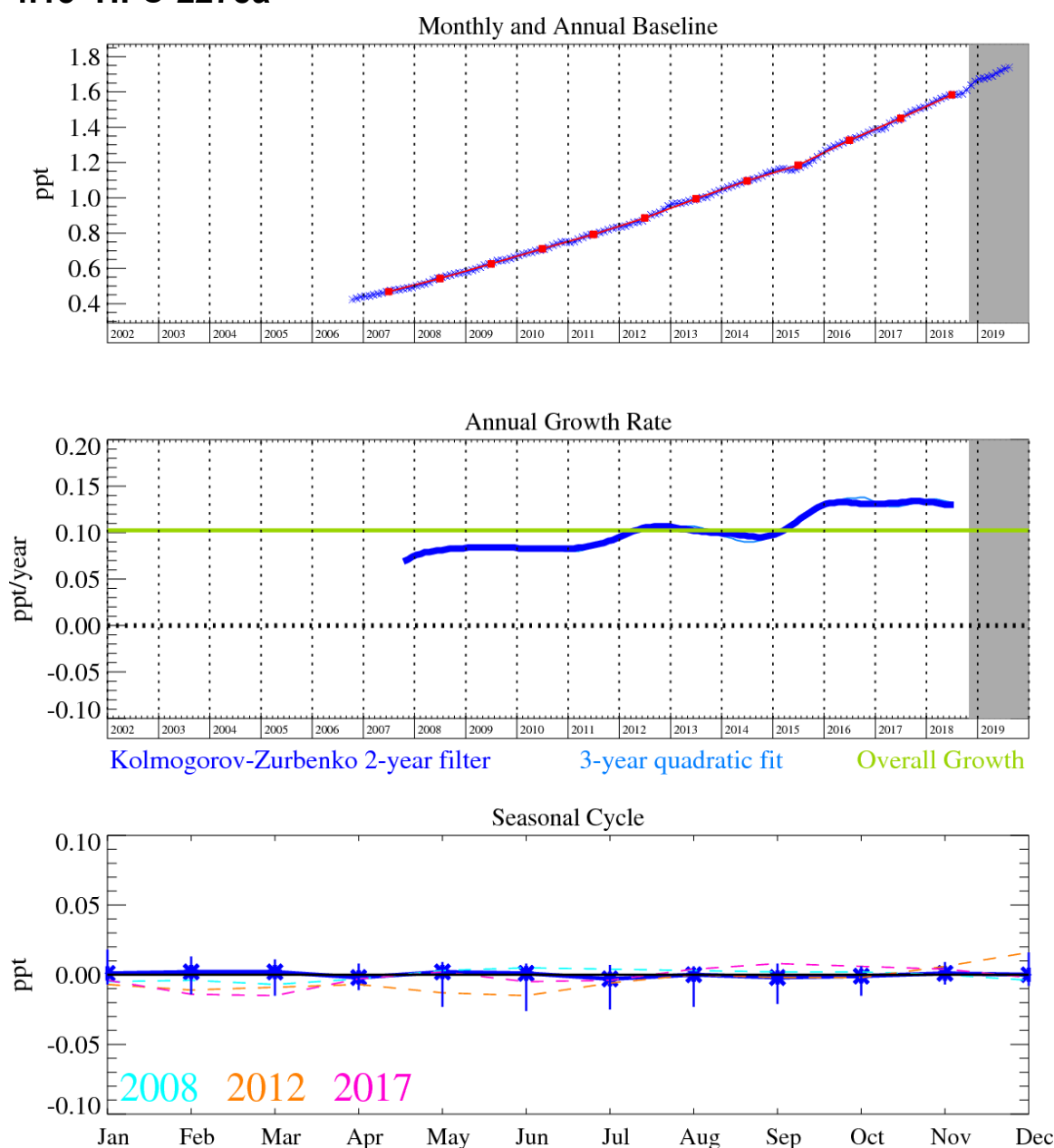
Figure 60: HFC-227ea: Monthly (blue) and annual (red) Northern Hemisphere baseline mole fractions (top plot). Annual (blue) and overall (green) average growth rate (middle plot). Seasonal cycle (de-trended) with year-to-year variability (lower plot). Grey area covers un-ratified provisional data.

HFC-227ea (C_3HF_7) was added to the Medusa analysis in October 2006. HFC-227ea is used as a propellant for medical aerosols and a fire-fighting agent and to a lesser extent in metered-dose inhalers, and foam blowing (atmospheric lifetime 35.8 years and GWP_{100} of 3580).

The InTEM results for the UK are significantly lower (~60%) than the inventory estimates. There is a definite increase in the emissions estimate from 2013-2015 which approximately follows the rise in the inventory. The InTEM results then level off, with good agreement between the MHD only and multi-site inversions. The results for NWEU are closer to the inventory estimate, but with greater uncertainties. There is a slight rise in the InTEM results, but it is not as steep as that seen in the inventory. There is less agreement between the model runs than for the UK, with the multi-site inversions giving lower predictions than the MHD-only inversion.
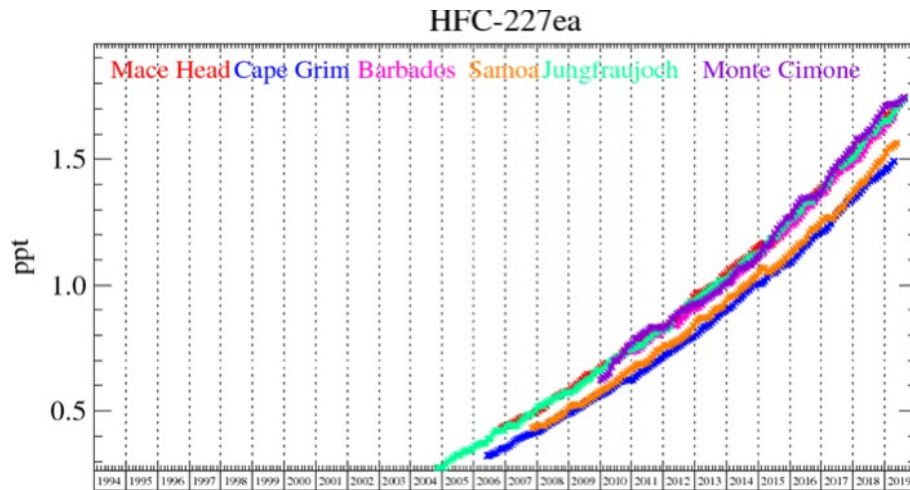
Figure 61: Background HFC-227ea mole fractions at several global AGAGE stations both in the Northern and Southern Hemispheres.
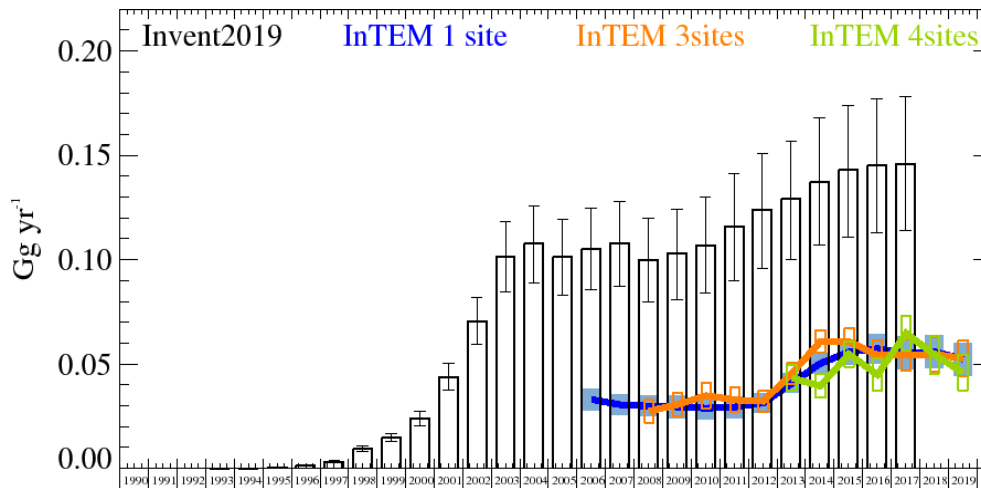
Figure 62: HFC-227ea: UK emission estimates (Gg yr^{-1}) from the UNFCCC Inventory (black) and InTEM (annually averaged): (a) MHD (3yr) with global meteorology (blue), (b) 3 sites (2yr) (MHD+JFJ+CMN) with global meteorology (orange), and (c) 4 sites (1yr) (MHD+JFJ+CMN+TAC) with UKV 1.5 km nested in global meteorology (green). The uncertainty bars represent 1 std.
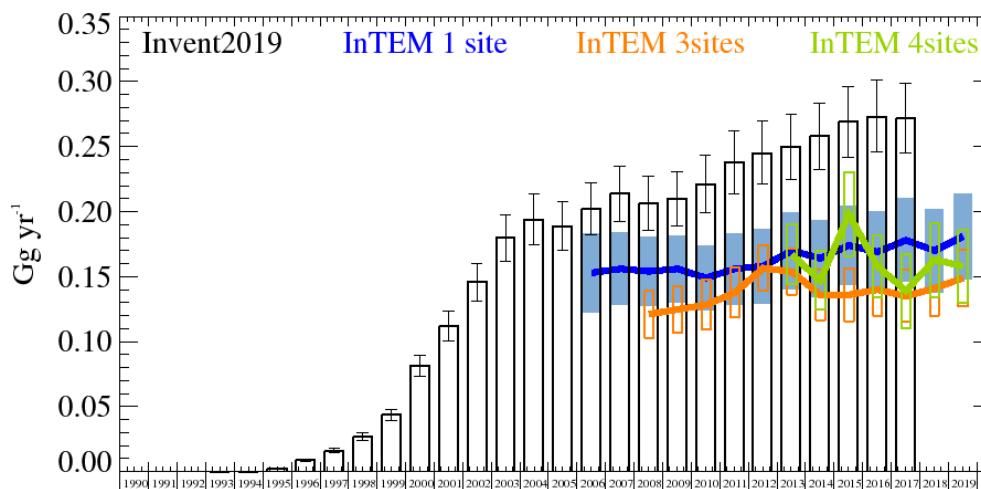
Figure 63: HFC-227ea: NWEU emission estimates (Gg yr^{-1}) from the UNFCCC Inventory (black) and InTEM (annually averaged): (a) MHD (3yr) with global meteorology (blue), (b) 3 sites (2yr) (MHD+JFJ+CMN) with global meteorology (orange), and (c) 4 sites (1yr) (MHD+JFJ+CMN+TAC) with UKV 1.5 km nested in global meteorology (green). The uncertainty bars represent 1 std.

Maximum value = 1.29 kg/km²/yr   Maximum value = 1.85 kg/km²/yr

0.00   0.06   0.18   0.57   1.80   0.00   0.06   0.18   0.57   1.80
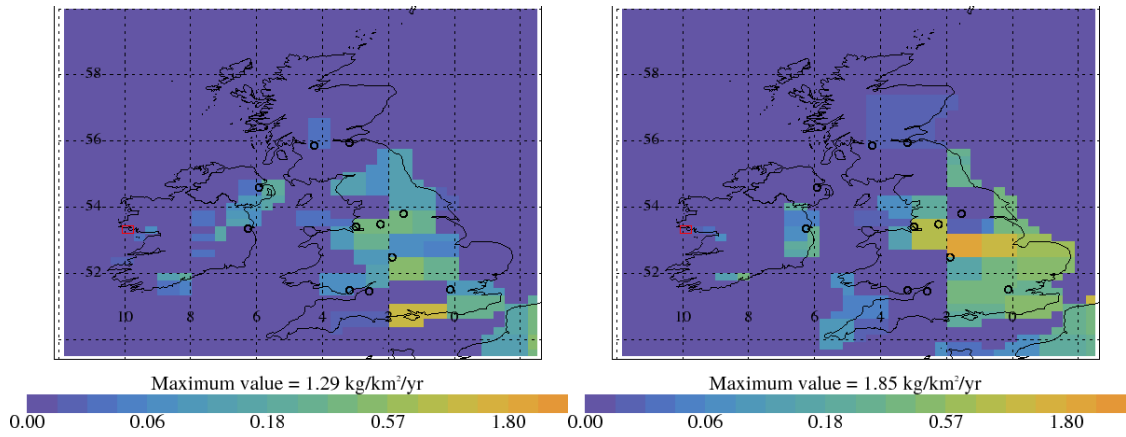
Figure 64: HFC-227ea emission estimate using MHD data for 2004-2008 (left) and 2014-2018 (right). Major cities shown as black circles and observation sites shown as red rectangle.

Maximum value = 1.09 kg/km²/yr   Maximum value = 1.05 kg/km²/yr

0.00   0.06   0.18   0.57   1.80   0.00   0.06   0.18   0.57   1.80
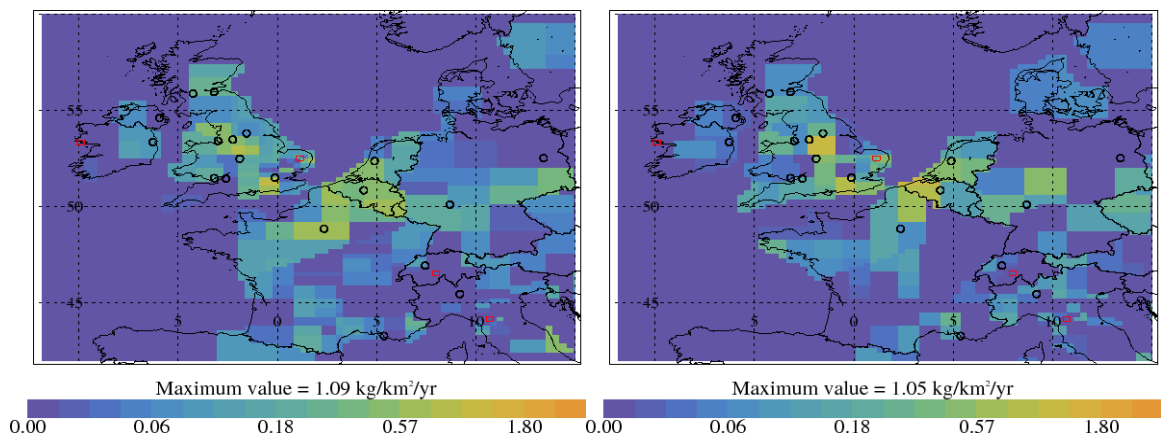
Figure 65: HFC-227ea emission estimate using data from 4 sites for 2013-2015 (left) and 2016-2018 (right). Major cities shown as black circles and observation sites shown as red rectangle.

Years	Inventory 1yr	MHD	3 sites	4 sites
1994	0.0000 (0.0000-0.0000)			
1995	0.0003 (0.0003-0.0004)			
1996	0.0013 (0.0011-0.0015)			
1997	0.0032 (0.0028-0.0036)			
1998	0.0095 (0.0083-0.0108)			
1999	0.0149 (0.0128-0.0169)			
2000	0.0241 (0.0206-0.0276)			
2001	0.0439 (0.0373-0.0506)			
2002	0.0705 (0.0594-0.0817)			
2003	0.1014 (0.0847-0.1181)			
2004	0.1076 (0.0891-0.1260)			
2005	0.1013 (0.0832-0.1195)			
2006	0.1050 (0.0855-0.1245)	0.0330 (0.0278-0.0382)		
2007	0.108 (0.087-0.128)	0.0305 (0.0256-0.0354)		
2008	0.100 (0.080-0.120)	0.0299 (0.0249-0.0349)	0.0275 (0.0220-0.0330)	
2009	0.103 (0.081-0.124)	0.0295 (0.0243-0.0347)	0.0306 (0.0248-0.0364)	
2010	0.107 (0.084-0.130)	0.0289 (0.0236-0.0342)	0.0349 (0.0287-0.0411)	
2011	0.116 (0.090-0.141)	0.0294 (0.0243-0.0345)	0.0328 (0.0270-0.0386)	
2012	0.124 (0.096-0.151)	0.0314 (0.0268-0.0360)	0.0322 (0.0272-0.0372)	
2013	0.129 (0.100-0.157)	0.0408 (0.0362-0.0454)	0.0455 (0.0403-0.0507)	0.0434 (0.0370-0.0498)
2014	0.137 (0.107-0.168)	0.0503 (0.0452-0.0554)	0.0608 (0.0553-0.0663)	0.0395 (0.0339-0.0451)
2015	0.143 (0.111-0.174)	0.0557 (0.0495-0.0619)	0.0608 (0.0545-0.0671)	0.0548 (0.0487-0.0609)
2016	0.145 (0.113-0.177)	0.0574 (0.0502-0.0646)	0.0542 (0.0469-0.0615)	0.0449 (0.0371-0.0527)
2017	0.146 (0.114-0.178)	0.0553 (0.0475-0.0631)	0.0544 (0.0467-0.0621)	0.0648 (0.0563-0.0733)
2018		0.0559 (0.0479-0.0639)	0.0547 (0.0465-0.0629)	0.0544 (0.0454-0.0634)
2019		0.0524 (0.0446-0.0602)	0.0528 (0.0443-0.0613)	0.0460 (0.0375-0.0545)

Table 22: HFC-227ea emission (Gg yr^{-1}) estimates for the UK with uncertainty (1std).

Years	Inventory 1yr	MHD	3 sites	4 sites
1994	0.0001 (0.0000-0.0001)			
1995	0.0019 (0.0017-0.0021)			
1996	0.0090 (0.0081-0.0099)			
1997	0.0160 (0.0150-0.0180)			
1998	0.0269 (0.0242-0.0296)			
1999	0.0437 (0.0393-0.0480)			
2000	0.0817 (0.0736-0.0899)			
2001	0.1119 (0.1007-0.1231)			
2002	0.1457 (0.1311-0.1603)			
2003	0.1797 (0.1617-0.1976)			
2004	0.1940 (0.1746-0.2134)			
2005	0.1889 (0.1700-0.2078)			
2006	0.202 (0.182-0.222)	0.153 (0.123-0.184)		
2007	0.214 (0.192-0.235)	0.156 (0.128-0.184)		
2008	0.206 (0.186-0.227)	0.154 (0.127-0.180)	0.1210 (0.1026-0.1394)	
2009	0.210 (0.189-0.231)	0.156 (0.131-0.182)	0.1248 (0.1067-0.1429)	
2010	0.221 (0.199-0.243)	0.149 (0.124-0.174)	0.1282 (0.1091-0.1473)	
2011	0.238 (0.214-0.262)	0.156 (0.129-0.184)	0.1376 (0.1184-0.1568)	
2012	0.245 (0.221-0.270)	0.158 (0.129-0.186)	0.1566 (0.1392-0.1740)	
2013	0.250 (0.225-0.275)	0.170 (0.141-0.200)	0.1539 (0.1361-0.1717)	0.167 (0.144-0.190)
2014	0.258 (0.232-0.283)	0.164 (0.135-0.194)	0.1359 (0.1161-0.1557)	0.147 (0.124-0.169)
2015	0.269 (0.242-0.296)	0.174 (0.144-0.205)	0.136 (0.116-0.157)	0.198 (0.165-0.230)
2016	0.273 (0.246-0.301)	0.169 (0.138-0.200)	0.140 (0.120-0.160)	0.158 (0.134-0.181)
2017	0.272 (0.245-0.299)	0.178 (0.146-0.210)	0.135 (0.115-0.155)	0.139 (0.111-0.168)
2018		0.170 (0.138-0.202)	0.141 (0.119-0.162)	0.163 (0.135-0.192)
2019		0.181 (0.148-0.214)	0.149 (0.127-0.171)	0.158 (0.130-0.186)

Table 23: HFC-227ea emission (Gg yr^{-1}) estimates for the NWEU with uncertainty (1std).

4.14 HFC-245fa
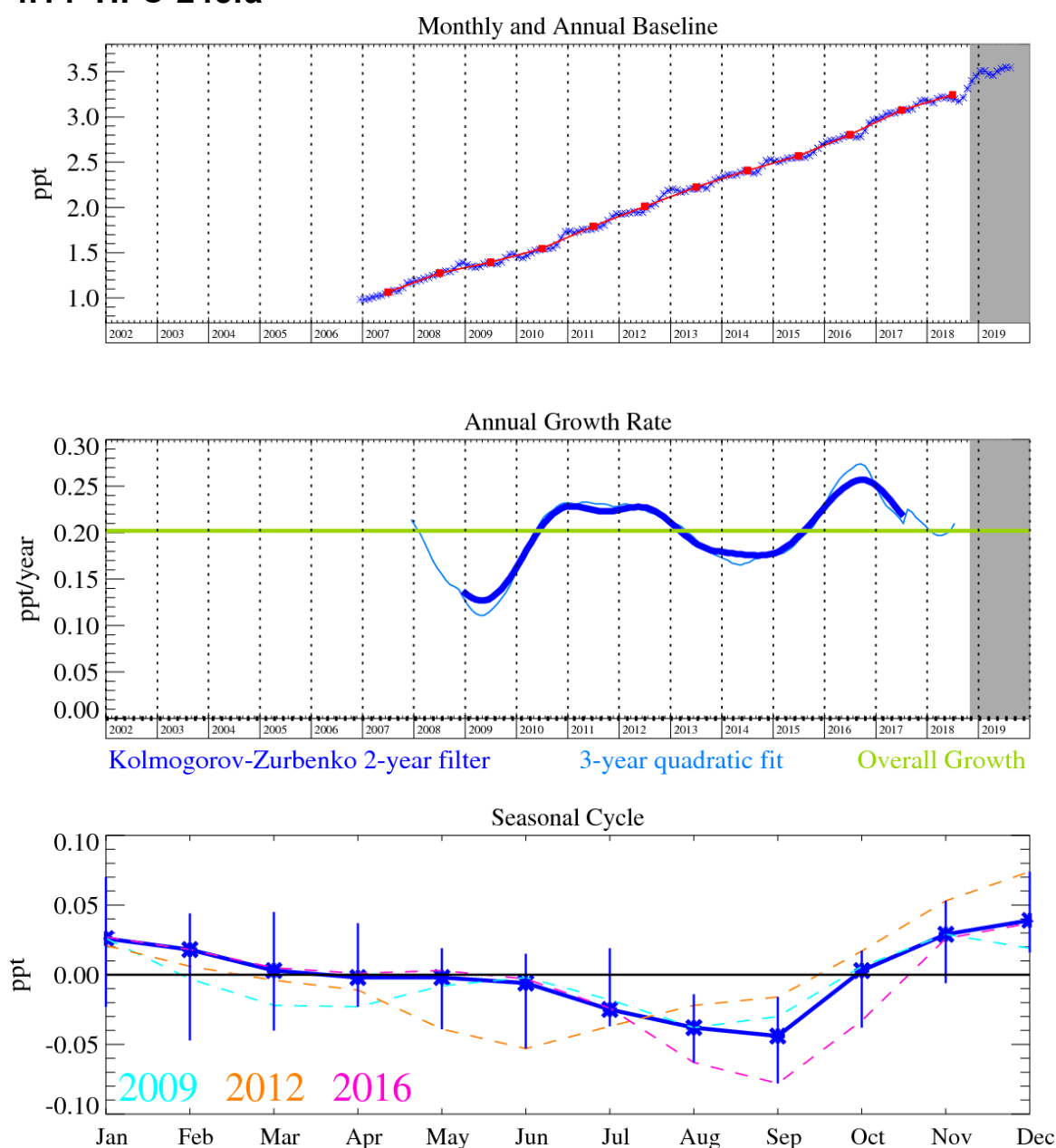
Figure 66: HFC-245fa: Monthly (blue) and annual (red) Northern Hemisphere baseline mole fractions (top plot). Annual (blue) and overall (green) average growth rate (middle plot). Seasonal cycle (de-trended) with year-to-year variability (lower plot). Grey area covers un-ratified provisional data.

The NH concentrations of HFC-245fa are steadily rising across the time-series of observations. The InTEM results for the UK generally underestimate the inventory. The MHD only estimates decline initially and then level off at around 50% or less than the inventory. The multi-site inversions however diverge from the MHD only run from 2012 onwards and show an upward trend. The uncertainties in all the InTEM inversions are large.

The results from NWEU are extremely well aligned to the inventory, with MHD only having the best fit to the inventory as the multi-site runs under-predict the inventory in later years. The sharp increase in emissions from 2013-2017 is captured very well. Looking at the spatial maps there is potentially a significant source in Belgium.
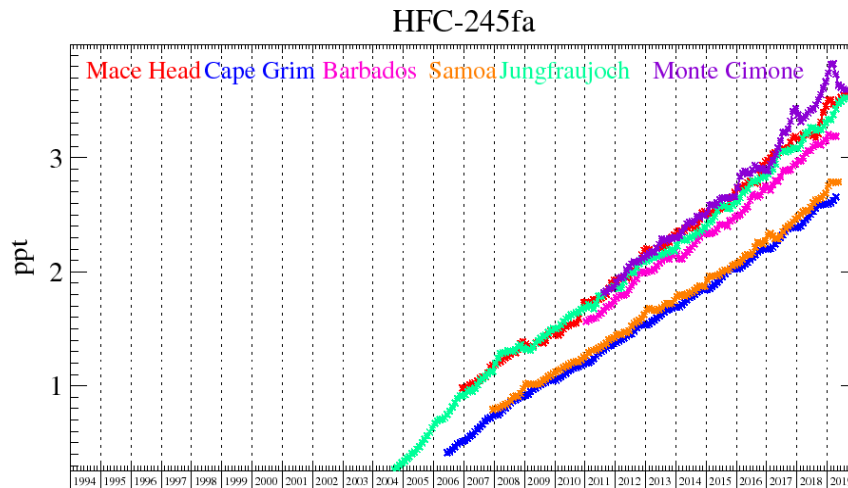
HFC-245fa

Figure 67: Background HFC-245fa mole fractions at several global AGAGE stations both in the Northern and Southern Hemispheres.
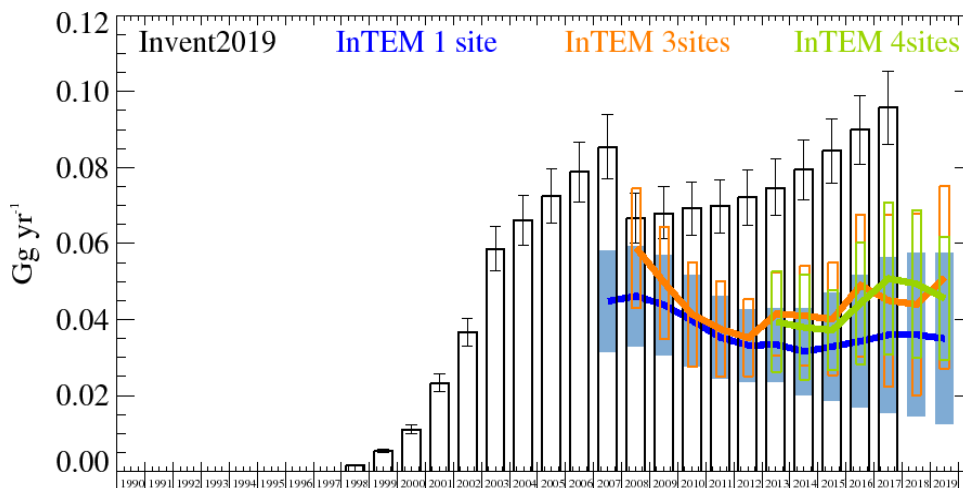
Figure 68: HFC-245fa: UK emission estimates (Gg yr^{-1}) from the UNFCCC Inventory (black) and InTEM (annually averaged): (a) MHD (3yr) with global meteorology (blue), (b) 3 sites (2yr) (MHD+JFJ+CMN) with global meteorology (orange), and (c) 4 sites (1yr) (MHD+JFJ+CMN+TAC) with UKV 1.5 km nested in global meteorology (green). The uncertainty bars represent 1 std.
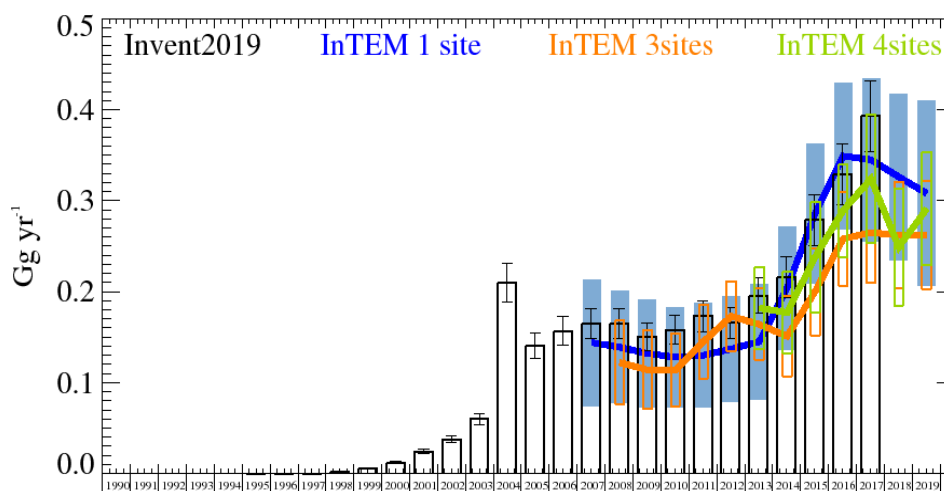
Figure 69: HFC-245fa: NWEU emission estimates (Gg yr^{-1}) from the UNFCCC Inventory (black) and InTEM (annually averaged): (a) MHD (3yr) with global meteorology (blue), (b) 3 sites (2yr) (MHD+JFJ+CMN) with global meteorology (orange), and (c) 4 sites (1yr) (MHD+JFJ+CMN+TAC) with UKV 1.5 km nested in global meteorology (green). The uncertainty bars represent 1 std.

Maximum value = 1.30 kg/km²/yr

0.00   0.06   0.18   0.57   1.80

Maximum value = 1.68 kg/km²/yr

0.00   0.06   0.18   0.57   1.80

Figure 70: HFC-245fa emission estimate using MHD data for 2004-2008 (left) and 2014-2018 (right). Major cities shown as black circles and observation sites shown as red rectangle.

Maximum value = 1.00 kg/km²/yr

0.00   0.06   0.18   0.57   1.80

Maximum value = 2.54 kg/km²/yr

0.00   0.06   0.18   0.57   1.80
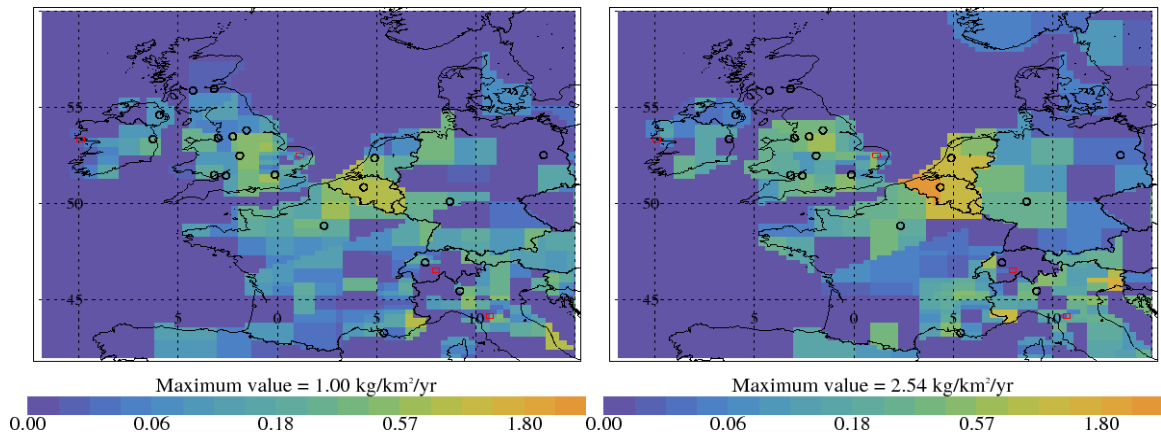
Figure 71: HFC-245fa emission estimate using data from 4 sites for 2013-2015 (left) and 2016-2018 (right). Major cities shown as black circles and observation sites shown as red rectangle.

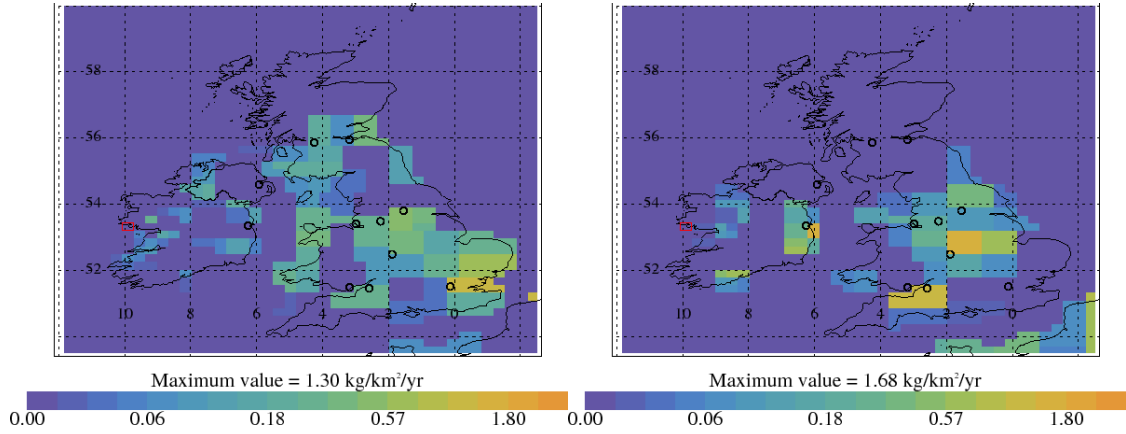| Years	Inventory 1yr	MHD	3 sites	4 sites
1998	0.0017 (0.0015-0.0019)			
1999	0.0054 (0.0049-0.0060)			
2000	0.0111 (0.0100-0.0122)			
2001	0.0233 (0.0210-0.0256)			
2002	0.0367 (0.0331-0.0404)			
2003	0.0585 (0.0527-0.0644)			
2004	0.0662 (0.0596-0.0728)			
2005	0.0725 (0.0653-0.0798)			
2006	0.0788 (0.0710-0.0867)			
2007	0.0854 (0.0769-0.0940)	0.0448 (0.0314-0.0582)		
2008	0.0667 (0.0600-0.0734)	0.0462 (0.0330-0.0594)	0.0588 (0.0430-0.0746)	
2009	0.0680 (0.0612-0.0749)	0.0438 (0.0307-0.0569)	0.0497 (0.0350-0.0644)	
2010	0.0692 (0.0623-0.0761)	0.0397 (0.0276-0.0518)	0.0413 (0.0275-0.0551)	
2011	0.0698 (0.0628-0.0768)	0.0353 (0.0245-0.0461)	0.0375 (0.0249-0.0501)	
2012	0.0721 (0.0649-0.0793)	0.0332 (0.0237-0.0427)	0.0352 (0.0251-0.0453)	
2013	0.0747 (0.0673-0.0822)	0.0334 (0.0237-0.0431)	0.0415 (0.0306-0.0524)	0.0394 (0.0262-0.0526)
2014	0.0794 (0.0714-0.0873)	0.0316 (0.0202-0.0430)	0.0410 (0.0278-0.0542)	0.0379 (0.0241-0.0517)
2015	0.0844 (0.0760-0.0928)	0.0329 (0.0187-0.0471)	0.0401 (0.0253-0.0549)	0.0372 (0.0266-0.0478)
2016	0.0899 (0.0809-0.0989)	0.0343 (0.0169-0.0517)	0.0490 (0.0303-0.0677)	0.0443 (0.0283-0.0603)
2017	0.0957 (0.0861-0.1053)	0.036 (0.016-0.057)	0.045 (0.023-0.068)	0.0508 (0.0309-0.0707)
2018		0.036 (0.015-0.058)	0.044 (0.020-0.068)	0.0494 (0.0300-0.0688)
2019		0.035 (0.013-0.058)	0.051 (0.027-0.075)	0.0456 (0.0294-0.0618)

Table 24: HFC-245fa emission (Gg yr⁻¹) estimates for the UK with uncertainty (1std).

Years	Inventory 1yr	MHD	3 sites	4 sites
1995	0.0000 (0.0000-0.0000)			
1996	0.0000 (0.0000-0.0000)			
1997	0.0000 (0.0000-0.0000)			
1998	0.0017 (0.0016-0.0019)			
1999	0.0055 (0.0049-0.0060)			
2000	0.0120 (0.0110-0.0130)			
2001	0.0242 (0.0218-0.0266)			
2002	0.0377 (0.0339-0.0415)			
2003	0.0598 (0.0538-0.0658)			
2004	0.2100 (0.1890-0.2310)			
2005	0.1400 (0.1260-0.1540)			
2006	0.1566 (0.1409-0.1723)			
2007	0.1647 (0.1482-0.1812)	0.144 (0.075-0.214)		
2008	0.1648 (0.1483-0.1813)	0.139 (0.077-0.200)	0.122 (0.076-0.168)	
2009	0.1504 (0.1353-0.1654)	0.132 (0.072-0.191)	0.114 (0.071-0.157)	
2010	0.1578 (0.1420-0.1736)	0.128 (0.073-0.183)	0.114 (0.073-0.154)	
2011	0.1730 (0.1557-0.1903)	0.130 (0.073-0.188)	0.145 (0.104-0.186)	
2012	0.1656 (0.1490-0.1821)	0.137 (0.079-0.195)	0.173 (0.135-0.212)	
2013	0.1953 (0.1758-0.2149)	0.145 (0.082-0.209)	0.164 (0.125-0.204)	0.182 (0.137-0.226)
2014	0.216 (0.194-0.238)	0.204 (0.137-0.272)	0.151 (0.107-0.195)	0.177 (0.133-0.222)
2015	0.279 (0.251-0.307)	0.286 (0.210-0.363)	0.200 (0.152-0.248)	0.238 (0.177-0.298)
2016	0.329 (0.296-0.362)	0.349 (0.269-0.429)	0.258 (0.206-0.310)	0.289 (0.238-0.340)
2017	0.393 (0.354-0.432)	0.345 (0.256-0.435)	0.265 (0.210-0.321)	0.324 (0.254-0.395)
2018		0.326 (0.235-0.418)	0.262 (0.204-0.320)	0.249 (0.184-0.313)
2019		0.308 (0.206-0.410)	0.262 (0.203-0.321)	0.291 (0.229-0.353)

Table 25: HFC-245fa emission (Gg yr^{-1}) estimates for the NWEU with uncertainty (1std).

4.15 HFC-43-10mee
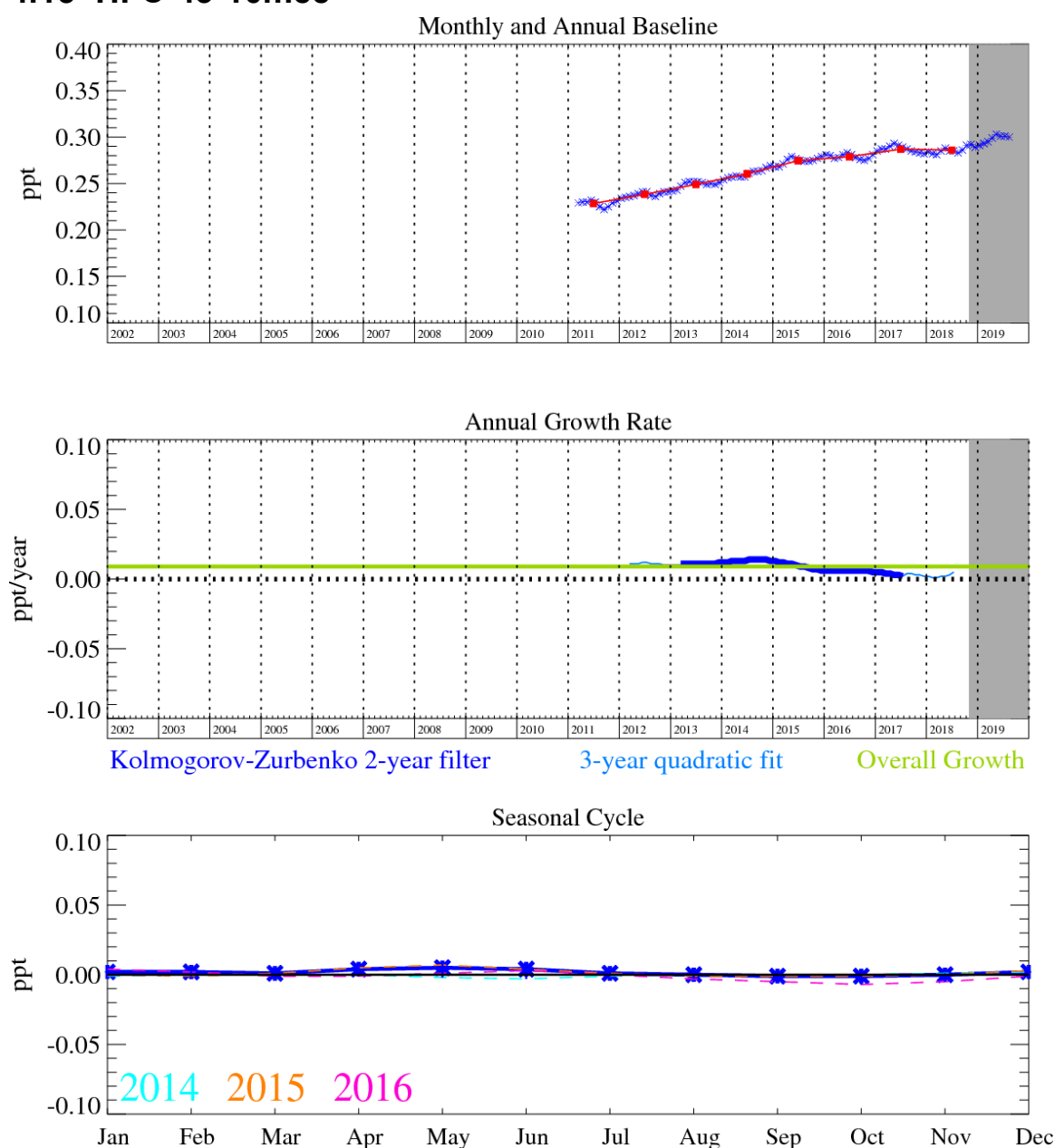
Figure 72: HFC-43-10mee: Monthly (blue) and annual (red) Northern Hemisphere baseline mole fractions (top plot). Annual (blue) and overall (green) average growth rate (middle plot). Seasonal cycle (de-trended) with year-to-year variability (lower plot). Grey area covers un-ratified provisional data.

HFC-43-10mee ($C_5H_2F_{10}$) was introduced in the mid 1990s as a replacement for CFC-113. It meets many requirements in the electronics industries and replaces PFCs in some uses such as a carrier fluid for lubricants applied to computer hard disks. It has an atmospheric lifetime of 16.1 years, a GWP_{100} of 1,650 and a radiative efficiency of 0.42 W m^{-2} ppb^{-1}. The NH concentration has grown very slowly since measurements began in 2011.

The UK inversion results for HFC-43-10mee underestimate the inventory, although the emissions are relatively small in both estimates and the InTEM results have quite large uncertainties. The INTEM results indicate a sharp drop off in emissions apart from the 4-sites inversion which is more in line with the inventory. The InTEM results for NWEU are almost double the inventory, though with large uncertainties and most error bars overlapping the inventory. However, it appears that several NWEU countries do not specify emissions of HFC-43-10mee in their UNFCCC submissions.
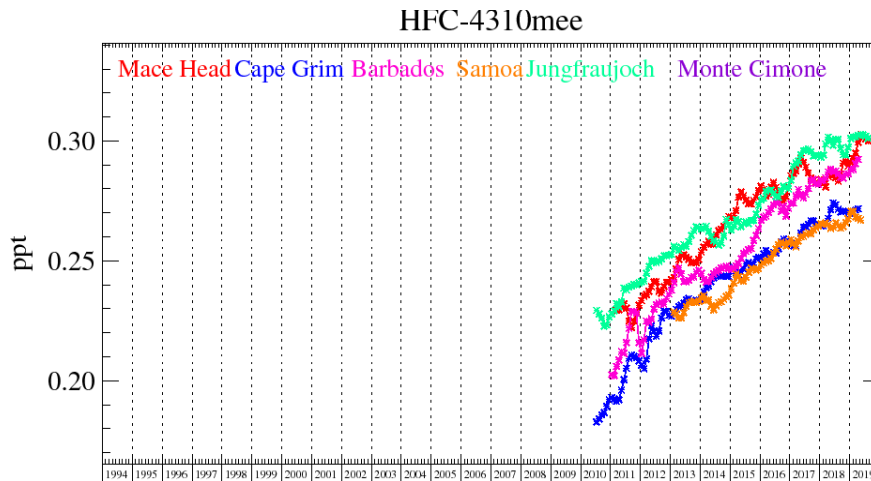
Figure 73: Background HFC-43-10mee mole fractions at several global AGAGE stations both in the Northern and Southern Hemispheres.
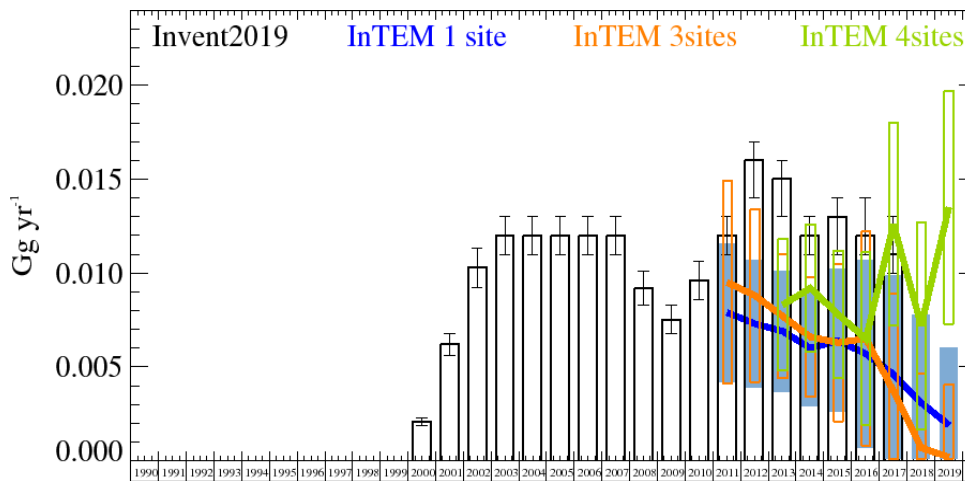
Figure 74: HFC-43-10mee: UK emission estimates (Gg yr^{-1}) from the UNFCCC Inventory (black) and InTEM (annually averaged): (a) MHD (3yr) with global meteorology (blue), (b) 3 sites (2yr) (MHD+JFJ) with global meteorology (orange), and (c) 4 sites (1yr) (MHD+JFJ+TAC) with UKV 1.5 km nested in global meteorology (green). The uncertainty bars represent 1 std.
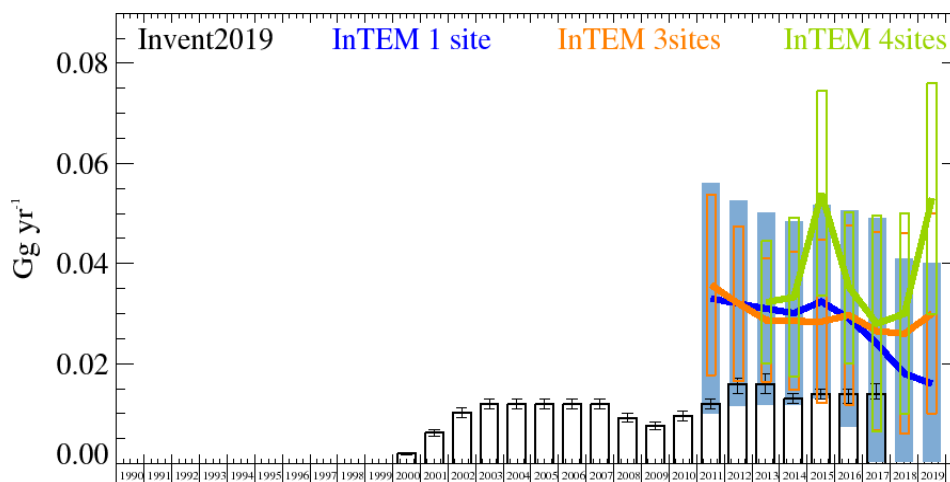
Figure 75: HFC-43-10mee: NWEU emission estimates (Gg yr^{-1}) from the UNFCCC Inventory (black) and InTEM (annually averaged): (a) MHD (3yr) with global meteorology (blue), (b) 3 sites (2yr) (MHD+JFJ) with global meteorology (orange), and (c) 4 sites (1yr) (MHD+JFJ+TAC) with UKV 1.5 km nested in global meteorology (green). The uncertainty bars represent 1 std.

Maximum value = 2.57e-01 kg/km²/yr   Maximum value = 2.26e-01 kg/km²/yr

0.00e+00   7.13e-03   2.25e-02   7.12e-02   2.25e-01   0.00e+00   7.13e-03   2.25e-02   7.12e-02   2.25e-01

Figure 76: HFC-43-10-mee emission estimate using data from 3 sites for 2013-2015 (left) and 2016-2018 (right). Major cities shown as black circles and observation sites shown as red rectangle.

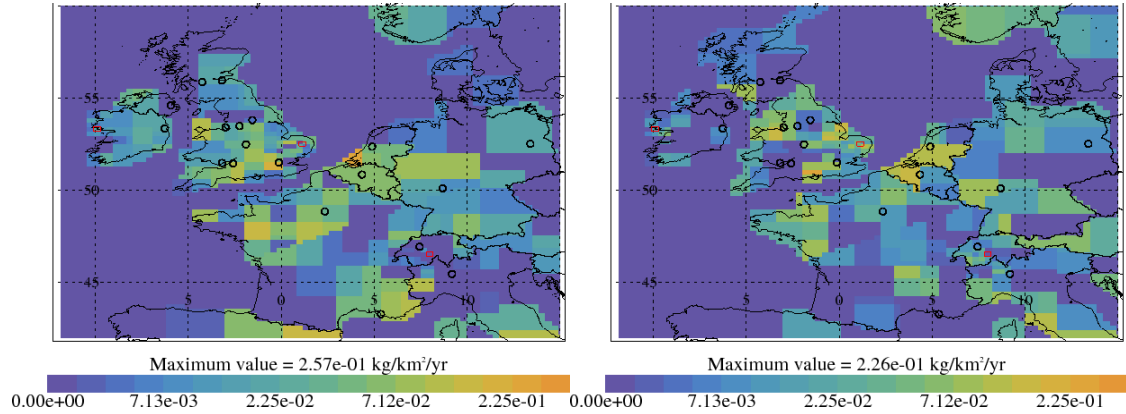| Years	Inventory 1yr	MHD	2 sites	3 sites
2003	0.012 (0.011-0.013)			
2004	0.012 (0.011-0.013)			
2005	0.012 (0.011-0.013)			
2006	0.012 (0.011-0.013)			
2007	0.012 (0.011-0.013)			
2008	0.009 (0.008-0.010)			
2009	0.008 (0.007-0.008)			
2010	0.010 (0.009-0.011)			
2011	0.012 (0.011-0.013)	0.0079 (0.0042-0.0116)	0.0095 (0.0041-0.0149)	
2012	0.016 (0.014-0.017)	0.0073 (0.0039-0.0107)	0.0088 (0.0042-0.0134)	
2013	0.015 (0.013-0.016)	0.0069 (0.0037-0.0101)	0.0077 (0.0044-0.0110)	0.0083 (0.0048-0.0118)
2014	0.012 (0.011-0.013)	0.0060 (0.0029-0.0091)	0.0066 (0.0034-0.0098)	0.0092 (0.0058-0.0126)
2015	0.013 (0.011-0.014)	0.0064 (0.0026-0.0102)	0.0063 (0.0021-0.0105)	0.0078 (0.0044-0.0112)
2016	0.012 (0.011-0.014)	0.0057 (0.0007-0.0107)	0.0065 (0.0008-0.0122)	0.0065 (0.0019-0.0111)
2017	0.011 (0.010-0.013)	0.0046 (0.0000-0.0105)	0.0037 (0.0000-0.0104)	0.0126 (0.0072-0.0180)
2018		0.0031 (0.0000-0.0094)	0.0007 (0.0000-0.0079)	0.0072 (0.0017-0.0127)
2019		0.0019 (0.0000-0.0083)	0.0002 (0.0000-0.0077)	0.0135 (0.0073-0.0197)

Table 26: HFC-43-10mee emission (Gg yr^{-1}) estimates for the UK with uncertainty (1std).

Years	Inventory 1yr	1s 3y	3s 2y	4s 1y
2003	0.012 (0.011-0.013)			
2004	0.012 (0.011-0.013)			
2005	0.012 (0.011-0.013)			
2006	0.012 (0.011-0.013)			
2007	0.012 (0.011-0.013)			
2008	0.009 (0.008-0.010)			
2009	0.008 (0.007-0.008)			
2010	0.010 (0.009-0.011)			
2011	0.012 (0.011-0.013)	0.033 (0.010-0.056)	0.036 (0.018-0.054)	
2012	0.016 (0.014-0.017)	0.032 (0.011-0.052)	0.032 (0.017-0.048)	
2013	0.016 (0.014-0.018)	0.031 (0.012-0.050)	0.029 (0.016-0.041)	0.032 (0.020-0.045)
2014	0.013 (0.012-0.014)	0.030 (0.012-0.049)	0.029 (0.015-0.042)	0.033 (0.017-0.049)
2015	0.014 (0.013-0.015)	0.032 (0.013-0.052)	0.028 (0.012-0.045)	0.054 (0.034-0.075)
2016	0.014 (0.012-0.015)	0.029 (0.008-0.051)	0.030 (0.012-0.048)	0.035 (0.020-0.050)
2017	0.014 (0.013-0.016)	0.024 (0.000-0.050)	0.027 (0.007-0.046)	0.028 (0.007-0.050)
2018		0.018 (0.000-0.046)	0.026 (0.006-0.046)	0.030 (0.010-0.050)
2019		0.016 (0.000-0.048)	0.030 (0.010-0.050)	0.053 (0.030-0.076)

Table 27: HFC-43-10mee emission (Gg yr^{-1}) estimates for the NWEU with uncertainty (1std).

4.16 HFC-365mfc
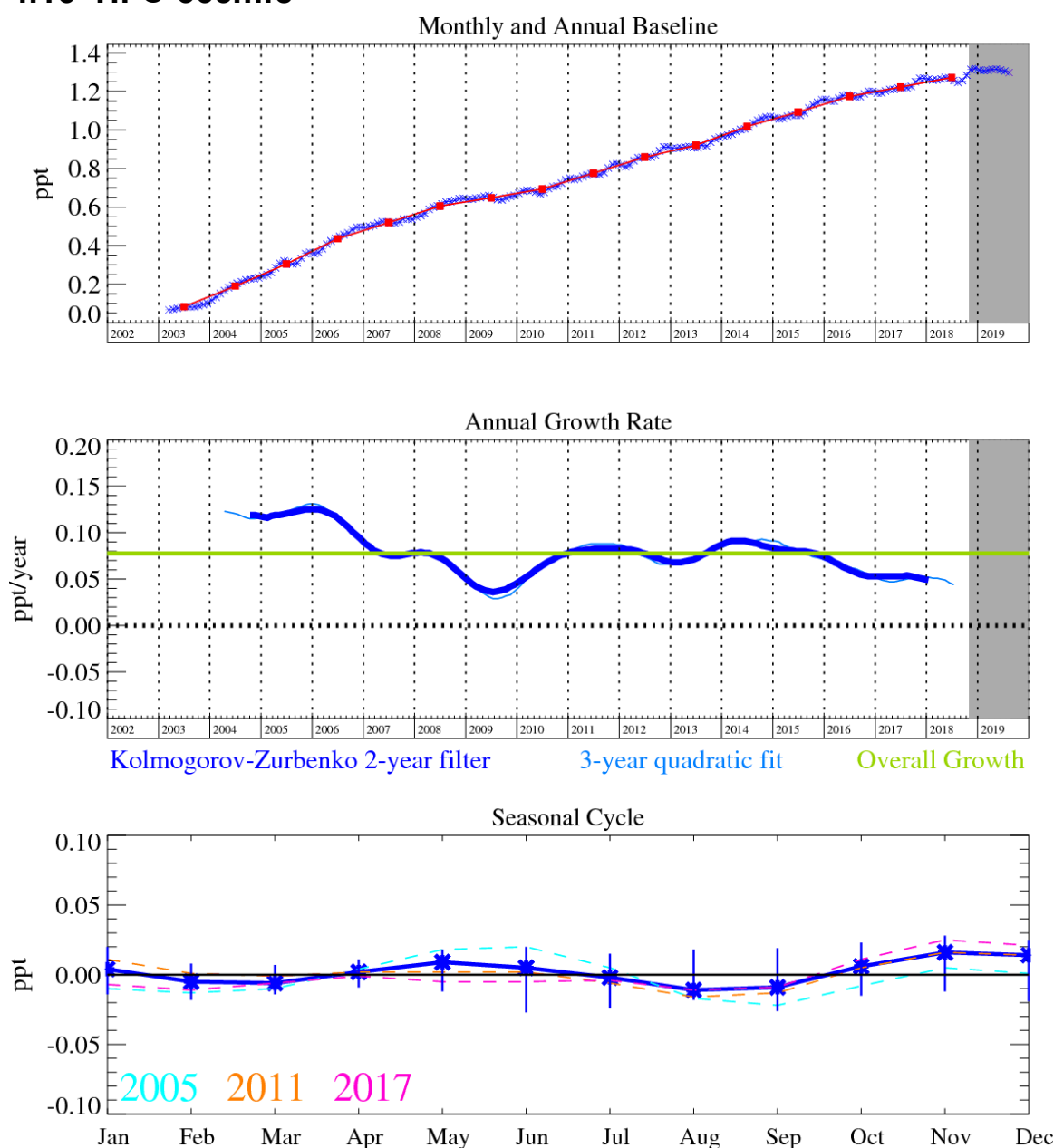
Figure 77: HFC-365mfc: Monthly (blue) and annual (red) Northern Hemisphere baseline mole fractions (top plot). Annual (blue) and overall (green) average growth rate (middle plot). Seasonal cycle (de-trended) with year-to-year variability (lower plot). Grey area covers un-ratified provisional data.

HFC-365mfc ($C_4H_5F_5$) is used predominantly for polyurethane structural foam blowing as a replacement for HCFC-141b, and to a minor extent as a blend component for solvents. It has an atmospheric lifetime of 8.6 years and an estimated GWP of 790-997 (100-year time horizon).

The inventory shows a steady growth followed by a sharp decline between 2007 and 2008 and then a flat period followed by a modest rise. The MHD only inversion captures the initial rise and subsequent decline with good agreement in annual emission totals. The multi-site data is well aligned with MHD only from 2009 onwards and all model inversions under-predict the inventory before rising to give better agreement (2014-2015) and then dropping off steadily as the inventory continues to rise.

The NWEU InTEM results show generally good agreement with the inventory, with all inversions slightly over-predicting until 2015 when the multi-site inversions slightly under-predict the inventory but with overlapping error bars. The emissions are broadly population based.
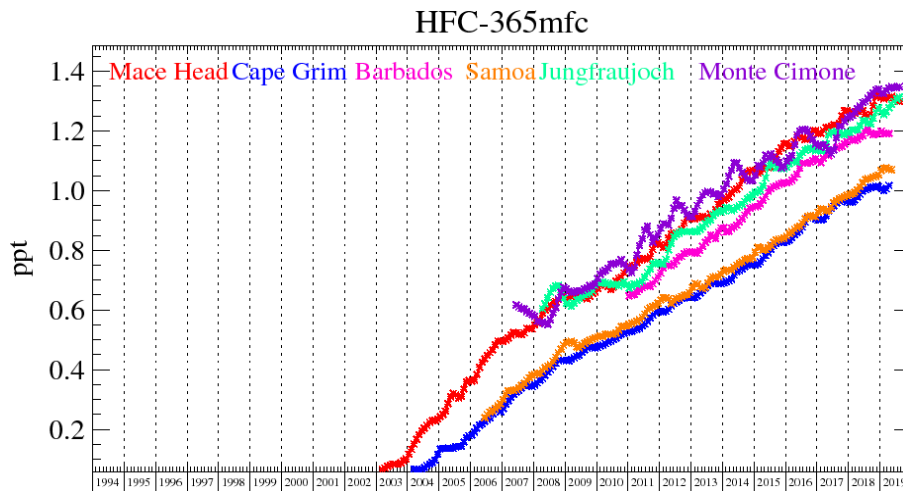
Figure 78: Background HFC-365mfc mole fractions at several global AGAGE stations both in the Northern and Southern Hemispheres.
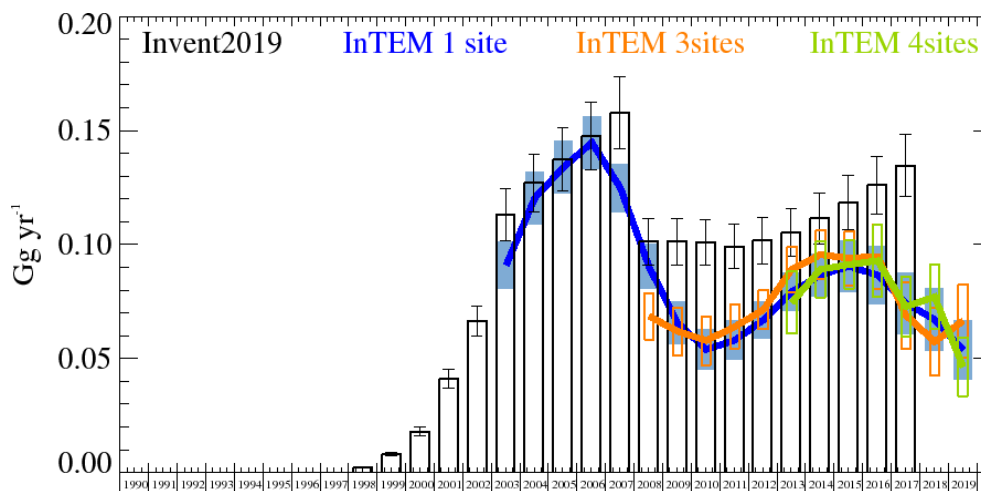
Figure 79: HFC-365mfc: UK emission estimates (Gg yr^{-1}) from the UNFCCC Inventory (black) and InTEM (annually averaged): (a) MHD (3yr) with global meteorology (blue), (b) 3 sites (2yr) (MHD+JFJ+CMN) with global meteorology (orange), and (c) 4 sites (1yr) (MHD+JFJ+CMN+TAC) with UKV 1.5 km nested in global meteorology (green). The uncertainty bars represent 1 std.
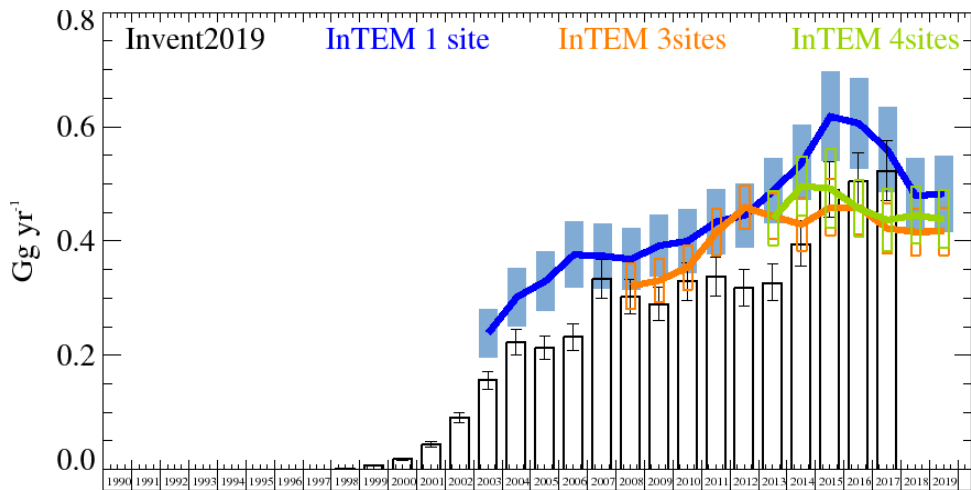
Figure 80: HFC-365mfc: NWEU emission estimates (Gg yr^{-1}) from the UNFCCC Inventory (black) and InTEM (annually averaged): (a) MHD (3yr) with global meteorology (blue), (b) 3 sites (2yr) (MHD+JFJ+CMN) with global meteorology (orange), and (c) 4 sites (1yr) (MHD+JFJ+CMN+TAC) with UKV 1.5 km nested in global meteorology (green). The uncertainty bars represent 1 std.

Figure 81: HFC-365mfc emission estimate using MHD data for 2004-2008 (left) and 2014-2018 (right). Major cities shown as black circles and observation sites shown as red rectangle.

Figure 82: HFC-365mfc emission estimate using data from 4 sites for 2013-2015 (left) and 2016-2018 (right). Major cities shown as black circles and observation sites shown as red rectangle.

74

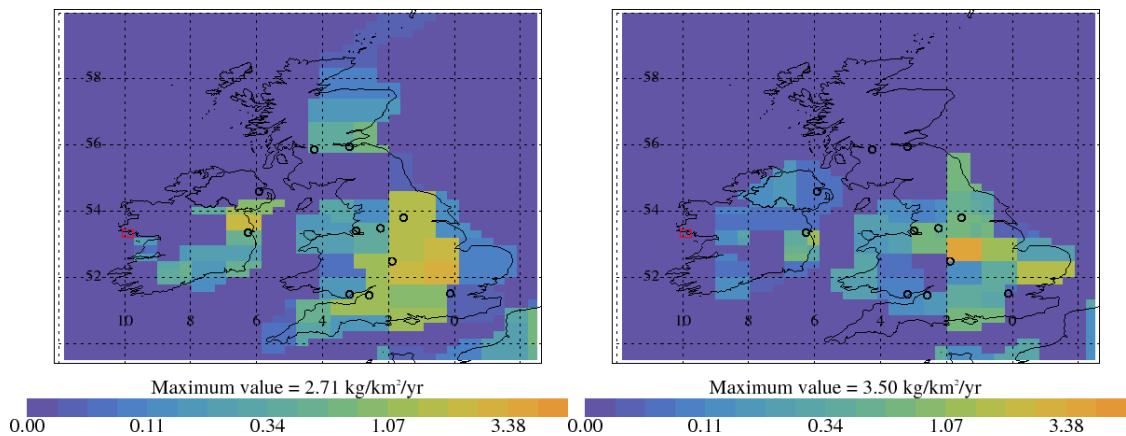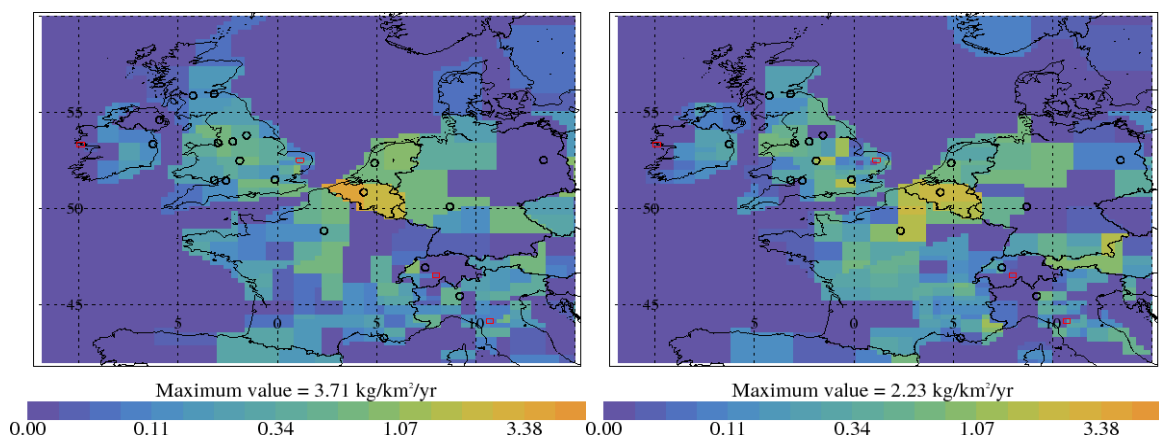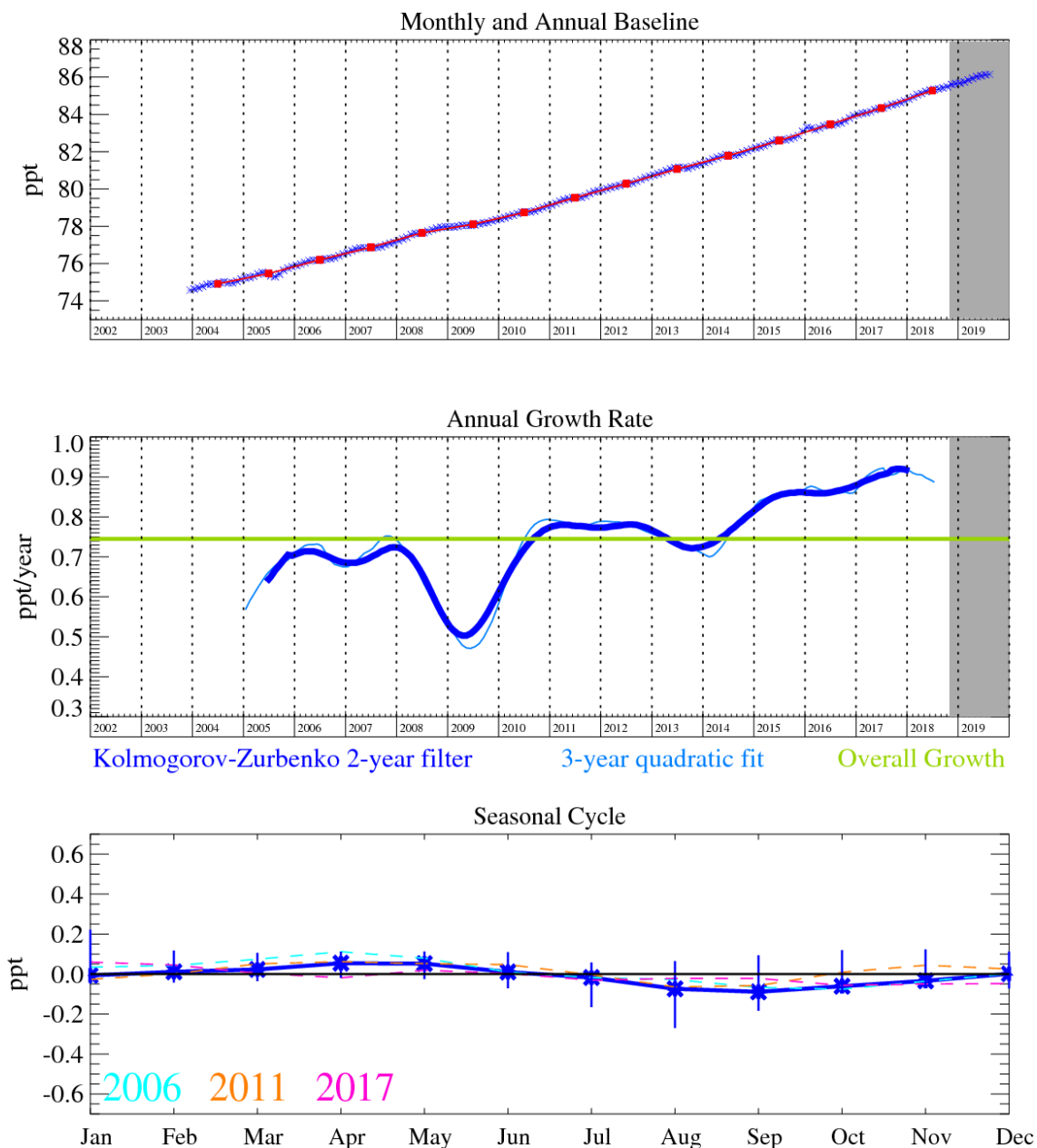| Years	Inventory 1yr	MHD	3 sites	4 sites
1998	0.0023 (0.0021-0.0026)			
1999	0.0080 (0.0072-0.0088)			
2000	0.0180 (0.0162-0.0198)			
2001	0.041 (0.037-0.045)			
2002	0.066 (0.060-0.073)			
2003	0.113 (0.102-0.124)			
2004	0.127 (0.114-0.140)	0.120 (0.109-0.132)		
2005	0.137 (0.124-0.151)	0.134 (0.123-0.145)		
2006	0.148 (0.133-0.162)	0.145 (0.133-0.156)		
2007	0.158 (0.142-0.174)	0.125 (0.114-0.135)		
2008	0.101 (0.091-0.111)	0.090 (0.080-0.100)		
2009	0.101 (0.091-0.112)	0.066 (0.056-0.075)	0.062 (0.052-0.072)	
2010	0.101 (0.091-0.111)	0.054 (0.045-0.063)	0.058 (0.047-0.069)	
2011	0.099 (0.089-0.109)	0.058 (0.049-0.067)	0.064 (0.054-0.074)	
2012	0.102 (0.092-0.112)	0.067 (0.059-0.075)	0.071 (0.063-0.080)	
2013	0.105 (0.095-0.116)	0.079 (0.071-0.087)	0.089 (0.079-0.099)	0.075 (0.061-0.088)
2014	0.112 (0.100-0.123)	0.086 (0.077-0.096)	0.096 (0.085-0.106)	0.089 (0.077-0.102)
2015	0.118 (0.107-0.130)	0.090 (0.079-0.102)	0.094 (0.082-0.106)	0.091 (0.081-0.102)
2016	0.126 (0.113-0.139)	0.087 (0.074-0.099)	0.095 (0.081-0.109)	0.093 (0.077-0.109)
2017	0.135 (0.121-0.148)	0.074 (0.061-0.088)	0.069 (0.054-0.083)	0.073 (0.060-0.086)
2018		0.067 (0.053-0.081)	0.057 (0.042-0.072)	0.077 (0.063-0.091)
2019				0.046 (0.034-0.059)

Table 28: HFC-365mfc emission (Gg yr^{-1}) estimates for the UK with uncertainty (1std).

Years	Inventory 1yr	MHD	3 sites	4 sites
1998	0.0023 (0.0021-0.0026)			
1999	0.0080 (0.0072-0.0088)			
2000	0.0180 (0.0162-0.0198)			
2001	0.044 (0.039-0.048)			
2002	0.091 (0.082-0.100)			
2003	0.156 (0.141-0.172)			
2004	0.223 (0.200-0.245)	0.30 (0.25-0.35)		
2005	0.213 (0.192-0.234)	0.33 (0.28-0.38)		
2006	0.232 (0.209-0.255)	0.38 (0.32-0.43)		
2007	0.33 (0.30-0.37)	0.37 (0.32-0.43)		
2008	0.30 (0.27-0.33)	0.37 (0.31-0.42)		
2009	0.29 (0.26-0.32)	0.39 (0.34-0.45)	0.33 (0.29-0.37)	
2010	0.33 (0.30-0.36)	0.40 (0.34-0.46)	0.35 (0.31-0.39)	
2011	0.34 (0.30-0.37)	0.43 (0.38-0.49)	0.41 (0.37-0.46)	
2012	0.32 (0.29-0.35)	0.45 (0.39-0.50)	0.46 (0.42-0.50)	
2013	0.33 (0.29-0.36)	0.49 (0.43-0.54)	0.44 (0.40-0.48)	0.44 (0.39-0.49)
2014	0.40 (0.36-0.43)	0.54 (0.47-0.60)	0.43 (0.38-0.48)	0.50 (0.44-0.55)
2015	0.49 (0.44-0.54)	0.62 (0.54-0.70)	0.46 (0.41-0.51)	0.49 (0.42-0.56)
2016	0.50 (0.45-0.56)	0.61 (0.53-0.68)	0.46 (0.41-0.51)	0.46 (0.41-0.51)
2017	0.52 (0.47-0.58)	0.56 (0.49-0.64)	0.42 (0.38-0.47)	0.44 (0.38-0.49)
2018		0.48 (0.41-0.55)	0.42 (0.38-0.46)	0.45 (0.40-0.49)
2019				0.44 (0.39-0.49)

Table 29: HFC-365mfc emission (Gg yr^{-1}) estimates for the NWEU with uncertainty (1std).

4.17 PFC-14

Monthly and Annual Baseline

Annual Growth Rate

Kolmogorov-Zurbenko 2-year filter   3-year quadratic fit   Overall Growth

Seasonal Cycle

2006   2011   2017

Figure 83: PFC-14: Monthly (blue) and annual (red) Northern Hemisphere baseline mole fractions (top plot). Annual (blue) and overall (green) average growth rate (middle plot). Seasonal cycle (de-trended) with year-to-year variability (lower plot). Grey area covers un-ratified provisional data.

PFC-14 (CF_4) possesses the longest known lifetime of anthropogenic molecules (>50,000 years), which, when coupled with its high absolute radiative forcing (0.08 W m^{-2} ppb^{-1}) gives rise to a high GWP_{100} of 5,820 and can equate to upwards of 1% of total radiative forcing. Its primary emission source is as an unwanted by-product of aluminium smelting during a fault condition known as an anode event. Thus, the frequency of occurrence and duration of anode events will determine its regional and global emissions. CF_4 has some additional minor applications in the semiconductor industry (as a source of F radicals), but the industry has generally shied away from using CF_4. The aluminium industry has recognised the CF_4 (and C_2F_6) emission problem and is in the process of replacing older, less efficient plant with more efficient designs, and automated and quicker intervention policies to prevent the occurrence of these anode effects. Alcoa and Rio Tinto are also developing carbon free anode/cathode technology that is claimed to inhibit all direct

greenhouse gas emission from smelters and scheduled to be commercially available from 2024. It is also thought that CF_4 has a natural source from crustal degassing. The current growth rate of atmospheric CF_4 in the NH is close to 0.8 ppt yr^{-1}. This compound will accumulate in the atmosphere due to its very long atmospheric lifetime.
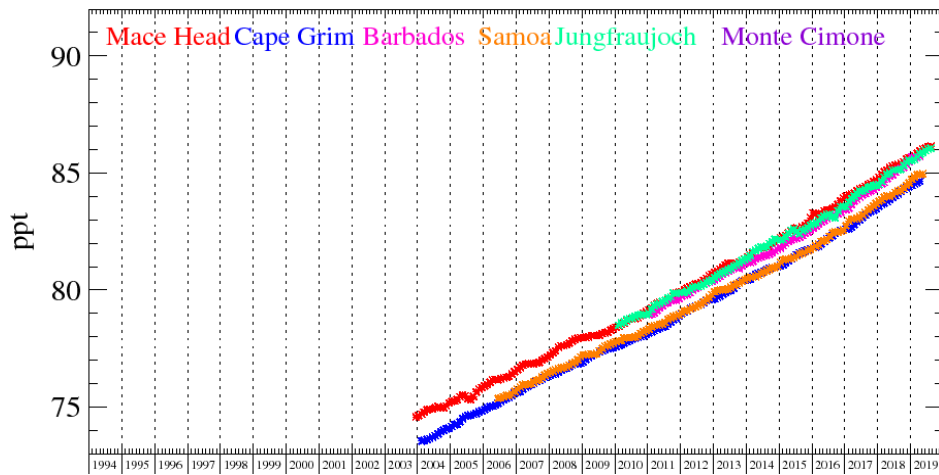
Figure 84: Background PFC-14 mole fractions at several global AGAGE stations both in the Northern and Southern Hemispheres.
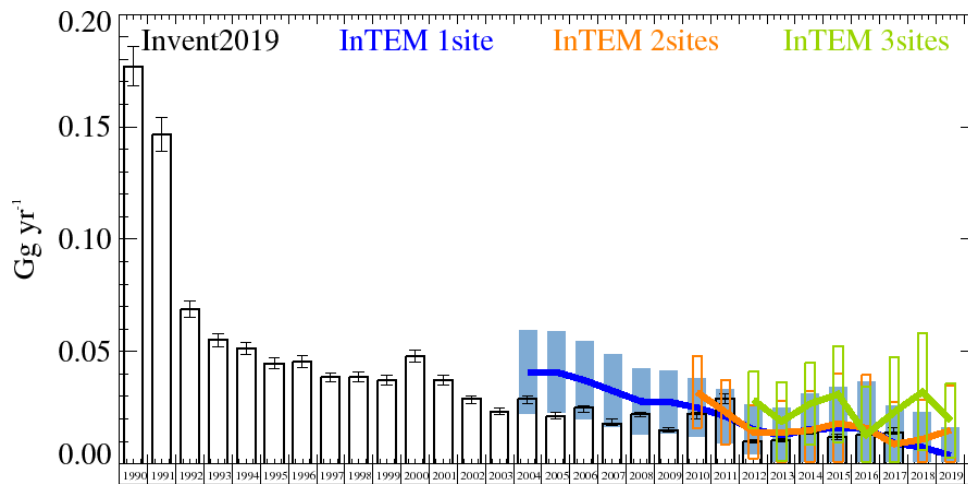
Figure 85: PFC-14: UK emission estimates (Gg yr^{-1}) from the UNFCCC Inventory (black) and InTEM (annually averaged): (a) MHD (3yr) with global meteorology (blue), (b) 2 sites (2yr) (MHD+JFJ) with global meteorology (orange), and (c) 3 sites (1yr) (MHD+JFJ+TAC) with UKV 1.5 km nested in global meteorology (green). The uncertainty bars represent 1 std.
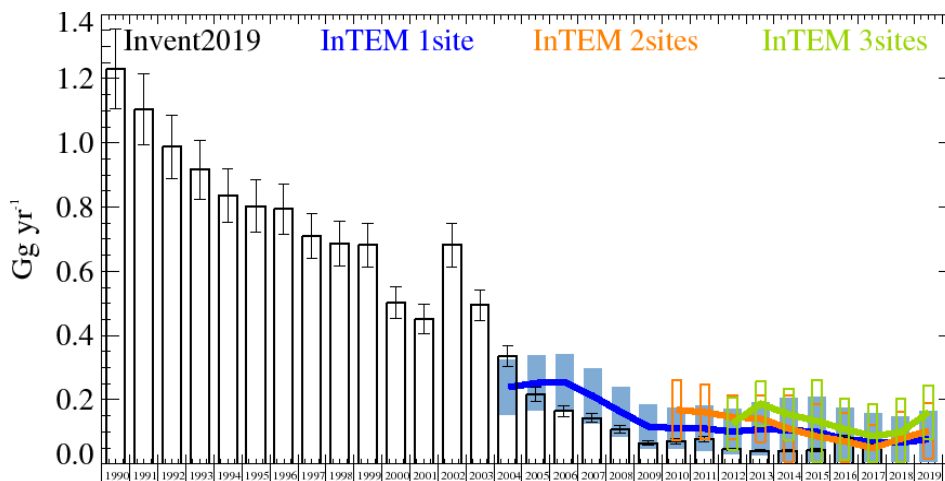
Figure 86: PFC-14: NWEU emission estimates (Gg yr^{-1}) from the UNFCCC Inventory (black) and InTEM (annually averaged): (a) MHD (3yr) with global meteorology (blue), (b) 2 sites (2yr) (MHD+JFJ) with global meteorology (orange), and (c) 3 sites (1yr) (MHD+JFJ+TAC) with UKV 1.5 km nested in global meteorology (green). The uncertainty bars represent 1 std.
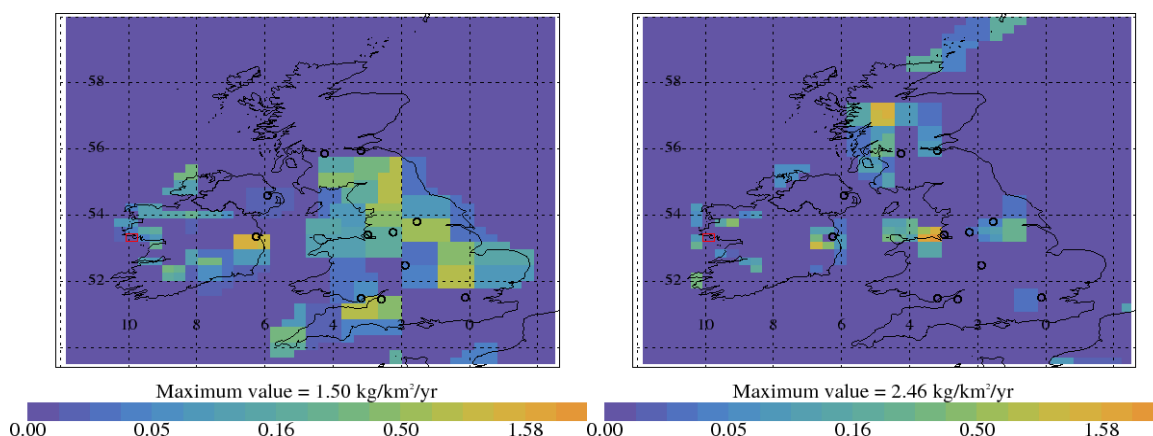
Figure 87: PFC-14 emission estimate using MHD data for 2004-2008 (left) and 2014-2018 (right). Major cities shown as black circles and observation sites shown as red rectangle.
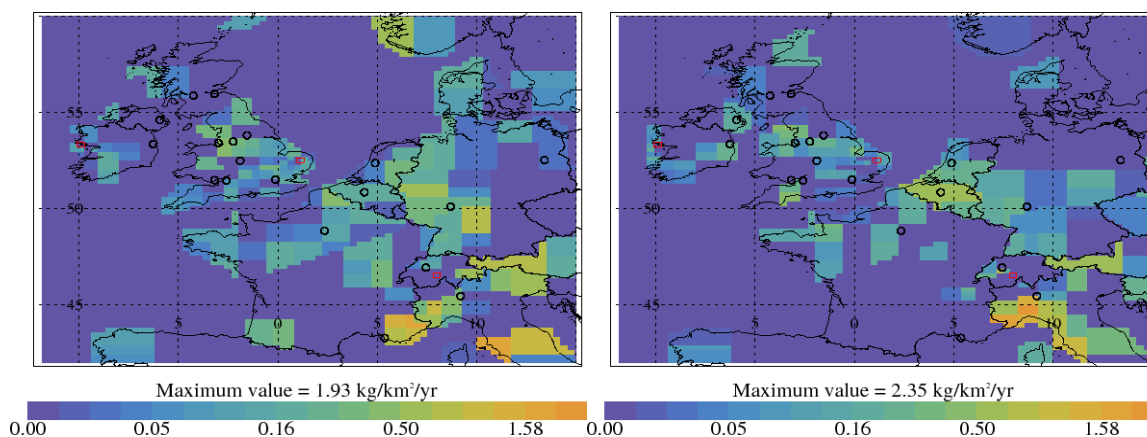
Figure 88: PFC-14 emission estimate using data from 3 sites for 2013-2015 (left) and 2016-2018 (right). Major cities shown as black circles and observation sites shown as red rectangle.

The large uncertainties in the InTEM results overlap with the inventory estimates although the results are generally higher. In the InTEM inversions, the statistical match in time-series between the model time-series and the observations is not strong. This is because the emissions are principally intermittent from point sources (anode effect events at aluminium smelters). If the locations of the smelters are included and solved for as single

grid cells (25 km) then the agreement between model and observation is much improved. The largest smelter in the UK, at Lynemouth on the north east coast of England ceased operations in March 2012. The 4-site InTEM results at the higher time resolution (annual) show elevated emissions compared to the inventory, estimated to be principally emanating from a source near Liverpool, although the uncertainties are large. The MHD-only InTEM estimates show a significant source from near Dublin, Ireland in 2004-2008.

Years	Inventory 1yr	MHD	2 sites	3 sites
1997	0.0385 (0.0364-0.0406)			
1998	0.0385 (0.0364-0.0407)			
1999	0.0372 (0.0351-0.0393)			
2000	0.0480 (0.0450-0.0510)			
2001	0.0375 (0.0353-0.0396)			
2002	0.0286 (0.0269-0.0303)			
2003	0.0233 (0.0220-0.0247)			
2004	0.0286 (0.0269-0.0303)			
2005	0.0214 (0.0201-0.0227)	0.041 (0.023-0.059)		
2006	0.0247 (0.0231-0.0262)	0.037 (0.020-0.055)		
2007	0.0185 (0.0173-0.0197)	0.032 (0.016-0.049)		
2008	0.0220 (0.0206-0.0234)	0.028 (0.013-0.043)		
2009	0.0147 (0.0137-0.0156)	0.028 (0.014-0.042)		
2010	0.0216 (0.0202-0.0230)	0.025 (0.012-0.038)		
2011	0.0288 (0.0270-0.0307)	0.021 (0.009-0.033)	0.023 (0.009-0.038)	
2012	0.0101 (0.0094-0.0108)	0.015 (0.004-0.026)	0.014 (0.002-0.026)	0.028 (0.016-0.041)
2013	0.0104 (0.0097-0.0111)	0.013 (0.001-0.025)	0.014 (0.000-0.028)	0.019 (0.001-0.036)
2014	0.0143 (0.0133-0.0153)	0.015 (0.000-0.032)	0.015 (0.000-0.035)	0.027 (0.008-0.045)
2015	0.0122 (0.0114-0.0130)	0.016 (0.000-0.037)	0.018 (0.000-0.044)	0.031 (0.010-0.053)
2016	0.0135 (0.0125-0.0144)	0.016 (0.000-0.041)	0.016 (0.000-0.047)	0.013 (0.000-0.043)
2017	0.0145 (0.0135-0.0155)	0.009 (0.000-0.034)	0.009 (0.000-0.037)	0.023 (0.000-0.049)
2018		0.007 (0.000-0.031)	0.011 (0.000-0.036)	0.030 (0.010-0.060)
2019				0.019 (0.003-0.036)

Table 30: PFC-14 emission (Gg yr^{-1}) estimates for the UK with uncertainty (1std).

Years	Inventory 1yr	MHD	2 sites	3 sites
1997	0.71 (0.64-0.78)			
1998	0.69 (0.62-0.76)			
1999	0.68 (0.61-0.75)			
2000	0.50 (0.45-0.55)			
2001	0.45 (0.41-0.50)			
2002	0.68 (0.61-0.75)			
2003	0.49 (0.44-0.54)			
2004	0.34 (0.30-0.37)			
2005	0.217 (0.195-0.239)	0.25 (0.16-0.34)		
2006	0.165 (0.148-0.181)	0.25 (0.17-0.34)		
2007	0.143 (0.128-0.157)	0.21 (0.13-0.30)		
2008	0.108 (0.097-0.119)	0.16 (0.09-0.24)		
2009	0.064 (0.058-0.071)	0.12 (0.05-0.18)		
2010	0.070 (0.063-0.077)	0.11 (0.05-0.18)		
2011	0.078 (0.070-0.086)	0.11 (0.04-0.18)	0.16 (0.08-0.25)	
2012	0.045 (0.041-0.050)	0.10 (0.03-0.17)	0.15 (0.08-0.22)	0.13 (0.04-0.21)
2013	0.041 (0.037-0.045)	0.11 (0.03-0.19)	0.14 (0.07-0.21)	0.19 (0.12-0.26)
2014	0.041 (0.037-0.045)	0.11 (0.01-0.21)	0.11 (0.01-0.21)	0.15 (0.07-0.23)
2015	0.043 (0.039-0.048)	0.10 (0.00-0.22)	0.09 (0.00-0.20)	0.13 (0.01-0.26)
2016	0.081 (0.073-0.089)	0.08 (0.00-0.19)	0.07 (0.00-0.18)	0.11 (0.01-0.20)
2017	0.058 (0.052-0.063)	0.07 (0.00-0.17)	0.05 (0.00-0.14)	0.09 (0.00-0.20)
2018		0.07 (0.00-0.17)	0.08 (0.00-0.17)	0.10 (0.00-0.21)
2019				0.16 (0.08-0.25)

Table 31: PFC-14 emission (Gg yr^{-1}) estimates for the NWEU with uncertainty (1std).

4.18 PFC-116
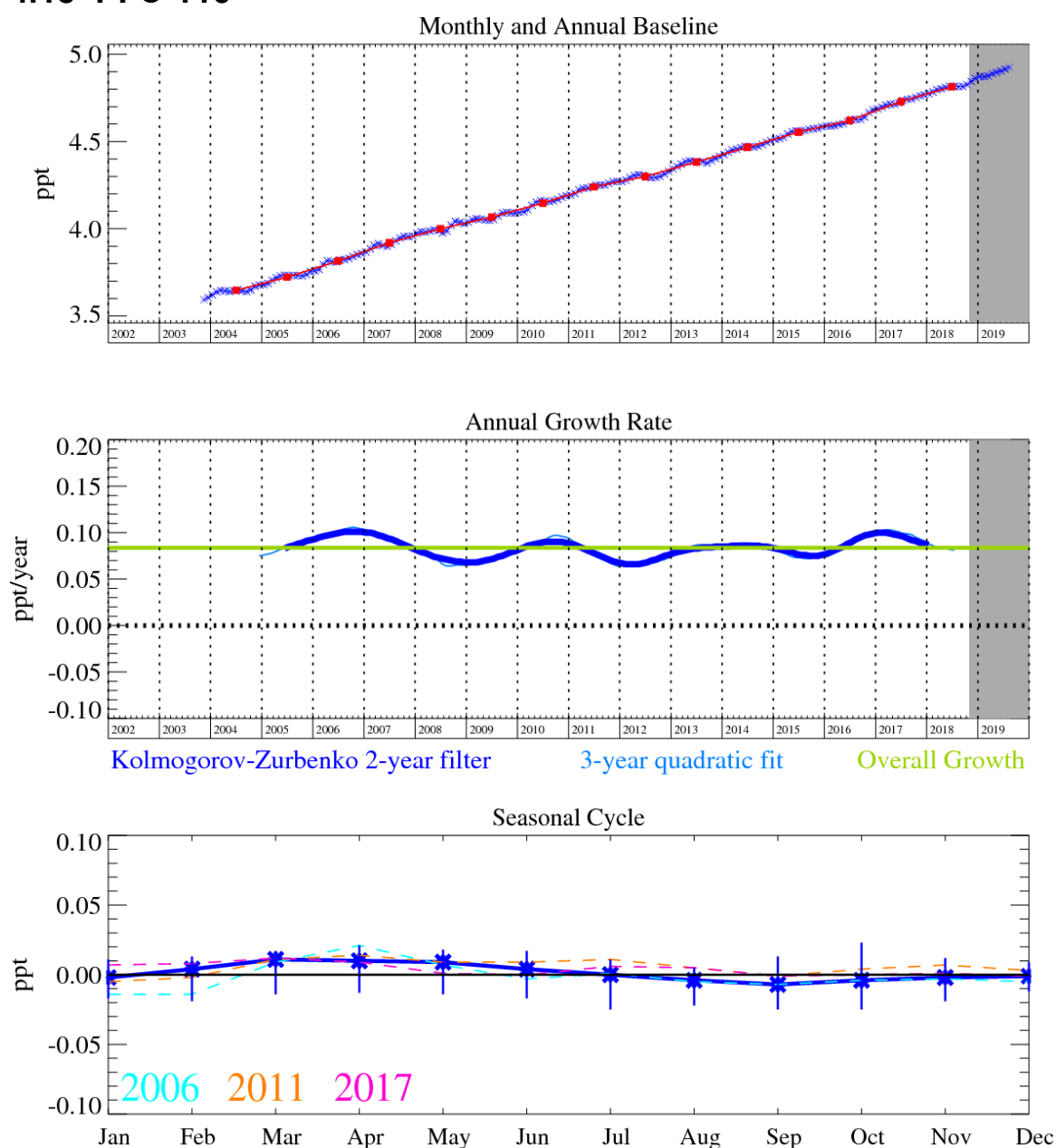
Figure 89: PFC-116: Monthly (blue) and annual (red) Northern Hemisphere baseline mole fractions (top plot). Annual (blue) and overall (green) average growth rate (middle plot). Seasonal cycle (de-trended) with year-to-year variability (lower plot). Grey area covers un-ratified provisional data.

PFC-116 (C_2F_6) is a potent greenhouse gas with an atmospheric lifetime of >10,000 years. It has many common sources to CF_4, and serves to help explain why most of the CF_4 above-baseline (pollution) events are correlated with those of C_2F_6. However, we note that they are more frequent. This is due to the dominant source of C_2F_6 being from plasma etching in the semiconductor industry.

The InTEM uncertainty ranges for the UK emissions are large but consistently overlap the inventory estimates. The 2004-2008 InTEM estimates show a strong emission source south west of Dublin, Ireland that fades in the more recent years.
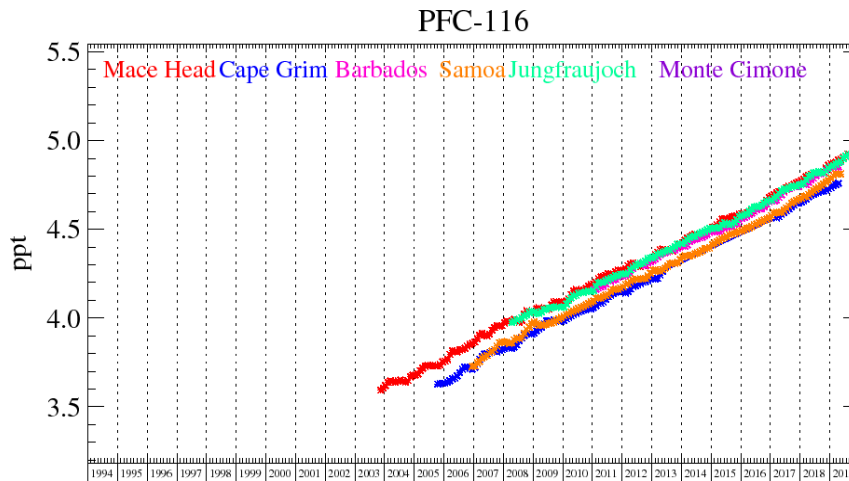
Figure 90: Background PFC-116 mole fractions at several global AGAGE stations both in the Northern and Southern Hemispheres.
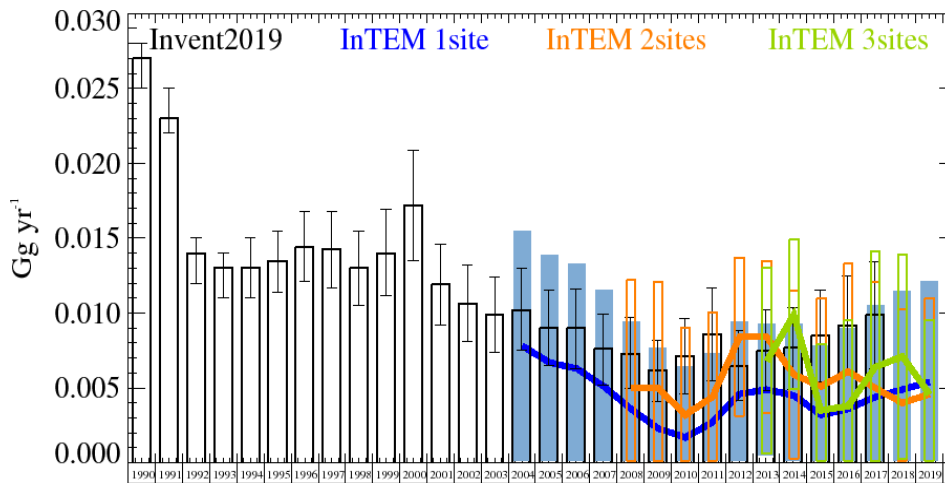
Figure 91: PFC-116: UK emission estimates (Gg yr^{-1}) from the UNFCCC Inventory (black) and InTEM (annually averaged): (a) MHD (3yr) with global meteorology (blue), (b) 2 sites (2yr) (MHD+JFJ) with global meteorology (orange), and (c) 3 sites (1yr) (MHD+JFJ+TAC) with UKV 1.5 km nested in global meteorology (green). The uncertainty bars represent 1 std.
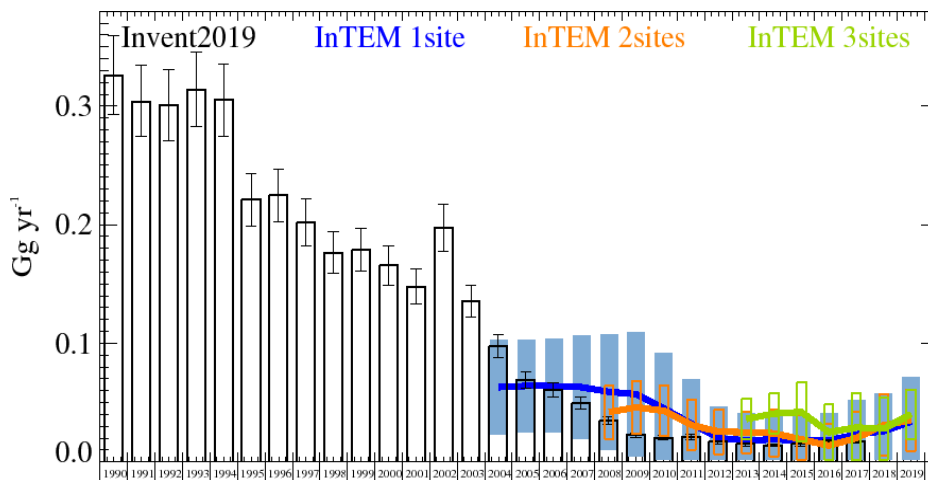
Figure 92: PFC-116: NWEU emission estimates (Gg yr^{-1}) from the UNFCCC Inventory (black) and InTEM (annually averaged): (a) MHD (3yr) with global meteorology (blue), (b) 2 sites (2yr) (MHD+JFJ) with global meteorology (orange), and (c) 3 sites (1yr) (MHD+JFJ+TAC) with UKV 1.5 km nested in global meteorology (green). The uncertainty bars represent 1 std.
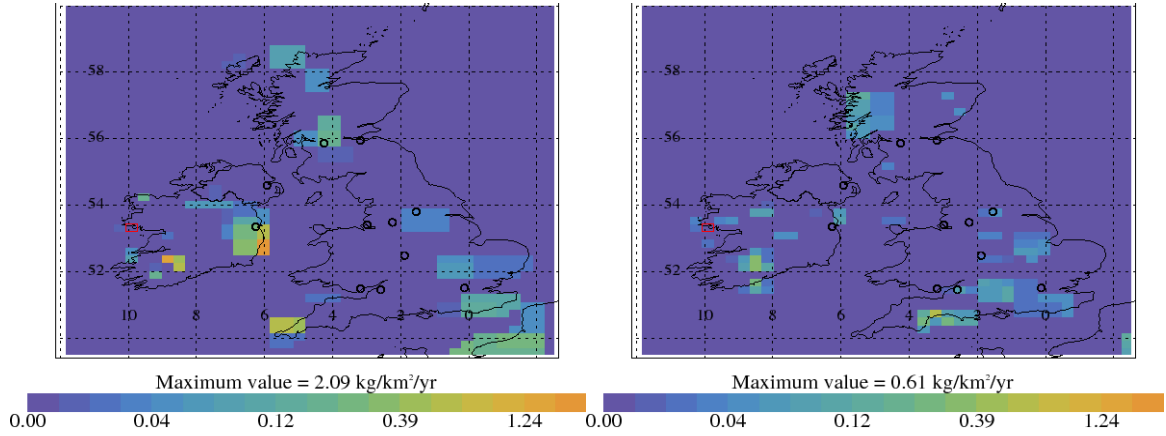
Figure 93: PFC-116 emission estimate using MHD data for 2004-2008 (left) and 2014-2018 (right). Major cities shown as black circles and observation sites shown as red rectangle.
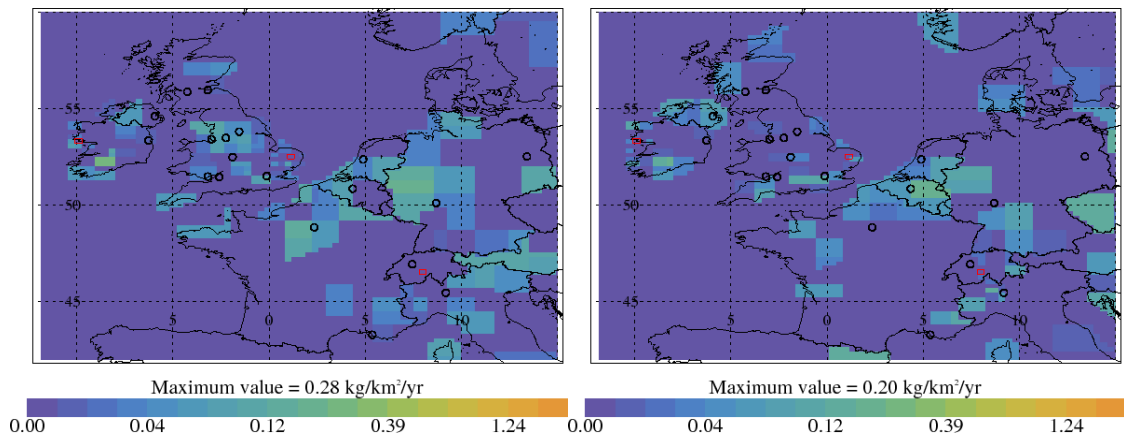
Figure 94: PFC-116 emission estimate using data from 3 sites for 2013-2015 (left) and 2016-2018 (right). Major cities shown as black circles and observation sites shown as red rectangle.

| Years	Inventory 1yr	MHD	2 sites	3 sites
1997	0.014 (0.012-0.017)			
1998	0.013 (0.011-0.016)			
1999	0.014 (0.011-0.017)			
2000	0.017 (0.013-0.021)			
2001	0.012 (0.009-0.015)			
2002	0.011 (0.008-0.013)			
2003	0.010 (0.007-0.012)			
2004	0.010 (0.007-0.013)			
2005	0.009 (0.006-0.012)	0.007 (0.000-0.014)		
2006	0.009 (0.006-0.012)	0.006 (0.000-0.014)		
2007	0.008 (0.005-0.010)	0.005 (0.000-0.013)		
2008	0.007 (0.005-0.010)	0.004 (0.000-0.012)		
2009	0.006 (0.004-0.008)	0.002 (0.000-0.011)	0.005 (0.000-0.014)	
2010	0.007 (0.005-0.010)	0.002 (0.000-0.009)	0.003 (0.000-0.012)	
2011	0.009 (0.005-0.012)	0.003 (0.000-0.009)	0.004 (0.000-0.011)	
2012	0.007 (0.004-0.009)	0.005 (0.000-0.010)	0.008 (0.003-0.014)	
2013	0.007 (0.005-0.010)	0.005 (0.001-0.009)	0.008 (0.003-0.013)	0.007 (0.001-0.013)
2014	0.008 (0.005-0.010)	0.004 (0.000-0.009)	0.006 (0.000-0.012)	0.010 (0.005-0.015)
2015	0.008 (0.005-0.011)	0.003 (0.000-0.009)	0.005 (0.000-0.012)	0.004 (0.000-0.009)
2016	0.009 (0.006-0.012)	0.004 (0.000-0.011)	0.006 (0.000-0.014)	0.004 (0.000-0.011)
2017	0.010 (0.006-0.013)	0.004 (0.000-0.012)	0.005 (0.000-0.014)	0.006 (0.000-0.015)
2018		0.005 (0.000-0.013)	0.004 (0.000-0.013)	0.007 (0.000-0.014)
2019				0.005 (0.000-0.010)

Table 32: PFC-116 emission (Gg yr^{-1}) estimates for the UK with uncertainty (1std).

Years	Inventory 1yr	MHD	2 sites	3 sites
1990	0.33 (0.29-0.36)			
1991	0.30 (0.27-0.33)			
1992	0.30 (0.27-0.33)			
1993	0.31 (0.28-0.35)			
1994	0.30 (0.27-0.34)			
1995	0.221 (0.199-0.243)			
1996	0.225 (0.202-0.247)			
1997	0.202 (0.182-0.222)			
1998	0.176 (0.159-0.194)			
1999	0.179 (0.161-0.197)			
2000	0.166 (0.149-0.182)			
2001	0.148 (0.133-0.163)			
2002	0.197 (0.178-0.217)			
2003	0.135 (0.122-0.149)			
2004	0.097 (0.088-0.107)			
2005	0.069 (0.062-0.076)	0.06 (0.03-0.10)		
2006	0.061 (0.055-0.067)	0.06 (0.02-0.10)		
2007	0.050 (0.045-0.055)	0.06 (0.02-0.11)		
2008	0.035 (0.031-0.038)	0.06 (0.01-0.11)		
2009	0.022 (0.020-0.025)	0.06 (0.00-0.11)	0.046 (0.024-0.068)	
2010	0.020 (0.018-0.022)	0.05 (0.00-0.09)	0.043 (0.021-0.064)	
2011	0.021 (0.019-0.023)	0.03 (0.00-0.07)	0.031 (0.010-0.052)	
2012	0.017 (0.015-0.018)	0.02 (0.00-0.05)	0.025 (0.007-0.044)	
2013	0.015 (0.013-0.016)	0.02 (0.00-0.05)	0.025 (0.007-0.043)	0.036 (0.019-0.053)
2014	0.014 (0.013-0.015)	0.02 (0.00-0.05)	0.024 (0.004-0.044)	0.041 (0.024-0.058)
2015	0.015 (0.013-0.016)	0.02 (0.00-0.05)	0.019 (0.000-0.041)	0.042 (0.017-0.067)
2016	0.018 (0.016-0.019)	0.02 (0.00-0.05)	0.014 (0.000-0.037)	0.025 (0.002-0.049)
2017	0.018 (0.016-0.019)	0.02 (0.00-0.06)	0.020 (0.000-0.045)	0.03 (0.00-0.06)
2018		0.03 (0.00-0.06)	0.03 (0.01-0.06)	0.03 (0.00-0.05)
2019				0.04 (0.02-0.06)

Table 33: PFC-116 emission (Gg yr^{-1}) estimates for the NWEU with uncertainty (1std).

4.19 PFC-218
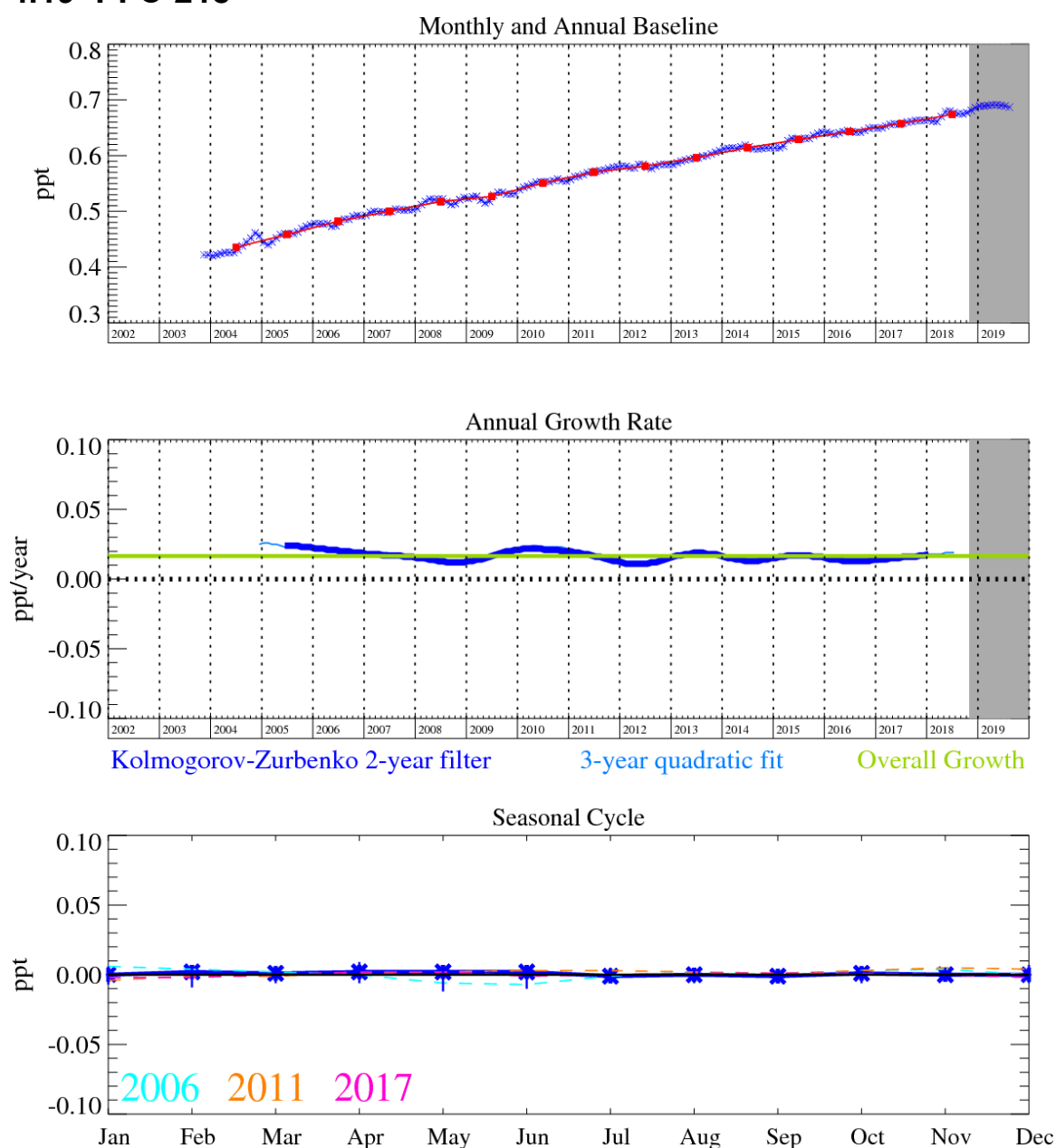
Figure 95: PFC-218: Monthly (blue) and annual (red) Northern Hemisphere baseline mole fractions (top plot). Annual (blue) and overall (green) average growth rate (middle plot). Seasonal cycle (de-trended) with year-to-year variability (lower plot). Grey area covers un-ratified provisional data.

PFC-218 (C_3F_8) has an atmospheric lifetime of 2600 years and a GWP_{100} of 8690. It is also used in semiconductor manufacturing, but to a lesser extent than C_2F_6. It also has a very small contribution from aluminium smelting and has an increasing contribution from refrigeration use. Observations of above-baseline C_3F_8 emissions are less frequent than those of C_2F_6 but are of a higher relative magnitude.

The MHD-only InTEM and inventory results are remarkably consistent in trend, both showing dips in emissions in 2008 – 2010. The MHD-only InTEM estimates are lower than those estimated in the inventory although the uncertainties fully overlap. The 4-site InTEM estimates show a dip in 2015-6, they estimate a significant UK emission source in NW England, in the Manchester / Liverpool area.
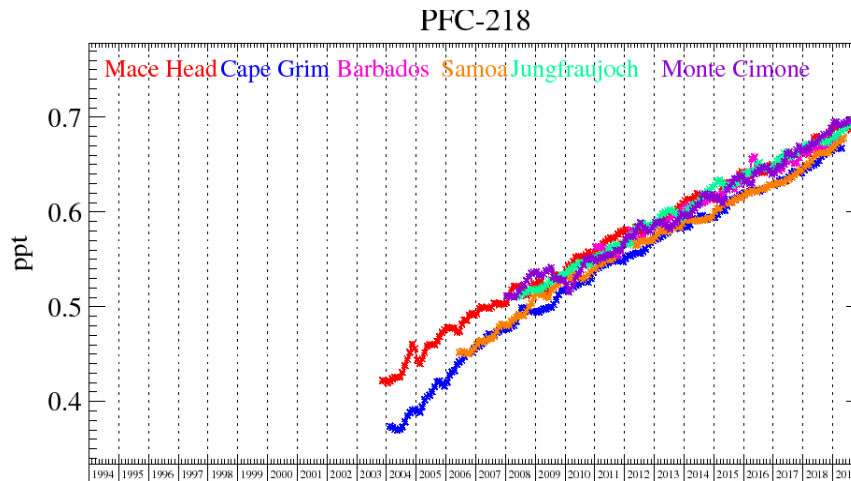
Figure 96: Background PFC-218 mole fractions at several global AGAGE stations both in the Northern and Southern Hemispheres.
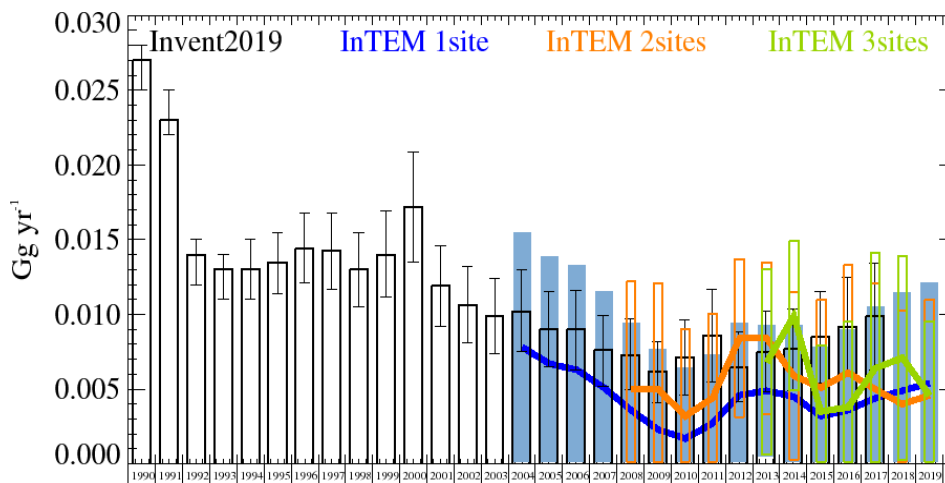
Figure 97: PFC-218: UK emission estimates (Gg yr^{-1}) from the UNFCCC Inventory (black) and InTEM (annually averaged): (a) MHD (3yr) with global meteorology (blue), (b) 3 sites (2yr) (MHD+JFJ+CMN) with global meteorology (orange), and (c) 4 sites (1yr) (MHD+JFJ+CMN+TAC) with UKV 1.5 km nested in global meteorology (green). The uncertainty bars represent 1 std.
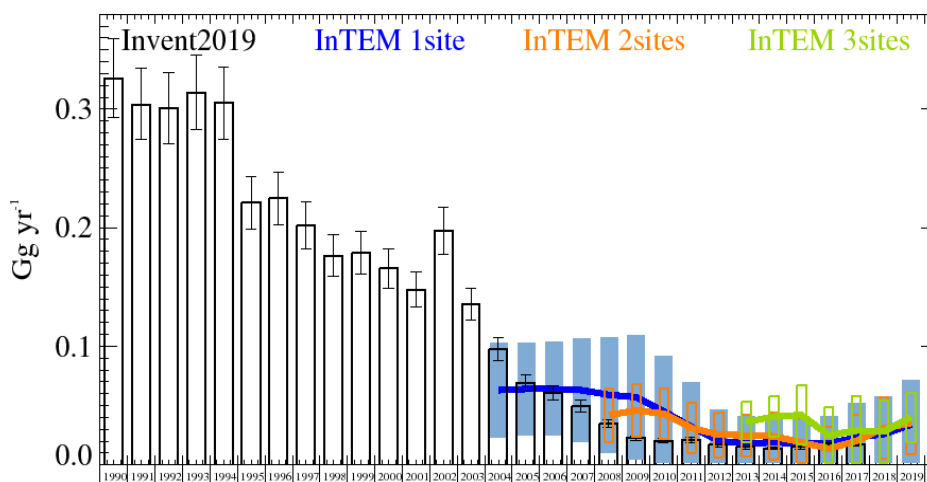
Figure 98: PFC-218: NWEU emission estimates (Gg yr^{-1}) from the UNFCCC Inventory (black) and InTEM (annually averaged): (a) MHD (3yr) with global meteorology (blue), (b) 3 sites (2yr) (MHD+JFJ+CMN) with global meteorology (orange), and (c) 4 sites (1yr) (MHD+JFJ+CMN+TAC) with UKV 1.5 km nested in global meteorology (green). The uncertainty bars represent 1 std.

Maximum value = 5.69e-01 kg/km^2/yr   Maximum value = 7.89e-01 kg/km^2/yr

0.00e+00   1.78e-02   5.63e-02   1.78e-01   5.63e-01   0.00e+00   1.78e-02   5.63e-02   1.78e-01   5.63e-01
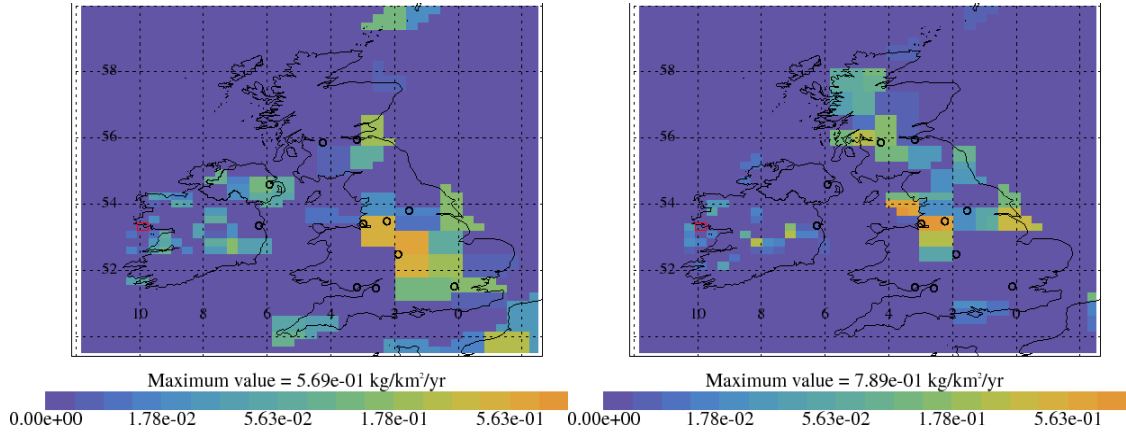
Figure 99: PFC-218 emission estimate using MHD data for 2004-2008 (left) and 2014-2018 (right). Major cities shown as black circles and observation sites shown as red rectangle.

Maximum value = 4.66e-01 kg/km^2/yr   Maximum value = 3.25e-01 kg/km^2/yr

0.00e+00   1.78e-02   5.63e-02   1.78e-01   5.63e-01   0.00e+00   1.78e-02   5.63e-02   1.78e-01   5.63e-01
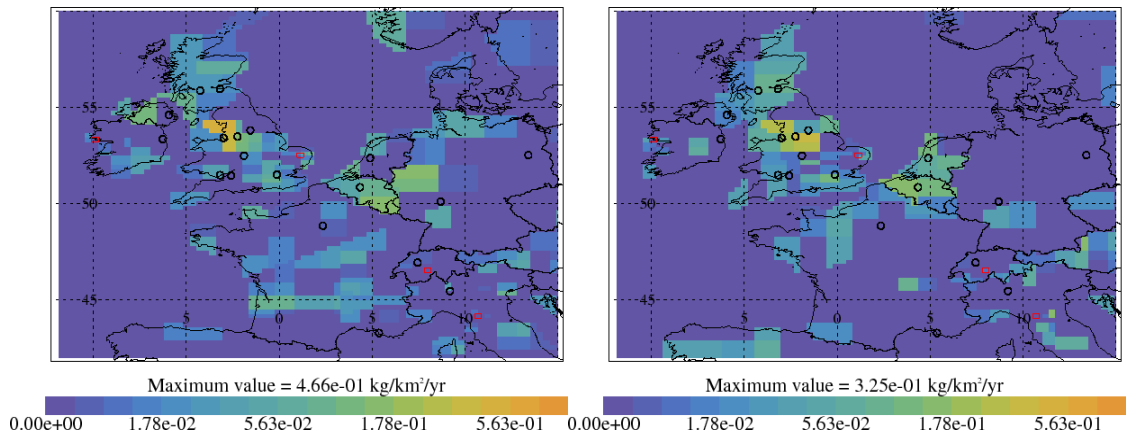
Figure 100: PFC-218 emission estimate using data from 4 sites for 2013-2015 (left) and 2016-2018 (right). Major cities shown as black circles and observation sites shown as red rectangle.

Years	Inventory 1yr	MHD	3 sites	4 sites
1996	0.0018 (0.0013-0.0022)			
1997	0.0018 (0.0014-0.0023)			
1998	0.0033 (0.0024-0.0041)			
1999	0.0018 (0.0013-0.0022)			
2000	0.0020 (0.0015-0.0025)			
2001	0.0062 (0.0047-0.0076)			
2002	0.0063 (0.0049-0.0078)			
2003	0.0065 (0.0050-0.0079)			
2004	0.010 (0.008-0.013)			
2005	0.013 (0.010-0.015)	0.020 (0.015-0.025)		
2006	0.010 (0.008-0.012)	0.019 (0.015-0.024)		
2007	0.0064 (0.0051-0.0076)	0.017 (0.012-0.021)		
2008	0.0015 (0.0012-0.0018)	0.014 (0.009-0.019)		
2009	0.0015 (0.0012-0.0018)	0.011 (0.006-0.016)	0.014 (0.008-0.019)	
2010	0.0046 (0.0038-0.0054)	0.010 (0.005-0.015)	0.011 (0.006-0.017)	
2011	0.011 (0.009-0.013)	0.009 (0.005-0.013)	0.010 (0.005-0.014)	
2012	0.011 (0.009-0.013)	0.010 (0.007-0.013)	0.009 (0.006-0.013)	
2013	0.017 (0.014-0.019)	0.012 (0.009-0.015)	0.012 (0.009-0.015)	0.013 (0.009-0.017)
2014	0.009 (0.007-0.010)	0.013 (0.009-0.017)	0.016 (0.012-0.021)	0.015 (0.010-0.019)
2015	0.015 (0.013-0.017)	0.015 (0.010-0.020)	0.015 (0.010-0.021)	0.016 (0.012-0.021)
2016	0.016 (0.013-0.018)	0.013 (0.007-0.019)	0.010 (0.005-0.016)	0.011 (0.005-0.017)
2017	0.016 (0.014-0.018)	0.013 (0.007-0.019)	0.009 (0.004-0.015)	0.018 (0.012-0.024)
2018		0.012 (0.006-0.018)	0.009 (0.004-0.015)	0.015 (0.010-0.020)
2019				0.013 (0.008-0.017)

**Table 34: PFC-218 emission (Gg yr^{-1}) estimates for the UK with uncertainty (1std).**

Years	Inventory 1yr	MHD	3 sites	4 sites
1990	0.025 (0.022-0.027)			
1991	0.024 (0.021-0.026)			
1992	0.026 (0.023-0.028)			
1993	0.026 (0.023-0.028)			
1994	0.031 (0.028-0.034)			
1995	0.037 (0.034-0.041)			
1996	0.039 (0.035-0.043)			
1997	0.042 (0.038-0.047)			
1998	0.028 (0.025-0.030)			
1999	0.0132 (0.0119-0.0146)			
2000	0.0144 (0.0130-0.0159)			
2001	0.019 (0.017-0.021)			
2002	0.019 (0.017-0.021)			
2003	0.020 (0.018-0.022)			
2004	0.024 (0.022-0.027)			
2005	0.027 (0.025-0.030)	0.05 (0.03-0.07)		
2006	0.026 (0.023-0.028)	0.05 (0.03-0.07)		
2007	0.020 (0.018-0.022)	0.05 (0.03-0.07)		
2008	0.0126 (0.0114-0.0139)	0.04 (0.02-0.07)		
2009	0.0090 (0.0081-0.0099)	0.03 (0.01-0.06)	0.026 (0.012-0.039)	
2010	0.0091 (0.0082-0.0100)	0.02 (0.00-0.05)	0.021 (0.009-0.032)	
2011	0.0139 (0.0125-0.0153)	0.02 (0.00-0.04)	0.016 (0.006-0.026)	
2012	0.0126 (0.0114-0.0139)	0.02 (0.00-0.04)	0.018 (0.009-0.027)	
2013	0.018 (0.016-0.020)	0.02 (0.00-0.04)	0.021 (0.012-0.030)	0.034 (0.024-0.044)
2014	0.010 (0.009-0.011)	0.02 (0.00-0.04)	0.025 (0.014-0.035)	0.027 (0.016-0.038)
2015	0.016 (0.014-0.017)	0.03 (0.00-0.05)	0.026 (0.013-0.038)	0.040 (0.030-0.060)
2016	0.016 (0.015-0.018)	0.03 (0.00-0.05)	0.017 (0.004-0.030)	0.028 (0.015-0.041)
2017	0.016 (0.015-0.018)	0.03 (0.00-0.05)	0.013 (0.001-0.024)	0.028 (0.013-0.042)
2018		0.03 (0.00-0.05)	0.016 (0.006-0.027)	0.026 (0.014-0.038)
2019				0.028 (0.016-0.040)

Table 35: PFC-218 emission (Gg yr^{-1}) estimates for the NWEU with uncertainty (1std).

4.20 PFC-318

Monthly and Annual Baseline

Annual Growth Rate

Kolmogorov-Zurbenko 2-year filter   3-year quadratic fit   Overall Growth

Seasonal Cycle

2012   2014   2017
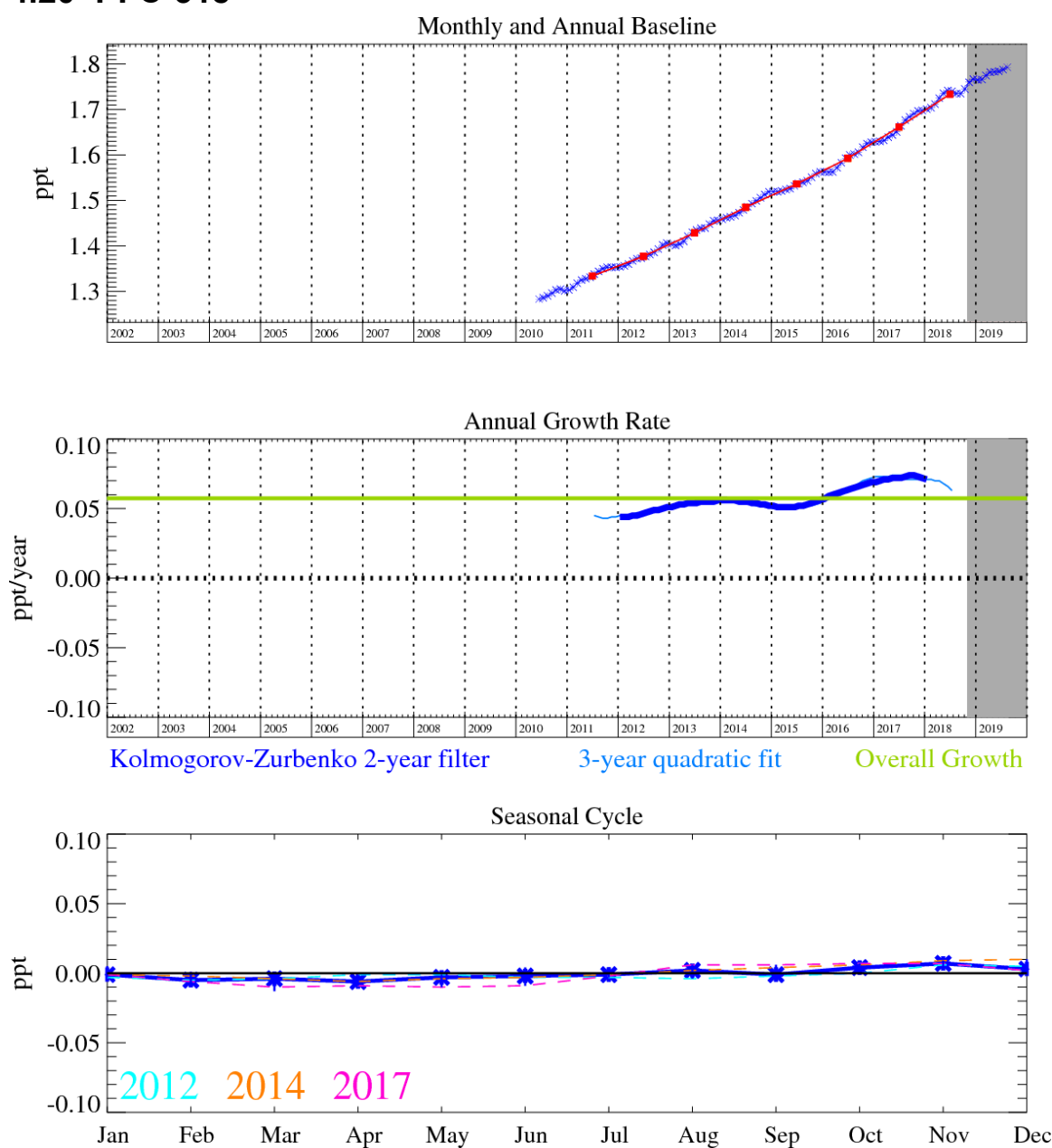
Figure 101: PFC-318: Monthly (blue) and annual (red) Northern Hemisphere baseline mole fractions (top plot). Annual (blue) and overall (green) average growth rate (middle plot). Seasonal cycle (de-trended) with year-to-year variability (lower plot). Grey area covers un-ratified provisional data.

PFC-318 (c-C_4F_8) is increasingly used in the semiconductor and electronics industries for cleaning, plasma etching and deposition gas, also it has a minor use in aerolysed foods, retinal detachment surgery, size estimation of natural gas and oil reservoirs, specialist military applications, tracer experiments and may also replace SF_6 as an electrically insulating gas. It has an atmospheric lifetime of 3,200 years, a GWP_{100} of 10,300 and a radiative efficiency of 0.32 W m^{-2} ppb^{-1}.

The reported UK inventory emissions of PFC-318 are very small (less than 0.00001 Gg yr-1) compared to the InTEM emission estimates (~0.006 Gg yr-1); however, the InTEM estimates have very significant uncertainty extending close to zero. The InTEM estimates with 4-sites, MHD+JFJ+CMN+TAC, show a significant source of PFC-318 from The Netherlands.
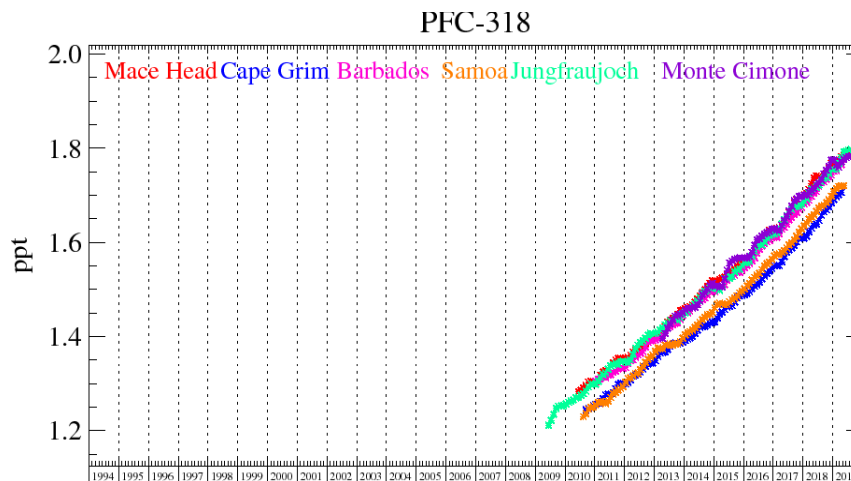
Figure 102: Background PFC-318 mole fractions at several global AGAGE stations both in the Northern and Southern Hemispheres.
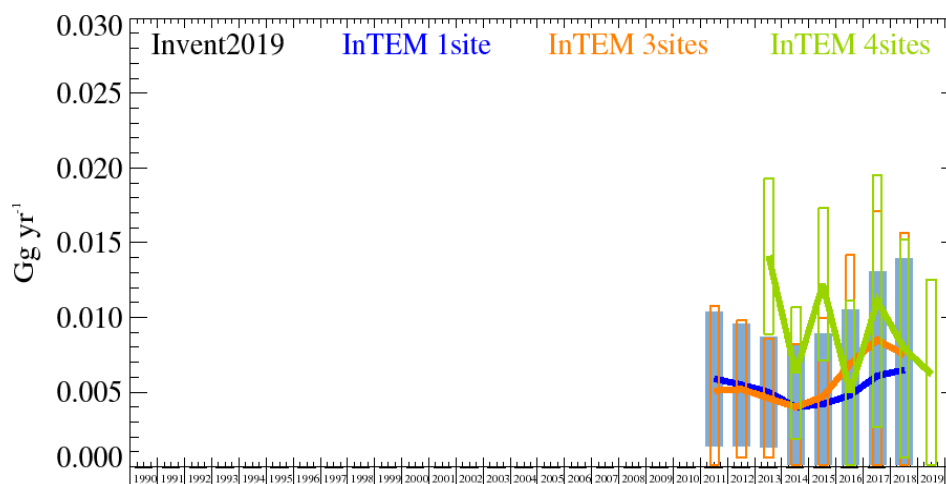
Figure 103: PFC-318: UK emission estimates (Gg yr^{-1}) from the UNFCCC Inventory (black) and InTEM (annually averaged): (a) MHD (3yr) with global meteorology (blue), (b) 3 sites (2yr) (MHD+JFJ+CMN) with global meteorology (orange), and (c) 4 sites (1yr) (MHD+JFJ+CMN+TAC) with UKV 1.5 km nested in global meteorology (green). The uncertainty bars represent 1 std.
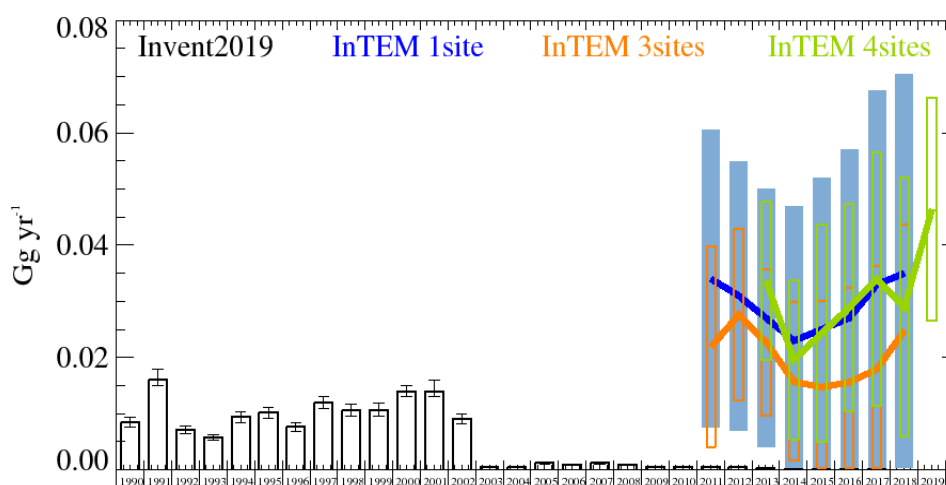
Figure 104: PFC-318: NWEU emission estimates (Gg yr^{-1}) from the UNFCCC Inventory (black) and InTEM (annually averaged): (a) MHD (3yr) with global meteorology (blue), (b) 3 sites (2yr) (MHD+JFJ+CMN) with global meteorology (orange), and (c) 4 sites (1yr) (MHD+JFJ+CMN+TAC) with UKV 1.5 km nested in global meteorology (green). The uncertainty bars represent 1 std.
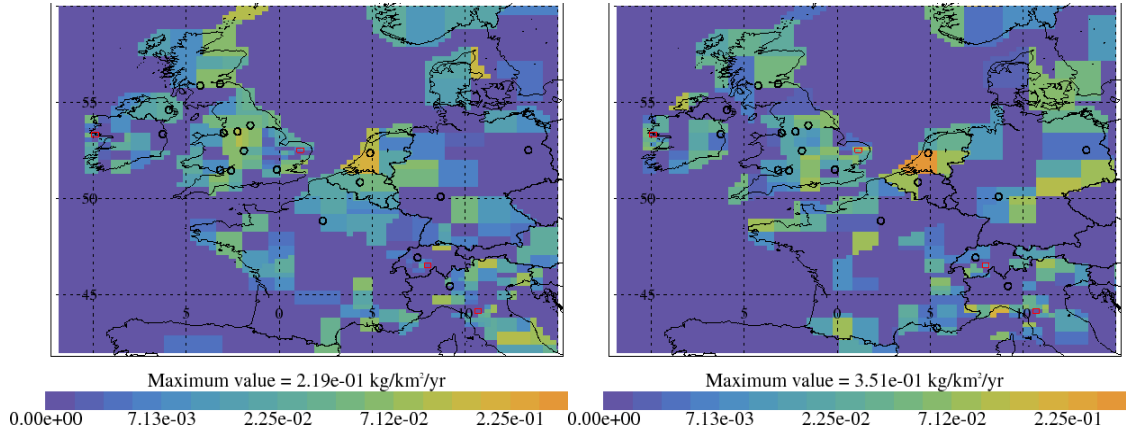
Figure 105: PFC-318 emission estimate using data from 4 sites for 2013-2015 (left) and 2016-2018 (right). Major cities shown as black circles and observation sites shown as red rectangle.

Years	Inventory 1yr	MHD	3 sites	4 sites
1990	0.000001 (0.000001-0.000001)			
1991	0.000001 (0.000001-0.000002)			
1992	0.000002 (0.000001-0.000002)			
1993	0.000002 (0.000002-0.000002)			
1994	0.000002 (0.000002-0.000002)			
1995	0.000003 (0.000002-0.000003)			
1996	0.000003 (0.000003-0.000003)			
1997	0.000003 (0.000003-0.000004)			
1998	0.000004 (0.000003-0.000004)			
1999	0.000004 (0.000004-0.000005)			
2000	0.000005 (0.000005-0.000006)			
2001	0.000003 (0.000003-0.000003)			
2002	0.000003 (0.000003-0.000003)			
2003	0.000003 (0.000003-0.000004)			
2004	0.000003 (0.000003-0.000003)			
2005	0.000003 (0.000003-0.000003)			
2006	0.000003 (0.000003-0.000003)			
2007	0.000003 (0.000003-0.000004)			
2008	0.000003 (0.000003-0.000004)			
2009	0.000004 (0.000003-0.000004)			
2010	0.000004 (0.000003-0.000004)			
2011	0.000004 (0.000003-0.000004)	0.0059 (0.0014-0.0104)	0.0051 (0.0000-0.0113)	
2012	0.000004 (0.000004-0.000005)	0.0055 (0.0014-0.0096)	0.0052 (0.0006-0.0098)	
2013	0.000005 (0.000004-0.000005)	0.0050 (0.0013-0.0087)	0.0046 (0.0006-0.0086)	0.0141 (0.0089-0.0193)
2014	0.000005 (0.000004-0.000005)	0.0040 (0.0000-0.0082)	0.0040 (0.0000-0.0085)	0.0063 (0.0019-0.0107)
2015	0.000005 (0.000005-0.000006)	0.0042 (0.0000-0.0095)	0.0047 (0.0000-0.0105)	0.0122 (0.0071-0.0173)
2016	0.000006 (0.000005-0.000006)	0.0048 (0.0000-0.0114)	0.0069 (0.0000-0.0146)	0.0050 (0.0000-0.0122)
2017	0.000006 (0.000006-0.000007)	0.0061 (0.0000-0.0140)	0.0085 (0.0000-0.0172)	0.0111 (0.0027-0.0195)
2018		0.0065 (0.0000-0.0149)	0.0075 (0.0000-0.0163)	0.0079 (0.0006-0.0152)
2019				0.0062 (0.0000-0.0127)

**Table 36: PFC-318 emission (Gg yr^{-1}) estimates for the UK with uncertainty (1std).**

Years	Inventory 1yr	MHD	3 sites	4 sites
1990	0.0084 (0.0076-0.0093)			
1991	0.0164 (0.0148-0.0180)			
1992	0.0072 (0.0065-0.0079)			
1993	0.0057 (0.0052-0.0063)			
1994	0.0094 (0.0084-0.0103)			
1995	0.0102 (0.0092-0.0112)			
1996	0.0077 (0.0069-0.0084)			
1997	0.0118 (0.0106-0.0129)			
1998	0.0106 (0.0096-0.0117)			
1999	0.0107 (0.0096-0.0118)			
2000	0.0140 (0.0126-0.0154)			
2001	0.0144 (0.0129-0.0158)			
2002	0.0091 (0.0082-0.0100)			
2003	0.0005 (0.0005-0.0006)			
2004	0.0005 (0.0005-0.0006)			
2005	0.0012 (0.0011-0.0013)			
2006	0.0010 (0.0009-0.0011)			
2007	0.0013 (0.0011-0.0014)			
2008	0.0010 (0.0009-0.0011)			
2009	0.0005 (0.0005-0.0006)			
2010	0.0005 (0.0004-0.0005)			
2011	0.0006 (0.0005-0.0006)	0.03 (0.01-0.06)	0.022 (0.004-0.040)	
2012	0.0004 (0.0004-0.0005)	0.031 (0.007-0.055)	0.028 (0.012-0.043)	
2013	0.0003 (0.0003-0.0004)	0.027 (0.004-0.050)	0.023 (0.010-0.036)	0.034 (0.019-0.048)
2014	0.0001 (0.0001-0.0001)	0.023 (0.000-0.048)	0.016 (0.002-0.030)	0.020 (0.005-0.034)
2015	0.0001 (0.0001-0.0001)	0.02 (0.00-0.05)	0.015 (0.000-0.031)	0.024 (0.005-0.044)
2016	0.0002 (0.0002-0.0002)	0.03 (0.00-0.06)	0.016 (0.000-0.034)	0.029 (0.010-0.047)
2017	0.0002 (0.0002-0.0002)	0.03 (0.00-0.07)	0.018 (0.000-0.037)	0.034 (0.012-0.057)
2018		0.04 (0.00-0.07)	0.025 (0.006-0.044)	0.029 (0.006-0.052)
2019				0.046 (0.026-0.066)

Table 37: PFC-318 emission (Gg yr^{-1}) estimates for the NWEU with uncertainty (1std).

4.21 SF$_6$
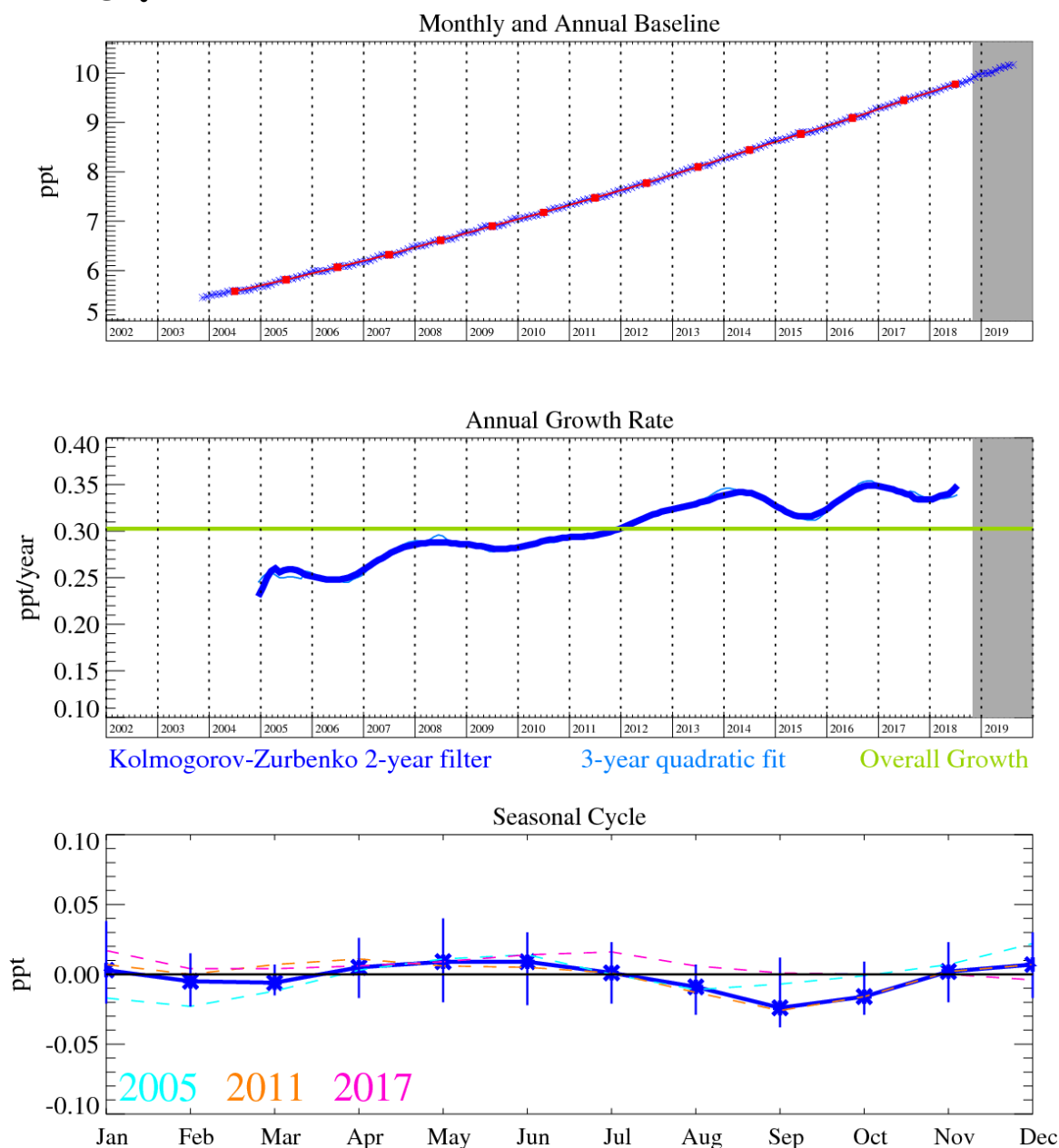
Figure 106: SF$_6$: Monthly (blue) and annual (red) Northern Hemisphere baseline mole fractions (top plot). Annual (blue) and overall (green) average growth rate (middle plot). Seasonal cycle (de-trended) with year-to-year variability (lower plot). Grey area covers un-ratified provisional data.

SF$_6$ is an important greenhouse gas since it has a long atmospheric lifetime of 3,200 years and a high radiative efficiency; giving rise to a GWP$_{100}$ of 22,800. Although having minor usage in the semiconductor industry, it is predominantly used in electrical circuit breakers, heavy-duty gas-insulated switchgear (GIS) for systems with voltages from 5,000-38,000 volts, and other switchgear used in the electrical transmission systems to manage high voltages (>38 kV). The electrical power industry uses roughly 80% of all SF$_6$ produced worldwide. Although the units themselves are hermetically sealed and pressurised, aging equipment, breakdown and disposal, alongside leakage from wear-and-tear will cause this sector to emit SF$_6$. A minor use of this gas is also reported in its use as a blanketing (i.e. oxygen inhibiting inert gas) agent during magnesium production. Hence SF$_6$ will have many, and more diffuse, sources relative to the other perfluorinated species. Its atmospheric trend was predicted to rise at a rate faster than linear, as older electrical

switchgear is switched to higher efficiency units; this is corroborated by the constantly increasing atmospheric growth rate since measurements began.
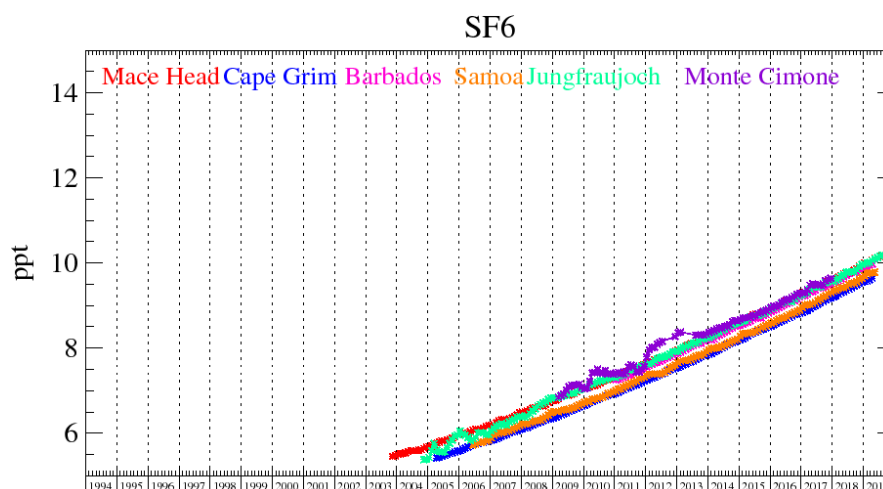
Figure 107: Background SF$_6$ mole fractions at several global AGAGE stations both in the Northern and Southern Hemispheres.
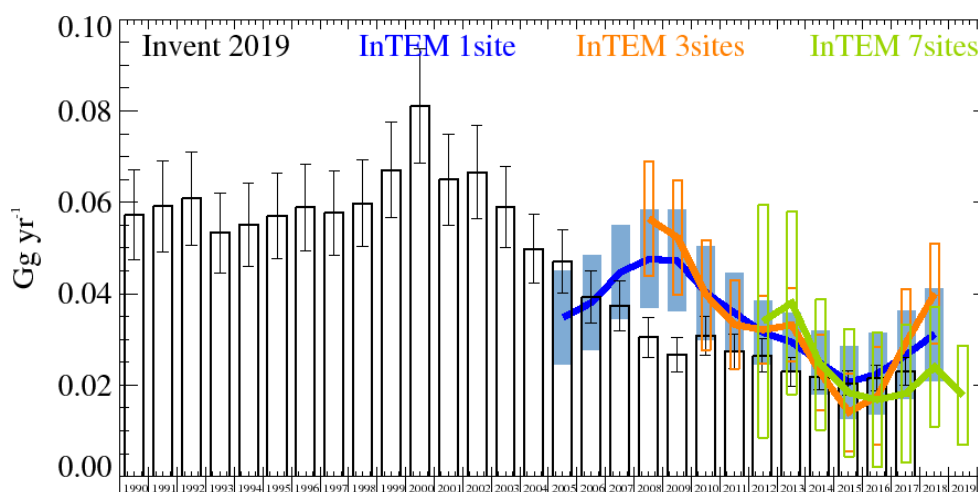
Figure 108: SF$_6$: UK emission estimates (Gg yr^{-1}) from the UNFCCC Inventory (black) and InTEM (annually averaged): (a) MHD (3yr) with global meteorology (blue), (b) 3 sites (2yr) (MHD+JFJ+CMN) with global meteorology (orange), and (c) 7 sites (2mth) (DECC+JFJ+CMN) with UKV 1.5 km nested in global meteorology (green). The uncertainty bars represent 1 std.

After 2006, the UK InTEM estimates using MHD-only are consistently elevated compared to the inventory; the InTEM uncertainty ranges do overlap the inventory estimates however from 2010. The rise in InTEM MHD-only emission estimates for the UK from 2006 to 2009 are at odds with a decline in the inventory. There is reasonable agreement between the different inversion estimates, but they start to diverge more in 2018, though all showing an upward trend.

The NWEU InTEM results are in very good agreement with the trend seen in the Inventory. The MHD-only inversion consistently under-predicts however the InTEM 7-site inversion is in very close agreement with the inventory. The south of Germany is estimated to be a growing source of SF$_6$.

There is also evidence of a seasonal cycle in the emission of SF$_6$, especially in the NWEU results, with more emission in the winter months. It is not clear why this may be.
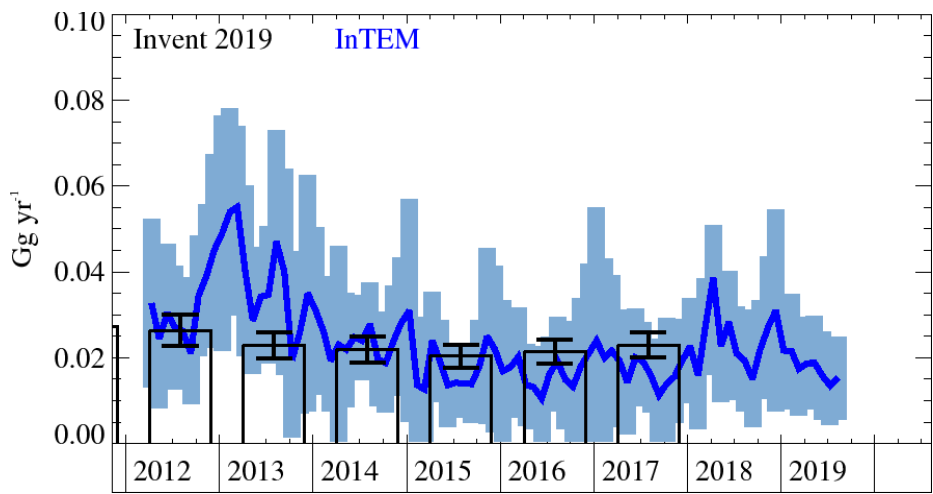
Figure 109: SF₆: UK emission estimates (Gg yr⁻¹) from the UNFCCC Inventory (black) and InTEM 2-month 7 sites (DECC+JFJ+CMN) with UKV 1.5 km meteorology (blue). The uncertainty bars represent 1 std.
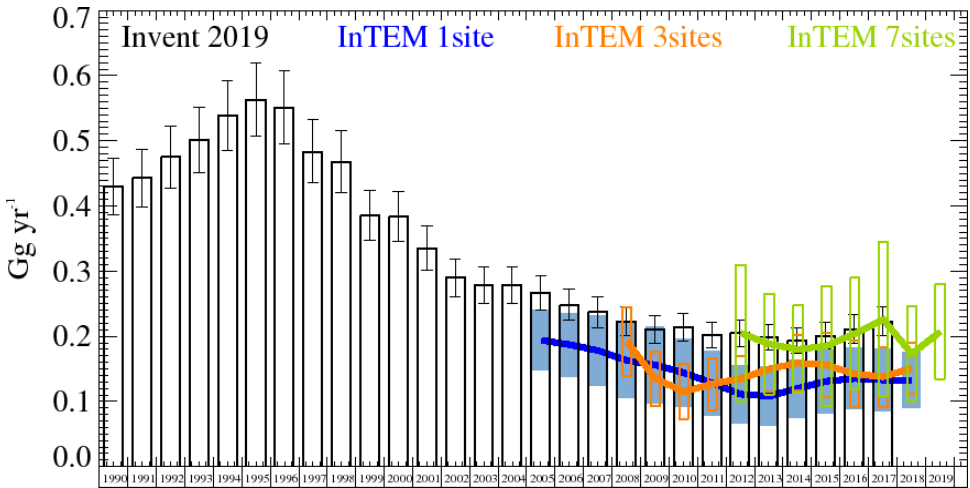
Figure 110: SF₆: NWEU emission estimates (Gg yr⁻¹) from the UNFCCC Inventory (black) and InTEM (annually averaged): (a) MHD (3yr) with global meteorology (blue), (b) 3 sites (2yr) (MHD+JFJ+CMN) with global meteorology (orange), and (c) 7 sites (2mth) (DECC+JFJ+CMN) with UKV 1.5 km nested in global meteorology (green). The uncertainty bars represent 1 std.
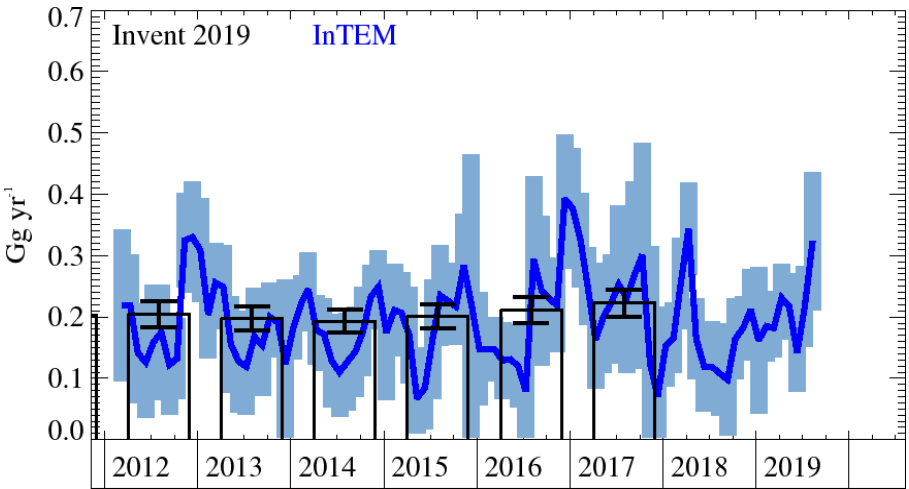
Figure 111: SF₆: NWEU emission estimates (Gg yr⁻¹) from the UNFCCC Inventory (black) and InTEM 2-month 7 sites (DECC+JFJ+CMN) with UKV 1.5 km meteorology (blue). The uncertainty bars represent 1 std.
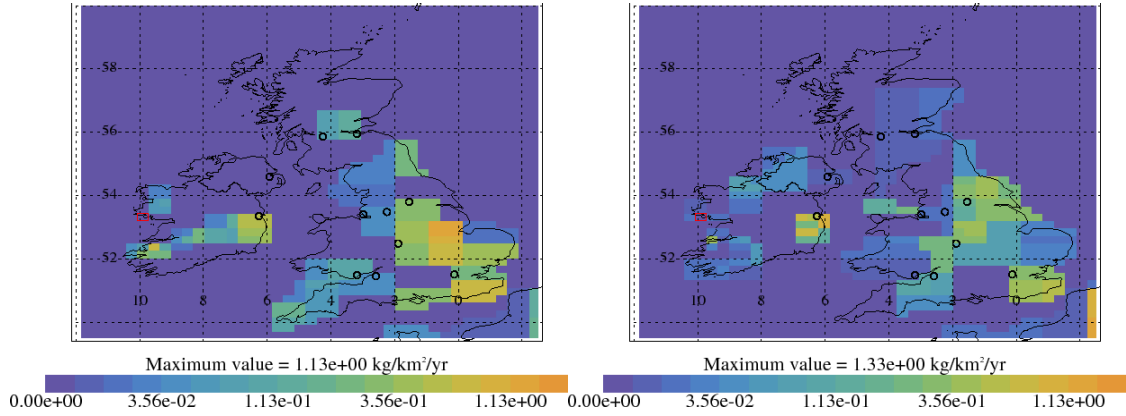
Figure 112: SF₆ emission estimate using MHD data for 2004-2008 (left) and 2014-2018 (right). Major cities shown as black circles and observation sites shown as red rectangle.
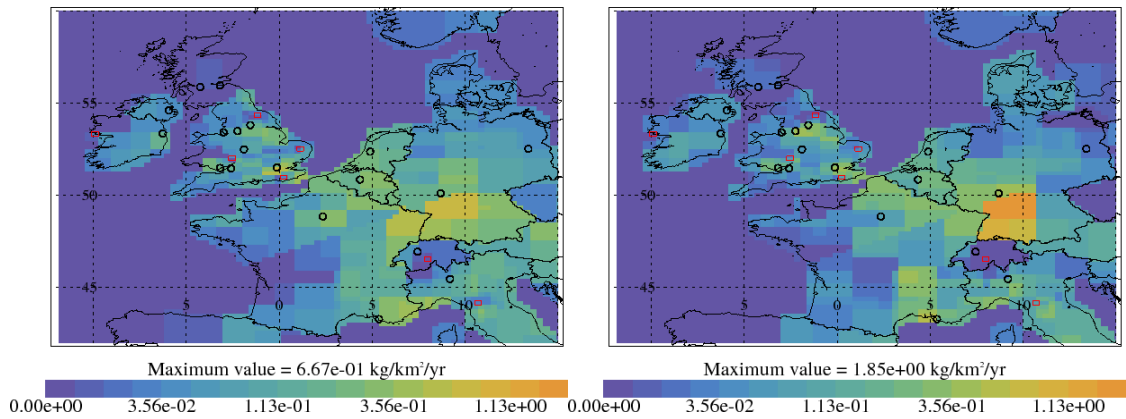

Figure 113: SF₆ emission estimate using data from 7 sites for 2013-2015 (left) and 2016-2018 (right). Major cities shown as black circles and observation sites shown as red rectangle.

Years	Inventory 1yr	MHD	3 sites	7 sites
1997	0.0577 (0.0485-0.0669)			
1998	0.0598 (0.0503-0.0692)			
1999	0.0671 (0.0566-0.0776)			
2000	0.0810 (0.0685-0.0936)			
2001	0.0650 (0.0550-0.0750)			
2002	0.0666 (0.0565-0.0768)			
2003	0.0589 (0.0500-0.0678)			
2004	0.0498 (0.0424-0.0573)			
2005	0.0470 (0.0401-0.0540)	0.0348 (0.0245-0.0451)		
2006	0.0393 (0.0336-0.0451)	0.0381 (0.0278-0.0484)		
2007	0.0374 (0.0319-0.0428)	0.0447 (0.0344-0.0550)		
2008	0.0305 (0.0261-0.0349)	0.0476 (0.0369-0.0583)	0.0564 (0.0438-0.0690)	
2009	0.0266 (0.0228-0.0303)	0.0472 (0.0361-0.0583)	0.0523 (0.0398-0.0648)	
2010	0.0308 (0.0265-0.0351)	0.0402 (0.0300-0.0504)	0.0397 (0.0276-0.0518)	
2011	0.0273 (0.0235-0.0311)	0.0358 (0.0271-0.0445)	0.0332 (0.0235-0.0429)	
2012	0.0264 (0.0228-0.0301)	0.0315 (0.0246-0.0384)	0.0321 (0.0247-0.0395)	0.0340 (0.0080-0.0590)
2013	0.0229 (0.0198-0.0260)	0.0294 (0.0229-0.0359)	0.0332 (0.0252-0.0412)	0.0380 (0.0180-0.0580)
2014	0.0219 (0.0190-0.0249)	0.0249 (0.0179-0.0319)	0.0227 (0.0144-0.0310)	0.0245 (0.0102-0.0388)
2015	0.0204 (0.0177-0.0231)	0.0206 (0.0127-0.0285)	0.0141 (0.0056-0.0226)	0.0183 (0.0043-0.0323)
2016	0.0215 (0.0187-0.0243)	0.0225 (0.0135-0.0315)	0.0176 (0.0069-0.0283)	0.0168 (0.0020-0.0316)
2017	0.0230 (0.0200-0.0260)	0.0266 (0.0169-0.0363)	0.0293 (0.0176-0.0410)	0.0182 (0.0031-0.0333)
2018		0.0311 (0.0210-0.0412)	0.0400 (0.0290-0.0510)	0.0240 (0.0109-0.0371)
2019				0.0178 (0.0069-0.0287)

Table 38: SF₆ emission (Gg yr⁻¹) estimates for the UK with uncertainty (1std).

Years	Inventory 1yr	1s 3y	3s 2y	7s 1y
1994	0.539 (0.485-0.593)			
1995	0.563 (0.507-0.620)			
1996	0.551 (0.496-0.607)			
1997	0.483 (0.435-0.532)			
1998	0.468 (0.421-0.515)			
1999	0.385 (0.347-0.424)			
2000	0.384 (0.346-0.422)			
2001	0.335 (0.302-0.369)			
2002	0.290 (0.261-0.319)			
2003	0.279 (0.251-0.306)			
2004	0.279 (0.251-0.307)			
2005	0.267 (0.240-0.293)	0.194 (0.148-0.240)		
2006	0.248 (0.224-0.273)	0.187 (0.138-0.236)		
2007	0.237 (0.213-0.260)	0.178 (0.124-0.232)		
2008	0.223 (0.201-0.245)	0.163 (0.106-0.221)	0.192 (0.139-0.245)	
2009	0.210 (0.189-0.231)	0.156 (0.097-0.214)	0.135 (0.093-0.177)	
2010	0.214 (0.193-0.235)	0.144 (0.091-0.196)	0.115 (0.072-0.157)	
2011	0.202 (0.182-0.222)	0.128 (0.079-0.177)	0.127 (0.087-0.167)	
2012	0.205 (0.184-0.225)	0.111 (0.067-0.155)	0.135 (0.101-0.170)	0.205 (0.100-0.309)
2013	0.198 (0.178-0.218)	0.108 (0.063-0.153)	0.150 (0.115-0.185)	0.188 (0.110-0.265)
2014	0.193 (0.174-0.213)	0.120 (0.076-0.165)	0.159 (0.116-0.202)	0.180 (0.113-0.247)
2015	0.201 (0.181-0.221)	0.131 (0.082-0.180)	0.156 (0.107-0.206)	0.185 (0.093-0.278)
2016	0.211 (0.190-0.233)	0.135 (0.088-0.182)	0.142 (0.091-0.193)	0.204 (0.118-0.290)
2017	0.223 (0.201-0.245)	0.133 (0.085-0.181)	0.138 (0.092-0.184)	0.226 (0.108-0.344)
2018		0.133 (0.090-0.177)	0.151 (0.112-0.189)	0.173 (0.100-0.246)
2019				0.207 (0.135-0.280)

Table 39: SF$_6$ emission (Gg yr^{-1}) estimates for the NWEU with uncertainty (1std).

4.22 NF₃
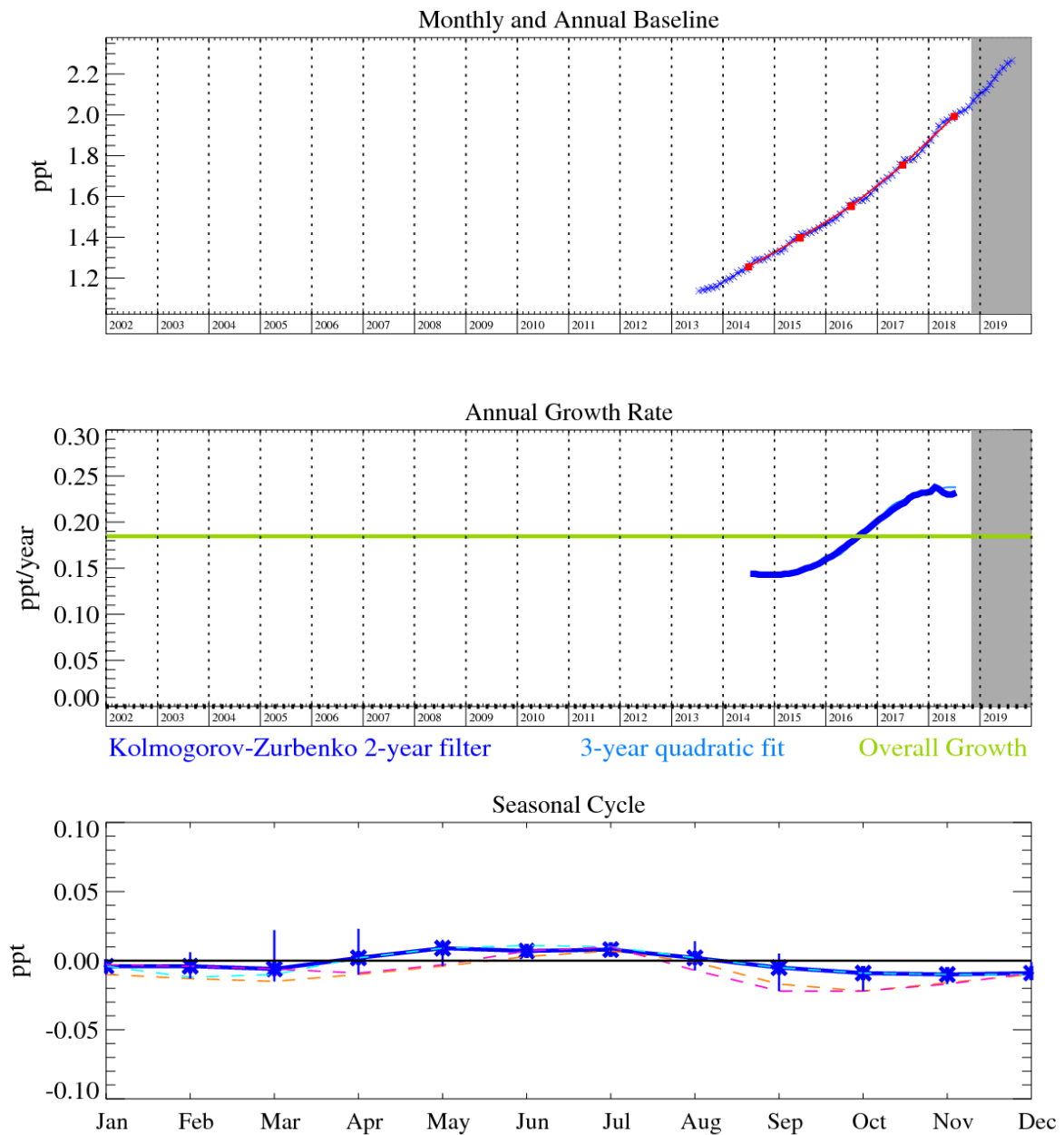
Figure 114: NF₃: Monthly (blue) and annual (red) Northern Hemisphere baseline mole fractions (top plot). Annual (blue) and overall (green) average growth rate (middle plot). Seasonal cycle (de-trended) with year-to-year variability (lower plot). Grey area covers un-ratified provisional data.

Production of nitrogen trifluoride (NF₃) has increased rapidly to meet demand, it is used in the manufacture of semiconductors, flat panel displays and photovoltaic cells. The new ambient air measurements from the Advanced Global Atmospheric Gases Experiment have shown the rapidly rising global atmospheric abundance of this gas due to this market expansion. Although the current contribution of NF₃ to radiative forcing is small, its potential to impact the climate is significant (its GWP₁₀₀ is 16,100).

The UK and NWEU emissions of this gas, both estimated in the inventory and using InTEM, are very small. The pollution events seen at Mace Head are almost all lost within the baseline noise. The only exception to this was an episode when the air travelled quickly and directly from the NE USA (please refer to the 2015 report for more details).
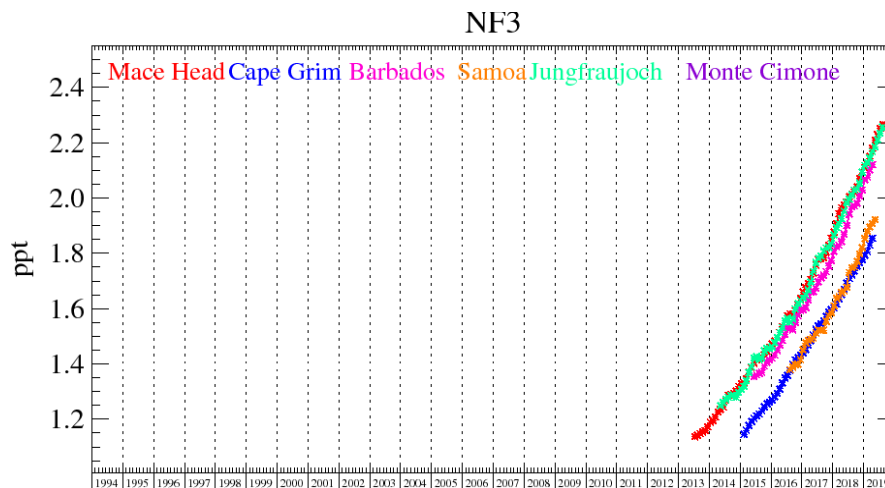
Figure 115: Background NF₃ mole fractions at several global AGAGE stations both in the Northern and Southern Hemispheres.
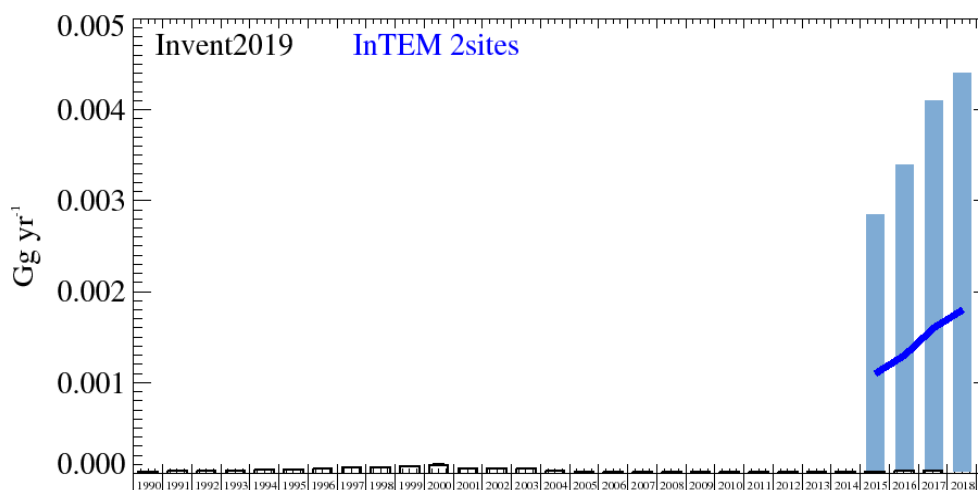
Figure 116: NF₃: UK emission estimates (Gg yr⁻¹) from the UNFCCC Inventory (black) and InTEM (annually averaged): 2 sites (2yr) (MHD+JFJ) with global meteorology (blue). The uncertainty bars represent 1 std.
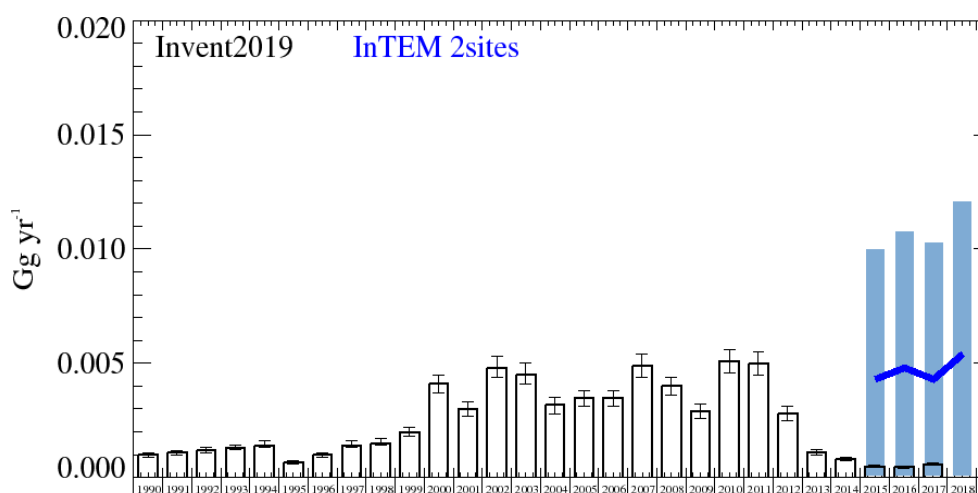
Figure 117: NF₃: NWEU emission estimates (Gg yr⁻¹) from the UNFCCC Inventory (black) and InTEM (annually averaged): 2 sites (2yr) (MHD+JFJ) with global meteorology (blue). The uncertainty bars represent 1 std.

Maximum value = 4.27e-02 kg/km²/yr

0.00e+00   1.78e-03   5.63e-03   1.78e-02   5.63e-02
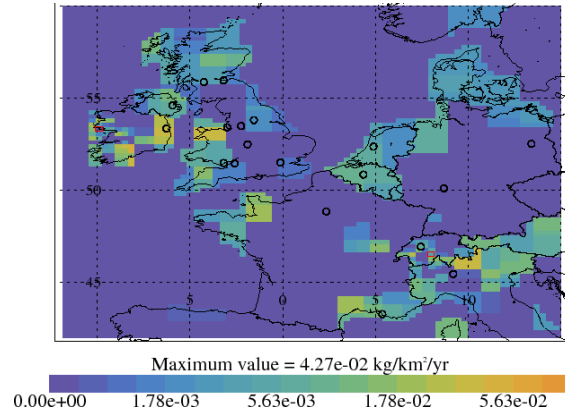
Figure 118: NF₃ emission estimate using data from 2 sites for 2014-2018. Major cities shown as black circles and observation sites shown as red rectangle.

5 Global Mole Fractions and Global Emissions

5.1 Introduction

Global emissions and mean lower tropospheric mole fraction estimates were made using baseline AGAGE observations from five "background" AGAGE stations (Mace Head, Ireland; Trinidad Head, California; Ragged Point, Barbados; Cape Matatula, American Samoa; and Cape Grim, Tasmania) using the method outlined in Rigby et al., [2014]. A two-dimensional model of global atmospheric chemistry and transport was used to simulate baseline mole fractions in four latitudinal bands, separated at the equator and ±30 degrees [*Rigby et al.*, 2013]. The modelled mole fractions were brought into consistency with the AGAGE observations using a Bayesian method in which an initial estimate of the emissions growth rate was adjusted in the inversion. Uncertainties in the derived global emissions estimates are determined by the observational uncertainty, model uncertainty and uncertainties in the atmospheric lifetimes of each gas. Global mole fractions and the emissions of each of the measured gases for each year are detailed.

5.2 Recent trends in non-CO2 Kyoto gases

5.2.1 CH_4

The average methane mole fraction over the past 5 years has grown at 9 ppt yr^{-1}. This positive growth trend been maintained since 2007, before which (between 2000 and 2006), growth was close to zero. The previous Reports have noted that there are several competing explanations for these changes in growth rate. The uncertainty surrounding the potential changes in methane sources and its atmospheric sink (primarily the OH radical in the troposphere) persists. Recent studies have suggested that changes in livestock and/or fossil fuel emissions may have contributed to recent mole fraction growth [*Wolf et al.*, 2017; *Worden et al.*, 2017]. However, the reasons for the pause in methane growth and its renewed rise remain highly uncertain.

5.2.2 N_2O

Nitrous oxide is the third most important greenhouse gas after CO_2 and CH_4 and it plays a major role in ozone depletion. Its growth rate has remained close to 0.8 ppt yr^{-1} for at least the last decade. During this time, global emissions remained close to 28 Tg yr^{-1}. There has been little work re-examining the global budget of nitrous oxide since the previous Report. The relative contribution of anthropogenic and natural emissions remains relatively uncertain at the global scale.

5.2.3 HFCs

Emissions and global mole fractions of all of the major HFCs grew between 2017 and 2018. There is a well-known gap between the total CO_2-equivalent HFC emissions reported by the UNFCCC and the total global emissions derived from atmospheric measurements (e.g. Rigby et al., [2014]). Evidence from atmospheric observations has suggested that this gap is largely due to emissions from non-reporting (non-Annex-1) countries, although discrepancies were found at the species-specific level between top-down and bottom-up reports for Annex-1 countries (e.g. Lunt et al., [2015]). A recent study of European emissions also finds consistency between reported and top-down emissions when HFCs are aggregated but some disagreement for individual gases [*Graziosi et al.*, 2017], whilst a regional study in the USA found aggregated emissions that were lower than the USA's UNFCCC reports [*Hu et al.*, 2017]. A recent study has shown that global emissions of HFC-23 increased rapidly after the Clean Development Mechanism (CDM) measures tackling HFC-23 emissions ended in 2009 [*Simmonds et al.*, 2018]. Emissions reached a maximum in 2014 and dropped until 2016. The cause of this decrease may be

linked to efforts to reduce emissions by the Chinese government. However, this decline appears to have halted, and emissions grew between 2017 and 2018.

5.2.4 PFCs, SF_6 and NF_3

Emissions of PFC-14 (CF_4), the most abundant PFC, remained flat between 2017 and 2018 following a recent rise. Emissions of PFC-116 and PFC-218 have remained relatively constant in recent years. Emissions of SF_6 and NF_3 have continued to grow strongly. There has been little change in our understanding of the sources of these long-lived greenhouse gases since the previous Report.

Date	CH4 (ppb)	N2O (ppb)	HFC-23 (ppt)	HFC-32 (ppt)	HFC-125 (ppt)
1978	(-)	300 (298 - 301)	(-)	(-)	(-)
1979	(-)	301 (299 - 302)	(-)	(-)	(-)
1980	(-)	301 (300 - 303)	(-)	(-)	(-)
1981	(-)	302 (300 - 303)	(-)	(-)	(-)
1982	(-)	303 (301 - 304)	(-)	(-)	(-)
1983	(-)	304 (302 - 305)	(-)	(-)	(-)
1984	(-)	304 (303 - 305)	(-)	(-)	(-)
1985	1684 (1676 - 1694)	304 (303 - 306)	(-)	(-)	(-)
1986	1665 (1657 - 1675)	305 (304 - 307)	(-)	(-)	(-)
1987	1677 (1669 - 1689)	306 (304 - 307)	(-)	(-)	(-)
1988	1693 (1684 - 1703)	307 (305 - 308)	(-)	(-)	(-)
1989	1709 (1700 - 1720)	308 (306 - 309)	(-)	(-)	(-)
1990	1714 (1705 - 1725)	309 (307 - 310)	(-)	(-)	(-)
1991	1731 (1722 - 1740)	310 (308 - 311)	(-)	(-)	(-)
1992	1735 (1727 - 1745)	310 (308 - 311)	(-)	(-)	(-)
1993	1738 (1730 - 1749)	310 (309 - 312)	(-)	(-)	(-)
1994	1744 (1736 - 1753)	311 (309 - 312)	(-)	(-)	(-)
1995	1747 (1739 - 1757)	312 (310 - 313)	(-)	(-)	(-)
1996	1749 (1741 - 1758)	313 (311 - 314)	(-)	(-)	(-)
1997	1753 (1744 - 1762)	314 (312 - 315)	(-)	(-)	(-)
1998	1763 (1754 - 1772)	314 (313 - 316)	(-)	0.124 (0.0668 - 0.189)	0.995 (0.943 - 1.05)
1999	1771 (1762 - 1780)	315 (314 - 317)	(-)	0.172 (0.112 - 0.239)	1.23 (1.16 - 1.29)
2000	1773 (1765 - 1782)	316 (315 - 318)	(-)	0.229 (0.180 - 0.280)	1.53 (1.46 - 1.61)
2001	1772 (1763 - 1782)	317 (315 - 319)	(-)	0.303 (0.243 - 0.362)	1.93 (1.84 - 2.05)
2002	1772 (1763 - 1782)	318 (316 - 319)	(-)	0.412 (0.357 - 0.476)	2.35 (2.24 - 2.48)
2003	1776 (1767 - 1786)	318 (317 - 320)	(-)	0.564 (0.520 - 0.609)	2.88 (2.74 - 3.03)
2004	1775 (1766 - 1784)	319 (317 - 320)	(-)	0.836 (0.804 - 0.867)	3.44 (3.29 - 3.62)
2005	1774 (1766 - 1784)	320 (318 - 321)	(-)	1.21 (1.17 - 1.25)	4.07 (3.88 - 4.27)
2006	1774 (1765 - 1784)	320 (319 - 322)	(-)	1.61 (1.56 - 1.66)	4.79 (4.59 - 5.02)
2007	1781 (1772 - 1791)	321 (320 - 323)	21.0 (20.7 - 21.5)	2.13 (2.06 - 2.19)	5.62 (5.38 - 5.92)
2008	1789 (1779 - 1798)	322 (321 - 324)	21.9 (21.4 - 22.3)	2.69 (2.61 - 2.76)	6.61 (6.31 - 6.93)
2009	1792 (1783 - 1802)	323 (321 - 324)	22.6 (22.1 - 23.0)	3.28 (3.18 - 3.38)	7.68 (7.34 - 8.05)
2010	1797 (1788 - 1807)	324 (322 - 325)	23.3 (22.8 - 23.7)	4.09 (3.96 - 4.22)	8.95 (8.54 - 9.41)
2011	1804 (1795 - 1814)	325 (323 - 326)	24.1 (23.6 - 24.5)	5.15 (4.98 - 5.30)	10.5 (9.99 - 11.0)
2012	1809 (1799 - 1818)	326 (324 - 327)	25.0 (24.5 - 25.4)	6.24 (6.04 - 6.43)	12.1 (11.6 - 12.8)
2013	1814 (1805 - 1824)	327 (325 - 328)	26.0 (25.5 - 26.5)	7.51 (7.27 - 7.73)	14.0 (13.4 - 14.7)
2014	1823 (1814 - 1833)	328 (326 - 329)	27.0 (26.6 - 27.6)	8.97 (8.68 - 9.25)	16.1 (15.4 - 16.9)
2015	1834 (1825 - 1844)	329 (327 - 330)	28.0 (27.5 - 28.6)	10.7 (10.4 - 11.0)	18.5 (17.7 - 19.4)
2016	1842 (1832 - 1851)	329 (328 - 331)	29.0 (28.4 - 29.5)	12.6 (12.2 - 13.0)	20.8 (20.0 - 21.9)
2017	1849 (1840 - 1859)	330 (329 - 332)	30.0 (29.4 - 30.5)	15.1 (14.6 - 15.6)	23.6 (22.6 - 24.8)
2018	1859 (1850 - 1870)	331 (330 - 333)	31.1 (30.6 - 31.7)	17.6 (17.1 - 18.2)	26.6 (25.5 - 28.0)

Table 40: Modelled global mole fractions with uncertainties

Date	HFC-134a (ppt)	HFC-143a (ppt)	HFC-152a (ppt)	HFC-227ea (ppt)
1978	(-)	(-)	(-)	(-)
1979	(-)	(-)	(-)	(-)
1980	(-)	0.0936 (0.0233 - 0.161)	(-)	(-)
1981	(-)	0.207 (0.0713 - 0.383)	(-)	(-)
1982	(-)	0.189 (0.0782 - 0.300)	(-)	(-)
1983	(-)	0.189 (0.145 - 0.244)	(-)	(-)
1984	(-)	0.204 (0.0871 - 0.340)	(-)	(-)
1985	(-)	0.237 (0.172 - 0.293)	(-)	(-)
1986	(-)	0.285 (0.242 - 0.330)	(-)	(-)
1987	(-)	0.304 (0.218 - 0.383)	(-)	(-)
1988	(-)	0.362 (0.301 - 0.412)	(-)	(-)
1989	(-)	0.421 (0.367 - 0.474)	(-)	(-)
1990	(-)	0.478 (0.416 - 0.540)	(-)	(-)
1991	(-)	0.532 (0.478 - 0.577)	(-)	(-)
1992	(-)	0.568 (0.510 - 0.617)	(-)	(-)
1993	(-)	0.613 (0.553 - 0.667)	(-)	(-)
1994	1.04 (0.941 - 1.15)	0.686 (0.626 - 0.737)	0.830 (0.798 - 0.874)	(-)
1995	2.00 (1.92 - 2.09)	0.805 (0.755 - 0.850)	1.06 (1.03 - 1.10)	(-)
1996	3.44 (3.35 - 3.54)	0.989 (0.927 - 1.03)	1.17 (1.13 - 1.21)	(-)
1997	5.36 (5.25 - 5.47)	1.24 (1.16 - 1.30)	1.29 (1.25 - 1.33)	(-)
1998	7.99 (7.84 - 8.14)	1.61 (1.53 - 1.66)	1.55 (1.50 - 1.60)	(-)
1999	11.1 (10.9 - 11.3)	2.00 (1.91 - 2.06)	1.70 (1.65 - 1.76)	(-)
2000	14.5 (14.2 - 14.7)	2.45 (2.35 - 2.51)	1.88 (1.83 - 1.95)	(-)
2001	18.0 (17.7 - 18.3)	2.96 (2.84 - 3.07)	2.11 (2.05 - 2.18)	(-)
2002	21.8 (21.4 - 22.1)	3.58 (3.43 - 3.69)	2.42 (2.33 - 2.50)	(-)
2003	25.9 (25.5 - 26.3)	4.20 (4.03 - 4.34)	2.84 (2.75 - 2.93)	(-)
2004	30.3 (29.8 - 30.8)	4.92 (4.75 - 5.06)	3.27 (3.16 - 3.37)	(-)
2005	34.7 (34.1 - 35.3)	5.71 (5.51 - 5.87)	3.76 (3.65 - 3.89)	(-)
2006	39.0 (38.3 - 39.7)	6.63 (6.40 - 6.81)	4.50 (4.36 - 4.65)	0.365 (0.335 - 0.398)
2007	43.4 (42.7 - 44.1)	7.59 (7.34 - 7.80)	5.29 (5.12 - 5.47)	0.430 (0.395 - 0.471)
2008	48.1 (47.2 - 48.8)	8.63 (8.34 - 8.87)	5.83 (5.63 - 6.02)	0.497 (0.461 - 0.545)
2009	52.8 (51.9 - 53.6)	9.74 (9.40 - 10.0)	5.99 (5.79 - 6.18)	0.574 (0.529 - 0.631)
2010	57.8 (56.8 - 58.8)	10.9 (10.5 - 11.2)	6.28 (6.08 - 6.48)	0.655 (0.606 - 0.716)
2011	62.8 (61.8 - 63.8)	12.1 (11.7 - 12.4)	6.62 (6.41 - 6.84)	0.737 (0.680 - 0.806)
2012	67.7 (66.6 - 68.8)	13.4 (12.9 - 13.8)	6.78 (6.56 - 7.01)	0.822 (0.761 - 0.900)
2013	72.7 (71.5 - 73.9)	14.8 (14.2 - 15.2)	6.74 (6.53 - 6.96)	0.922 (0.857 - 1.01)
2014	77.9 (76.7 - 79.2)	16.2 (15.6 - 16.7)	6.65 (6.44 - 6.87)	1.02 (0.944 - 1.12)
2015	83.4 (82.0 - 84.7)	17.7 (17.1 - 18.2)	6.62 (6.41 - 6.84)	1.12 (1.04 - 1.23)
2016	89.4 (87.9 - 90.8)	19.3 (18.7 - 19.9)	6.71 (6.50 - 6.91)	1.24 (1.15 - 1.35)
2017	95.8 (94.2 - 97.2)	21.0 (20.3 - 21.6)	6.85 (6.64 - 7.09)	1.37 (1.26 - 1.49)
2018	102 (100. - 103)	22.6 (21.8 - 23.2)	7.01 (6.81 - 7.22)	1.50 (1.38 - 1.64)

Table 41: Modelled global mole fractions with uncertainties

Date	HFC-236fa (ppt)	HFC-245fa (ppt)	HFC-365mfc (ppt)	CF4 (ppt)
1978	(-)	(-)	(-)	50.8 (49.4 - 52.0)
1979	(-)	(-)	(-)	52.2 (50.7 - 53.5)
1980	(-)	(-)	(-)	53.5 (52.0 - 54.7)
1981	(-)	(-)	(-)	54.6 (53.1 - 55.9)
1982	(-)	(-)	(-)	55.6 (54.1 - 56.9)
1983	(-)	(-)	(-)	56.6 (55.1 - 58.0)
1984	(-)	(-)	(-)	57.7 (56.2 - 59.1)
1985	(-)	(-)	(-)	58.7 (57.2 - 60.1)
1986	(-)	(-)	(-)	59.7 (58.2 - 61.0)
1987	(-)	(-)	(-)	60.7 (59.1 - 62.2)
1988	(-)	(-)	(-)	61.7 (60.2 - 63.2)
1989	(-)	(-)	(-)	62.8 (61.1 - 64.3)
1990	(-)	(-)	(-)	63.8 (62.2 - 65.3)
1991	(-)	(-)	(-)	64.8 (63.1 - 66.3)
1992	(-)	(-)	(-)	65.7 (64.0 - 67.2)
1993	(-)	(-)	(-)	66.5 (64.8 - 68.0)
1994	(-)	(-)	(-)	67.2 (65.5 - 68.8)
1995	(-)	(-)	(-)	67.9 (66.2 - 69.6)
1996	(-)	(-)	(-)	68.7 (66.9 - 70.3)
1997	(-)	(-)	(-)	69.4 (67.6 - 71.1)
1998	(-)	(-)	(-)	70.1 (68.3 - 71.8)
1999	(-)	(-)	(-)	70.8 (69.0 - 72.5)
2000	(-)	(-)	(-)	71.5 (69.6 - 73.2)
2001	(-)	(-)	(-)	72.1 (70.2 - 73.8)
2002	(-)	(-)	(-)	72.8 (70.9 - 74.5)
2003	(-)	(-)	0.0608 (0.0482 - 0.0717)	73.5 (71.6 - 75.3)
2004	(-)	(-)	0.128 (0.106 - 0.147)	74.3 (72.3 - 76.0)
2005	(-)	(-)	0.219 (0.183 - 0.249)	75.0 (73.0 - 76.7)
2006	0.0582 (0.0456 - 0.0699)	0.604 (0.559 - 0.657)	0.318 (0.262 - 0.360)	75.7 (73.7 - 77.4)
2007	0.0655 (0.0516 - 0.0793)	0.835 (0.774 - 0.908)	0.408 (0.342 - 0.468)	76.4 (74.4 - 78.2)
2008	0.0732 (0.0575 - 0.0880)	1.03 (0.950 - 1.11)	0.481 (0.398 - 0.548)	77.1 (75.1 - 78.9)
2009	0.0812 (0.0637 - 0.0981)	1.19 (1.10 - 1.29)	0.537 (0.445 - 0.620)	77.7 (75.6 - 79.5)
2010	0.0897 (0.0705 - 0.108)	1.34 (1.24 - 1.45)	0.589 (0.491 - 0.680)	78.3 (76.2 - 80.1)
2011	0.0992 (0.0779 - 0.120)	1.51 (1.41 - 1.63)	0.649 (0.541 - 0.751)	79.0 (76.9 - 80.8)
2012	0.110 (0.0863 - 0.131)	1.70 (1.59 - 1.84)	0.712 (0.592 - 0.815)	79.7 (77.6 - 81.6)
2013	0.120 (0.0944 - 0.144)	1.88 (1.76 - 2.04)	0.777 (0.651 - 0.891)	80.5 (78.4 - 82.4)
2014	0.131 (0.103 - 0.157)	2.05 (1.91 - 2.23)	0.846 (0.712 - 0.968)	81.2 (79.0 - 83.1)
2015	0.142 (0.111 - 0.169)	2.23 (2.07 - 2.42)	0.919 (0.770 - 1.05)	81.9 (79.7 - 83.8)
2016	0.153 (0.119 - 0.183)	2.43 (2.26 - 2.62)	0.992 (0.835 - 1.13)	82.7 (80.5 - 84.6)
2017	0.164 (0.128 - 0.197)	2.63 (2.45 - 2.84)	1.06 (0.890 - 1.21)	83.6 (81.5 - 85.6)
2018	0.176 (0.138 - 0.212)	2.83 (2.63 - 3.08)	1.13 (0.946 - 1.28)	84.6 (82.4 - 86.5)

Table 42: Modelled global mole fractions with uncertainties

Date	C2F6 (ppt)	C3F8 (ppt)	SF6 (ppt)	NF3 (ppt)
1978	1.04 (1.00 - 1.07)	(-)	0.659 (0.640 - 0.680)	(-)
1979	1.13 (1.09 - 1.16)	(-)	0.755 (0.737 - 0.775)	(-)
1980	1.21 (1.18 - 1.26)	(-)	0.857 (0.837 - 0.880)	(-)
1981	1.30 (1.26 - 1.34)	(-)	0.975 (0.951 - 1.00)	(-)
1982	1.37 (1.33 - 1.41)	(-)	1.10 (1.08 - 1.13)	(-)
1983	1.44 (1.40 - 1.49)	0.0715 (0.0663 - 0.0764)	1.22 (1.19 - 1.25)	(-)
1984	1.53 (1.49 - 1.58)	0.0762 (0.0723 - 0.0799)	1.34 (1.31 - 1.37)	(-)
1985	1.62 (1.58 - 1.67)	0.0823 (0.0782 - 0.0861)	1.48 (1.45 - 1.51)	(-)
1986	1.71 (1.66 - 1.77)	0.0892 (0.0848 - 0.0933)	1.65 (1.61 - 1.68)	(-)
1987	1.80 (1.75 - 1.85)	0.0964 (0.0919 - 0.101)	1.81 (1.77 - 1.85)	(-)
1988	1.89 (1.84 - 1.95)	0.104 (0.0992 - 0.108)	1.97 (1.93 - 2.02)	(-)
1989	1.98 (1.93 - 2.05)	0.111 (0.106 - 0.116)	2.15 (2.11 - 2.20)	(-)
1990	2.07 (2.02 - 2.15)	0.118 (0.113 - 0.124)	2.35 (2.30 - 2.40)	(-)
1991	2.16 (2.10 - 2.24)	0.126 (0.121 - 0.132)	2.56 (2.51 - 2.61)	(-)
1992	2.25 (2.19 - 2.32)	0.135 (0.129 - 0.141)	2.77 (2.72 - 2.83)	(-)
1993	2.34 (2.28 - 2.41)	0.145 (0.139 - 0.151)	2.98 (2.92 - 3.05)	(-)
1994	2.42 (2.36 - 2.50)	0.157 (0.150 - 0.163)	3.21 (3.14 - 3.27)	(-)
1995	2.51 (2.46 - 2.59)	0.171 (0.164 - 0.178)	3.45 (3.38 - 3.51)	(-)
1996	2.62 (2.56 - 2.70)	0.189 (0.180 - 0.196)	3.69 (3.61 - 3.76)	(-)
1997	2.73 (2.67 - 2.82)	0.209 (0.200 - 0.217)	3.92 (3.83 - 4.00)	(-)
1998	2.86 (2.79 - 2.95)	0.232 (0.222 - 0.241)	4.14 (4.05 - 4.23)	(-)
1999	2.99 (2.91 - 3.08)	0.257 (0.246 - 0.267)	4.34 (4.25 - 4.44)	(-)
2000	3.11 (3.04 - 3.22)	0.284 (0.272 - 0.295)	4.53 (4.44 - 4.63)	(-)
2001	3.23 (3.16 - 3.34)	0.312 (0.299 - 0.325)	4.73 (4.63 - 4.83)	(-)
2002	3.35 (3.28 - 3.45)	0.342 (0.327 - 0.356)	4.94 (4.84 - 5.04)	(-)
2003	3.46 (3.39 - 3.57)	0.371 (0.355 - 0.386)	5.17 (5.06 - 5.27)	(-)
2004	3.57 (3.48 - 3.68)	0.400 (0.383 - 0.415)	5.39 (5.29 - 5.50)	(-)
2005	3.66 (3.57 - 3.78)	0.428 (0.410 - 0.444)	5.62 (5.52 - 5.74)	(-)
2006	3.76 (3.67 - 3.88)	0.454 (0.435 - 0.471)	5.87 (5.75 - 5.99)	(-)
2007	3.85 (3.76 - 3.97)	0.477 (0.458 - 0.495)	6.14 (6.02 - 6.27)	(-)
2008	3.94 (3.85 - 4.06)	0.499 (0.479 - 0.518)	6.42 (6.29 - 6.55)	(-)
2009	4.01 (3.92 - 4.14)	0.519 (0.498 - 0.539)	6.70 (6.57 - 6.84)	(-)
2010	4.09 (4.00 - 4.22)	0.537 (0.516 - 0.558)	6.99 (6.85 - 7.13)	(-)
2011	4.17 (4.07 - 4.31)	0.555 (0.533 - 0.576)	7.28 (7.14 - 7.43)	(-)
2012	4.25 (4.15 - 4.38)	0.572 (0.550 - 0.594)	7.59 (7.44 - 7.74)	(-)
2013	4.33 (4.23 - 4.46)	0.588 (0.565 - 0.612)	7.90 (7.75 - 8.06)	1.04 (1.00 - 1.08)
2014	4.41 (4.31 - 4.54)	0.603 (0.579 - 0.628)	8.23 (8.06 - 8.40)	1.16 (1.12 - 1.20)
2015	4.49 (4.39 - 4.63)	0.619 (0.594 - 0.644)	8.56 (8.38 - 8.73)	1.30 (1.26 - 1.34)
2016	4.57 (4.47 - 4.72)	0.634 (0.608 - 0.660)	8.89 (8.72 - 9.08)	1.45 (1.41 - 1.50)
2017	4.66 (4.56 - 4.81)	0.650 (0.622 - 0.676)	9.24 (9.06 - 9.43)	1.63 (1.58 - 1.68)
2018	4.75 (4.64 - 4.91)	0.665 (0.638 - 0.690)	9.59 (9.40 - 9.79)	1.82 (1.77 - 1.88)

Table 43: Modelled global mole fractions with uncertainties

Date	CH4 (Tg/yr)	N2O (Tg/yr)	HFC-23 (Gg/yr)	HFC-32 (Gg/yr)	HFC-125 (Gg/yr)
1978	(-)	24.4 (22.0 - 27.0)	(-)	(-)	(-)
1979	(-)	22.9 (20.8 - 25.2)	(-)	(-)	(-)
1980	(-)	23.0 (20.6 - 25.2)	(-)	(-)	(-)
1981	(-)	25.3 (23.0 - 27.6)	(-)	(-)	(-)
1982	(-)	26.7 (24.6 - 29.0)	(-)	(-)	(-)
1983	(-)	22.4 (20.3 - 24.9)	(-)	(-)	(-)
1984	(-)	22.5 (20.4 - 24.6)	(-)	(-)	(-)
1985	357.0 (294.3 - 418.7)	23.3 (21.0 - 25.8)	(-)	(-)	(-)
1986	478.8 (411.3 - 544.4)	24.7 (22.4 - 27.2)	(-)	(-)	(-)
1987	501.8 (432.5 - 573.5)	24.8 (22.5 - 27.2)	(-)	(-)	(-)
1988	536.0 (473.1 - 595.9)	25.4 (23.2 - 27.8)	(-)	(-)	(-)
1989	492.6 (423.5 - 554.3)	26.4 (24.1 - 28.9)	(-)	(-)	(-)
1990	548.6 (483.9 - 610.7)	27.3 (25.1 - 29.7)	(-)	(-)	(-)
1991	542.8 (478.8 - 609.8)	24.3 (22.1 - 26.6)	(-)	(-)	(-)
1992	490.7 (420.8 - 558.7)	22.4 (20.2 - 24.7)	(-)	(-)	(-)
1993	527.1 (464.4 - 591.7)	22.4 (19.9 - 24.9)	(-)	(-)	(-)
1994	518.1 (450.3 - 584.3)	25.0 (23.0 - 27.7)	(-)	(-)	(-)
1995	515.2 (446.1 - 574.8)	25.4 (23.1 - 27.7)	(-)	(-)	(-)
1996	516.6 (445.7 - 582.9)	26.7 (24.4 - 28.9)	(-)	(-)	(-)
1997	515.9 (448.9 - 579.1)	25.7 (23.5 - 28.2)	(-)	(-)	(-)
1998	552.2 (483.5 - 614.9)	26.0 (23.7 - 28.3)	(-)	0.846 (-0.328 - 2.06)	7.40 (6.75 - 7.89)
1999	522.3 (457.9 - 587.4)	26.4 (24.1 - 28.9)	(-)	0.660 (-0.476 - 1.70)	6.24 (5.75 - 6.69)
2000	514.1 (444.4 - 575.7)	27.3 (25.1 - 29.8)	(-)	0.657 (-0.275 - 1.63)	8.57 (7.78 - 9.18)
2001	517.4 (450.3 - 580.7)	24.8 (22.8 - 27.0)	(-)	1.35 (0.219 - 2.45)	9.06 (8.33 - 9.89)
2002	520.3 (454.3 - 586.5)	24.5 (22.3 - 27.1)	(-)	1.67 (0.550 - 3.03)	11.2 (10.4 - 12.0)
2003	526.5 (453.5 - 591.2)	25.8 (23.8 - 28.1)	(-)	3.11 (2.12 - 3.89)	13.6 (12.5 - 14.5)
2004	509.7 (441.8 - 579.8)	24.9 (22.7 - 27.4)	(-)	4.17 (3.81 - 4.52)	14.3 (13.2 - 15.5)
2005	522.4 (456.8 - 584.3)	25.7 (23.6 - 28.3)	(-)	5.41 (4.97 - 5.88)	16.6 (15.4 - 17.8)
2006	512.8 (444.3 - 577.2)	25.2 (23.1 - 27.5)	(-)	6.82 (6.19 - 7.44)	19.2 (17.5 - 20.4)
2007	543.0 (470.5 - 607.7)	26.7 (24.6 - 29.2)	11.8 (10.9 - 12.5)	8.24 (7.52 - 8.98)	21.8 (20.3 - 23.4)
2008	532.9 (462.0 - 599.3)	26.8 (24.4 - 29.4)	11.3 (10.7 - 11.9)	9.84 (8.91 - 10.8)	26.1 (24.1 - 27.9)
2009	524.5 (455.0 - 592.3)	26.1 (24.0 - 28.3)	9.64 (9.05 - 10.1)	11.2 (10.1 - 12.4)	27.9 (25.6 - 30.0)
2010	549.6 (478.2 - 617.0)	26.7 (24.4 - 29.4)	10.4 (9.82 - 11.0)	15.5 (14.1 - 17.2)	35.1 (32.5 - 37.5)
2011	538.5 (467.5 - 604.1)	27.5 (25.2 - 30.0)	11.6 (11.0 - 12.2)	18.1 (16.4 - 19.8)	39.3 (36.7 - 42.2)
2012	539.6 (469.8 - 605.6)	27.1 (24.7 - 29.3)	12.9 (12.3 - 13.5)	20.9 (18.8 - 23.2)	44.4 (40.9 - 47.6)
2013	545.4 (477.3 - 611.9)	27.8 (25.8 - 30.3)	14.0 (13.2 - 14.6)	24.5 (22.1 - 27.1)	49.7 (46.2 - 53.0)
2014	557.1 (488.1 - 624.1)	28.3 (25.6 - 30.6)	14.5 (13.9 - 15.1)	29.7 (26.9 - 32.8)	58.1 (54.0 - 61.9)
2015	558.5 (486.7 - 628.3)	26.8 (24.4 - 29.2)	13.1 (12.5 - 13.7)	34.1 (30.3 - 38.2)	60.4 (55.4 - 64.3)
2016	557.2 (484.5 - 625.7)	27.5 (25.5 - 29.9)	12.9 (12.3 - 13.5)	39.7 (35.7 - 44.2)	66.6 (62.1 - 71.6)
2017	555.1 (487.3 - 620.0)	28.8 (26.5 - 31.5)	14.9 (14.1 - 15.5)	49.7 (45.0 - 55.1)	77.3 (70.8 - 82.9)
2018	580.8 (500.8 - 646.6)	28.5 (25.9 - 31.0)	15.9 (15.1 - 16.5)	50.0 (44.4 - 56.2)	77.9 (71.7 - 83.0)

Table 44: Modelled global emissions with uncertainties

Date	HFC-134a (Gg/yr)	HFC-143a (Gg/yr)	HFC-152a (Gg/yr)	HFC-227ea (Gg/yr)
1978	(-)	(-)	(-)	(-)
1979	(-)	(-)	(-)	(-)
1980	(-)	2.30 (0.184 - 4.94)	(-)	(-)
1981	(-)	0.939 (-1.707 - 3.89)	(-)	(-)
1982	(-)	-0.496 (-3.004 - 1.80)	(-)	(-)
1983	(-)	0.172 (-2.028 - 1.59)	(-)	(-)
1984	(-)	0.0445 (-1.884 - 1.93)	(-)	(-)
1985	(-)	0.605 (-1.526 - 2.54)	(-)	(-)
1986	(-)	0.817 (-0.716 - 2.14)	(-)	(-)
1987	(-)	0.407 (-0.532 - 1.52)	(-)	(-)
1988	(-)	1.39 (0.0434 - 2.64)	(-)	(-)
1989	(-)	0.773 (-0.438 - 1.82)	(-)	(-)
1990	(-)	0.924 (-0.142 - 2.13)	(-)	(-)
1991	(-)	1.10 (-0.370 - 2.46)	(-)	(-)
1992	(-)	0.573 (-0.934 - 1.76)	(-)	(-)
1993	(-)	1.34 (-0.120 - 3.09)	(-)	(-)
1994	15.1 (12.8 - 18.4)	1.10 (-0.215 - 2.26)	10.9 (9.72 - 12.4)	(-)
1995	21.3 (20.3 - 22.3)	2.45 (1.18 - 3.49)	11.0 (9.69 - 12.6)	(-)
1996	33.2 (32.0 - 34.7)	3.46 (2.49 - 4.57)	11.8 (10.5 - 13.4)	(-)
1997	43.3 (41.6 - 45.3)	4.54 (3.37 - 5.77)	13.5 (12.1 - 15.3)	(-)
1998	60.3 (57.8 - 63.0)	5.63 (4.09 - 7.02)	14.8 (12.9 - 16.9)	(-)
1999	71.7 (68.6 - 75.1)	6.28 (4.79 - 8.01)	16.3 (14.3 - 18.7)	(-)
2000	80.0 (75.6 - 84.3)	7.33 (5.53 - 8.97)	18.3 (16.1 - 20.9)	(-)
2001	86.5 (81.5 - 91.0)	9.06 (7.12 - 10.9)	19.8 (17.3 - 22.6)	(-)
2002	100. (94.3 - 106)	9.69 (7.74 - 11.7)	23.6 (20.6 - 26.7)	(-)
2003	109 (102 - 116)	11.5 (9.91 - 13.7)	27.2 (24.0 - 30.7)	(-)
2004	117 (109 - 125)	11.8 (11.0 - 12.7)	30.1 (26.2 - 34.4)	(-)
2005	125 (116 - 132)	13.9 (13.0 - 14.7)	36.1 (31.9 - 41.1)	(-)
2006	128 (117 - 138)	15.5 (14.7 - 16.5)	43.1 (37.9 - 49.0)	2.21 (1.78 - 2.69)
2007	138 (127 - 148)	16.0 (15.1 - 17.1)	48.2 (41.7 - 55.4)	2.21 (1.90 - 2.49)
2008	149 (136 - 160)	18.5 (17.3 - 19.7)	48.8 (42.3 - 56.1)	2.53 (2.24 - 2.88)
2009	156 (143 - 169)	18.7 (17.2 - 19.8)	47.8 (41.2 - 55.1)	2.76 (2.41 - 3.13)
2010	170 (155 - 183)	20.5 (19.1 - 21.8)	52.6 (45.5 - 60.7)	2.98 (2.59 - 3.34)
2011	172 (155 - 188)	21.5 (20.4 - 23.1)	53.9 (46.1 - 62.0)	3.06 (2.58 - 3.46)
2012	179 (162 - 195)	23.1 (21.5 - 24.6)	52.4 (44.4 - 61.5)	3.36 (2.94 - 3.81)
2013	187 (168 - 203)	24.4 (22.9 - 26.1)	51.0 (43.2 - 60.1)	3.73 (3.24 - 4.19)
2014	201 (182 - 219)	25.9 (24.4 - 27.7)	50.6 (43.1 - 58.9)	3.82 (3.32 - 4.27)
2015	212 (190 - 231)	27.6 (25.8 - 29.6)	50.9 (43.6 - 60.1)	3.97 (3.47 - 4.55)
2016	229 (206 - 249)	29.4 (27.7 - 31.3)	52.3 (44.8 - 61.3)	4.54 (3.84 - 5.15)
2017	241 (217 - 264)	30.3 (28.3 - 32.4)	54.6 (46.9 - 63.8)	4.86 (4.12 - 5.55)
2018	238 (210 - 261)	29.0 (26.7 - 31.4)	54.3 (46.6 - 63.3)	5.13 (4.39 - 5.75)

Table 45: Modelled global emissions with uncertainties

Date	HFC-236fa (Gg/yr)	HFC-245fa (Gg/yr)	HFC-365mfc (Gg/yr)	CF4 (Gg/yr)
1978	(-)	(-)	(-)	21.2 (19.7 - 22.3)
1979	(-)	(-)	(-)	20.5 (19.2 - 21.4)
1980	(-)	(-)	(-)	19.4 (18.2 - 20.4)
1981	(-)	(-)	(-)	17.1 (16.1 - 18.4)
1982	(-)	(-)	(-)	15.7 (14.6 - 16.6)
1983	(-)	(-)	(-)	16.4 (15.2 - 17.4)
1984	(-)	(-)	(-)	16.5 (15.5 - 17.8)
1985	(-)	(-)	(-)	15.7 (14.7 - 16.9)
1986	(-)	(-)	(-)	15.6 (14.4 - 16.4)
1987	(-)	(-)	(-)	15.8 (14.6 - 16.8)
1988	(-)	(-)	(-)	16.1 (15.1 - 17.3)
1989	(-)	(-)	(-)	16.1 (15.0 - 17.1)
1990	(-)	(-)	(-)	16.0 (15.0 - 16.8)
1991	(-)	(-)	(-)	14.8 (13.8 - 15.7)
1992	(-)	(-)	(-)	13.0 (12.0 - 13.9)
1993	(-)	(-)	(-)	12.3 (11.4 - 13.3)
1994	(-)	(-)	(-)	11.7 (10.7 - 12.7)
1995	(-)	(-)	(-)	11.9 (11.0 - 12.9)
1996	(-)	(-)	(-)	11.5 (10.7 - 12.4)
1997	(-)	(-)	(-)	11.3 (10.5 - 12.1)
1998	(-)	(-)	(-)	11.1 (10.1 - 12.0)
1999	(-)	(-)	(-)	10.8 (9.74 - 11.7)
2000	(-)	(-)	(-)	10.5 (9.65 - 11.4)
2001	(-)	(-)	(-)	10.2 (9.20 - 11.1)
2002	(-)	(-)	(-)	10.7 (9.84 - 11.6)
2003	(-)	(-)	1.23 (0.967 - 1.49)	11.6 (10.7 - 12.5)
2004	(-)	(-)	2.34 (1.99 - 2.80)	11.3 (10.6 - 12.0)
2005	(-)	(-)	2.98 (2.56 - 3.53)	10.7 (10.1 - 11.4)
2006	0.196 (0.151 - 0.247)	7.43 (6.53 - 8.32)	3.36 (2.91 - 3.95)	11.3 (10.6 - 12.0)
2007	0.206 (0.162 - 0.258)	7.40 (6.39 - 8.16)	3.28 (2.77 - 3.96)	10.8 (10.2 - 11.4)
2008	0.217 (0.175 - 0.270)	7.37 (6.25 - 8.24)	3.13 (2.64 - 3.89)	10.6 (10.1 - 11.2)
2009	0.225 (0.183 - 0.284)	7.15 (6.09 - 8.13)	2.93 (2.46 - 3.60)	9.06 (8.47 - 9.63)
2010	0.246 (0.190 - 0.311)	7.89 (6.59 - 8.87)	3.13 (2.61 - 3.78)	10.1 (9.51 - 10.7)
2011	0.274 (0.218 - 0.345)	8.79 (7.57 - 10.0)	3.43 (2.81 - 4.21)	11.3 (10.6 - 12.0)
2012	0.289 (0.232 - 0.362)	9.48 (8.06 - 11.0)	3.65 (3.05 - 4.49)	11.3 (10.7 - 12.0)
2013	0.295 (0.241 - 0.369)	9.71 (8.11 - 11.1)	3.88 (3.38 - 4.80)	11.1 (10.5 - 11.7)
2014	0.299 (0.237 - 0.370)	10.2 (8.37 - 11.8)	4.20 (3.54 - 5.22)	11.1 (10.4 - 11.7)
2015	0.305 (0.240 - 0.385)	11.0 (9.06 - 12.6)	4.46 (3.65 - 5.51)	11.9 (11.3 - 12.5)
2016	0.320 (0.255 - 0.402)	11.9 (9.86 - 13.7)	4.60 (3.81 - 5.64)	13.0 (12.3 - 13.8)
2017	0.334 (0.263 - 0.412)	12.7 (10.6 - 14.7)	4.70 (3.83 - 5.72)	14.1 (13.3 - 14.8)
2018	0.344 (0.266 - 0.432)	13.1 (10.8 - 15.2)	4.85 (4.01 - 6.17)	14.0 (13.1 - 14.8)

Table 46: Modelled global emissions with uncertainties

Date	C2F6 (Gg/yr)	C3F8 (Gg/yr)	SF6 (Gg/yr)	NF3 (Gg/yr)
1978	2.21 (1.88 - 2.56)	(-)	2.51 (2.16 - 2.81)	(-)
1979	2.24 (2.00 - 2.50)	(-)	2.58 (2.29 - 2.86)	(-)
1980	2.15 (1.97 - 2.37)	(-)	2.74 (2.51 - 2.97)	(-)
1981	1.89 (1.73 - 2.09)	(-)	3.10 (2.86 - 3.37)	(-)
1982	1.74 (1.53 - 1.99)	(-)	3.13 (2.92 - 3.39)	(-)
1983	1.91 (1.70 - 2.13)	0.263 (0.205 - 0.326)	2.98 (2.76 - 3.24)	(-)
1984	2.17 (1.95 - 2.39)	0.256 (0.205 - 0.314)	3.38 (3.05 - 3.60)	(-)
1985	2.17 (1.96 - 2.37)	0.250 (0.199 - 0.298)	3.90 (3.65 - 4.21)	(-)
1986	2.16 (1.92 - 2.39)	0.254 (0.208 - 0.300)	4.20 (3.92 - 4.48)	(-)
1987	2.18 (1.97 - 2.39)	0.248 (0.208 - 0.293)	4.19 (3.90 - 4.48)	(-)
1988	2.25 (2.06 - 2.44)	0.244 (0.205 - 0.286)	4.34 (4.03 - 4.66)	(-)
1989	2.26 (2.05 - 2.46)	0.242 (0.205 - 0.282)	4.70 (4.40 - 4.95)	(-)
1990	2.23 (2.06 - 2.46)	0.248 (0.215 - 0.288)	5.16 (4.88 - 5.51)	(-)
1991	2.16 (1.96 - 2.39)	0.265 (0.228 - 0.297)	5.43 (5.14 - 5.76)	(-)
1992	2.09 (1.88 - 2.31)	0.297 (0.260 - 0.330)	5.40 (5.14 - 5.68)	(-)
1993	2.12 (1.95 - 2.33)	0.348 (0.308 - 0.382)	5.52 (5.21 - 5.76)	(-)
1994	2.16 (1.94 - 2.38)	0.418 (0.379 - 0.449)	5.88 (5.52 - 6.17)	(-)
1995	2.35 (2.12 - 2.55)	0.504 (0.455 - 0.537)	6.19 (5.92 - 6.49)	(-)
1996	2.60 (2.37 - 2.81)	0.598 (0.551 - 0.636)	6.13 (5.78 - 6.44)	(-)
1997	2.86 (2.68 - 3.03)	0.690 (0.632 - 0.736)	5.84 (5.58 - 6.22)	(-)
1998	3.02 (2.84 - 3.21)	0.772 (0.715 - 0.818)	5.57 (5.25 - 5.91)	(-)
1999	3.11 (2.93 - 3.32)	0.843 (0.784 - 0.889)	5.21 (4.90 - 5.50)	(-)
2000	3.03 (2.84 - 3.20)	0.900 (0.847 - 0.955)	5.04 (4.78 - 5.32)	(-)
2001	2.90 (2.73 - 3.10)	0.941 (0.883 - 0.994)	5.21 (4.92 - 5.55)	(-)
2002	2.86 (2.67 - 3.06)	0.965 (0.899 - 1.03)	5.61 (5.30 - 5.87)	(-)
2003	2.72 (2.56 - 2.89)	0.971 (0.906 - 1.03)	5.81 (5.60 - 6.09)	(-)
2004	2.46 (2.26 - 2.63)	0.952 (0.885 - 1.01)	5.83 (5.58 - 6.08)	(-)
2005	2.32 (2.16 - 2.50)	0.906 (0.841 - 0.962)	6.11 (5.82 - 6.35)	(-)
2006	2.31 (2.15 - 2.47)	0.842 (0.792 - 0.889)	6.50 (6.23 - 6.75)	(-)
2007	2.27 (2.10 - 2.43)	0.772 (0.722 - 0.823)	6.98 (6.69 - 7.24)	(-)
2008	2.08 (1.95 - 2.24)	0.709 (0.657 - 0.756)	7.25 (6.97 - 7.55)	(-)
2009	1.89 (1.76 - 2.02)	0.657 (0.606 - 0.704)	7.20 (6.90 - 7.49)	(-)
2010	1.93 (1.76 - 2.07)	0.617 (0.562 - 0.662)	7.37 (7.10 - 7.64)	(-)
2011	1.93 (1.78 - 2.08)	0.581 (0.533 - 0.634)	7.65 (7.36 - 7.95)	(-)
2012	1.91 (1.75 - 2.06)	0.552 (0.505 - 0.589)	7.95 (7.65 - 8.21)	(-)
2013	1.93 (1.76 - 2.08)	0.534 (0.491 - 0.572)	8.20 (7.93 - 8.50)	1.39 (1.31 - 1.48)
2014	1.95 (1.81 - 2.10)	0.524 (0.481 - 0.560)	8.39 (8.10 - 8.69)	1.55 (1.47 - 1.67)
2015	2.00 (1.83 - 2.13)	0.519 (0.472 - 0.554)	8.45 (8.13 - 8.75)	1.76 (1.68 - 1.85)
2016	2.12 (1.98 - 2.28)	0.515 (0.468 - 0.555)	8.73 (8.47 - 9.06)	2.01 (1.91 - 2.11)
2017	2.20 (2.05 - 2.37)	0.515 (0.469 - 0.565)	8.92 (8.58 - 9.26)	2.27 (2.17 - 2.38)
2018	2.12 (1.92 - 2.31)	0.515 (0.456 - 0.571)	9.04 (8.71 - 9.33)	2.43 (2.31 - 2.57)

Table 47: Modelled global emissions with uncertainties

6 UK HFC-125 emissions

HFC-125 (CHF_2CF_3) is the third most abundant HFC in the global atmosphere, behind HFC-134a and HFC-23. Its atmospheric abundance has increased near-exponentially in the global atmosphere since it was first detected over 20 years ago. HFC-125 is mainly used in refrigerant blends for commercial refrigeration, such as R-410A (50% by weight HFC-125 and 50% by weight HFC-32) and R-407C (52% by weight HFC-134a, 25% by weight HFC-125 and 23% by weight HFC-32), replacing the ozone depleting refrigerant HCFC-22. With a 100-year global warming potential (GWP_{100}) of 3450, HFC-125 is a potent greenhouse gas. Consequently, annual emissions of HFC-125 are reported by the UK government to the United Nations Framework Convention on Climate Change (UNFCCC).

The UK collates its emissions from refrigeration and air-conditioning (RAC) sectors (which account for 100% of the UK's HFC-125 emissions) via the RAC model. This model splits UK RAC emissions into 6 sectors, which are further divided into a total of 13 subsectors (Table 1). In each subsector, emissions are calculated using a bottom-up approach, whereby activity data (e.g. the number of commercial refrigeration systems in the UK) are multiplied by an emissions factor (e.g. average leak rate) to estimate an emissions total. This method is applied for each stage of the product life cycle – manufacture, operation and disposal. For all the end uses discussed in this work, most emissions are assumed to occur during operation (e.g. leakage during routine use).

A breakdown of UK HFC-125 emissions from 1990 – 2015 shows that the largest contributing sectors are commercial refrigeration and stationary air-conditioning. Within these, the two dominant RAC sectors, centralised supermarket refrigeration systems and small stationary air-conditioning, each account for roughly 22.5% of total UK HFC-125 emissions.

While the RAC model activity data is informed by a significant quantity of data from industry, the use of a single set of emission factors in each subsector results in potentially highly uncertain estimates of emissions. In this work, we compare the UK HFC-125 emissions inventory to top-down estimates derived using the UK DECC network and InTEM and show that a significant discrepancy exists between reporting methods. Assumptions made within the RAC-4/6 sectors were examined in order to understand the potential origin of these discrepancies.

RAC sector	Source	RAC category
RAC-1	Domestic refrigeration	Domestic refrigeration
RAC-2	Small hermetic stand-alone refrigeration	Commercial refrigeration
RAC-3	Condensing units	Commercial refrigeration
RAC-4	Large supermarket refrigeration systems	Commercial refrigeration
RAC-5	Industrial refrigeration	Industrial refrigeration
RAC-6	Small stationary air-conditioning	Stationary air-conditioning
RAC-7	Medium stationary air-conditioning	Stationary air-conditioning
RAC-8	Large stationary air-conditioning (chillers)	Stationary air-conditioning
RAC-9	Heat pumps	Stationary air-conditioning
RAC-10	Land transport refrigeration	Transport refrigeration
RAC-11	Marine transport refrigeration	Transport refrigeration
RAC-12	Light-duty mobile air-conditioning	Mobile air-conditioning
RAC-13	Other mobile air-conditioning	Mobile air-conditioning

6.1   Methodology

A similar method to that described in Say et al., [2016] was used to examine the RAC model. In short, the original model was adapted in Python, to reduce computational expense and increase the flexibility of key input parameters such as 'refill', which determines the frequency with which a refrigeration/air-conditioning unit's coolant charge is replenished. Input parameters were then varied within their respective uncertainty ranges, and the revised model output compared to the InTEM emissions. In each case, the following input parameters were explored:

- Refill (described above). In the original model, refill was fixed at either 0% or 100%, meaning each unit is assumed to be refilled annually, or not at all. In the Python adapted model, refill can be anywhere in the range between 0% and 100%.

- Lifetime – the assumed average lifetime of units in a given RAC sector.

- Operational loss factor – the assumed loss rate (% total charge per year) during routine operation of units in each RAC sector.

- Manufacturing loss factor – the assumed loss rate (% total charge per year) during manufacture of units in each RAC sector.

- Disposal loss factor – the assumed loss rate (% total charge per year) during disposal of units in each RAC sector.

6.2   Results and discussion

6.2.1   RAC-4 – Centralised supermarket refrigeration systems

The results for the RAC-4 sensitivity study are shown in Figure 119. A reduction of the refill rate (default 100%) results in a significant decrease in UK HFC-125 emissions. In 2010, this decrease is equivalent to 27% of the UK inventory. However, despite a lack of industrial data, a complete reduction in refill rate is highly unlikely to be a true reflection of the UK market given the high leakage rates typically exhibited by supermarket refrigeration systems. REAL Zero, a company contracted by the Institute of Refrigeration to investigate the source of refrigerant leaks in the context of the EU F-gas regulations, published a case study in which four R-404A (44% by weight HFC-125, 52% by weight HFC-143a, 4% by weight HFC-134a) cooled commercial refrigeration systems were monitored over the course of year. Of these four units, 3 required refill after a year. Based on this very small study, a refill rate of 75% is more appropriate, though a larger scale study is required before changes are officially made to the RAC model.

The unit lifetime parameter was varied between 7 and 20 years (default 18 years). Reduction in lifetime only results in modifications to the inventory after 2001 when the first units reach the end of life. After this point, an assumed lifetime of 7 years results in an average decrease in the inventory of 0.12 Gg.

Variations in the assumed loss rates for manufacture and disposal (within the recommended ranges) did not result in any significant changes to the UK HFC-125 emissions inventory, a reflection of the very small contribution emissions from the manufacture and disposal of centralised supermarket refrigeration systems make to total emissions. In comparison, very large variations were observed upon variation of the operational loss factor. The default 2010 loss rate of 18% was varied between 10% and 35%, based on the lower and upper bounds of the recommended IPCC range respectively. While the majority of the IPCC range is above the default parameter, reducing the operational loss rate to 10% does yield an appreciable reduction in total emissions, equivalent to approximately 17% of the inventory in 2010.
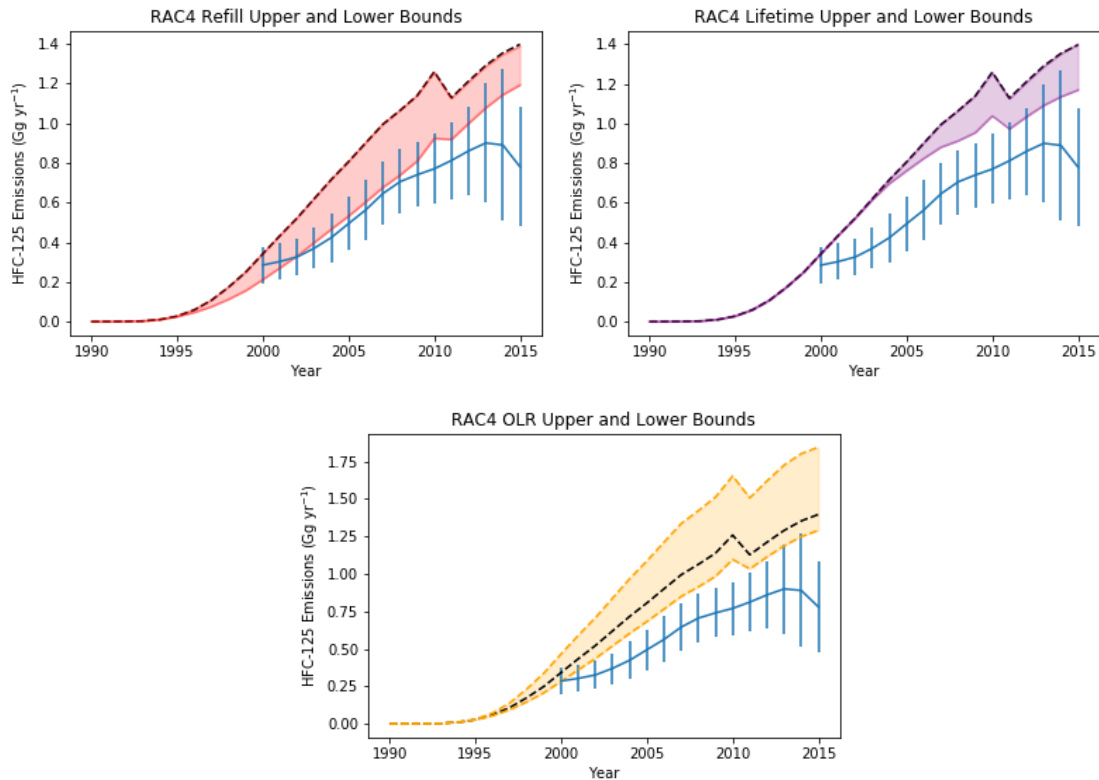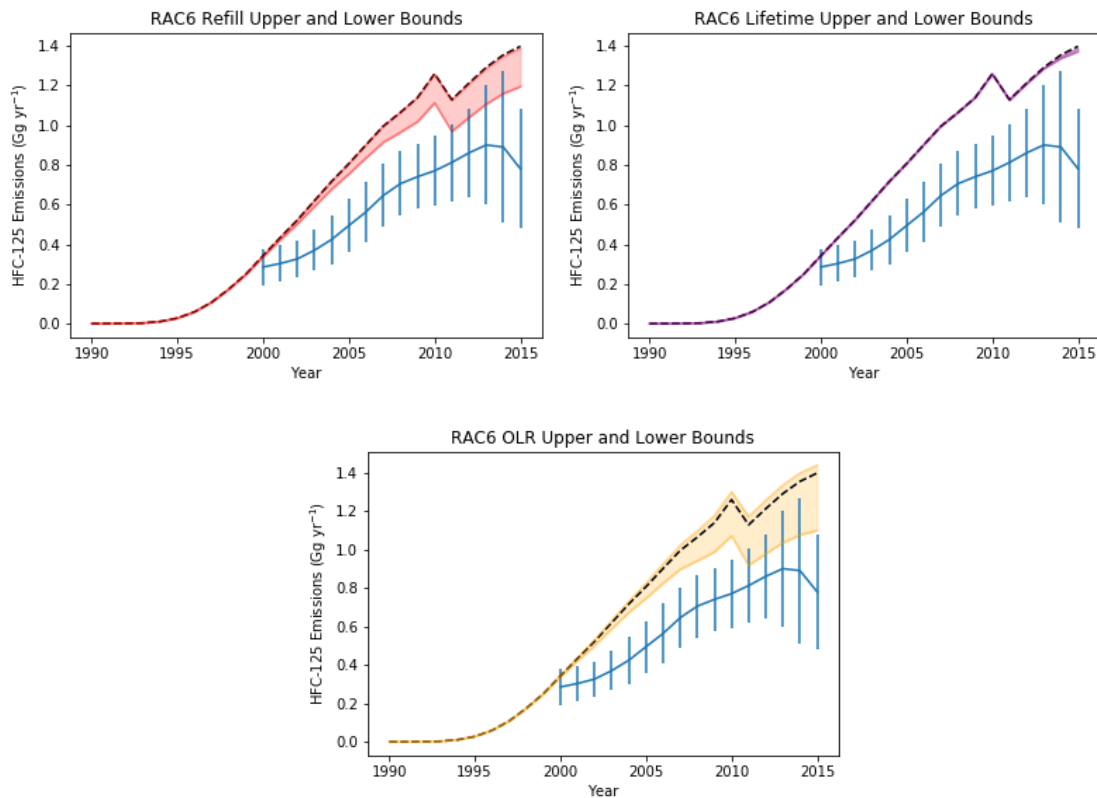
Figure 119: Showing the sensitivity of UK bottom-up HFC-125 emissions (Gg yr-1, black dashed line and shading) to changes in RAC-4 input parameters, compared to annual emissions estimated using InTEM (blue line and error bars). OLR – Operational Loss Rate. The results for manufacturing and disposal loss rate sensitivities are not shown due to the very low sensitivity of the inventory to changes in these parameters.

6.2.2 RAC-6 – Small stationary air-conditioning

The results of the RAC-6 sensitivity study are shown in Figure 120. In comparison to RAC-4, changes to the input parameters in RAC-6 have less overall impact on the UK's HFC-125 inventory. However, reduction of the RAC-6 refill to 0% does have a significant impact on the inventory, yielding a 0.19 Gg decrease of the inventory in 2015. In addition, there is strong evidence that a refill rate of 100% (the default) is an overestimate of the market refill frequency. Daikin, one of the five largest manufacturers of small stationary air-conditioning, states that 'regassing of our air-conditioning units will never be required if installed correctly'. Likewise, Fujitsu state 'If an air conditioning is installed correctly then it should never need to be regassed'. While we were unable to find any experimental data to back up these claims, the advice from manufacturers is strongly suggestive of a reduced refill rate in future iterations of the RAC model.

Sensitivity of the UK inventory to variations in the assumed RAC-6 lifetime, manufacturing loss rate and disposal loss rate is negligible. As with RAC-4, the inventory is most sensitive to variations in operational loss rate. The default 2010 loss rate (3%) was varied within the recommended range of 0.5% to 8%, with the lower bound yielding a 21% decrease in total emissions in 2015. While an operational loss rate of 0.5% does provide a notable reduction in discrepancy between reporting methods, a value of this magnitude is unlikely due to base emissions caused by unit malfunction and catastrophic failure.

Figure 120: Showing the sensitivity of UK bottom-up HFC-125 emissions (Gg yr-1, black dashed line and shading) to changes in RAC-6 input parameters, compared to annual emissions estimated using InTEM (blue line and error bars). OLR – Operational Loss Rate. The results for manufacturing and disposal loss rate sensitivities are not shown due to the very low sensitivity of the inventory to changes in these parameters.

Based on the sensitivity analysis of RAC-4 and RAC-6, an updated UK HFC-125 emissions inventory was estimated (red line, Fig. 3). The revised inventory is based on a RAC-4 refill rate of 75% (e.g. three quarters of centralised supermarket refrigeration systems refilled annually) following the case study by REAL Zero, and a RAC-6 refill rate of 20%, a conservative estimate based on the recommendation of air-conditioning manufacturers while assuming that one in five units will still require annual refill.
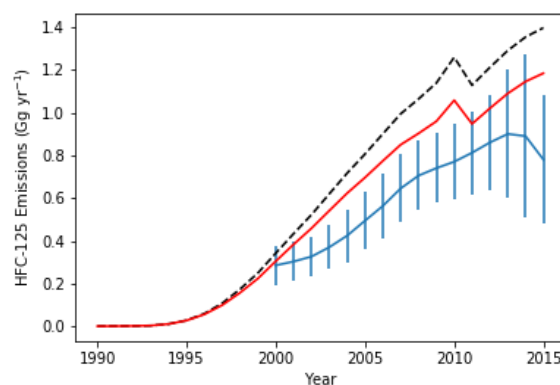
Figure 121: A revised UK HFC-125 emissions inventory (red line), compared to the original inventory (dashed black line) and InTEM top-down estimates (blue line and error bars).

While the revised inventory remains higher than the mean InTEM estimate in all reported years, the reductions in refill results in a considerable smaller discrepancy between methods than that observed previously. In 2015, the revised inventory is over 0.2 Gg smaller than the original estimate, an approximate 15% reduction. With further investigation of the RAC-4/6 operational loss rates, which are highly uncertain but to which

113

the total inventory is highly sensitive, the discrepancy between reporting methods has the potential to be fully explained.

6.3   Conclusions

The UK's HFC-125 inventory is significantly larger than the top-down emissions, derived using InTEM, throughout much of the reporting period. HFC-125 is used in multiple RAC sectors, predominantly as a blend component. Together, RAC-4 (centralised supermarket refrigeration systems) and RAC-6 (small stationary air-conditioning) account for 45% of total UK HFC-125 emissions. The assumptions made by the inventory in calculating emissions from these sectors were examined, using the methodology described previously in Say et al., [2016]. The sensitivity of the UK inventory to changes in RAC-4/6 default model parameters was calculated using a Pythonic version of the RAC model. Reduction of the RAC-4 refill parameter from 100% (annual refill) to 0% (no refill) yielded a significant reduction of the inventory estimates, with the revised estimates overlapping the InTEM uncertainties in all years except 2015. However, supermarket refrigeration systems are notoriously leaky, and almost certainly require multiple refills over the course of their operational life. Smaller reductions were also observed upon setting the RAC-6 refill rate to 0%. However, in contrast to RAC-4, a large reduction in refill rate appears justified – multiple leading manufacturers of small stationary air-conditioning units state that refill of their units is not required during operational lifetime, assuming these units are installed correctly. Further emissions reductions were achieved via reduction of the RAC-6 operational loss factor, down from a default of 3% in 2010 to 0.5%, as per the lower bound of the recommended range. However, catastrophic failures (e.g. unit malfunction) are likely to prevent loss rates of that magnitude from being achieved.

A revised inventory was calculated based on revised refill rates of 75% and 20% for RAC-4 and RAC-6 respectively, based on the limited independent data available. The revised inventory estimates reduce the discrepancy between methods substantially – between 2011 and 2014, the bottom-up estimates are within the InTEM uncertainties. Further work is required to provide a more comprehensive assessment of UK refill rates – however, the data that is available strongly suggests that the magnitude of the UK's HFC-125 inventory estimates are artificially inflated by over-conservative refill rate estimates in RAC-4 and 6.

7 UK Methane Emissions using Remotely Sensed Data

7.1 Introduction

The UK uses the DECC network of tall tower measurements to perform greenhouse gas inversions for the UK, but does not currently use any of the available satellite measurements for greenhouse gas inversions. Satellite measurements use different methodology to surface sites: satellites measure columns of air, with sensitivity throughout the atmospheric column, whereas *in situ* sites are most sensitive to the nearby surface. The potential benefit of space-based remote sensing data is that it can cover a wider spatial area than fixed *in situ* measurement stations. However, the cost comes in the form of lower measurement precision, and, because the entire atmospheric column is measured, lower sensitivity to surface fluxes. This report investigates the usefulness of observations from the Greenhouse Gases Observing Satellite (GOSAT) [*Kuze et al.*, 2016] for providing an additional verification of the inversion of methane fluxes in the UK.

7.2 Method

Here, we describe a set of inversions that were performed to determine whether GOSAT data could add value to UK methane emissions estimates. We performed three inversions, one using the DECC network, one using the DECC network with GOSAT, and one using only GOSAT.
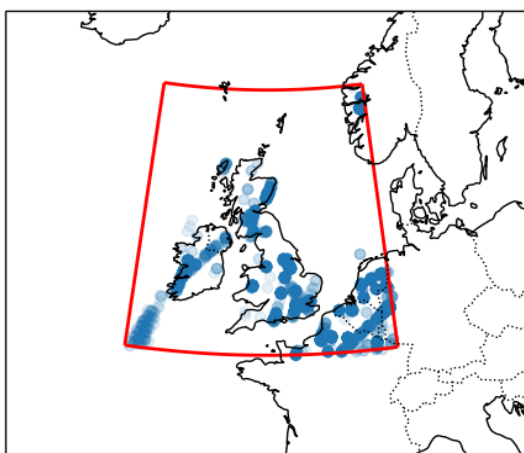
Figure 122 The domain used for GOSAT observations within North-West Europe (red box). Circles indicate GOSAT observations between 2010 and 2017 inclusive. Darker circles indicate multiple observations over the time period.

7.2.1 Satellite Data

GOSAT provides near-global measurements of column methane. To perform a UK inversion a regional subset of the GOSAT data was taken, shown in Figure 122. The data used is the level 2 product from the University of Leicester [*Parker et al.*, 2011]. Figure 123 shows the frequency of observations for each month of the available data, between 2010 and 2017 inclusive. There is a substantial seasonal change in the number of available soundings. During the winter there are relatively few observations (~15 per month), with more available during the summer (~59 per month). This is compared to ~720 hourly averaged observations per site per month in the tall tower network. The seasonal change in the number of GOSAT observations is driven by the change in solar zenith angle, with few observations being possible when the sun is very low in the sky, and cloud cover. GOSAT observations have a relatively high uncertainty compared to the *in situ* data; between 2010-2017, GOSAT average measurement uncertainty is 11 ppb compared to 1.5 ppb for the Mace Head data.
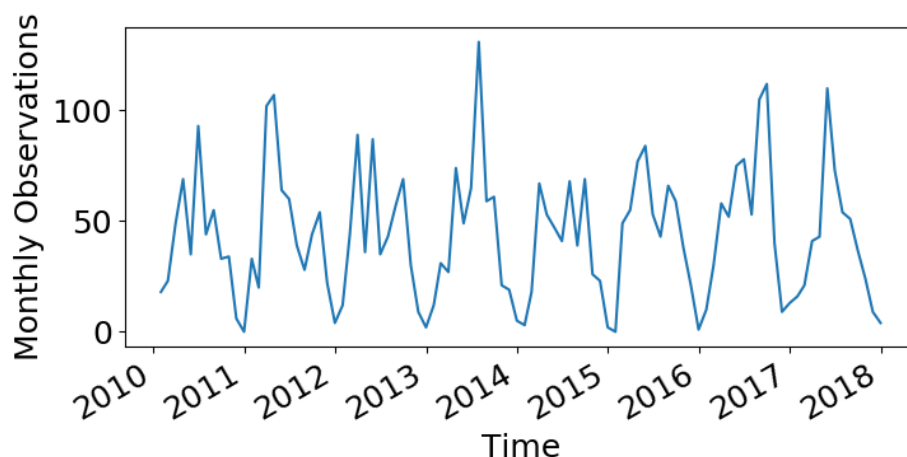
Figure 123 The total number of observations for each month of the GOSAT data, showing seasonal variation with lows in winter.

7.2.2 Prior Emissions

UK anthropogenic emissions are taken from the 2016 National Atmospheric Emissions Inventory (NAEI). Outside of the UK, Emission Database for Global Atmospheric Research (EDGAR) inventory values are used. The combined emissions map is shown in Figure 124. Boundary conditions are taken from the Copernicus Atmosphere Monitoring Service (CAMS) global methane reanalysis product, and incorporated into the NAME inversions as described in previous publications [*Lunt et al.*, 2016; *Ganesan et al.*, 2017].
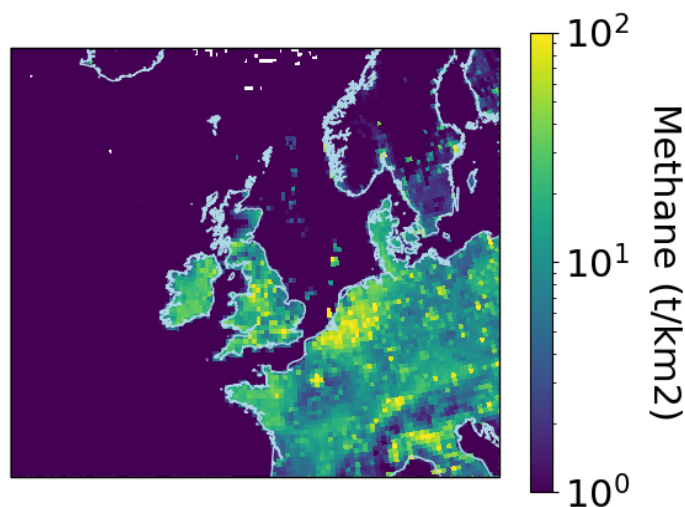
Figure 124 A subset of prior emissions using NAEI within the UK and EDGAR outside. The full domain used reaches North America to the west, and all of Europe to the east.

7.2.3 Modelling

The inversion is performed using a Trans-dimensional Markov Chain Monte Carlo (TDMCMC) method, adapted for remotely sensed data, as explained in detail elsewhere [*Lunt et al.*, 2016; *Ganesan et al.*, 2017]. This method uses Bayesian statistics to estimate gridded posterior emissions and their uncertainties using prior emissions information and atmospheric observations combined and the NAME model. The trans-dimensional component of the model allows the basis function used to aggregate the emissions and sensitivities to be adjusted during the inversion in order to avoid issues associated with subjectively chosen basis functions. The uncertainty in the basis functions used in this process is propagated to the final posterior distribution of emissions. Annual emissions and monthly boundary conditions were solved for in the inversion. Where DECC network data were used, the daily average at each site was taken.

7.3 Results

7.3.1 Annual Emission Estimates

Annual emission estimates from the inversions are shown in Figure 125. The figure shows that, compared to the DECC-only inversion, the inclusion of GOSAT observations has a small impact on the inferred annual emissions and their uncertainty. The GOSAT-only inversion has very large uncertainty compared to the inversions using the DECC network data. These findings are likely because of the relatively small number of observations and high uncertainty of the GOSAT data, compared to the *in situ* observations. Furthermore, because GOSAT is sensitive to the whole atmospheric column, the data are less strongly influenced by surface emissions than the DECC network measurements.
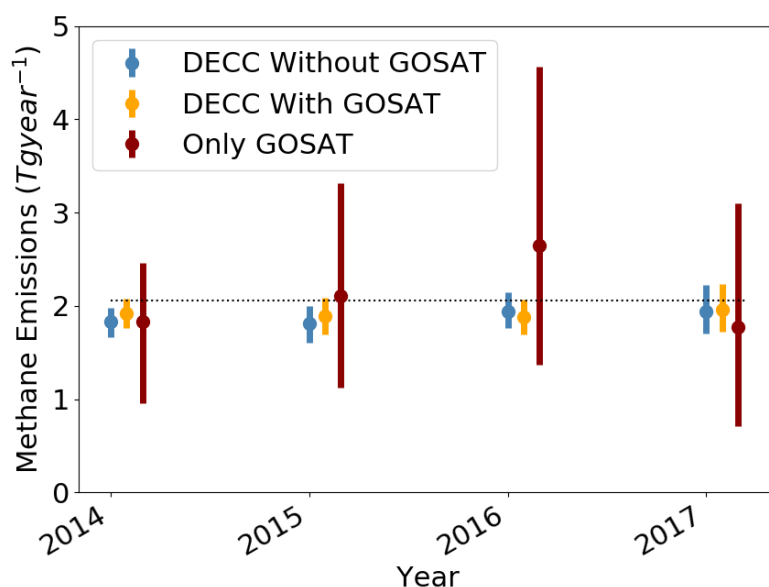
Figure 125 Annual emissions estimates from the DECC inversions with and without the GOSAT observations included, and for inversions only using GOSAT. Results are shown as mean values with 5th-95th percentile ranges and the dotted line showing the mean emissions of the prior used.

7.4 Conclusion and Future Work

Data from the GOSAT satellite has been used to perform annual inversion estimates of UK methane emissions from 2014 to 2017 inclusive. GOSAT has much fewer observations, lower sensitivity to surface emissions and higher measurement uncertainty compared to the DECC network sites. Including GOSAT data in inversions using the DECC network provides little additional refinement on emissions estimates.

The next-generation satellite instruments such as The TROPOspheric Monitoring Instrument (TROPOMI) may be able to overcome this issue [*Hu et al.*, 2018]. TROPOMI has a much higher spatial resolution than GOSAT, allowing measurements to be made through gaps in cloud cover, with potential for more observations in a single day than GOSAT achieves in a month over the UK. In this work, we have developed the inverse modelling framework to use satellite observations for UK methane emissions estimation, which we will now apply to TROPOMI and future satellite missions.

8 Results and analysis of additional gases

8.1 Introduction

This section discusses the atmospheric trends and regional emissions of the other gases that are measured at Mace Head. The table below describes, if applicable, the principle uses of each of the gases, their radiative efficiency, atmospheric lifetime, global warming potential in a 100-year framework (GWP_{100}) and ozone depleting potential (ODP). In the following sections each of these gases are presented.

Gas	Primary use	Radiative Efficiency ($W\ m^{-2}\ ppb^{-1}$)	Atmospheric Lifetime (years)	GWP_{100}	ODP
CFC-11	Widespread	0.26	45	4,660	1
CFC-12	Refrigerant	0.32	100	10,200	0.82
CFC-113	Coolant, electronics	0.30	85	5,820	0.85
CFC-115	Refrigerant	0.20	1,020	7,670	0.57
HCFC-124	Refrigerant, fire suppression	0.20	5.9	527	0.02
HCFC-141b	Foam blowing	0.16	9.2	782	0.12
HCFC-142b	Chem. synthesis/foam blowing	0.19	17.2	1,980	0.06
HCFC-22	Propellant, air conditioning	0.21	11.9	1,760	0.04
HFC-236fa	Fire extinguisher	0.24	242	8060	
HFC-245fa	Foam blowing	0.24	7.7	858	
SO_2F_2	Fumigant	0.2	36	4090	
CH_3Cl	Natural, refrigerant	0.01	1	12	0.02
CH_2Cl_2	Foam plastic, solvent, natural		144 days		
$CHCl_3$	Bi-product, natural		149 days		
CCl_4	Fire suppression, precursor	0.17	26	1,730	0.82
CH_3CCl_3	Solvent	0.07	5.0	160	0.16
$CHClCCl_2$	Degreasing solvent		5 days	5	
CCl_2CCl_2	Solvent, dry cleaning		90 days	15	
CH_3Br	Natural (seaweed), fumigant		0.8		
CH_2Br_2	Natural (seaweed)		123 days		
$CHBr_3$	Fumigant, natural (seaweed)		24 days		0.66
$CBrClF_2$	Fire suppression (military)	0.29	16	1,750	7.9
$CBrF_3$	Fire suppression	0.30	65	6,290	15.9
$C_2Br_2F_4$	Fire suppression	0.31	20	1,470	13.0
CH_3I	Natural (seaweed)		7 days		
C_2H_6	Combustion, gas leakage				
CO	Combustion		30-90 days		
O_3	Reactions in atmosphere				
H_2	Combustion, photolysis				

Table 48: The principle uses of the gases observed at Mace Head, their radiative efficiency, atmospheric lifetime, global warming potential in a 100-year framework (GWP_{100}) and ozone depleting potential (ODP). The gases listed in red are specifically covered by the Montreal Protocol. All of the gases with a GWP are GHGs but not all GHGs are covered by the Kyoto Protocol.
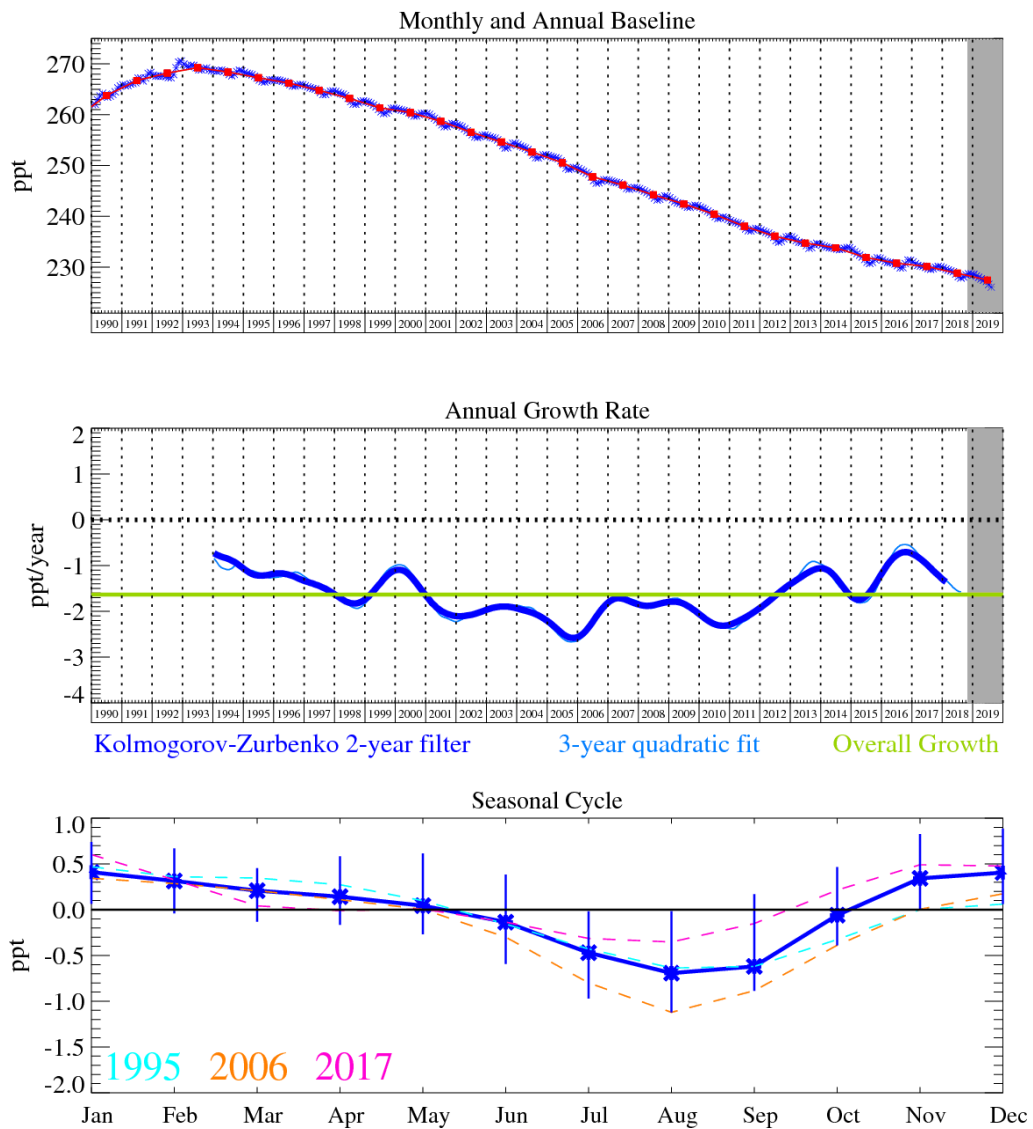
8.2 CFC-11

Figure 126: CFC-11: Monthly (blue) and annual (red) Northern Hemisphere baseline mole fractions (top plot). Annual (blue) and overall (green) average growth rate (middle plot). Seasonal cycle (de-trended) with year-to-year variability (lower plot). Grey area covers un-ratified provisional data.
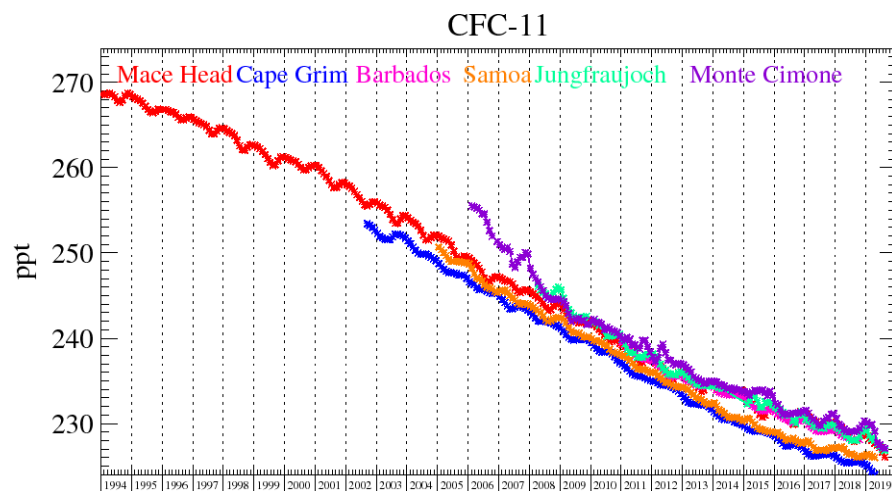

Figure 127: Background CFC-11 mole fractions at several global AGAGE stations both in the Northern and Southern Hemispheres.
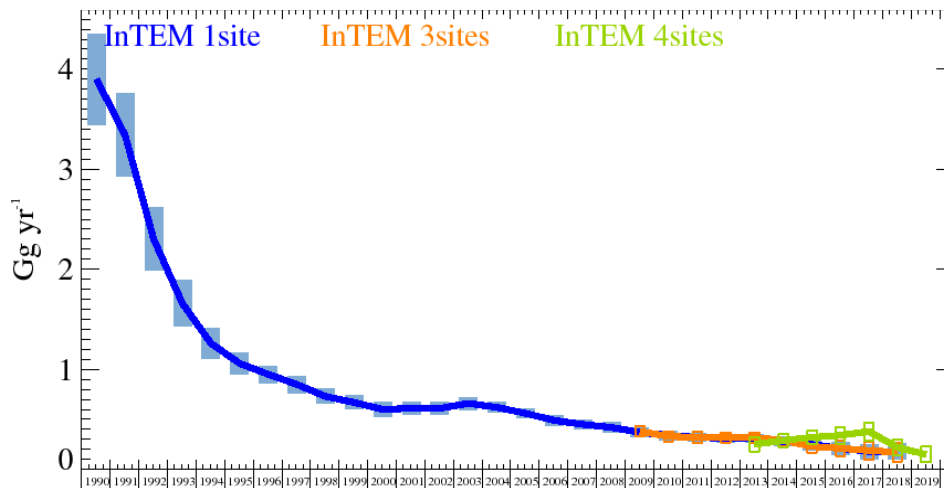
Figure 128: CFC-11: UK emission estimates (Gg yr^{-1}) using InTEM (annually averaged): (a) MHD (3yr) with global meteorology (blue), (b) 3 sites (2yr) (MHD+JFJ+CMN) with global meteorology (orange), and (c) 4 sites (1yr) (MHD +JFJ+CMN+TAC) with UKV 1.5 km nested in global meteorology (green). The uncertainty bars represent 1 std.
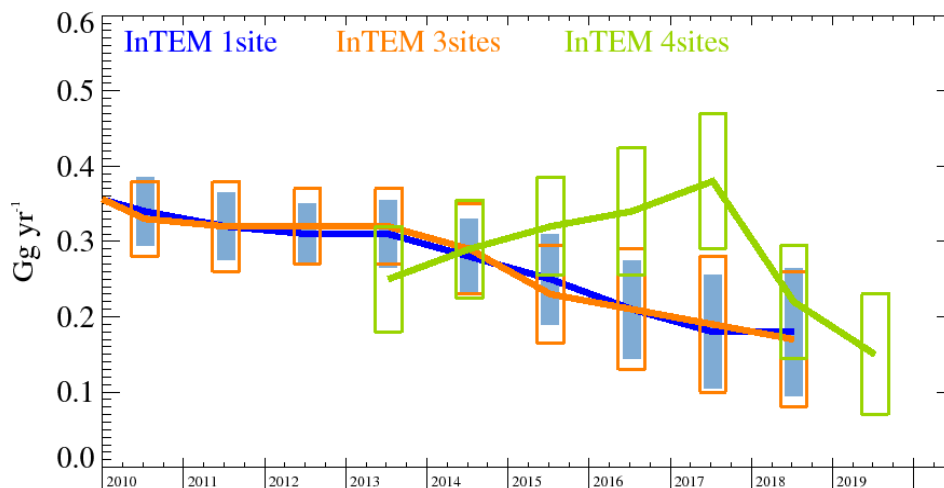
Figure 129: CFC-11 (expanded Y-axis): UK emission estimates (Gg yr^{-1}) using InTEM (annually averaged): (a) MHD (3yr) with global meteorology (blue), (b) 3 sites (2yr) (MHD+JFJ+CMN) with global meteorology (orange), and (c) 4 sites (1yr) (MHD+JFJ+CMN+TAC) with UKV 1.5 km nested in global meteorology (green). The uncertainty bars represent 1 std.
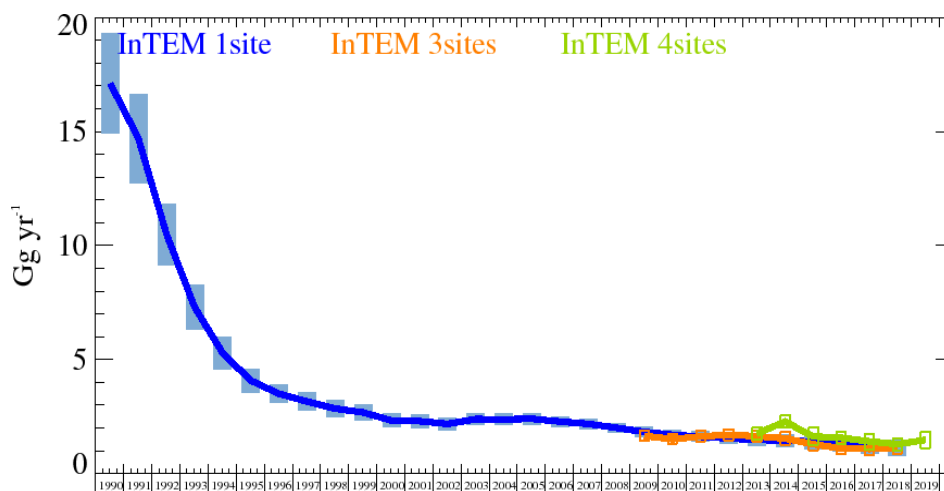
Figure 130: CFC-11: NWEU emission estimates (Gg yr^{-1}) using InTEM (annually averaged): (a) MHD (3yr) with global meteorology (blue), (b) 3 sites (2yr) (MHD+JFJ+CMN) with global meteorology (orange), and (c) 4 sites (1yr)
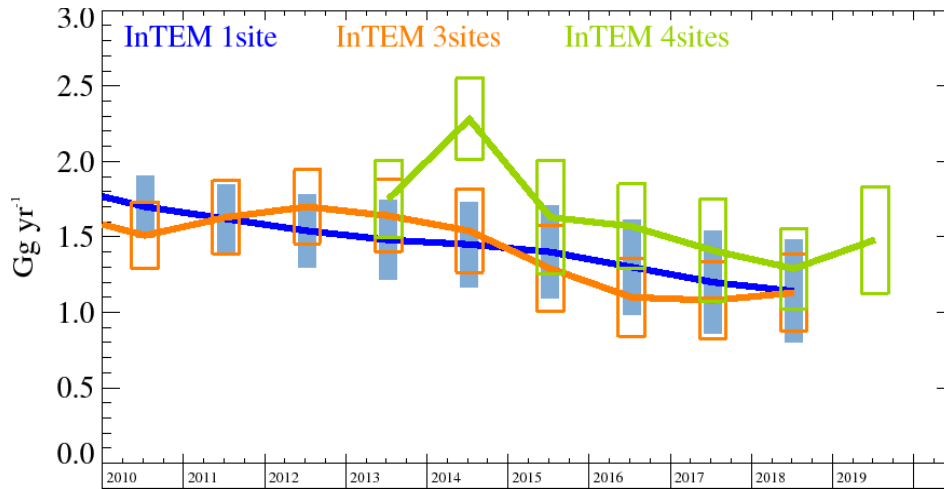
Figure 131: CFC-11 (expanded Y-axis): NWEU emission estimates (Gg yr^{-1}) using InTEM (annually averaged): (a) MHD (3yr) with global meteorology (blue), (b) 3 sites (2yr) (MHD+JFJ+CMN) with global meteorology (orange), and (c) 4 sites (1yr) (MHD+JFJ+CMN+TAC) with UKV 1.5 km nested in global meteorology (green). The uncertainty bars represent 1 std.

Years	MHD	3 sites	4 sites
1990	3.90 (3.45-4.36)		
1991	3.34 (2.92-3.75)		
1992	2.30 (1.98-2.61)		
1993	1.66 (1.43-1.89)		
1994	1.26 (1.11-1.42)		
1995	1.06 (0.95-1.17)		
1996	0.95 (0.86-1.03)		
1997	0.85 (0.76-0.93)		
1998	0.73 (0.66-0.81)		
1999	0.67 (0.60-0.74)		
2000	0.60 (0.53-0.67)		
2001	0.61 (0.55-0.68)		
2002	0.61 (0.54-0.67)		
2003	0.66 (0.59-0.72)		
2004	0.62 (0.56-0.67)		
2005	0.56 (0.51-0.61)		
2006	0.49 (0.44-0.54)		
2007	0.45 (0.40-0.50)		
2008	0.42 (0.37-0.47)		
2009	0.37 (0.32-0.41)	0.38 (0.33-0.43)	
2010	0.34 (0.29-0.38)	0.33 (0.28-0.38)	
2011	0.32 (0.27-0.36)	0.32 (0.26-0.38)	
2012	0.31 (0.27-0.35)	0.32 (0.27-0.37)	
2013	0.31 (0.26-0.35)	0.32 (0.27-0.37)	0.25 (0.18-0.32)
2014	0.28 (0.23-0.33)	0.29 (0.23-0.35)	0.29 (0.23-0.36)
2015	0.25 (0.19-0.31)	0.23 (0.17-0.30)	0.32 (0.25-0.38)
2016	0.21 (0.15-0.28)	0.21 (0.13-0.29)	0.34 (0.26-0.43)
2017	0.18 (0.11-0.26)	0.19 (0.10-0.28)	0.38 (0.29-0.47)
2018	0.18 (0.09-0.26)	0.17 (0.08-0.26)	0.22 (0.15-0.30)
2019			0.15 (0.07-0.23)

Table 49: CFC-11 emission (Gg yr^{-1}) estimates for the UK with uncertainty (1std).

Years	MHD	3 sites	4 sites
1990	17.1 (14.9-19.3)		
1991	14.7 (12.8-16.7)		
1992	10.5 (9.2-11.9)		
1993	7.3 (6.3-8.3)		
1994	5.28 (4.57-6.00)		
1995	4.08 (3.57-4.59)		
1996	3.50 (3.10-3.89)		
1997	3.16 (2.77-3.54)		
1998	2.85 (2.48-3.22)		
1999	2.68 (2.34-3.01)		
2000	2.33 (2.03-2.63)		
2001	2.30 (2.01-2.59)		
2002	2.18 (1.90-2.46)		
2003	2.39 (2.11-2.66)		
2004	2.38 (2.12-2.64)		
2005	2.40 (2.16-2.65)		
2006	2.28 (2.04-2.52)		
2007	2.18 (1.95-2.41)		
2008	2.01 (1.79-2.22)		
2009	1.83 (1.62-2.04)	1.65 (1.43-1.88)	
2010	1.70 (1.49-1.90)	1.51 (1.29-1.73)	
2011	1.62 (1.39-1.85)	1.63 (1.39-1.88)	
2012	1.54 (1.29-1.78)	1.70 (1.46-1.95)	
2013	1.48 (1.22-1.75)	1.64 (1.40-1.88)	1.75 (1.49-2.00)
2014	1.45 (1.17-1.73)	1.54 (1.27-1.82)	2.28 (2.01-2.55)
2015	1.40 (1.09-1.71)	1.29 (1.00-1.57)	1.63 (1.25-2.00)
2016	1.30 (0.98-1.61)	1.10 (0.84-1.36)	1.57 (1.29-1.85)
2017	1.20 (0.86-1.54)	1.08 (0.83-1.34)	1.41 (1.07-1.75)
2018	1.14 (0.80-1.48)	1.13 (0.87-1.38)	1.29 (1.02-1.55)
2019			1.48 (1.13-1.84)

Table 50: CFC-11 emission (Gg yr^{-1}) estimates for the NWEU with uncertainty (1std).
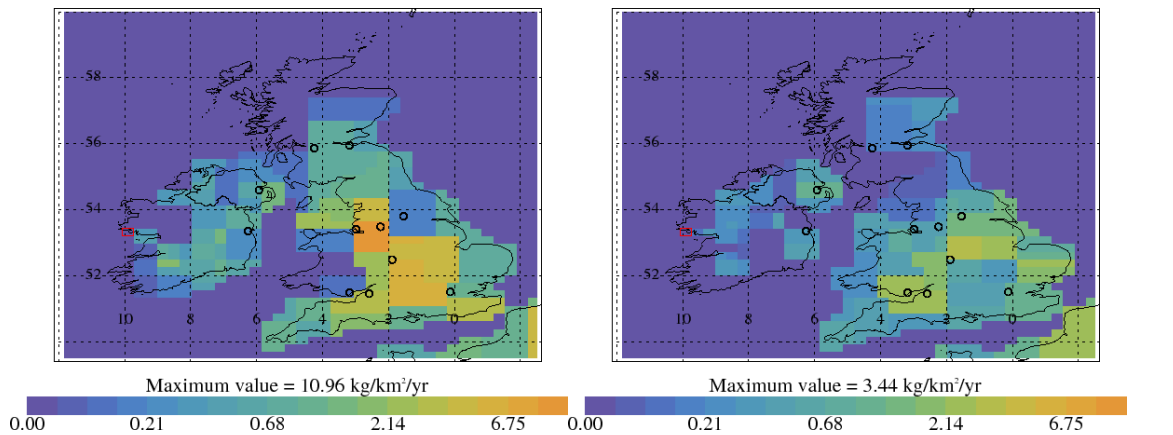
Figure 132: CFC-11 emission estimate using MHD data for 2004-2008 (left) and 2014-2018 (right). Major cities shown as black circles and observation sites shown as red rectangle.

Maximum value = 5.64 kg/km²/yr   Maximum value = 9.53 kg/km²/yr

0.00   0.21   0.68   2.14   6.75   0.00   0.21   0.68   2.14   6.75
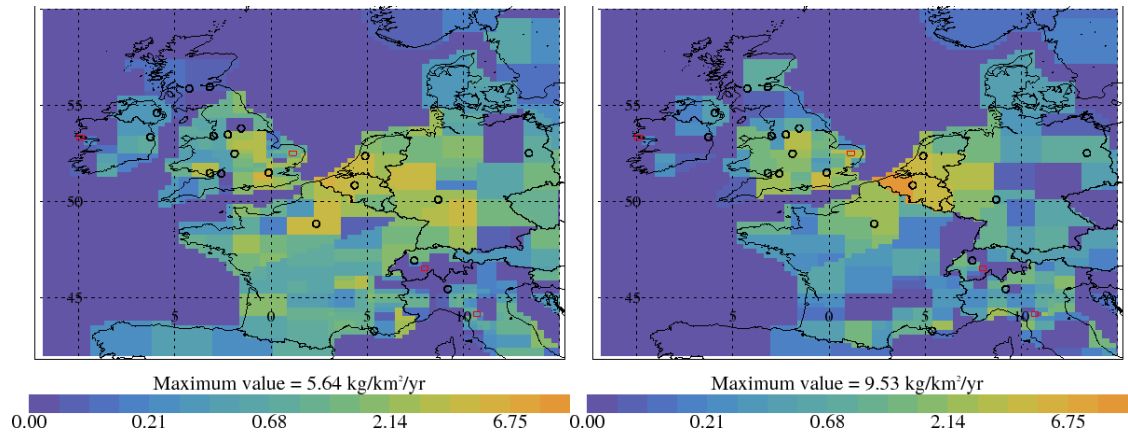
Figure 133: CFC-11 emission estimate using data from 3 sites for 2013-2015 (left) and 2016-2018 (right). Major cities shown as black circles and observation sites shown as red rectangle.
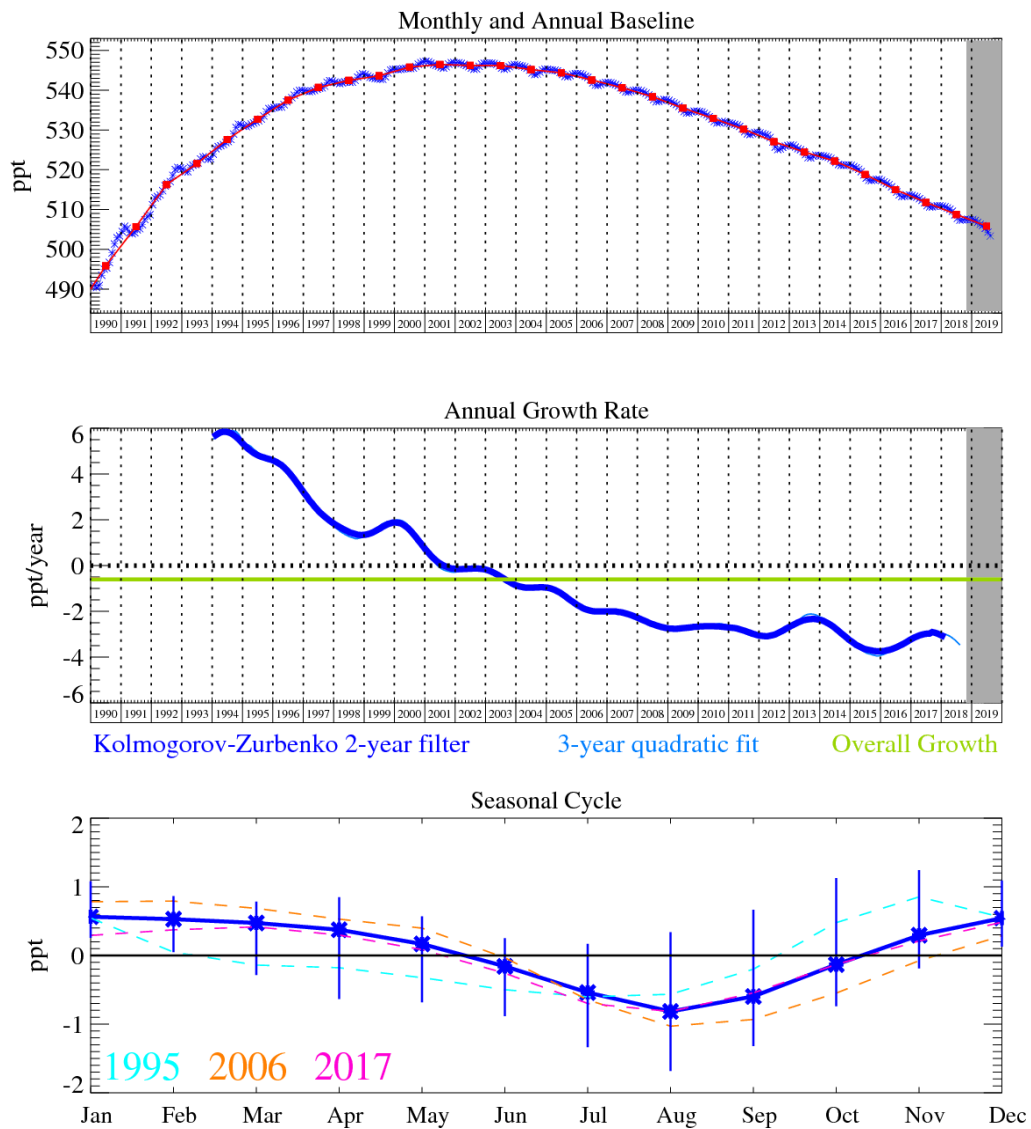
8.3   CFC-12

Monthly and Annual Baseline

Annual Growth Rate

Kolmogorov-Zurbenko 2-year filter   3-year quadratic fit   Overall Growth

Seasonal Cycle

1995   2006   2017

Figure 134: CFC-12: Monthly (blue) and annual (red) Northern Hemisphere baseline mole fractions (top plot). Annual (blue) and overall (green) average growth rate (middle plot). Seasonal cycle (de-trended) with year-to-year variability (lower plot). Grey area covers un-ratified provisional data.

CFC-12

Mace Head Cape Grim Barbados Samoa Jungfraujoch Monte Cimone
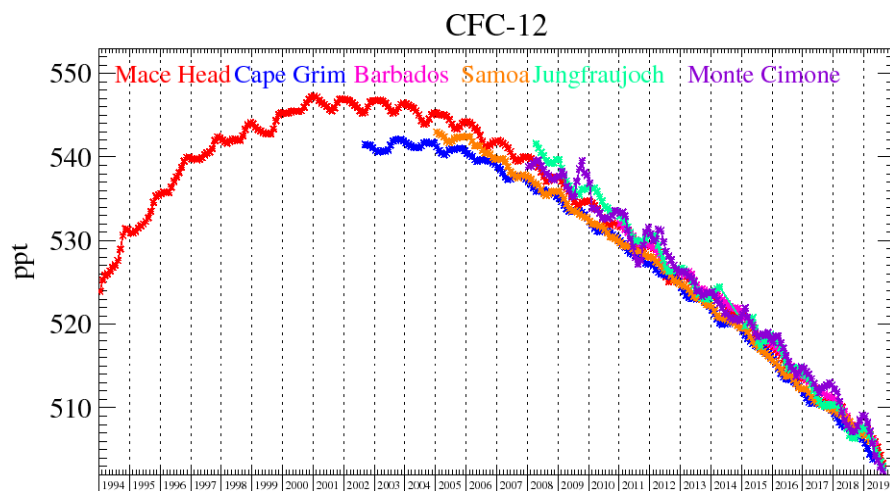
Figure 135: Background CFC-12 mole fractions at several global AGAGE stations both in the Northern and Southern Hemispheres.

124
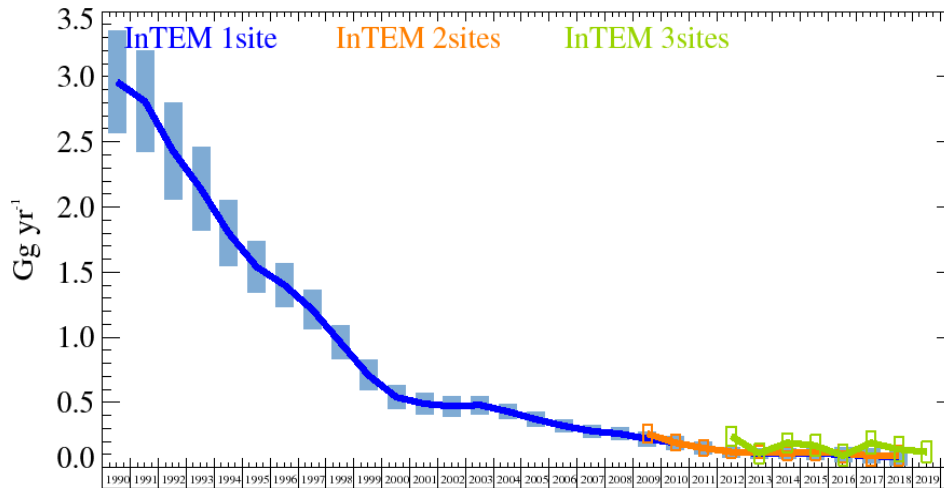
Figure 136: CFC-12: UK emission estimates (Gg yr^{-1}) using InTEM (annually averaged): (a) MHD (3yr) with global meteorology (blue), (b) 2 sites (2yr) (MHD+JFJ) with global meteorology (orange), and (c) 3 sites (1yr) (MHD +JFJ+TAC) with UKV 1.5 km nested in global meteorology (green). The uncertainty bars represent 1 std.
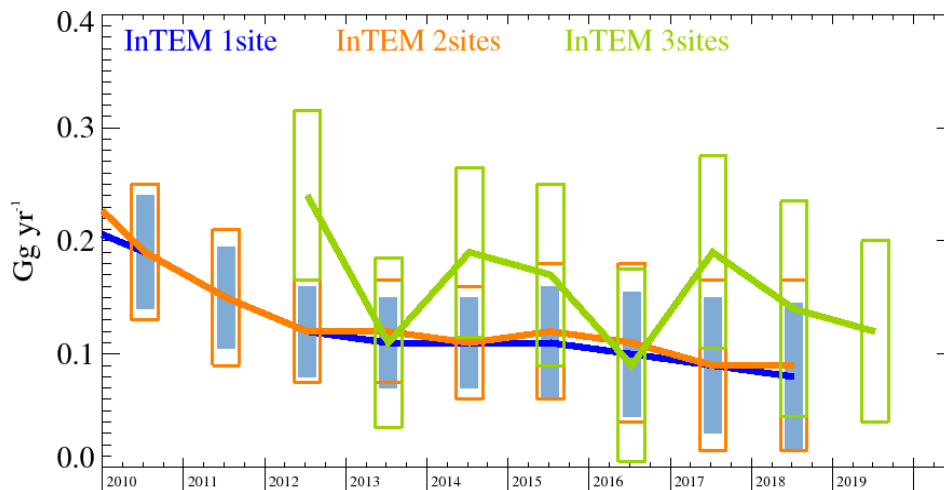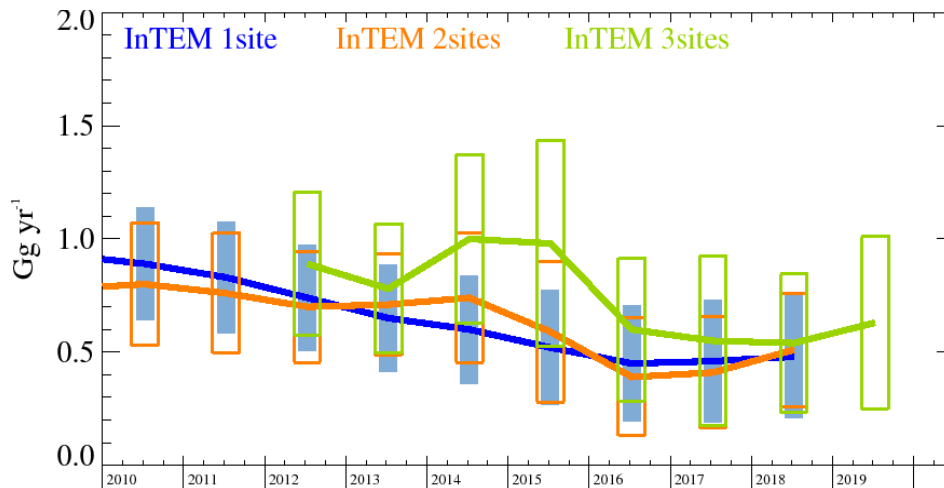

Figure 137: CFC-12 (expanded Y-axis): UK emission estimates (Gg yr^{-1}) using InTEM (annually averaged): (a) MHD (3yr) with global meteorology (blue), (b) 2 sites (2yr) (MHD+JFJ) with global meteorology (orange), and (c) 3 sites (1yr) (MHD+JFJ+TAC) with UKV 1.5 km nested in global meteorology (green). The uncertainty bars represent 1 std.
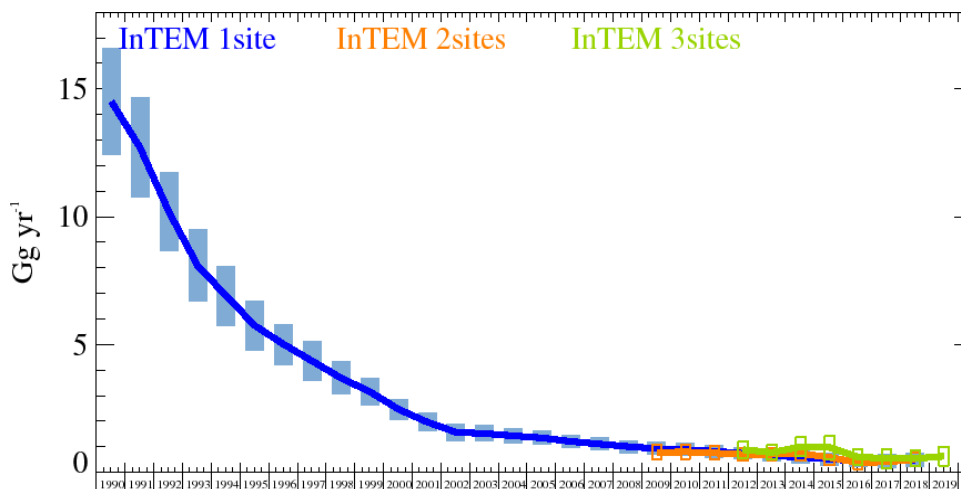
Figure 138: CFC-12: NWEU emission estimates (Gg yr^{-1}) using InTEM (annually averaged): (a) MHD (3yr) with global meteorology (blue), (b) 2 sites (2yr) (MHD+JFJ) with global meteorology (orange), and (c) 3 sites (1yr) (MHD+JFJ+TAC) with UKV 1.5 km nested in global meteorology (green). The uncertainty bars represent 1 std.

Figure 139: CFC-12 (expanded Y-axis): NWEU emission estimates (Gg yr⁻¹) using InTEM (annually averaged): (a) MHD (3yr) with global meteorology (blue), (b) 2 sites (2yr) (MHD+JFJ) with global meteorology (orange), and (c) 3 sites (1yr) (MHD+JFJ+TAC) with UKV 1.5 km nested in global meteorology (green). The uncertainty bars represent 1 std.

Years	MHD	2 sites	3 sites
1990	2.96 (2.57-3.36)		
1991	2.81 (2.42-3.20)		
1992	2.43 (2.06-2.80)		
1993	2.14 (1.82-2.46)		
1994	1.80 (1.55-2.06)		
1995	1.54 (1.34-1.74)		
1996	1.40 (1.23-1.56)		
1997	1.21 (1.06-1.36)		
1998	0.96 (0.83-1.09)		
1999	0.71 (0.60-0.83)		
2000	0.54 (0.45-0.63)		
2001	0.49 (0.41-0.58)		
2002	0.47 (0.39-0.54)		
2003	0.48 (0.41-0.55)		
2004	0.43 (0.37-0.49)		
2005	0.37 (0.32-0.43)		
2006	0.32 (0.27-0.37)		
2007	0.28 (0.23-0.33)		
2008	0.26 (0.21-0.31)		
2009	0.22 (0.17-0.28)	0.26 (0.19-0.32)	
2010	0.19 (0.14-0.24)	0.19 (0.13-0.25)	
2011	0.15 (0.10-0.19)	0.15 (0.09-0.21)	
2012	0.12 (0.08-0.16)	0.12 (0.08-0.17)	0.24 (0.17-0.32)
2013	0.11 (0.07-0.15)	0.12 (0.07-0.16)	0.11 (0.03-0.18)
2014	0.11 (0.07-0.15)	0.11 (0.06-0.16)	0.19 (0.12-0.27)
2015	0.11 (0.06-0.16)	0.12 (0.06-0.18)	0.17 (0.09-0.25)
2016	0.10 (0.05-0.16)	0.11 (0.04-0.18)	0.09 (0.01-0.18)
2017	0.09 (0.03-0.15)	0.09 (0.02-0.17)	0.19 (0.11-0.28)
2018	0.08 (0.02-0.15)	0.09 (0.01-0.16)	0.14 (0.05-0.24)
2019			0.12 (0.04-0.20)

Table 51: CFC-12 emission (Gg yr⁻¹) estimates for the UK with uncertainty (1std).
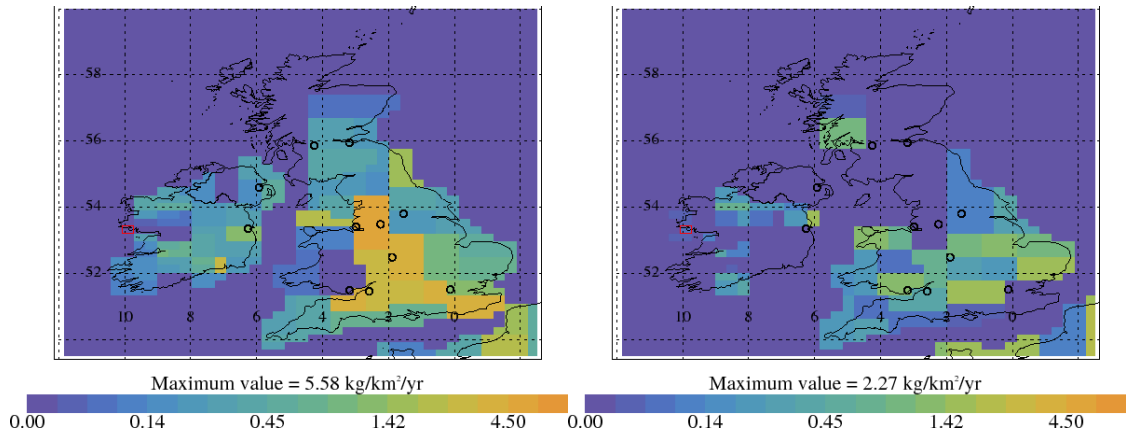
Figure 140: CFC-12 emission estimate using MHD data for 2004-2008 (left) and 2014-2018 (right). Major cities shown as black circles and observation sites shown as red rectangle.
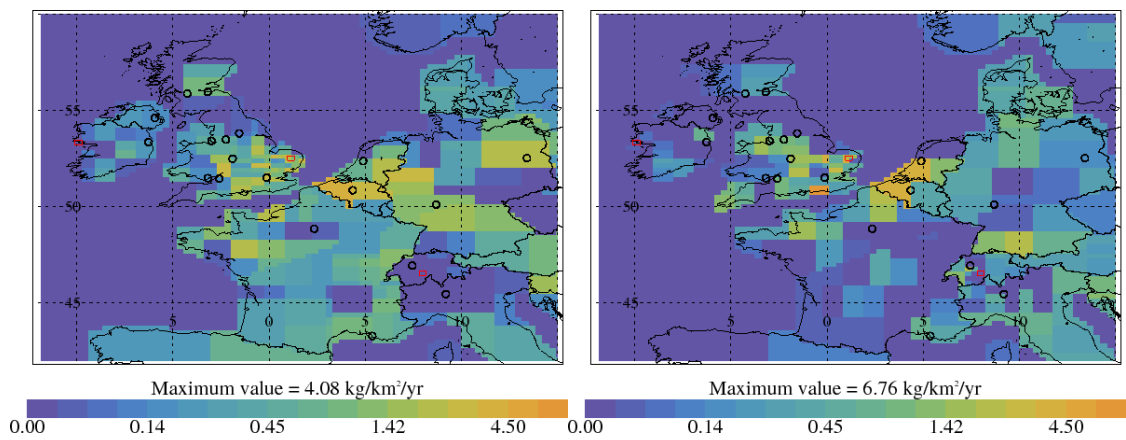
Figure 141: CFC-12 emission estimate using data from 3 sites for 2013-2015 (left) and 2016-2018 (right). Major cities shown as black circles and observation sites shown as red rectangle.

Years	MHD	2 sites	3 sites
1990	14.5 (12.4-16.6)		
1991	12.7 (10.8-14.7)		
1992	10.2 (8.6-11.7)		
1993	8.1 (6.7-9.5)		
1994	6.9 (5.8-8.1)		
1995	5.74 (4.78-6.70)		
1996	5.01 (4.21-5.80)		
1997	4.35 (3.58-5.11)		
1998	3.69 (3.04-4.34)		
1999	3.16 (2.62-3.70)		
2000	2.47 (2.06-2.87)		
2001	1.97 (1.60-2.34)		
2002	1.57 (1.24-1.91)		
2003	1.52 (1.20-1.83)		
2004	1.43 (1.13-1.73)		
2005	1.35 (1.08-1.62)		
2006	1.21 (0.95-1.47)		
2007	1.11 (0.86-1.35)		
2008	1.01 (0.76-1.26)		
2009	0.93 (0.68-1.18)	0.78 (0.49-1.07)	
2010	0.89 (0.64-1.14)	0.80 (0.53-1.07)	
2011	0.83 (0.58-1.07)	0.76 (0.50-1.03)	
2012	0.74 (0.51-0.98)	0.70 (0.45-0.94)	0.89 (0.57-1.20)
2013	0.65 (0.42-0.89)	0.71 (0.49-0.94)	0.78 (0.50-1.07)
2014	0.60 (0.36-0.84)	0.74 (0.46-1.03)	1.00 (0.63-1.37)
2015	0.52 (0.27-0.78)	0.59 (0.28-0.90)	0.98 (0.52-1.43)
2016	0.45 (0.20-0.71)	0.39 (0.13-0.65)	0.60 (0.29-0.92)
2017	0.46 (0.19-0.73)	0.41 (0.16-0.65)	0.55 (0.17-0.92)
2018	0.48 (0.21-0.75)	0.51 (0.26-0.76)	0.54 (0.24-0.85)
2019			0.63 (0.25-1.01)

Table 52: CFC-12 emission (Gg yr^{-1}) estimates for the UK with uncertainty (1std).
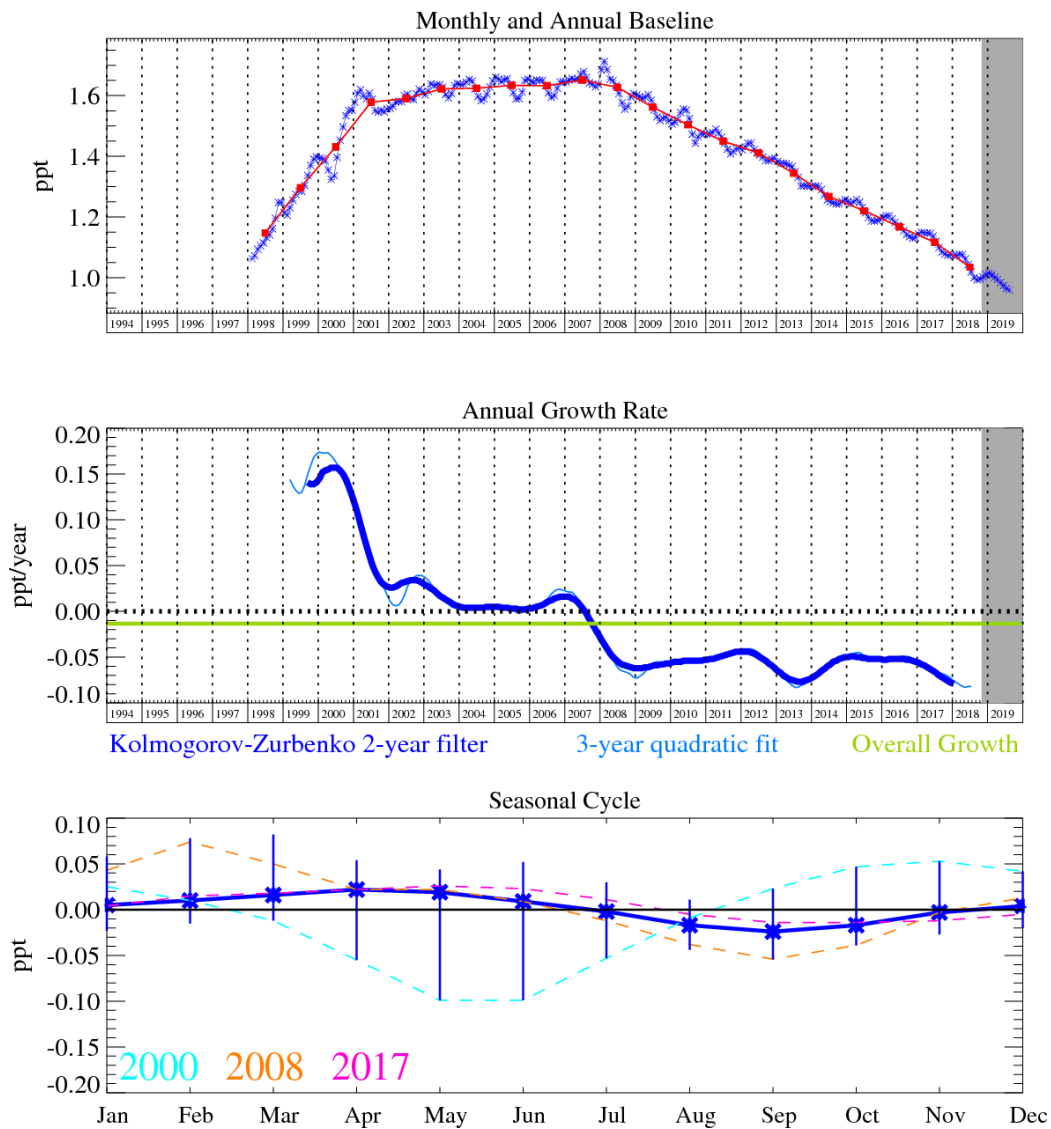
8.4 HCFC-124

Figure 142: HCFC-124: Monthly (blue) and annual (red) Northern Hemisphere baseline mole fractions (top plot). Annual (blue) and overall (green) average growth rate (middle plot). Seasonal cycle (de-trended) with year-to-year variability (lower plot). Grey area covers un-ratified provisional data.
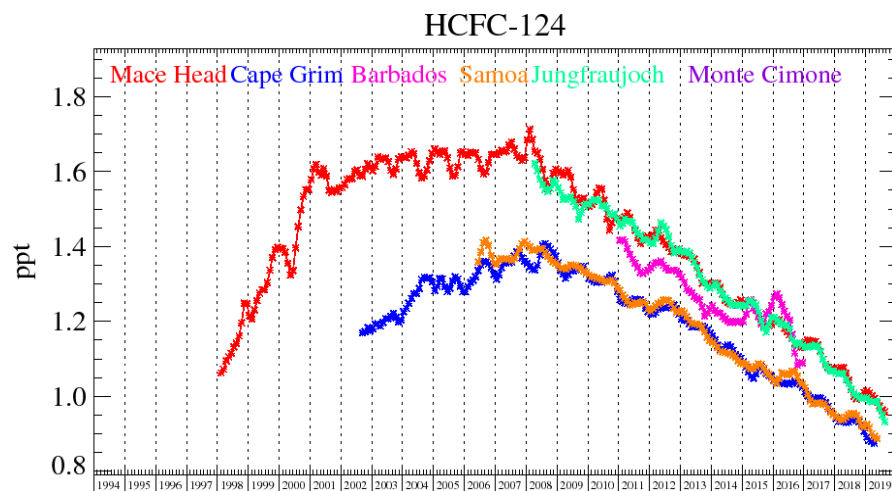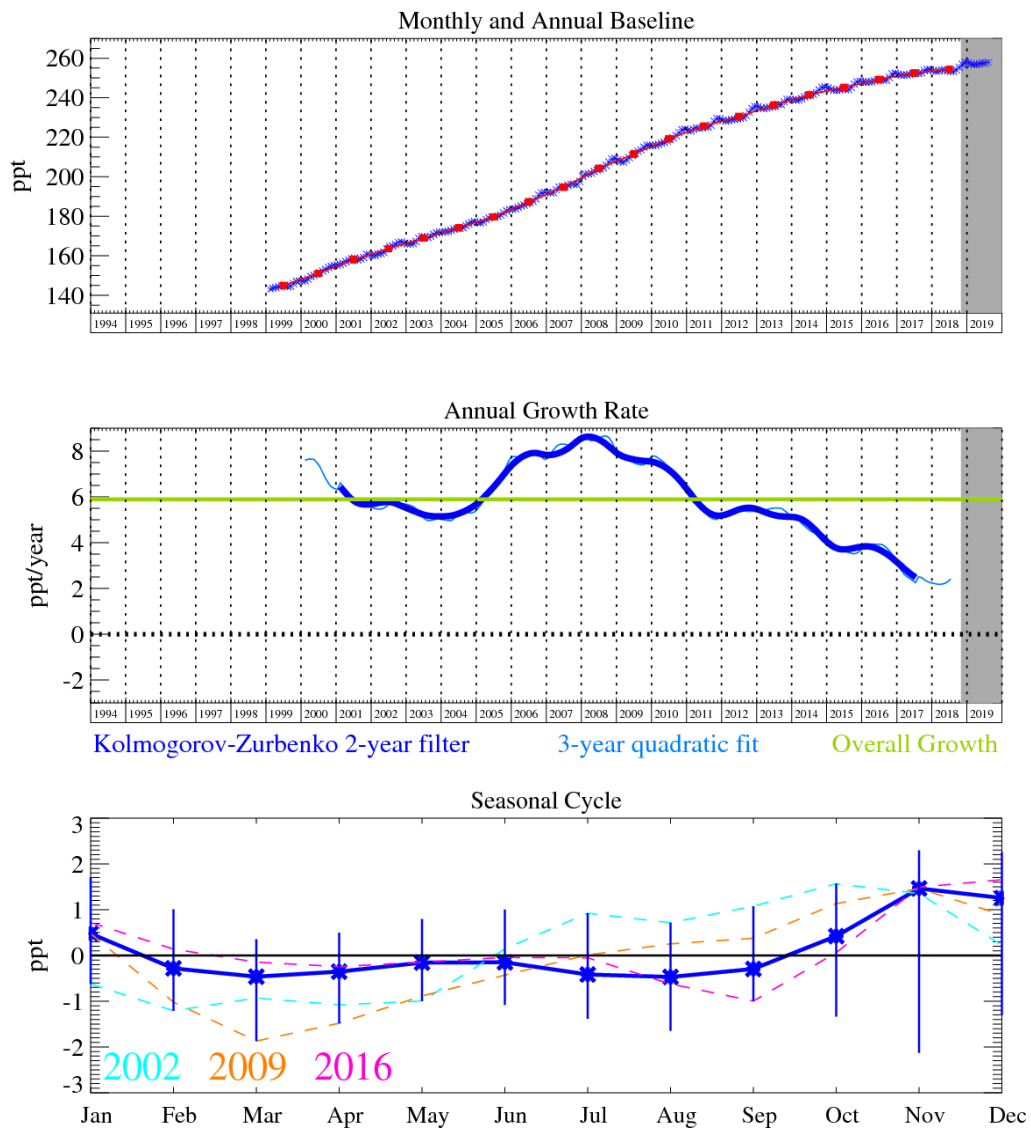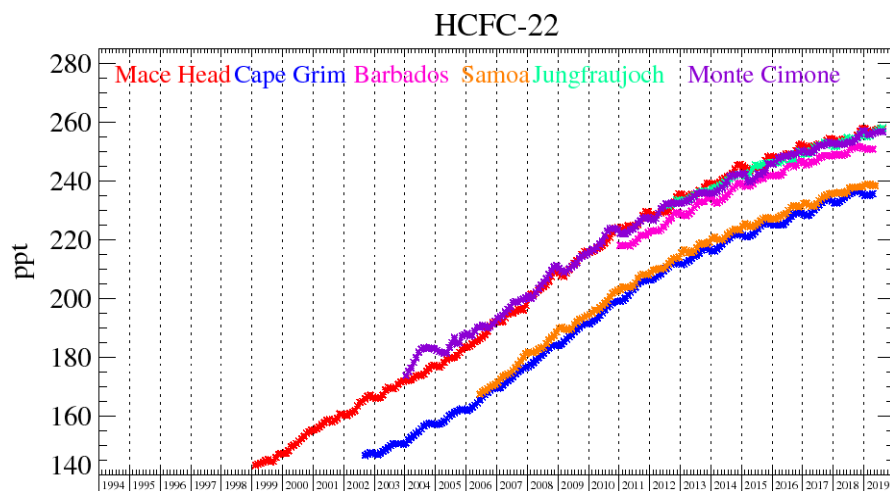

Figure 143: Background HCFC-124 mole fractions at several global AGAGE stations both in the Northern and Southern Hemispheres.
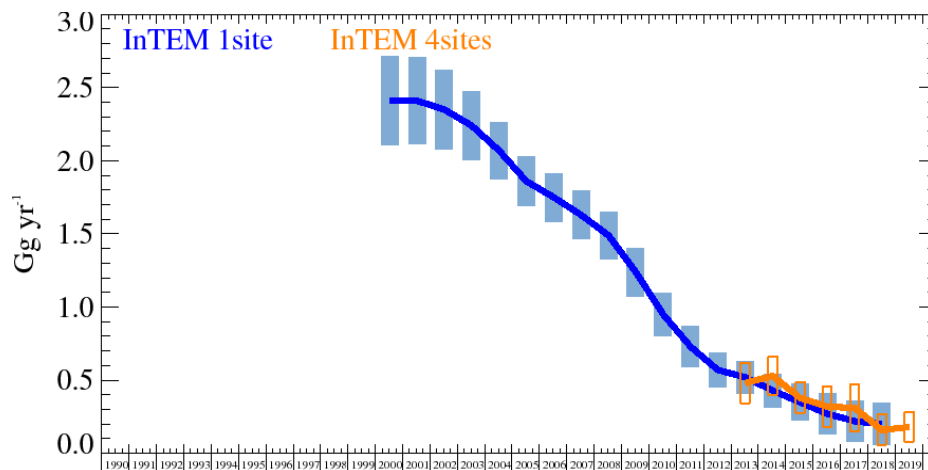
8.5   HCFC-22

Monthly and Annual Baseline

Annual Growth Rate

Kolmogorov-Zurbenko 2-year filter   3-year quadratic fit   Overall Growth

Seasonal Cycle

2002   2009   2016

Figure 144: HCFC-22: Monthly (blue) and annual (red) Northern Hemisphere baseline mole fractions (top plot). Annual (blue) and overall (green) average growth rate (middle plot). Seasonal cycle (de-trended) with year-to-year variability (lower plot). Grey area covers un-ratified provisional data.

HCFC-22

Mace Head Cape Grim Barbados Samoa Jungfraujoch Monte Cimone

Figure 145: Background HCFC-22 mole fractions at several global AGAGE stations both in the Northern and Southern Hemispheres.

Figure 146: HCFC-22: UK emission estimates (Gg yr^{-1}) using InTEM (annually averaged): (a) MHD (3yr) with global meteorology (blue) and (b) 4 sites (1yr) (MHD+JFJ+CMN+TAC) with UKV 1.5 km nested in global meteorology (green). The uncertainty bars represent 1 std.
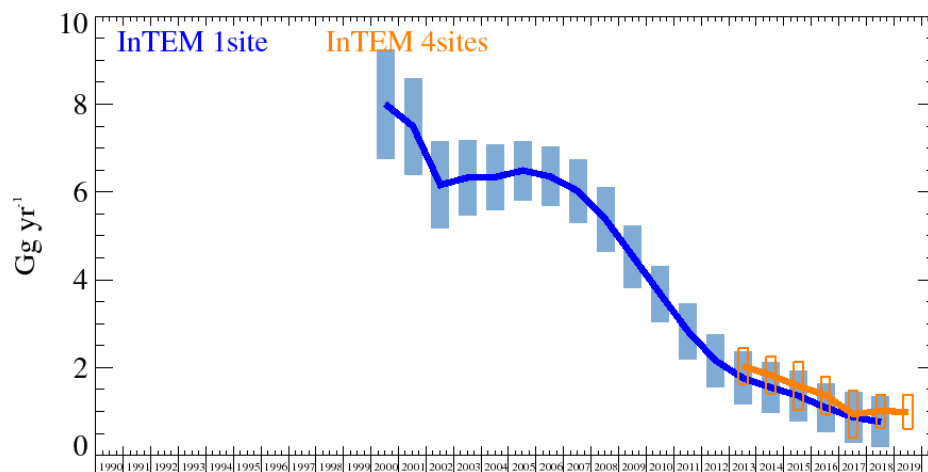

Figure 147: HCFC-22: NWEU emission estimates (Gg yr^{-1}) using InTEM (annually averaged): (a) MHD (3yr) with global meteorology (blue) and (b) 4 sites (1yr) (MHD+JFJ+CMN+TAC) with UKV 1.5 km nested in global meteorology (green). The uncertainty bars represent 1 std.

Years	MHD	4 sites
2000	2.41 (2.11-2.72)	
2001	2.41 (2.11-2.70)	
2002	2.35 (2.08-2.62)	
2003	2.24 (2.01-2.48)	
2004	2.07 (1.87-2.26)	
2005	1.86 (1.69-2.03)	
2006	1.75 (1.58-1.91)	
2007	1.63 (1.46-1.79)	
2008	1.49 (1.33-1.65)	
2009	1.24 (1.07-1.40)	
2010	0.95 (0.80-1.10)	
2011	0.73 (0.59-0.87)	
2012	0.57 (0.46-0.69)	
2013	0.52 (0.41-0.63)	0.48 (0.34-0.62)
2014	0.43 (0.32-0.55)	0.53 (0.40-0.66)
2015	0.35 (0.22-0.47)	0.38 (0.28-0.49)
2016	0.27 (0.13-0.41)	0.32 (0.18-0.46)
2017	0.22 (0.08-0.36)	0.31 (0.15-0.47)
2018	0.20 (0.06-0.35)	0.16 (0.06-0.27)
2019		0.18 (0.08-0.28)

Table 53: HCFC-22 emission (Gg yr^{-1}) estimates for the UK with uncertainty (1std).
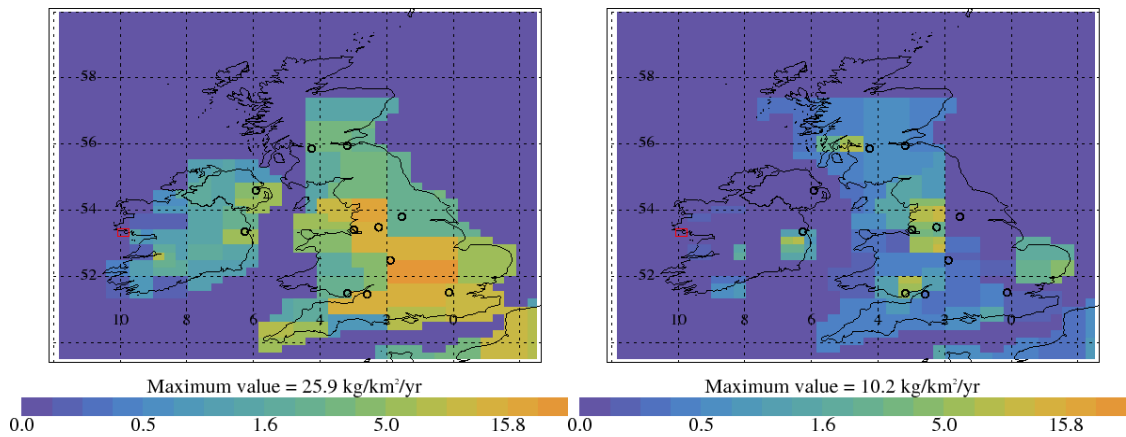
Figure 148: HCFC-22 emission estimate using MHD data for 2004-2008 (left) and 2014-2018 (right). Major cities shown as black circles and observation sites shown as red rectangle.
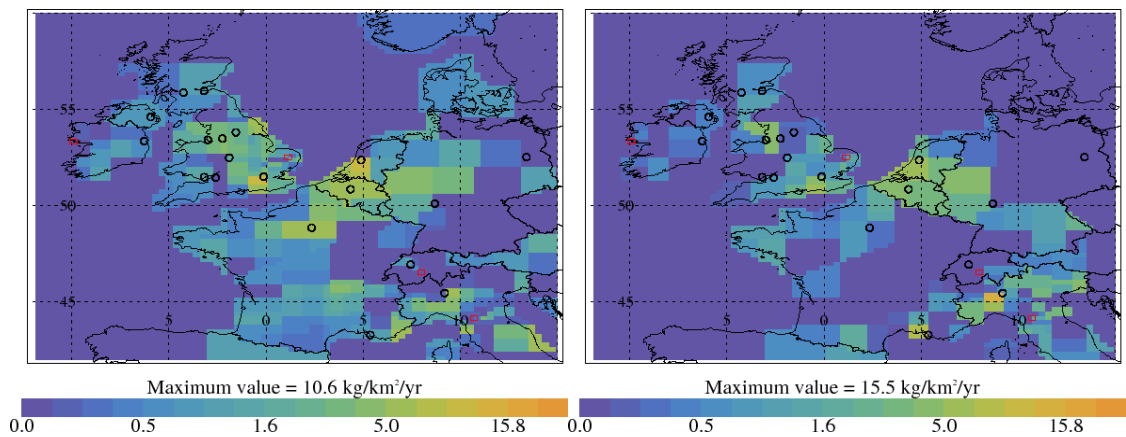

Figure 149: HCFC-22 emission estimate using data from 4 sites for 2013-2015 (left) and 2016-2018 (right). Major cities shown as black circles and observation sites shown as red rectangle.

Years	MHD	4 sites
2000	8.0 (6.8-9.3)	
2001	7.5 (6.4-8.6)	
2002	6.16 (5.17-7.15)	
2003	6.33 (5.48-7.19)	
2004	6.34 (5.59-7.08)	
2005	6.49 (5.82-7.17)	
2006	6.35 (5.68-7.03)	
2007	6.02 (5.29-6.75)	
2008	5.38 (4.65-6.11)	
2009	4.53 (3.82-5.24)	
2010	3.67 (3.03-4.31)	
2011	2.83 (2.19-3.46)	
2012	2.16 (1.56-2.75)	
2013	1.76 (1.15-2.36)	2.03 (1.62-2.43)
2014	1.55 (0.98-2.13)	1.83 (1.41-2.25)
2015	1.36 (0.78-1.94)	1.58 (1.03-2.13)
2016	1.09 (0.55-1.64)	1.37 (0.94-1.80)
2017	0.87 (0.30-1.44)	0.94 (0.40-1.48)
2018	0.76 (0.18-1.33)	1.01 (0.63-1.38)
2019		0.99 (0.59-1.38)

Table 54: HCFC-22 emission (Gg yr^{-1}) estimates for the NWEU with uncertainty (1std).

8.6   HCFC-141b

Monthly and Annual Baseline

Annual Growth Rate

Kolmogorov-Zurbenko 2-year filter   3-year quadratic fit   Overall Growth

Seasonal Cycle
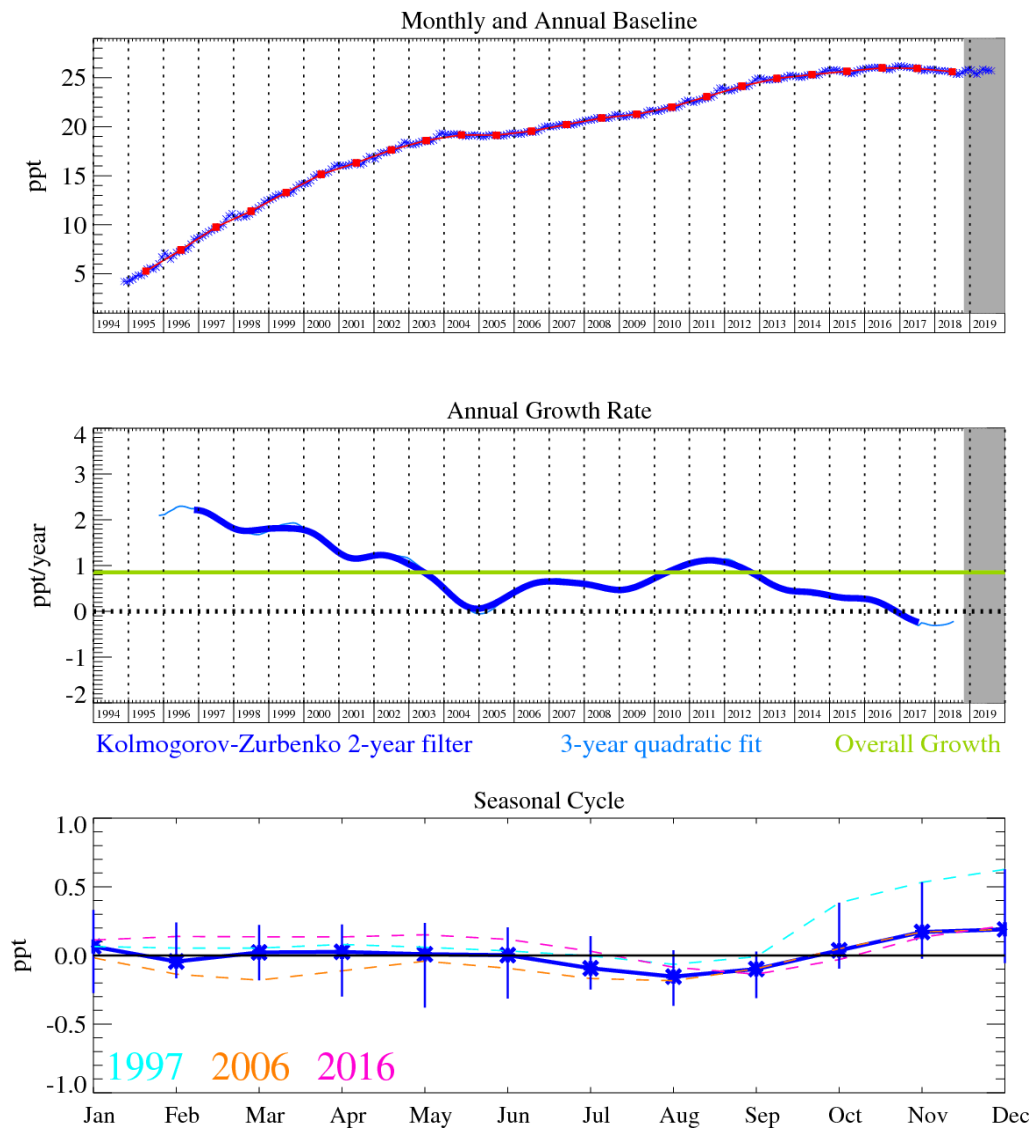

1997   2006   2016

Figure 150: HCFC-141b: Monthly (blue) and annual (red) Northern Hemisphere baseline mole fractions (top plot). Annual (blue) and overall (green) average growth rate (middle plot). Seasonal cycle (de-trended) with year-to-year variability (lower plot). Grey area covers un-ratified provisional data.
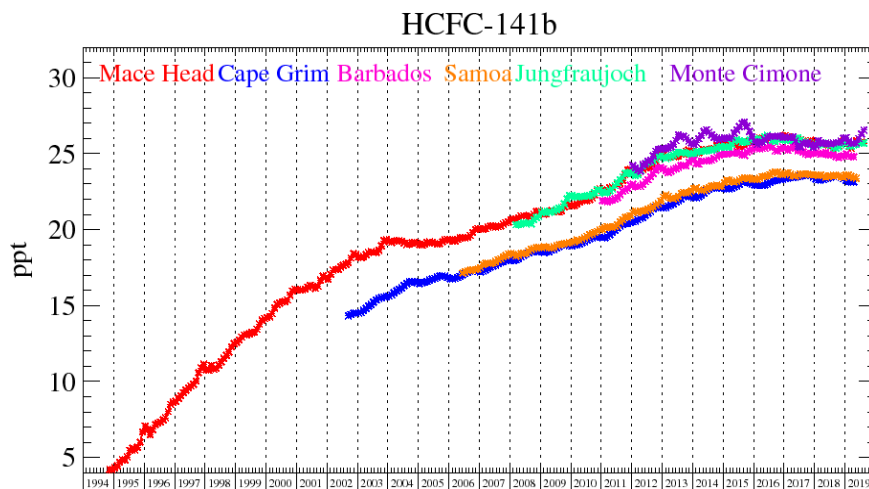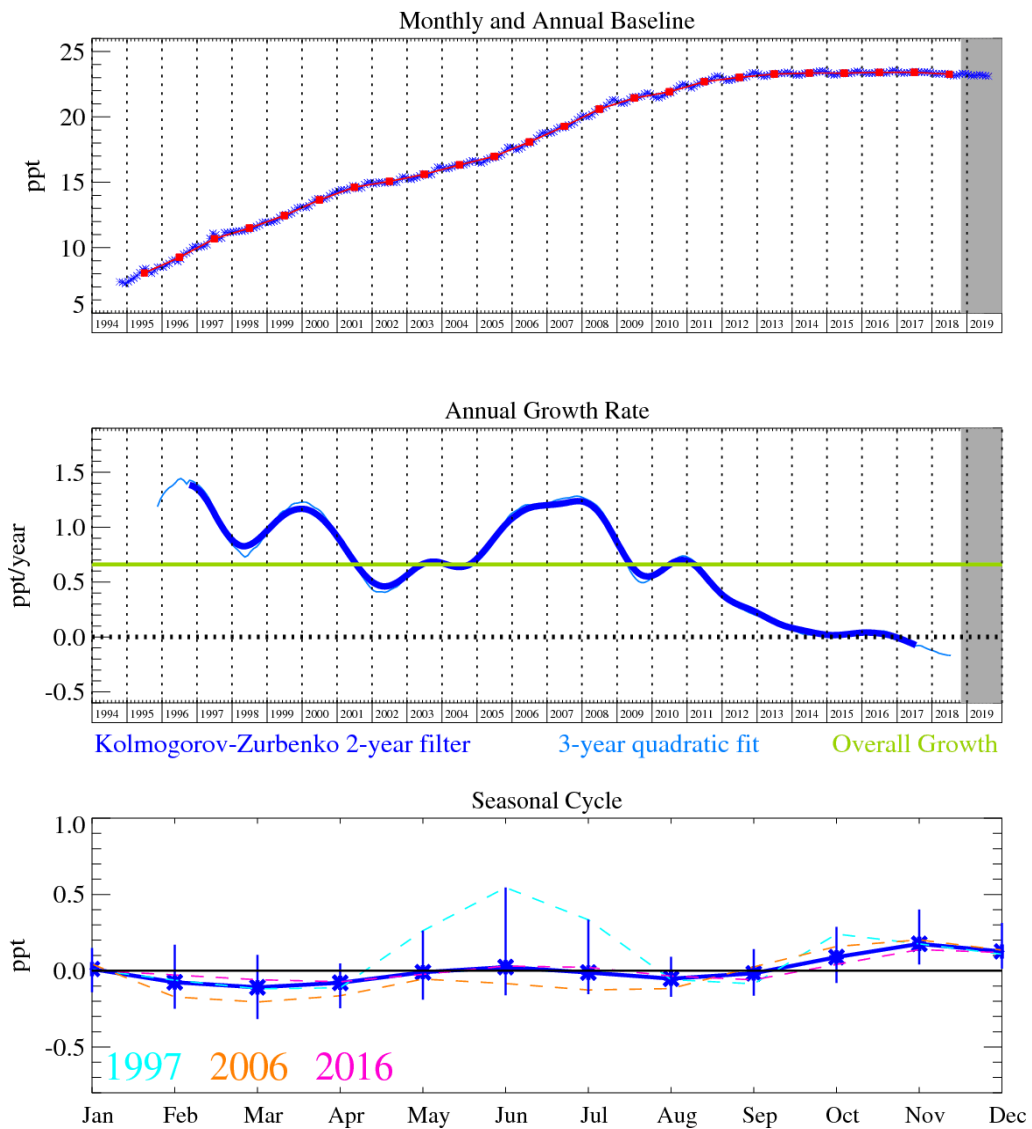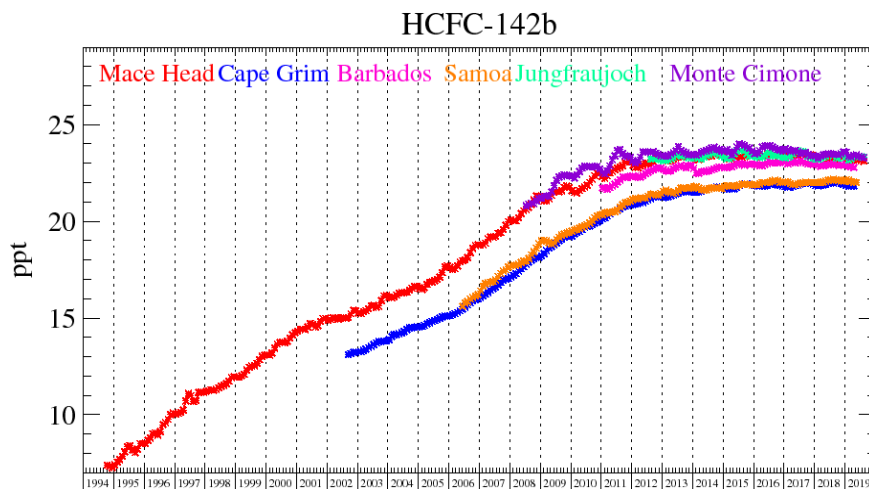
HCFC-141b

Mace Head Cape Grim Barbados Samoa Jungfraujoch Monte Cimone

Figure 151: Background HCFC-141b mole fractions at several global AGAGE stations both in the Northern and Southern Hemispheres.

8.7 HCFC-142b

Monthly and Annual Baseline

Annual Growth Rate

Kolmogorov-Zurbenko 2-year filter   3-year quadratic fit   Overall Growth

Seasonal Cycle

1997 2006 2016

Figure 152: HCFC-142b: Monthly (blue) and annual (red) Northern Hemisphere baseline mole fractions (top plot). Annual (blue) and overall (green) average growth rate (middle plot). Seasonal cycle (de-trended) with year-to-year variability (lower plot). Grey area covers un-ratified provisional data.

HCFC-142b

Mace Head Cape Grim Barbados Samoa Jungfraujoch Monte Cimone

Figure 153: Background HCFC-142b mole fractions at several global AGAGE stations both in the Northern and Southern Hemispheres.
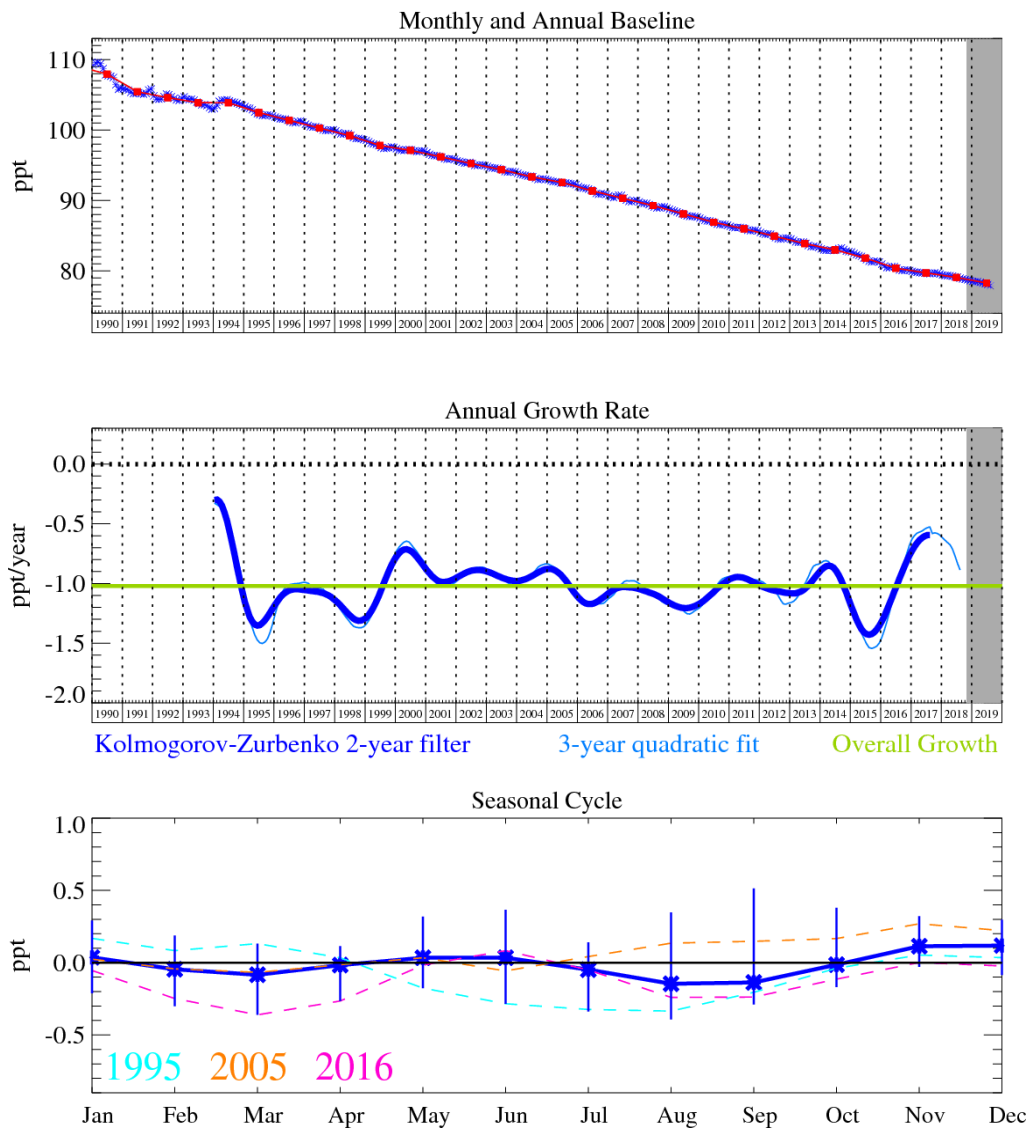
8.8 Carbon tetrachloride

Monthly and Annual Baseline

Annual Growth Rate

Kolmogorov-Zurbenko 2-year filter   3-year quadratic fit   Overall Growth

Seasonal Cycle

1995   2005   2016

Figure 154: CCl₄: Monthly (blue) and annual (red) Northern Hemisphere baseline mole fractions (top plot). Annual (blue) and overall (green) average growth rate (middle plot). Seasonal cycle (de-trended) with year-to-year variability (lower plot). Grey area covers un-ratified provisional data.

Carbon tetrachloride (CCl4)

Mace Head   Cape Grim   Barbados   Samoa   Jungfraujoch   Monte Cimone
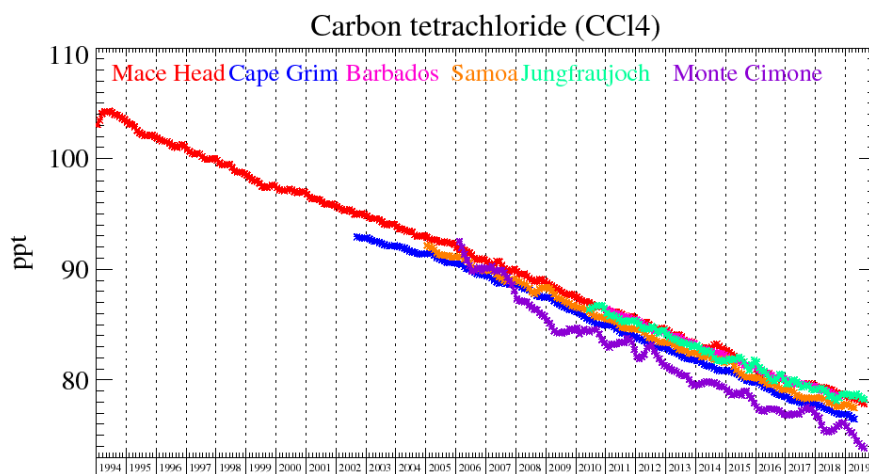
Figure 155: Background CCl₄ mole fractions at several global AGAGE stations both in the Northern and Southern Hemispheres.
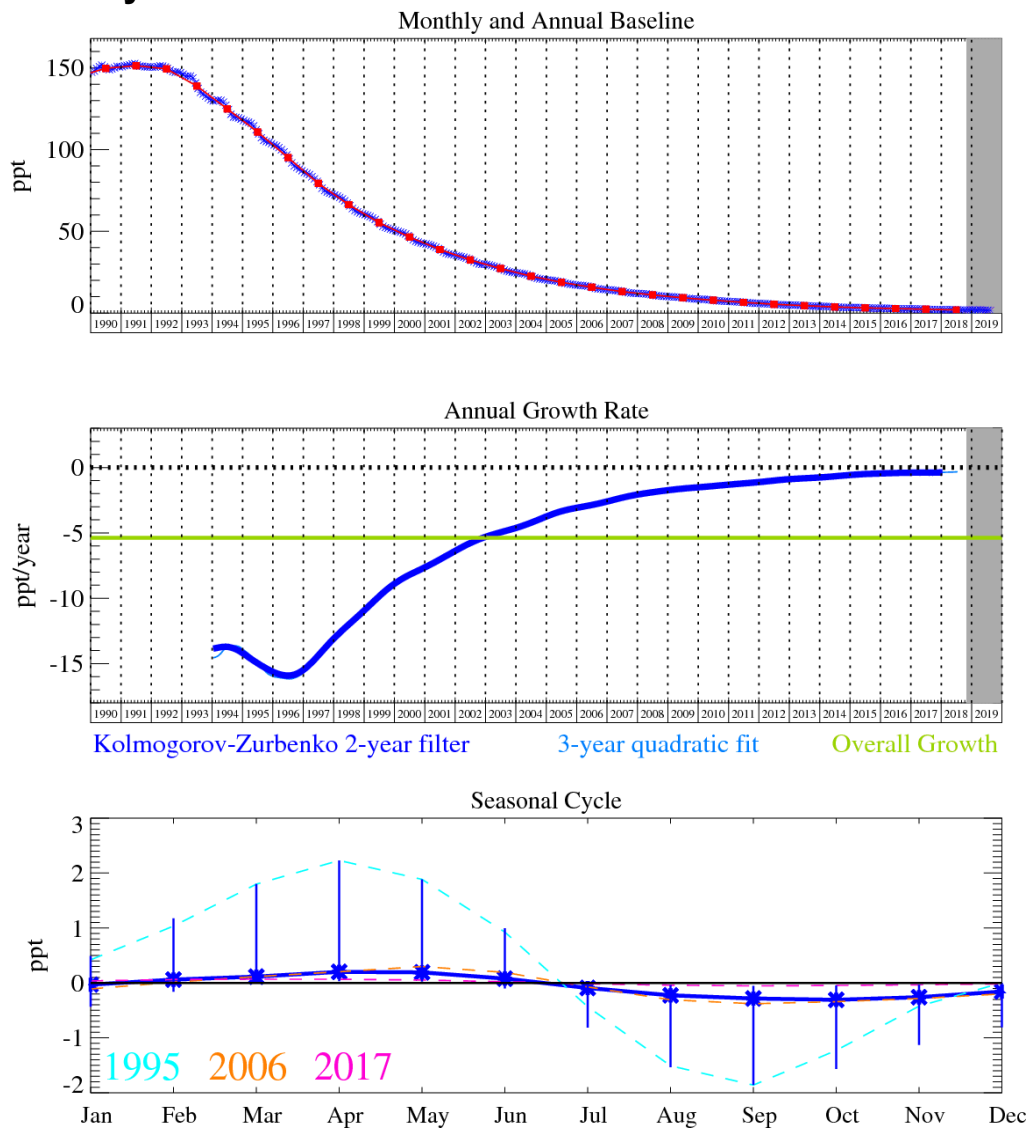
8.9 Methyl Chloroform

Monthly and Annual Baseline

Annual Growth Rate

Kolmogorov-Zurbenko 2-year filter   3-year quadratic fit   Overall Growth

Seasonal Cycle

1995   2006   2017

Figure 156: CH$_3$CCl$_3$: Monthly (blue) and annual (red) Northern Hemisphere baseline mole fractions (top plot). Annual (blue) and overall (green) average growth rate (middle plot). Seasonal cycle (de-trended) with year-to-year variability (lower plot). Grey area covers un-ratified provisional data.

Methyl chloroform (CH3CCl3)

Mace Head   Cape Grim   Barbados   Samoa   Jungfraujoch   Monte Cimone
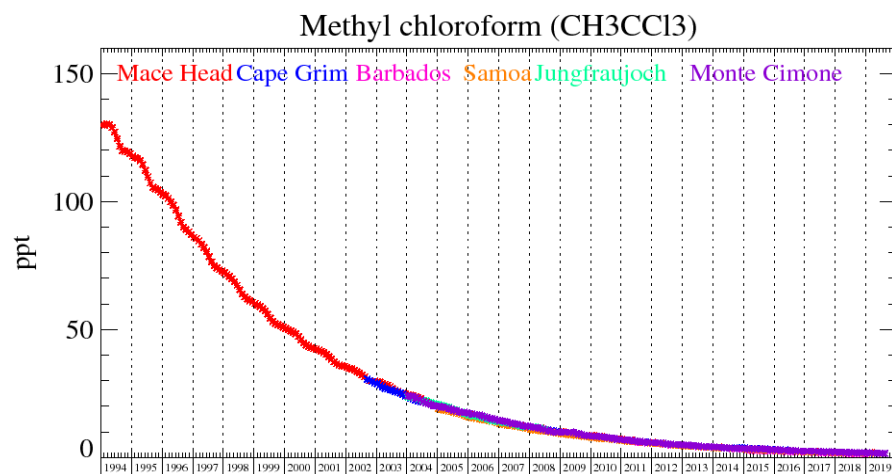
Figure 157: Background CH$_3$CCl$_3$ mole fractions at several global AGAGE stations both in the Northern and Southern Hemispheres.
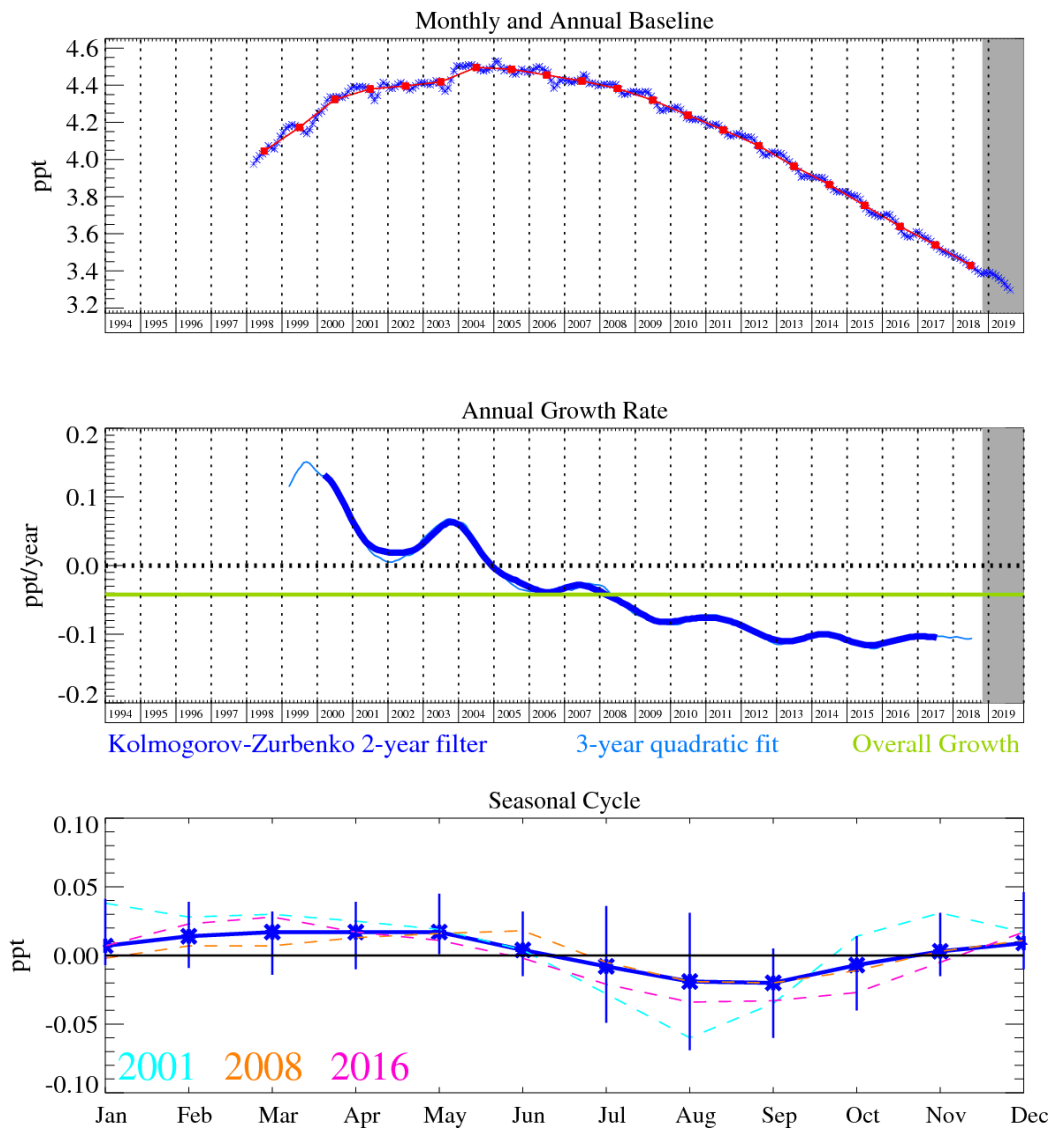
137

8.10 Halon-1211

Figure 158: Halon-1211: Monthly (blue) and annual (red) Northern Hemisphere baseline mole fractions (top plot). Annual (blue) and overall (green) average growth rate (middle plot). Seasonal cycle (de-trended) with year-to-year variability (lower plot). Grey area covers un-ratified provisional data.
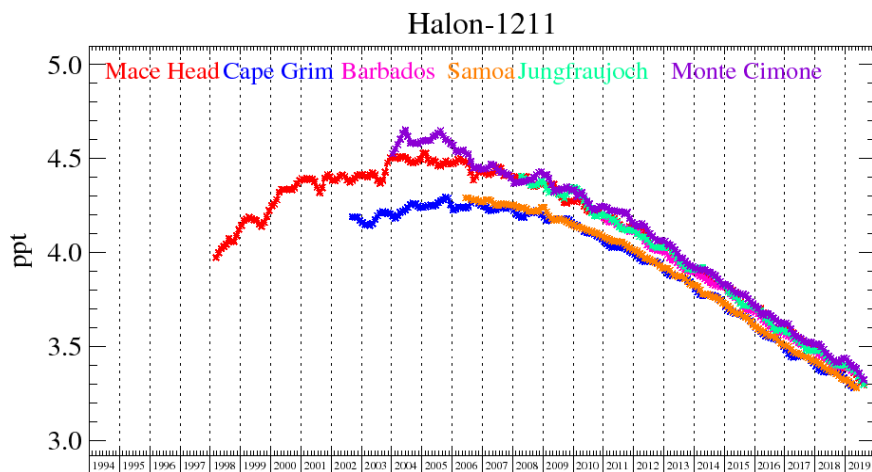

Figure 159: Background Halon-1211 mole fractions at several global AGAGE stations both in the Northern and Southern Hemispheres.
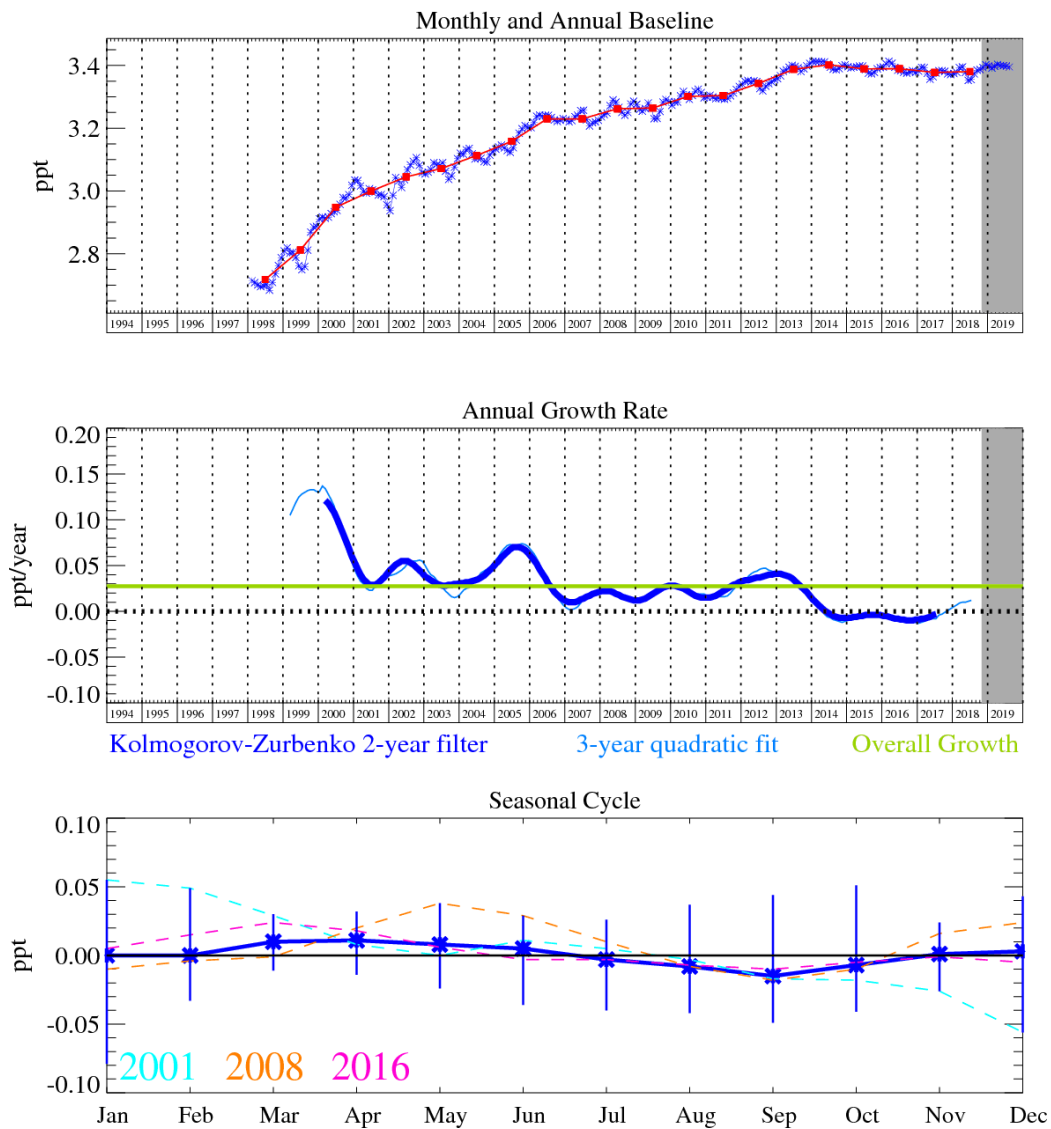
8.11 Halon-1301

Figure 160: Halon-1301: Monthly (blue) and annual (red) Northern Hemisphere baseline mole fractions (top plot). Annual (blue) and overall (green) average growth rate (middle plot). Seasonal cycle (de-trended) with year-to-year variability (lower plot). Grey area covers un-ratified provisional data.
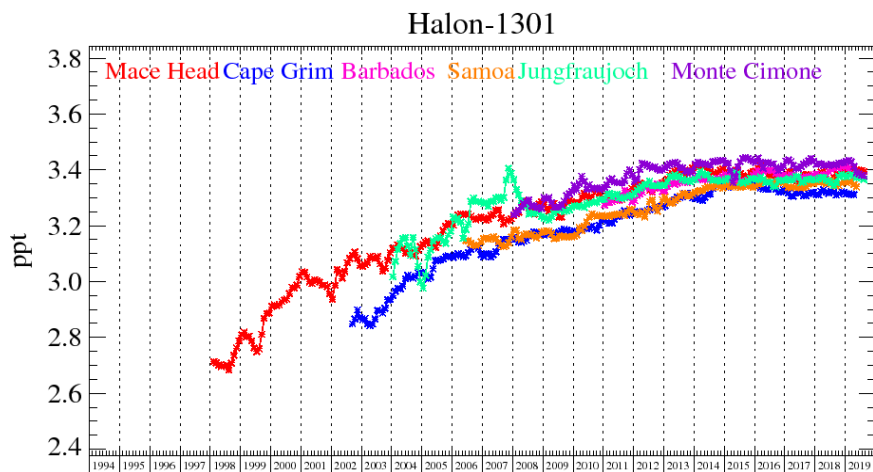

Figure 161: Background Halon-1301 mole fractions at several global AGAGE stations both in the Northern and Southern Hemispheres.

8.12 Halon-2402

Monthly and Annual Baseline

Annual Growth Rate

Kolmogorov-Zurbenko 2-year filter   3-year quadratic fit   Overall Growth

Seasonal Cycle
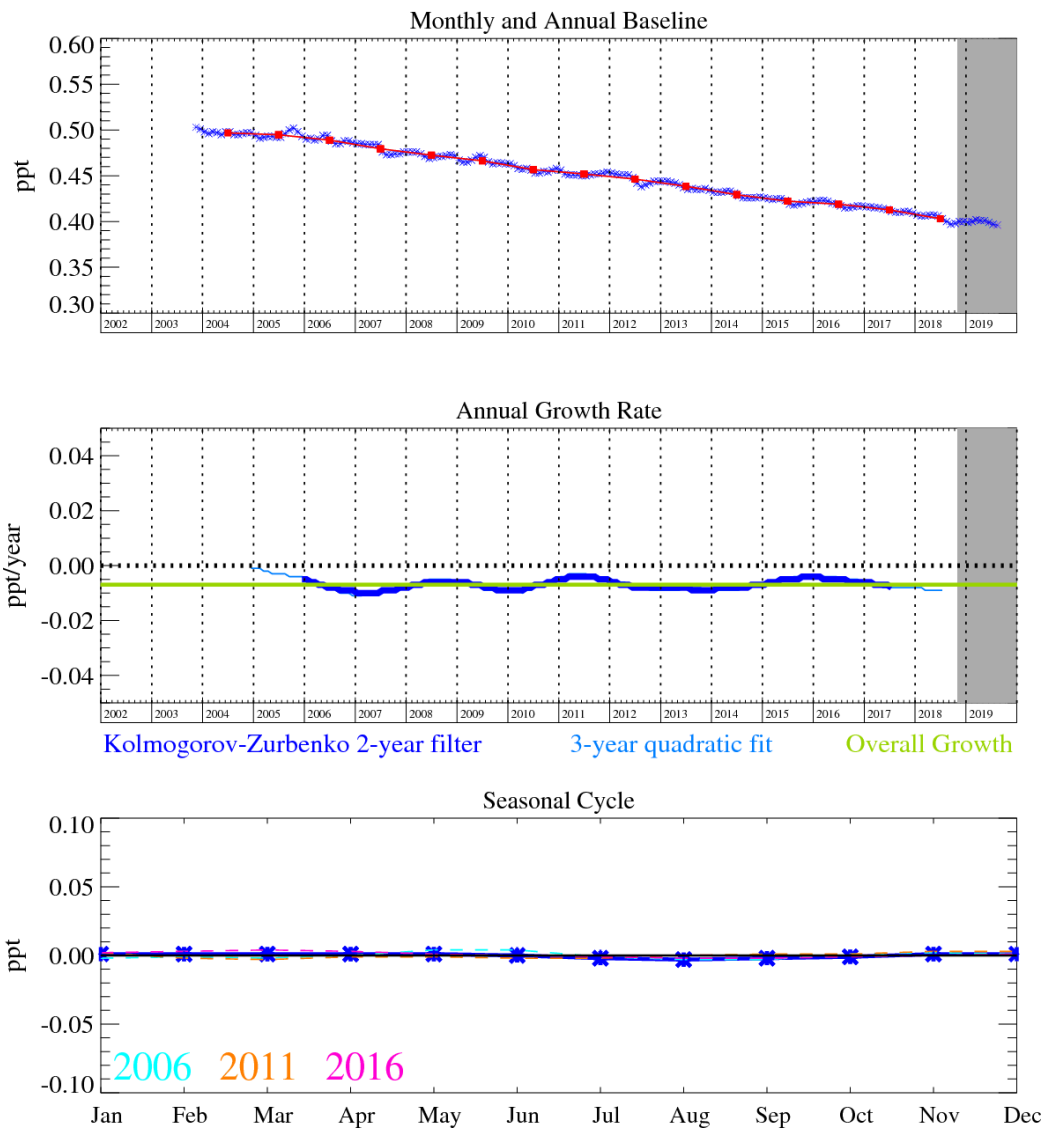

2006   2011   2016

Figure 162: Halon-2402: Monthly (blue) and annual (red) Northern Hemisphere baseline mole fractions (top plot). Annual (blue) and overall (green) average growth rate (middle plot). Seasonal cycle (de-trended) with year-to-year variability (lower plot). Grey area covers un-ratified provisional data.
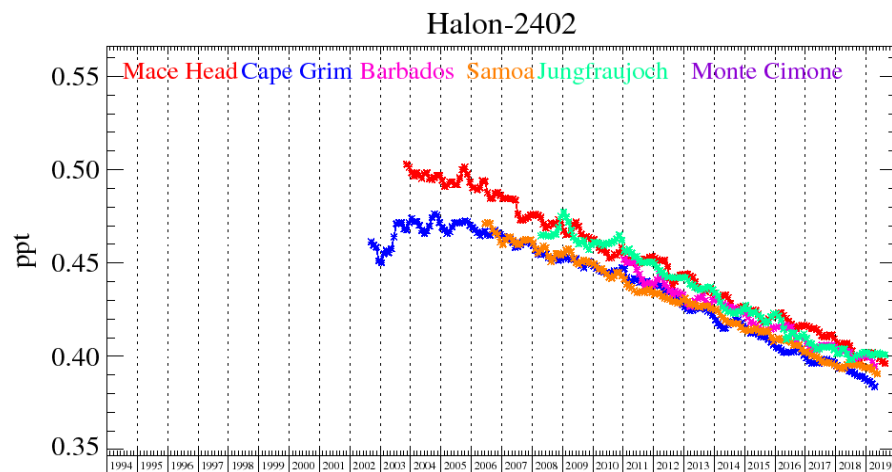
Halon-2402

Mace Head Cape Grim Barbados Samoa Jungfraujoch Monte Cimone

Figure 163: Background Halon-2402 mole fractions at several global AGAGE stations both in the Northern and Southern Hemispheres.

9 Bibliography

Ganesan, A. L., M. Rigby, M. F. Lunt, R. J. Parker, H. Boesch, N. Goulding, T. Umezawa, A. Zahn, A. Chatterjee, R. G. Prinn, Y. K. Tiwari, M. van der Schoot, and P. B. Krummel, **Atmospheric observations show accurate reporting and little growth in India's methane emissions**, *Nature Communications*, *8*(1), doi:10.1038/s41467-017-00994-7, 2017.

Graziosi, F., J. Arduini, F. Furlani, U. Giostra, P. Cristofanelli, X. Fang, O. Hermanssen, C. Lunder, G. Maenhout, S. O'Doherty, S. Reimann, N. Schmidbauer, M. K. Vollmer, D. Young, and M. Maione, **European emissions of the powerful greenhouse gases hydrofluorocarbons inferred from atmospheric measurements and their comparison with annual national reports to UNFCCC**, *Atmospheric Environment*, *158*, 85–97, doi:10.1016/j.atmosenv.2017.03.029, 2017.

Hu, H., J. Landgraf, R. Detmers, T. Borsdorff, J. Aan de Brugh, I. Aben, A. Butz, and O. Hasekamp, **Toward Global Mapping of Methane With TROPOMI: First Results and Intersatellite Comparison to GOSAT**, *Geophysical Research Letters*, *45*(8), 3682–3689, doi:10.1002/2018GL077259, 2018.

Hu, L., S. A. Montzka, S. J. Lehman, D. S. Godwin, B. R. Miller, A. E. Andrews, K. Thoning, J. B. Miller, C. Sweeney, C. Siso, J. W. Elkins, B. D. Hall, D. J. Mondeel, D. Nance, T. Nehrkorn, M. Mountain, M. L. Fischer, S. C. Biraud, H. Chen, and P. P. Tans, **Considerable contribution of the Montreal Protocol to declining greenhouse gas emissions from the United States: U.S. CFCs, HCFCs, and HFCs Emissions**, *Geophysical Research Letters*, *44*(15), 8075–8083, doi:10.1002/2017GL074388, 2017.

Kuze, A., H. suto, K. Shiomi, s. kawakami, M. Tanaka, Y. Ueda, A. Deguchi, J. Yoshida, Y. Yamamoto, F. Kataoka, T. E. Taylor, and H. Buijs, **Update on GOSAT TANSO-FTS performance, operations, and data products after more than six years in space**, *Atmospheric Measurement Techniques Discussions*, 1–38, doi:10.5194/amt-2015-333, 2016.

Lunt, M. F., M. Rigby, A. L. Ganesan, A. J. Manning, R. G. Prinn, S. O'Doherty, J. Mühle, C. M. Harth, P. K. Salameh, T. Arnold, R. F. Weiss, T. Saito, Y. Yokouchi, P. B. Krummel, L. P. Steele, P. J. Fraser, S. Li, S. Park, S. Reimann, M. K. Vollmer, C. Lunder, O. Hermansen, N. Schmidbauer, M. Maione, J. Arduini, D. Young, and P. G. Simmonds, **Reconciling reported and unreported HFC emissions with atmospheric observations**, *Proceedings of the National Academy of Sciences*, 201420247, doi:10.1073/pnas.1420247112, 2015.

Lunt, M. F., M. Rigby, A. L. Ganesan, and A. J. Manning, **Estimation of trace gas fluxes with objectively determined basis functions using reversible-jump Markov chain Monte Carlo**, *Geoscientific Model Development*, *9*(9), 3213–3229, doi:10.5194/gmd-9-3213-2016, 2016.

Parker, R., H. Boesch, A. Cogan, A. Fraser, L. Feng, P. I. Palmer, J. Messerschmidt, N. Deutscher, D. W. T. Griffith, J. Notholt, P. O. Wennberg, and D. Wunch, **Methane observations from the Greenhouse Gases Observing SATellite: Comparison to ground-based TCCON data and model calculations: GOSAT CH_4 OBSERVATIONS**, *Geophysical Research Letters*, *38*(15), doi:10.1029/2011GL047871, 2011.

Rigby, M., R. G. Prinn, S. O'Doherty, S. A. Montzka, A. McCulloch, C. M. Harth, J. Mühle, P. K. Salameh, R. F. Weiss, D. Young, P. G. Simmonds, B. D. Hall, G. S. Dutton, D. Nance, D. J. Mondeel, J. W. Elkins, P. B. Krummel, L. P. Steele, and P. J. Fraser, **Re-evaluation of the lifetimes of the major CFCs and CH_3CCl_3 using atmospheric trends**, *Atmospheric Chemistry & Physics*, *13*(5), 2691–2702, doi:10.5194/acp-13-2691-2013, 2013.

Rigby, M., R. G. Prinn, S. O'Doherty, B. R. Miller, D. Ivy, J. Mühle, C. M. Harth, P. K. Salameh, T. Arnold, R. F. Weiss, P. B. Krummel, L. P. Steele, P. J. Fraser, D. Young, and P. G. Simmonds, **Recent and future trends in synthetic greenhouse gas radiative forcing**, *Geophysical Research Letters*, *41*(7), 2623–2630, doi:10.1002/2013GL059099, 2014.

Say, D., A. J. Manning, S. O'Doherty, M. Rigby, D. Young, and A. Grant, **Re-Evaluation of the UK's HFC-134a Emissions Inventory Based on Atmospheric Observations**, *Environmental Science & Technology*, *50*(20), 11129–11136, doi:10.1021/acs.est.6b03630, 2016.

Simmonds, P. G., M. Rigby, A. McCulloch, M. K. Vollmer, S. Henne, J. Mühle, S. O'Doherty, A. J. Manning, P. B. Krummel, P. J. Fraser, D. Young, R. F. Weiss, P. K. Salameh, C. M. Harth, S. Reimann, C. M. Trudinger, L. P. Steele, R. H. J. Wang, D. J. Ivy, R. G. Prinn, B. Mitrevski, and D. M. Etheridge, **Recent increases in the atmospheric growth rate and emissions of HFC-23 (CHF$_3$) and the link to HCFC-22 (CHClF$_2$) production**, *Atmos. Chem. Phys.*, *18*(6), 4153–4169, doi:10.5194/acp-18-4153-2018, 2018.

Velders, G. J. M., D. W. Fahey, J. S. Daniel, M. McFarland, and S. O. Andersen, **The large contribution of projected HFC emissions to future climate forcing**, *Proceedings of the National Academy of Sciences*, *106*(27), 10949–10954, doi:10.1073/pnas.0902817106, 2009.

Wolf, J., G. R. Asrar, and T. O. West, **Revised methane emissions factors and spatially distributed annual carbon fluxes for global livestock**, *Carbon Balance and Management*, *12*(1), doi:10.1186/s13021-017-0084-y, 2017.

Worden, J. R., A. A. Bloom, S. Pandey, Z. Jiang, H. M. Worden, T. W. Walker, S. Houweling, and T. Röckmann, **Reduced biomass burning emissions reconcile conflicting estimates of the post-2006 atmospheric methane budget**, *Nature Communications*, *8*(1), doi:10.1038/s41467-017-02246-0, 2017.